The Effect of Cannabidiol in Tuberous Sclerosis Complex

PhD Thesis

Inês da Silva Serra, M.Pharm.

School of Psychology and Clinical Language Sciences, and School of Pharmacy

April 2019

Supervisors:

Prof. Claire Williams and Dr. Mark Dallas

Declaration:

I confirm that this is my own work and the use of all material from other sources has been properly and fully acknowledged.

Inês da Silva Serra

Acknowledgments:

I would like to begin this work by thanking my supervisors, Claire and Mark, for their support and patience throughout my experiments and writing. I would also like to thank Ben, who moved to the dark side, but whose "good job" was greatly missed and always kept me motivated. A special thanks to the tech help I had, especially from Shanice and Leo, whose assistance with my energetic rats allowed me more time for the fun bench work.

A massive note of gratitude to the people I met at K.U.Leuven, for making me feel at home in their laboratory and for teaching me so much about the wonderful zebrafish. A special thank you note to Riccardo who, since then, introduced a lot of constructive awkwardness into my life.

To my *Pharma* companions, who always heard my endless complaining with an impressive apparent interest: let us move our shenanigans elsewhere now. A special thanks to Orla, one of the most inspirational women I have ever met and whose strength helped me throughout this endeavour. I am also eternally grateful to my *Office Nerds*, who always took care of me when I needed the most and made me fell sane when everything else felt crazy.

My housemates Matt, Rebecca and Ben also deserve a special note in this work, particularly the last two, as they allowed me to be a shameless third wheel throughout my time in Reading and always made me feel comfortable in our tiny household.

Over on the other side, I would like to thank *Dois P.*, *Best B.* and *ASJ*. Whenever I came back home, you received me like I had never left and that made me feel like I belonged with you all the time. That helped me more than you know.

However, most of all, an enormous feeling of gratitude towards my family. To my mum, my dad and my brother. Also, to my grandparents, especially the ones who will not be here to see me graduate. I thank you endlessly for always providing for me and motivating me to follow my dreams, even if that meant studying for years and years in a row. You are my heroes and I hope I made you proud. This work is for you. I will now complain about something else… .

Abstract:

Tuberous Sclerosis Complex (TSC) is a rare genetic disease caused by *TSC1* or *TSC2* mutations, characterized by overactivation of mechanistic target of rapamycin (mTOR). Among others, this leads to increased cell growth, altered cellular structure and migration. Consequently, TSC patients exhibit multiorgan tumours, namely in the brain, with neurological and neuropsychiatric manifestations affecting the majority of individuals. Central nervous system (CNS) alterations are a significant contributor to decreased quality of life and increased morbidity and caregiver dependence.

Although pharmacological options are available to manage specific CNS features of TSC, these are limited and not curative, creating a high demand for new entities that address these symptoms. In the search for novel compounds that target CNS manifestations in TSC, I focused on cannabidiol, a phytocannabinoid present in *Cannabis*, seeking out to explore and identify which CBD effects could contribute positively to the management of TSC.

With a zebrafish model of TSC, I demonstrated that CBD reduced the activation of the mTOR downstream molecule rpS6, cell size and anxiety-like behaviour. Using a rat model of TSC, the Eker rat, I described a novel cerebellar characterization and identified mutation-dependent cell size and density alterations, modified by CBD. Following long-term CBD administration and behavioural analysis, I corroborated the mild phenotype of the Eker rat and the action of CBD on rpS6. The Eker mutation also appeared to have no effect on seizure susceptibility following short-term CBD treatment. In both cases, mutation and treatment revealed minimal disease-modifying effects.

The results presented in this thesis provide novel information on the *in vivo* effects of CBD in the presence of TSC mutations and additional insight on the appropriateness of TSC models to explore CNS manifestations. The data presented is a valuable contribution to the development of novel interventions for TSC and to the study of TSC itself.

Abbreviations:

4E-BP1 eukaryotic initiation factor 4E-binding protein

5-HT$_{1A}$ 5-hydroxytryptamine (serotonin) 1A

ABC Vineland Adaptive Behavior Composite

ACTH adrenocorticotropin hormone

ADOS autism diagnostic observation schedule

ADU arbitrary density units

AED anti-epileptic drug

AIU arbitrary intensity units

Akt protein kinase B (aka PKB)

AML angiomyolipoma

AMT α-[^{11}C]methyl-L-tryptophan

ANCOVA analysis of covariance

ANOVA analysis of variance

ARRIVE Animal Research: Reporting of In Vivo Experiments

ASD autism spectrum disorder

BSA bovine serum albumin

CARS Childhood Autism Rating Scale

CBD cannabidiol

CBDA cannabidiolic acid

CSF cerebro-spinal fluid

CNS central nervous system

CT computed tomography

DAPI 4′,6-diamidino-2-phenylindole

DEPTOR DEP domain-containing mTOR interacting protein

DMSO dimethyl sulfoxide

DN dysmorphic neuron

DNA deoxyribonucleic acid

DNAse deoxyribonuclease

dpf days post-fertilization**;**

DS Dravet syndrome

DSM-5 Diagnostic and Statistical Manual of Mental Disorders

EAE experimental autoimmune encephalomyelitis

ECoG electrocorticography

EDTA ethylenediaminetetraacetic acid

EEG Electroencephalography

eIF4E eukaryotic initiation factor 4E

EKR extracellular signal-regulated kinase

ENT1 equilibrative nucleoside transporter 1

EtOH ethanol

FCD focal cortical dysplasia

FKBP12 FK506-binding protein

GABA γ-aminobutyric acid

GAD67 glutamic acid decarboxylase 67

GC giant cell

GCL granule cell layer

GFAP glial fibrillary acidic protein

GIC Global Impression of Change

GPR55 G protein-coupled receptor 55

GSK-3β glycogen synthase kinase 3 beta

HEPES 4-(2-hydroxyethyl)-1-piperazine-ethanesulfonic acid

Het heterozygote

IAU intensity arbitrary units

IHC immunohistochemistry

IL-6 interleukin 6

ILAE International League Against Epilepsy

Ip intraperitoneal

IQ intelligent quotient

IS infantile spasms

LAM lymphangioleiomyomatosis

LC-MS liquid chromatography-mass spectrometry

LGS Lennox-Gastaut syndrome

MEF murine embryo fibroblasts
Mek mitogen-activated protein kinase
ML molecular layer
mLST8 mammalian lethal with SEC13 protein 8
MRI magnetic resonance imaging
MSEL Mullen Scales of Early Learning
mSin1 stress-activated protein kinase interacting protein 1
MTC maximum tolerated concentration
mTOR mechanistic target of rapamycin
NMDA N-methyl-D-aspartate
NMI no mutation identified
OCT optimal cutting temperature
PBS phosphate-buffered saline
PC Purkinje cell
PCL Purkinje cell layer
PCR polymerase chain reaction
PDK1 phosphorylated phosphoinositide-dependent protein kinase 1
PET positron emission tomography
PFA paraformaldehyde
Pfu *Pyrococcus furiosus*
PI3K phosphatidylinositol 3-kinase
pKB negative base-10 logarithm of the base dissociation constant
PKD polycystic kidney disease
PRAS40 proline-rich Akt substrate 40 kDa
rpS6 ribosomal protein 6
PTZ pentylenetetrazol
PV parvalbumin
QoL Quality of Life
Raptor rapamycin-associated protein of TOR
RCC renal cell carcinoma
Rheb Ras homolog enriched in brain
Rictor rapamycin-insensitive companion of mTOR
ROI region of interest
S6K ribosomal protein S6 kinase
Sc subcutaneous
SEGA subependymal giant cell astrocytoma
SEM standard error of the mean
SEN subependymal nodule
SREBP1 sterol regulatory element-binding protein activation 1
SUDEP sudden unexpected death in epilepsy
TACREN TSC Autism Center of Excellence Network
TAND TSC-associated neuropsychiatric disorders
TBS tris-buffered saline
TC tonic-clonic
TD typically developing
THC Δ-9-tetrahydrocannabinol
THCA Δ-9-tetrahydrocannabinolic acid
TILLING Targeting Induced Local Lesions IN Genomes
TOSCA TuberOus SClerosis registry to increase disease Awareness
TR Touch-response
TRPV1 transient receptor potential vanilloid 1
TSC Tuberous sclerosis complex;
TUNEL terminal deoxynucleotidyl transferase dUTP nick end labelling
TX-100 4-(1,1,3,3-Tetramethylbutyl)phenyl-polyethylene glycol
US ultrasound
VABS Vineland Adaptative Behaviour Scales
VAVFL associated visual field loss
WT wild-type

List of Figures:

List of Tables:

Publications, Communications and Awards:

Journal Publications

Supplemental vitamin B-12 enhances the neural response to sensory stimulation in the barrel cortex of healthy rats but does not affect spontaneous neural activity. Sungmin Kang, Yurie Hayashi, Michael Bruyns-Haylett, Daniel H. Baker, Marcia Boura, Xuedan Wang, Kimon-Andreas Karatzas, **Ines Serra**, Angela Bithell, Claire Williams, David T. Field, Ying Zheng. *The Journal of Nutrition (DOI: 10.1093/jn/nxz011). In Press.*

Contribution to the manuscript: analysed the data and edited the manuscript.

Cannabidiol modulates phosphorylated rpS6 signalling in a zebrafish model of Tuberous Sclerosis Complex. **Ines Serra**, Chloë Scheldeman, Michael Bazelot, Benjamin J. Whalley, Mark L. Dallas, Peter A. M. de Witte, Claire M. Williams. *Behavioural Brain Research,* 363, 135-144 (2019).

Contribution to the manuscript: designed and performed the experiments; analysed the data and designed figures; wrote manuscript.

mTOR-related neuropathology in mutant tsc2 zebrafish: Phenotypic, transcriptomic and pharmacological analysis. Chloë Scheldeman, James D. Mills, Aleksandra Siekierska, **Ines Serra**, Daniëlle Copmans, Anand M. Iyer, Benjamin J. Whalley, Jan Maes, Anna C. Jansen, Lieven Lagae, Eleonora Aronica, Peter A.M. de Witte. *Neurobiology of Disease*, 108, 225-237 (2017).

Contribution to the manuscript: performed experiments and edited the manuscript.

Patents

Use of cannabidiol in the treatment of tuberous sclerosis complex (WO2018234811). Benjamin Whalley, William Hind, Royston Gray, Michael Bazelot, Ines da Silva Serra, Claire Williams, Andrew Tee (2018).

Oral Communications

The effect of cannabidiol (CBD) in a zebrafish model of tuberous sclerosis complex (TSC). *8th European Workshop on Cannabinoid Research*, University of Roehampton, London, UK (September 2017)

The effect of CBD in a zebrafish model of TSC. *Early Career Researcher day at the International Research Conference on TSC and LAM*, Washington, DC., USA (June 2017)

Poster Communications

Cellular characterisation of the Eker rat cerebellum. *Cerebellum UK Conference*, Royal Holloway, UK (April 2018)

The effect of CBD in a zebrafish model of TSC. *International Research Conference on TSC and LAM*, Washington, DC., USA (June 2017)

Awards

First Prize in the Research Image Competition (*£100 prize money*). *University of Reading Doctoral Research Conference*, Reading, UK (June 2018)

Travel Award: *£100 Bursary (May 2018)* to attend the Cerebellum UK conference, Royal Holloway, UK (April 2018)

Travel Award: *£206 BPS member bursary (July 2017)* to attend the 8th European Workshop on Cannabinoid Research, University of Roehampton, London, UK (September 2017)

Shortlisted Image in the Research Image Competition. *University of Reading Doctoral Research Conference*, Reading, UK (June 2016)

Table of Contents:

Chapter 1: Introduction

1.1 Tuberous Sclerosis Complex

1.1.1 The history of TSC

In 1835, the French dermatologist, Pierre François Olive Rayer, published the "*Traite theorique et pratique des maladies de la peau*", a comprehensive compilation of skin disease descriptions and illustrations[1]. One of these illustrations showed a picture of a man with what Rayer called "vegetations vasculaires", today recognized as facial angiofibromas. This is considered the first mention of a manifestation we now know to be widely associated with Tuberous Sclerosis Complex (TSC). Although sporadic reports of TSC symptoms had been described, it was in 1880 that Desire-Magloire Bourneville published the first detailed description of a TSC case, which he called "sclerose tubereuse des circonvoluntions cerebrales"[2]. Here, he detailed the case of L. Marie, a girl who exhibited partial and generalized seizures since birth, cognitive delay and "*vasculo-papular eruptions on her nose, cheeks and forehead*". When Marie died at 15, Bourneville conducted a *post-mortem* examination where he also noted abnormalities in her brain, specifically nodular tumours near the cerebral ventricles (now called subependymal nodules), as well as sclerotic and white areas on cortical gyri (now known to be tubers). Additionally, he found small masses in her kidneys, although he did not make an association between these and the cerebral and cognitive pathology[2]. Today, the skin, brain and kidney tumours reported by Bourneville are still used as clinical diagnostic criteria for TSC[3].

In 1901 and 1905, Pellizzi and Perusini, respectively, published work on the pathology of TSC in the brain, including microscopy drawings of abnormal and heterotopic cells, alterations of myelination, and disorganized cortical organization[4,5]. More importantly, Perusini was the first to acknowledge that, in TSC patients, brain, heart, kidney and skin lesions often coexisted[5].

Given the diversity of pathological manifestations in TSC, but also its rarity, the disease was initially overlooked, and manifestations addressed as a set of distinct medical issues rather than a single pathology. Heinrich Vogt greatly advanced the field by proposing, in 1908, the "clinical triad" for TSC diagnosis. This comprised "*mental retardation, intractable epilepsy and adenoma sebaceum* (facial angiofibromas)". His proposal was widely accepted by the medical community as the first diagnostic criteria for TSC[6]. These criteria were helpful in diagnosing severe cases of TSC. However, due to the heterogeneity of manifestations and phenotypes now known to exist, a considerable number of patients were still undiagnosed. In 1942, Moolten coined the term Tuberous Sclerosis *Complex* to account for, not only the "sclerose tubereuse" found in the brain of patients and reported by Bourneville, but also the manifestations present in other organs and systems[7].

Diagnosing TSC was facilitated with the development and use of computed tomography (CT) in 1974 and of magnetic resonance imaging (MRI) in 1982. These techniques enabled the detection of tubers and subependymal nodules, two characteristic features of TSC[8]. Crucial to the improvement of the diagnosis criteria, and to the study of TSC itself, was the discovery of a possible TSC gene. Seminal work from Lagos and Gomez in 1967 suggested for the first time a hereditary component in disease transmission, with the report of a family that had been affected by TSC for 5 generations. In these individuals, a third had normal intelligence while the remaining two thirds presented with learning disabilities, which again confirmed the heterogeneity of TSC and forced a revision of the diagnosis criteria[8]. The experimental confirmation of a gene responsible for TSC was published in 1987, when Fryer and colleges, studying 19 different families, found a mutation on chromosome 9, region 9q34[9]. Soon after, in 1992, Northrup and colleagues identified a second TSC locus[10]. The exact location of this second locus was published in 1992, by linkage analysis of the 5 families previously classified as unlinked to chromosome 9, with Kandt and colleagues localizing this second TSC gene to chromosome 16, region p13[11] (Figure 1.1). Of importance to this finding was the observation that polycystic kidney disease (PKD) was very common in TSC patients. This enabled the use of the marker D16S283, close to the already known PKD1 gene, to localize the unknown *TSC2* gene.

The identification of the causative genes for TSC enabled research into the underlying molecular mechanisms of disease to start. The crucial point for the transition from observational patient studies into molecular manifestations of TSC was the cloning of the *TSC2* and *TSC1* genes, in 1993[12] and 1997[13], respectively, and the discovery that these genes coded for two tumour suppressor proteins, tuberin and hamartin.

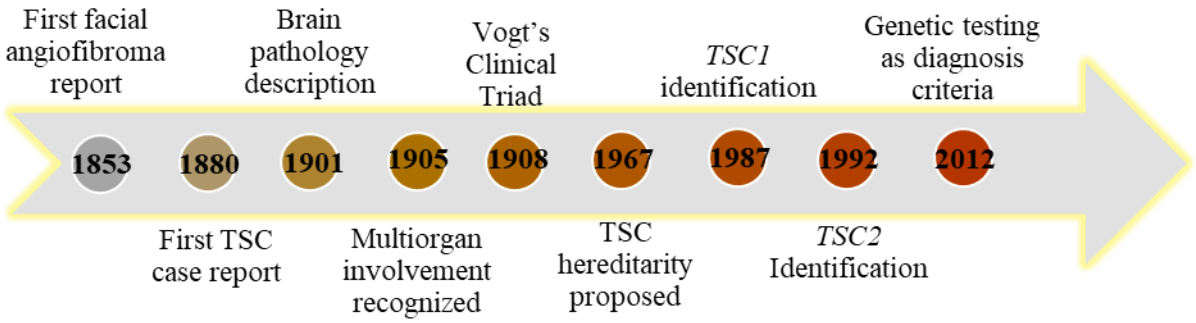

Figure 1.1: *The History of TSC*. Timeline with selected dates that contributed to the understanding of TSC and development of the diagnosis criteria. Please refer to the text body for the the corresponding references.

1.1.2 Diagnosis of TSC

Up until 1998, the diagnosis of TSC was purely based on clinical presentation. In 2012, these criteria were revised to include genetic criteria. A current definite diagnosis of TSC is possible if: (i) a pathogenic mutation is found in *TSC1* or *TSC2* or (ii) two major clinical features or (iii) one major and two minor or more clinical features are present[3]. Major and minor clinical features of TSC and their prevalence are presented in Table 1.1.

System	Manifestation	Prevalence	Diagnosis Criteria†
Brain	Subependymal nodules (SEN)	78.2 %[14]	M
	Subependymal giant cell astrocytoma (SEGA)	24.4 %[14]	M
	Cortical tubers and white matter abnormalities	70-90%[15]	M
Eye	Retinal hamartomas	40-50[16]	M
	Retinal achromic patch	12% [17]	m
Heart	Cardiac rhabdomyomas	60**%** [18]	M
Kidney	Angiomyolipoma	47.2 % [14]	M (≥2)
	Cysts	22.8 %[14]	m
	Renal cell carcinoma	2-4%[19]	NA
Liver	Liver angiomyolipoma	15 %[20]	NA
Lung	Lymphangioleiomyomatosis (LAM)	6.9 %[14]	M
	Multifocal micronodular pneumocyte hyperplasia	*Not available*[21]	NA
Skin	Hypomelanotic macules	66.8 %[14]	M (≥3, at least 5-mm diameter)
	Shagreen patches	27.4 %[14]	M
	Peri or subungual fibromas	16.7 %[14]	NA
	Facial angiofibromas	57.3 %[14]	M (≥3)
	Fibrous cephalic plaque	14.1 %[14]	
	Confetti lesions	8.6 %[14]	m
Nail	Ungual fibroma	20%[18]	M (≥2)
Mouth	Dental enamel Pits	90%[16]	m (≥3)
	Intraoral fibromas	69% [22]	m (≥2)
Behaviour	Intellectual disability	30%[15]	NA
	Attention deficit hyperactivity disorder	19.6 %[14]	NA
	Challenging behaviour	40-50%[15]	NA
	Mood, anxiety or depression disorders	20-50%[15]	NA
	Autism spectrum disorder	20.7 %[14]	NA
	Epilepsy	80-96%[15]	NA
	Infantile Spasm	38%[23]	NA

Table 1.1: *Pathological manifestations of Tuberous Sclerosis Complex*. Prevalence of different manifestations of TSC and their classification as diagnosis criteria. † M- Major feature, m- minor feature, NA- feature not included in the clinical diagnostic criteria.

Genetic testing was a major addition to the TSC diagnostic tools, as it allowed diagnosis of young patients who might not yet have developed the full phenotype or major clinical features. This enabled a better management of patients, as well as earlier medical intervention[24]. Additionally, genetic testing facilitated family planning, when one of the couple's members carried the disease[24]. For genetic testing purposes, a pathogenic mutation, defined as one that prevents protein synthesis or function[3], is expected to be detected by standard diagnostic techniques in 85% of patients[25]. The remaining 15% are classified as *no mutation identified* (NMI), explained later in this work, and diagnosis of these patients is primarily based on clinical criteria (Section 1.1.4.1).

A diagnosis of TSC can also be suspected with *in utero* examination, when cardiac rhabdomyomas are detected during a foetal ultrasound (US) examination. Diagnosis can be confirmed with foetal echocardiography[26,27]. Nonetheless, a definite case of TSC can only be assumed if either genetic testing is performed or if foetal cerebral MRI detects the presence of brain lesions. The latter was shown to occur in 49% of the cases[27].

1.1.3 Clinical manifestations of TSC

1.1.3.1 General considerations

The majority of TSC patients develop hamartomas in the brain, skin, heart and kidney[16,24,28], defined as "*a benign growth made up of an abnormal mixture of cells and tissues normally found in the area of the body where the growth occurs*"[29]. However, hamartoma development does not occur in all organs at the same time nor in equal number or severity. Some lesions are age-dependent and may be temporary. Cardiac rhabdomyomas, for example, are usually detected *in utero* but, although a main feature in foetuses and new-borns with TSC, complete remission is expected during childhood[16]. On the other hand, LAM, a progressive pulmonary disease that leads to severe respiratory insufficiency (OMIM 606690), is both age- and sex-dependent, mainly affecting premenopausal women and rarely present in men[16,30]. In fact, the most recent TOSCA (TuberOus SClerosis registry to increase disease Awareness) study, a systematization of the natural history and disease management of 2093 TSC patients, across 31 different countries[14], showed that although only 6.9% of their cohort had LAM, 94.4% of these were women[14]. Lesions can be non-progressive, as tubers, which remain relatively unchanged throughout an individual's lifespan. Whilst cell populations within tubers can undergo molecular modifications, namely increased apoptosis, the number and size of tubers remains constant[8,31,32]. Other lesions can increase or decrease in number, like the shagreen patches[16] or the previously mentioned cardiac rhabdomyomas, respectively. Progression of symptom severity can also occur, as it is the case with LAM or kidney

angiomyolipomas (AML), that can lead to retroperitoneal haemorrhage, chronic renal disease or renal failure[8,33].

In summary, patients with TSC develop lesions that can grow virtually anywhere in the body. However, the brain is one of the most critically affected organs. Tumour growth greatly impacts the quality of life (QoL) and autonomy of patients[34], and is correlated with significantly altered behaviour and neurological pathology[25,35]. As the brain is the main focus of this thesis, the central nervous system (CNS) pathology of TSC will now be described in more detail.

1.1.3.2 Tubers

More than 90% of TSC patients show changes in the CNS in the form of lesions (tubers, subependymal nodules or subependymal giant cell astrocytomas) or tuberous sclerosis- associated neuropsychiatric disorders (TAND)[18].

Tubers are the hallmark of TSC and are present in 82.2% of patients (Figure 1.2A)[14]. Tuber load can be highly variable, with a retrospective study indicating numbers between 5 and 50, averaging 18.8 tubers per patient[36,37]. Tubers can also have different sizes and one single patient can have tubers of multiple dimensions[25]. Although tubers do not grow nor increase in number post-natally, they can still undergo significant structural changes. A common modification is calcification, present in 37 to 46% of patients, and of higher incidence with age progression[38–41]. Mainly in the paediatric population, cyst-like structures can also develop within pre-existent tubers[40,41].

The exact origin of tubers is still uncertain. These structures seem to appear early in the embryonic period, with MRI detection reported as early as 19 weeks of gestation. These represent areas where neuronal migration failed to be properly completed and where the expression of early-stage neuronal migration markers is increased[26,32,42–44].

Macroscopically, tubers are sites of cortical dysplasia where the hexalaminar structure of a typical cortex is absent (Figure 1.2B)[18,45,46]. These are usually located in the frontal and parietal lobes in the interface between white and grey matter[32,47], in either hemisphere and in any cortical structure[31,36,38,48]. Additionally, a recent study comparing neuronal density in control, tuber and focal cortical dysplasia (FCD) tissue, reported general neuronal cell loss in tubers[44]. Microscopically, tubers contain three main types of cells: astrocytes, dysmorphic neurons (DNs) and giant cells (GCs) (Figure 1.2C-D)[39,46]. The number of astrocytes is increased by up to 3-fold in tuberal tissue, compared to nearby neocortex[49] and astrogliosis can be used as an indicator of the tuberal border, using markers for astrocytes such as glial fibrillary acidic protein (GFAP)[50]. DNs exhibit enlarged somas and aberrant dendrites, and are often mispositioned in the cortical layer organization[51]. GCs are specific to TSC and appear as single units or clumps of large cells with thickened processes. They exhibit a mixed phenotype, indicating not only a dysregulation of cell size control, but also of

differentiation[32,52]. GCs are immunoreactive for neuronal markers such as non-phosphorylated neurofilament SMI-311, but not NeuN as DNs, and for neuroglial progenitor markers, like vimentin[37,40,53]. Although DNs and GCs are common in TSC patients, their exact function and contribution to TSC pathology is still unknown. Electroencephalography (EEG) studies and electrophysiological recordings from dysplastic brain samples suggest that DNs may have abnormal firing properties which could lead to network defects and an epileptogenic phenotype. However, precise electrophysiological studies with DNs and GCs from TSC samples are still lacking[54–56].

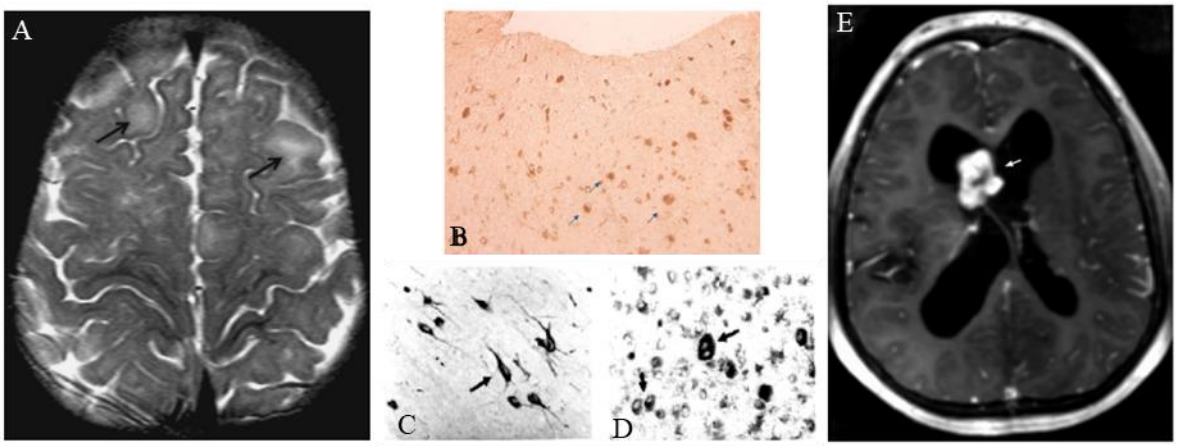

Figure 1.2: *Neurological manifestations in TSC*. Cortical tubers (A, arrows) are characterized by the lack of hexalaminar organization (B) and by the presence of dysplastic neurons (C) and giant cells (D), while SEGA can be found emerging from the ependyma into the ventricular compartments (E). Images reproduced and adapted from references 30, 37 and 174 with permission of Dr. Peter Crino and Dr. David Franz.

Historically, tubers are structures of great importance in TSC as they were considered from early on the focal origin of epileptic seizures[48]. Molecularly, this could be due to a hyperexcitable state of DN's, as these were shown to have increased transcripts and synthesis of AMPA and NMDA receptors[39,53,57,58]. Both DNs and GCs were also shown to have decreased transcripts of $GABA_A$ receptors, compared to control tissue, which could further potentiate an imbalance between excitatory and inhibitory networks[57]. Analysis of patient data corroborates the role of tubers in seizures. A high tuber load, regardless of tuber location, was positively associated with infantile spasms (IS)[36,48], with O'Callaghan and colleagues reporting a median of 20 tubers versus 8 in patients with and without history of IS, respectively[59]. Additionally, tuber burden appears to be inversely related to the age of seizure onset, an important determinant of neurocognitive outcome[36]. However, it is important to acknowledge that there are still patients without tubers that present with seizures, while others may have tubers and exhibit none[41].

The fact that some tuber-resected patients still exhibited seizures post-surgery led to the hypothesis that perituberal tissue could also have epileptogenic properties[60–62]. Major and colleagues reported a series of three clinical paediatric cases of tuber resection, with patients with intractable epilepsy and TSC. Upon intracranial electrocorticography (ECoG), tubers were found to be silent for epileptiform activity while the surrounding tissue presented with epileptogenic discharges[47]. Further studies on perituberal tissue revealed that, in addition to possible epileptogenic activity, this structure also exhibited abnormal cells. Although sparser compared to tubers, reactive astrocytes, that often but not always surrounded giant cells, and some dysmorphic neurons were also observed in the perituberal area[50,55,63].

1.1.3.3 SEN and SEGA

Subependymal nodules (SENs) are the second most common neurological manifestation in TSC, present in 78.2% of patients[14]. These are asymptomatic, potentially proliferative lesions, frequently located on the surface of the lateral or third ventricles[8,39,40]. SENs develop during gestation and can be detected *in utero* during the middle and final stages of foetal life[64,65]. SENs are usually benign and often undergo calcification[65,66]. In about 24% of patients, these lesions continue to grow postnatally and become subependymal giant cell astrocytomas (SEGA) (Figure 1.2E)[14,18,65]. Presently, it is challenging to predict if a SEN will grow into a SEGA, and monitoring lesions is the preferred course of action. After a TSC diagnosis, brain MRI, CT or US are performed every 1 to 3 years to detect and monitor these lesions. Serial imaging of SENs can inform about growth alterations and possible SEGA transformation, in which case frequency of examination should be increased[3,66]. Size-based conventions have also been used to aid the distinction between SENs and SEGAs. Lesions in the caudo-thalamic groove, with a diameter bigger than one centimetre, are commonly used parameters for identifying potentially proliferative lesions[65].

SEGAs can theoretically grow anywhere where SENs are present. However, because these can also be asymptomatic lesions, they are often detected only when symptoms arise. This is usually the case when SEGAs grow next to the foramina of Monro, narrow ducts that connect the third to the lateral ventricles. Obstructions to these areas can impede cerebrospinal fluid flow leading to the distention of the ventricular system, increased intracranial pressure and potentially abnormal head growth – a condition denominated hydrocephalus. Consequently, common symptoms of hydrocephalus include headaches, seizures, behavioural alterations, visual impairment and vomiting[67–69]. When left untreated, hydrocephalus is a life-threatening condition and a major cause of morbidity and mortality in the TSC population[23,70].

Histologically, SENs and SEGAs are difficult to distinguish as they exhibit similar cell types, namely fibrillated spindle cells, gemistocyte-like cells and giant cells (GC). Similarly to tubers, GCs are positive for both neuronal and glial markers, such as neuron specific enolase and

neural cell adhesion molecule, and GFAP, respectively[40,71–73]. GCs can be isolated but are more commonly found in clusters. In SEGAs specifically, they often exhibit a pseudorosette shape. Low mitosis levels, identified by the presence of mitotic nuclei and positive MIB-1 and cyclin D1 expression, and vascularization, detected by the presence of endothelial proliferation, are consistent with the slow and progressive growth of SEGAs[65,66,70,71,73].

Although it is commonly assumed that SEGAs derive from SENs, the mechanisms that originate these lesions are still under debate[65,74–76]. One of the reasons for this is the lack of SEN samples, as these are rarely a threat to patients and, therefore, not often resected[77]. When potential differences in pathway activation between these two lesions was investigated, hyperactivation of the mechanistic target of rapamycin (mTOR) pathway was confirmed in both SEN and SEGA samples, with increased expression of the mTOR downstream marker phosphorylated protein rpS6 (rpS6)[65,78,79]. Additionally, components of the protein kinase B (Akt) cascade, upstream of mTOR and that also receive feedback from the later, were also upregulated in both lesions, when compared with control brain tissue. These included phosphorylated phosphoinositide-dependent protein kinase 1 (pPDK1) (Ser241), pAkt (Ser473) and phosphorylated glycogen synthase kinase 3 beta (pGSK-3β) (Ser21/9). Interestingly, elements of the extracellular signal-regulated kinase (ERK) pathway, which also acts upstream of mTOR, were differentially upregulated. Specifically, pERK (Thr202/Tyr204) and phosphorylated mitogen-activated protein kinase kinase 1 and 2 (pMAP2K1 and pMAP2K2) (Ser221) were upregulated in all three SEGA samples, while the SEN sample had a similar expression to control tissue. The total amount of ERK was also increased in the SEN when compared to the control tissue. Although this study uses a small sample size, it does suggest that mechanisms additional to mTOR activation are required for the transformation of SEN into SEGA. Despite the need for more studies on SEGA development, the possible activation of secondary pathways is a critical theme for researchers in the TSC area as it may lead to the identification of potential new targets for therapies and treatments.

1.1.3.4 Epilepsy

Epilepsy is the most common neurologic symptom in TSC, present in 83.5% of patients[14], contrasting with its prevalence of 1% in general population[80]. Although all types of seizures can manifest, focal seizures are the most common in children often evolving across the lifespan into loss of awareness and generalized episodes, including tonic-clonic and myoclonic seizures[14,15,37,60]. The majority of TSC patients are diagnosed with epilepsy around the age of 3[14,23,35]. Early diagnosis, and treatment initiation, is critical as the age of onset of epilepsy is determinant for its prognosis. In a retrospective study, Chu-Shore and colleagues showed that, in their cohort of 291 TSC patients, 85.2% had had at least one seizure, and from these, 99.2% developed epilepsy later on[35]. Early seizure onset also impacted treatment outcome, as it was associated with an unfavourable

prognosis[64,81]. This relationship between age of onset and treatment outcome was present in the majority of patients, regardless of mutation type[82]. Seizure development also impacts cognition, with 60.9% of individuals with history of seizures being cognitively impaired. This contrasts with the 12.2% without a seizure record[35], suggesting that seizures are important contributors to cognitive decline. More recently, data from the TSC Autism Center of Excellence Network (TACERN), a multicentre prospective study, supported these findings revealing that early learning composite scores were worse for epileptic patients and declined over time, as opposed to non-epileptic patients[83]. Importantly, treatment-induced reduction in seizure frequency did not correlate with cognitive improvement. Instead, a significant improvement was only seen in patients who achieved complete seizure remission[83], defined by the ILAE as the absence of seizures of any type for at least 12 months[84,85]. This once again alerted for the importance of patient assessment and for the prescription of appropriate pharmacological treatment as soon as seizures are detected.

IS, also referred to as West Syndrome, are particularly relevant to the TSC paediatric population[86,87]. This is an extremely rare condition in the general population affecting 0.03% of children[86,87], but common in TSC affecting 38.8% of patients[14,23,35,37,82,87]. IS develop between the ages of 4 and 8 months, with a peak at 6 months of age, and are manifested by spasms of the upper body, or limb extensions, and hypsarrythmia on EEG[81,86–88]. These are a severe neurological manifestation as age of seizure onset impacts prognosis and is positively correlated with the development of treatment-resistant seizures[82]. In fact, it is estimated that between one to two thirds of TSC patients develop drug-resistant (refractory) epilepsy, defined by the International League Against Epilepsy (ILAE) as the "*failure of adequate trials of two tolerated and appropriately chosen and used AED schedules (whether as monotherapies or in combination) to achieve sustained seizure freedom*"[35,89–91]. In a study by Chu-Shore and colleagues, from 110 IS patients 94% exhibited seizures later in life. 75.4% of these went on to develop refractory epilepsy, whilst this was only present in 39.8% of the patients without IS history[35]. In another TSC cohort, patients who had not received treatment for IS or achieved seizure remission were strongly associated with the likelihood of drug-resistant focal epilepsy later in life[82]. Nonetheless, this study did find a high success rate of IS treatment, mainly with vigabatrin administration, with 63.3% of treated patients achieving seizure remission. This supports data from the TOSCA study where, from the 78.3% of patients receiving vigabatrin for IS, 71.5% achieved seizure control[14]. These highly relevant clinical results reinforce the need for a rapid treatment initiation after IS diagnosis.

1.1.3.5 Behaviour and Cognition

The neurological manifestations present in TSC patients contribute in various degrees to TSC-associated neuropsychiatric disorders (TAND). TAND can be highly heterogenous amongst individuals but they are present in up to half of the TSC patients[18,92–94]. TAND burden typically

change with age. For example, cognitive concerns are predominant in paediatric populations whilst depression is a major concern in adults[34]. Additionally, access to appropriate and TSC-specific health care facilities, as well as the presence of other comorbidities and response to treatment, also influence the impact of TAND on QoL[95].

Both paediatric and adult TSC patients report cognitive, depression, anxiety and autism spectrum disorders (ASD) symptoms as some of their major neuropsychiatric concerns[14,34,96] (Table 1.1). In a postal survey conducted in the UK, with 265 answered questionnaires from children and adolescents with TSC, de Vries and colleagues reported a 40% rate of anxiety in individuals and depressed mood in 23%. Aggressive outbursts were present in 58% of responders, cognitive disability in 64% and ASD in 48% of patients[97]. In a USA-based population, results were similar. 27% of patients had symptoms of anxiety, 27% mood disorders and 28% showed aggressive or disruptive behaviour. ASD prevalence was reported at 36% and cognitive impairment was present in 49% of patients[96]. In a wider TSC population survey, anxiety was reported in 13.7% of patients, depressive mood in 8.3%, severe aggression in 10.8% and ASD in 20.7%. Mild to profound intellectual disability was also detected in 54.9% of patients upon evaluation with intelligent quotient (IQ)-type studies and physician assessments[14].

As a whole, the diagnosis of anxiety disorders is present in up to half of TSC patients, with data indicating an age-dependent increase in prevalence[96–98]. Specific analysis of the TAND component of the TOSCA registry revealed that the prevalence of anxiety disorders was of 5.6% in TSC patients under the age of 2, of 34.2% in patients between the ages of 14 and 18, and of 72% in patients older than 40[98]. Contrastingly, epidemiological studies in general population report the presence of anxiety disorders in 10 to 34% of individuals[99]. These numbers reveal that anxiety disorders are a TSC comorbidity affecting a great number of individuals and that its presence and treatment should also be addressed when searching for novel therapeutic options.

TSC is the second biggest monogenic cause of ASD, preceded only by Fragile X Syndrome[37,100,101]. The prevalence of ASD in TSC has been reported to be between 20-40%[14,96,97,102,103], which greatly contrasts with the observed prevalence in the general population of 0.5-2%[104–107]. According to the NIH definition, ASD is "*a group of developmental disorders. ASD includes a wide range, "a spectrum," of symptoms, skills, and levels of disability*"[108]. These symptoms, according to the latest edition of the manual from the American Psychiatric Association's Diagnostic and Statistical Manual of Mental Disorders (DSM-5), can be grouped into two main categories: (1) deficits in social communication and interaction, which include problems in social-emotional reciprocity, nonverbal communicative behaviours, and developing, maintaining and understanding relationships; and (2) restricted and repetitive behaviour and interests, which comprises stereotyped actions, inflexibility to change and hyper- or hyposensitivity to sensory input[109].

In general population, ASD is typically diagnosed at the age of 4, although parental concerns have been reported by 2 years of age[110,111]. In fact, Richards and colleagues showed that, in a survey of 471 children with developmental delays aged 18 to 24 months, parents with behavioural concerns were significantly more likely to receive a diagnosis of ASD based on ADOS scores[111]. In this cohort, of the 93.4% of parents who revealed concerns about their child's development, particularly in the field of speech and communication, 94.4% later received a diagnosis of ASD for their child[111]. In TSC, ASD tends to be detected earlier, at around 3 years of age[112]. Nonetheless, prospective studies have detected atypical communication features as early as 6 months old[113] and altered cognitive abilities by the age of 9 months[112]. Earlier diagnoses likely represents the nature of TSC which is not only a known risk factor for autism and cognitive deficits but also possible to diagnose *in utero*[114]. This in turn provides an opportunity for earlier diagnosis of ASD, that could potentially lead to support therapy initiation during critical developmental periods[112,113,115].

Another peculiarity of the TSC-ASD population, besides age of diagnosis, is its gender distribution. While the distribution of ASD in general population is around 4 boys to 1 girl, across the full IQ range, it has a 1:1 prevalence in TSC[37,104,116–119]. However, this gender bias has been increasingly questioned and might actually be a consequence of the regular neuropsychiatric monitoring TSC patients receive. It has been proposed that non-TSC females are underdiagnosed with ASD because they exhibit a less visible phenotype, including anxiety and depression symptoms. On the other hand, males exhibit a more external phenotype with aggression and hyperactivity behaviours which draw more attention from carers and teachers[104,119].

A number of studies have now focused on understanding possible differences between syndromic TSC-ASD and non-syndromic ASD (nsASD) populations, and if their features could be used to define more adequate therapy schedules. Jeste and colleagues analysed a cohort of 82 nsASD, 18 TSC-ASD and 18 TSC-no ASD patients, with mean ages from 29.2 to 34.6 months. Here, no significant differences in cognition were found between the TSC-ASD and nsASD groups, assessed with the Mullen Scales of Early Learning (MSEL) test, whilst both the typically developing (TD) and the TSC-no ASD groups presented with higher cognition scores[115]. Additionally, ADOS scores clustered TSC-ASD with the nsASD group, and TD with the TSC-no ASD group. This was observed despite the similar epilepsy profile of the TSC-no ASD and the TSC-ASD groups, indicating that at this age epilepsy might not contribute substantially to the development of some ASD-like behaviours[115]. However, in an older TSC cohort (average 9.9 to 10.2 years old), Numis and colleagues showed that age of seizure onset, seizure frequency, and interictal but not ictal epileptiform activity on EEG, were all significantly associated with ASD symptomatology[116].

In another study, Jeste and colleagues followed longitudinally a TSC population of 3 to 36-month-olds[113]. They found that, as a whole, the TSC group showed developmental delays at all ages compared to the TD group. Furthermore, specific domains like fine motor skills, visual reception

and behavioural interaction were affected by the age of 6 months, with all other domains (gross motor, receptive language and expressive language skills) affected by 9 months of age. Comparing the TSC-ASD with the TSC-no ASD groups at 12 months, the former exhibited lower scores in the visual reception, fine motor, expressive language and receptive language parameters. From 12 to 36 months, the trajectories of developmental quotient, nonverbal IQ and verbal IQ were also different in both groups, with TSC-ASD showing no improvement, or even a decline, as opposed to the TSC-no ASD group[113]. Although it was expected that the TSC-ASD group presented itself with cognitive and behavioural changes compared to the TSC-no ASD group, this study emphasises that the diagnosis of TSC itself modifies behavioural and cognitive gain during infantile development. This highlights the importance of initiating therapeutic interventions at early developmental time points, in order to improve some ASD-related symptoms[120]. Furthermore, although studies focusing on different possible types of ASD, especially with respect to TSC, are still scarce, evidence points towards a common mechanism of development, and that further differences between groups, regarding communication, learning and behaviour, might be potentiated later in life due to other contributing factors such as epilepsy.

Although the exact causes of autism are still unknown, considerable work has been done in the search for specific brain areas or molecular markers involved in autism[100,121–123]. One of the brain areas that has been commonly reported to be altered in ASD patients is the cerebellum, although conflicting results have been described[106,124–127]. Functional measurements with diffusion weighted MRI tractography in fifteen 3-13 year old children have suggested reduced functional connectivity between PC and the cerebellar dentate nuclei, supporting the presence of white matter changes in ASD[128]. MRI studies have also shown reduced cerebellar volume in ASD patients[122,129], while Levitt and colleagues found this difference only in low IQ individuals[129]. In a meta-analysis of paediatric population studies, grey matter volume in the cerebellum was also reduced[130]. However, others have found no alterations regarding cerebellar size[121,131,132]. Post-mortem studies with ASD brains from children, young adults and adult cerebelli have repeatedly shown a decrease in the number of Purkinje cells (PC) compared to control brain tissue[124,125,133–135], and the cross-sectional area of these cells has also been reported to be smaller in ASD brains[136]. Nonetheless, other cells from the cerebellum, namely basket cells and stellate cells, do not seem to be altered[137]. Structure-focused studies have reported area reductions in the vermal[138] and right crus I/II areas[139], while there is also evidence for increased volume in the vermis VIIIA and B areas[139]. ASD has been proposed as a neurodevelopmental dysfunction where imbalances in central excitation and inhibition contribute to altered behaviour[140]. Indeed, evidence suggests specific changes to GABA system components in ASD[105,124]. Specifically, GAD 65 and 67 proteins[141–143], as well as GABA receptor subunits mRNA and protein, were decreased in ASD cerebelli[136,144,145]. Levels of parvalbumin mRNA, a calcium binding protein abundant in the cerebellum, were also decreased[146]. Although highly relevant, post-mortem studies have their own limitations. First, due to the scarcity

of samples, it is difficult to match brains in relation to age and comorbidities which introduces significant variability into the studies; and second, samples are not always preserved using standard guidelines which impacts the quality of tissue and outcome of experiments and analysis[105,124]. Overall, post-mortem studies are invaluable to our understanding of ASD, but more and larger cohort studies are necessary to better understand which alterations are consistent across patients.

In the case of TSC, there is some evidence for the role of the cerebellum in ASD pathology. Weber and colleagues analysed MRI and behavioural data from 29 TSC patients, from prenatal to 9 years old. Although no association was found between the Childhood Autism Rating Scale (CARS) scores and the total number or location of cortical tubers, children with a higher cerebellar tuber load did exhibit higher CARS scores. Similar results were found when the Vineland Adaptive Behavior Composite (ABC) scores were considered[147]. Another paediatric study with 78 TSC patients revealed analogous results, with patients with cerebellar lesions exhibiting higher autistic symptomatology scores than those without any cerebellar tubers[148]. Finally, in a study by Sundberg and colleagues, brain tissue from TSC patients with and without ASD, was used to generate human induced pluripotent stem cells. After differentiation into Purkinje cells, electrophysiological characterization revealed that cell lines from TSC-ASD patients had an hypoexcitability response compared to the ones from the TSC-no ASD group[149]. In sum, although considerable work is still required to properly address the role of the cerebellum in TSC-ASD, available evidence indicates the possibility of disease-specific alterations that may contribute to a specific ASD phenotype in TSC.

Despite the importance of ASD and TAND in general, and of their contribution to decreased QoL, a study conducted in 2010 revealed that only 18% of patients received active treatment or therapy for their TAND[18,93,95,150]. In an attempt to improve access to treatment, the neuropsychiatric panel of the International Consensus Conference for TSC created a "TAND checklist", aiming at compiling main psychological and social concerns and facilitating treatment prioritization[150]. Although this checklist is easy and accessible to use, the TOSCA study revealed that, by 2017, a considerable number of patients were still lacking TAND assessments. Only 39.2% of TSC patients had received an IQ-type test and data on behavioural and psychiatric disorders was missing in 25.5 to 38.2% of patients[14].

One of the reasons for lack of diagnosis and consequent delay in initiating treatment regimens for TAND is their uniqueness; symptoms are distinct and specific for each patient, requiring individual care and attention. Looking to facilitate patient treatment and promote an earlier detection of TAND, Leclezio and colleagues studied the possibility of grouping TAND features in clusters. Using TAND checklist answers from 56 patients, cluster analysis was conducted on 29 different parameters selected from the checklist. This analysis identified the presence of 6 natural TAND clusters: "Behavioural dysregulation", "Mood/mixed", "ASD-like", "Hyperactive/impulsive", "Neuropsychological" and "Scholastic"[95]. Although the first of its kind,

this study suggested the possibility of patient grouping into specific TAND categories. Clinically, this could enable the creation of TAND therapy "starter packs" allowing for rapid treatment initiation and *a posteriori* adaptations according to individual progression.

In addition to the burden of TAND on patients themselves, and their contribution to disease morbidity, TAND also have a considerable economical impact[34]. A survey of 676 TSC patients and carers revealed that 99% of children and 98% of adults had been to the doctor at least once in the past year and that 37% of children and adults were hospitalized for 5.2 days, on average, during this same period[34]. In countries where health care is not readily available or affordable, this could have a determining impact on access to treatment. In addition, doctor visits often include changes in medication, especially given that this is a highly refractory epileptic population[151]. In fact, the economic costs of epileptic TSC patients can be more than 3-fold that of the general population when there is also associated epilepsy[152]. Taken together, this reveals a major unmet medical need in relation to TAND that requires not only more medical attention but also new support measures.

1.1.4 Management of CNS manifestations in TSC

As previously described, TSC is a multiorgan pathology that can affect different biological systems in distinct manners. However, CNS involvement is predominant in TSC patients, with seizures, tumour growth and TAND being highly prevalent in these individuals. As the brain is the main focus of this thesis, further attention will be given to the available therapeutic options for the management of neurological and neuropsychiatric symptoms in TSC.

1.1.4.1 Anti-epileptic drugs

Intractable epilepsy, which affects 20 to 30% of the epileptic population[151,153,154], is present in around 85% of patients with TSC[14,35,60,82]. Consequently, even though epilepsy management begins following prescription guidelines, patients often require add-on treatments, including surgery, to attempt seizure control. Carbamazepine, valproate and lamotrigine are commonly used drugs, but therapy prescription greatly depends on the type of seizures exhibited by the patient and on the response to treatment itself[3,81,155]. In the case of IS, the first-line treatment is vigabatrin. This can, and is advised, to be used in very young patients including under 2 years of age[3,80,155]. Nonetheless, the use of vigabatrin has increased over the years and is now prescribed to older children and adults as long as seizure remission persists[80,156]. In fact, the most recent TOSCA study revealed that vigabatrin was prescribed to 78.3% of patients receiving any pharmacological treatment for IS, but also in 65.1% of the patients with focal seizures[14].

It is important to acknowledge that although vigabatrin is the advised first-line treatment in TSC IS, in centres and hospitals that do not specialize in TSC, prescription of this drug is often

avoided due to vigabatrin-associated visual field loss (VAVFL). While initial reports of VAVFL were highly variable, with small studies reporting anything from 9% to 92% of patients affected[80,81,157,158], a Cochrane review including data from 755 patients, although none of these with TSC, reported an increased rate of visual abnormalities in vigabatrin-treated groups that was not statistically significant[156]. Therefore, although more studies are needed regarding the risk of VAVFL in TSC, it is clear that the benefit from achieving seizure control especially when these begin at very young ages supports the risk of vigabatrin use in paediatric and older TSC populations[155].

Interestingly, despite the effect of vigabatrin in TSC, in the NICE guidelines for the pharmacological treatment of epilepsy this is either a third option or not even recommended for other types of epilepsy, as it has been shown to be less effective in inducing seizure freedom than other approved AED[159–161]. Considering specifically the paediatric population, vigabatrin seems to be particularly effective. In a cohort of 103 epileptic patients, median 8 months old, a first follow-up after approximately 1.6 months of vigabatrin therapy revealed a 24.2% rate of seizure freedom, increasing to 37.5% in the last follow-up appointment at 12.1 months[162]. Furthermore, although seizure freedom was not related to seizure aetiology, patients with TSC revealed a higher reduction in seizure frequency when compared to other seizure causes[162]. Another study also suggested that vigabatrin could be particularly effective in TSC. In this retrospective study, from the 84 paediatric patients treated for IS with vigabatrin, half became spasm free. From these, 82% had TSC while only 37% had TSC in the non-responder group. However, regarding 59 patients that were also being treated for partial seizures with vigabatrin as an add-on therapy, aetiology did not seem to impact the response rate[163].

The reason why vigabatrin seems to be particularly effective in TSC may be due to its proposed mechanism of action. Primarily, vigabatrin is known to irreversibly inhibit GABA transaminase. This increases GABA brain levels, potentiating inhibitory transmission and decreasing neuronal excitation[156,157,164]. An additional secondary mechanism of action was proposed by Zhang and colleagues, using the $Tsc1^{GFAP}CKO$ mouse model[153]. Upon vigabatrin treatment, an expected reduction in seizure frequency was seen with video-EEG. However, in brain and cultured astrocytes from treated mice, a reduction in phosphorylated rpS6 to total rpS6 ratio, a readout of mTOR activity, was observed. This effect seemed to be specific of vigabatrin as phenobarbital, a different AED, had no effect on rpS6 phosphorylation levels[153,165]. This study highlights that vigabatrin could provide treatment of seizures associated with mTORopathies and merits further investigation.

When no improvement with vigabatrin is seen, or if this drug is unavailable, steroidal drugs such as adrenocorticotropin hormone (ACTH) are usually the second-line treatment for TSC-associated IS[3,80,81]. This is rarely used for seizures in adult patients[14,166]. Regarding other seizure types, treatment follows the standard AED prescription guidelines[166].

1.1.4.2 mTOR inhibitors

Given the overactivation of the mTOR pathway caused by *TSC* mutations, the study of mTOR inhibitors as a potential therapy for TSC manifestations was always of interest. Indeed, these compounds have shown promising effects in both *in vitro* and *in vivo* studies in addressing distinct pathological features of TSC, which ultimately led to its approval for clinical use[167,168]. Currently, the 2012 Consensus guidelines for the management of TSC comprehend the use of mTOR inhibitors in patients with AML, asymptomatic and with a diameter larger than 3 cm, to prevent or delay renal damage. Moreover, mTOR inhibitors are also advised for patients with fast progressing LAM and were shown to aid the preservation of pulmonary function[3].

Regarding the CNS, the use of mTOR inhibitors is recommended for the management of SEGA when these are asymptomatic or when resective surgery is not feasible[3]. As mentioned before, one of the most significant issues with the presence of SEGA is its contribution to hydrocephalus and, in these cases, surgical resection is still the first-line treatment. Although this procedure has a good prognosis, the management of SEGA with mTOR inhibitors is now increasing[67,70]. For example, the EXIST-1 trial examined the effect of the mTOR inhibitor Everolimus in long-term SEGA management. In this prospective, double-blind, placebo-controlled trial, a cohort of 111 patients was followed over the course of 4 years and, of these, 58% responded to therapy. These exhibited a median reduction in total SEGA volume between -38% and -54%, over the treatment period[169]. Although a potentially good non-invasive alternative to surgery, careful consideration should be made regarding the use of mTOR inhibitors as SEGA regrowth, although rare, has been associated with therapy cessation[66,170].

More recently, the use of mTOR inhibitors for seizure control has also been proposed. Initial indications of this effect were based on data from animal models of TSC and other epileptic syndromes[81,154,155,171]. The exact mechanism by which mTOR inhibitors may reduce seizures is still unkown[172]. However, the biological functions of this kinase suggest how its inhibition could potentially have beneficial effects on seizures.

mTOR is involved in the control of cell division, growth and migration, and synaptic modulation[173–175]. In cases where mTOR overactivation is present, common CNS findings include hippocampal and cortical disorganization and hypertrophy[171,176], and increased inflammatory mediators and astrogliosis[153,171,176]. Moreover, mTOR was shown to regulate synaptic processes, such as local protein synthesis in dendrites[174,177], and the expression and function of neurotransmitter transporters, such as GLT-1 and GLAST, voltage-gated ion channels, as Kiv1.1, and ionotropic glutamate receptors, like AMPAR and NMDAR[171,176,178–181]. As these processes and proteins have all been implicated in epileptogenesis, this sets the rationale for trials using mTOR inhibitors for seizure control in TSC patients.

When clinical studies with Everolimus started, their primary outcome measure was SEGA size. However, seizure reduction was also reported in some patients[182,183]. In 2013, Krueger and colleagues published the first prospective study specifically aimed at analysing the effect of Everolimus in TSC-related epilepsy. In this study, 20 patients with a median age of 8 years old and refractory epilepsy were followed for 16 weeks. 75% of patients reported an overall 73% decrease in seizure frequency, with vEEG findings supporting reduced seizure frequency and duration in 17 patients. In this study, Everolimus was also reported to improve questionnaire-assessed QoL parameters such as "Attention and concentration", "Behaviour", "Social interaction" and "Social activities". In addition, specific positive behaviours (*Adaptive social*) were improved, while negative ones (*Conduct problem* and *Insecure/anxious*) were reduced[172]. A different cohort of 7 children with TSC and intractable epilepsy were treated with Everolimus for 36 weeks by Wiegand and colleagues. 4 out of the 7 children had a reduction in the mean number of daily seizures and 3 out of 7 had an increase in the percentage of seizure-free days compared to baseline values[184]. Of note, the two patients that did not exhibit an improvement in seizure presentation also lacked increased seizure-free days, suggesting that these two patients could represent a population less responsive to mTOR inhibitors. In another small open-label trial, Cardamone and colleagues monitored Sirolimus (rapamycin) treatment for varying periods of time (6 to 36 months). While one patient did not improve seizure frequency, all other 6 reported decreases in the number of seizures. Two patients reported to be seizure free for 6 months and one for 12. Parent-reported improvements on communication and social skills were also observed[185]. Altogether, these clinical studies suggested that mTOR inhibitors could improve the seizure profile of TSC patients.

To address possible long-term effects of Everolimus, Krueger and colleagues followed-up on 18 of their previous 20 patients, after 4 years treatment[186]. During this time, 3 patients left the study due to lack of efficacy and 1 due to withdrawn consent. For the remainder, response to Everolimus was overall positive. For patients who had previously shown a favourable response (*more than 50% seizure reduction*), a 75% to 93% overall seizure reduction was observed, depending on the analysed time-point. For partial responders, there was a 6 to 13% seizure reduction, although this value was reduced to 0% of baseline during the last time-point analysed (48 months). Therefore, for a percentage of patients that initially demonstrated a small response to Everolimus, this was no longer present after 48 months of treatment. Additionally, while the 2013 study had reported statistically significant improvements in several qualitative behaviour and QoL parameters, this significance was not achieved at the 48-month follow-up. Overall, this study suggests that while Everolimus appears to be an initially good therapeutic option for TSC patients with epilepsy, sustained effects after long treatment periods might not be observed. Molecularly, this reduction in mTOR inhibitor effect after long-term exposure may be due to the establishment of negative feedback loops that promote Akt stimulation[187].

So far, at least one patient was reported to wean off AEDs and maintain seizure control solely with Everolimus[186]. On the other hand, cessation of mTOR inhibitors, as mentioned before regarding SEGA, has also been associated with seizure relapse[155,188,189]. This suggests the need for continuous mTOR inhibitor treatment in order to sustain seizure control. However, although the described studies imply a good seizure and behaviour profile of mTOR inhibitors, the assessment of their effects is also limited by sample size. This prevents the evaluation of the contribution of parameters such as age and type of seizure to the overall therapy effect. Additionally, as open-label trials, mTOR inhibitors were used as add-on therapies. Therefore, the impact of the primary AED to the final outcome should also be taken into account. Another limitation of these mTOR inhibitor/seizure studies is that they often assess patients with SEGAs. Therefore, SEGA growth and its contribution to seizures should also be considered. In conclusion, larger multi-centre studies are necessary to: (1) build better controlled samples, (2) fully clarify the role of mTOR inhibitors in seizure control, and (3) understand if their use outweighs possible side or long-term effects. Nonetheless, although mTOR inhibitors do not seem to be a cure for intractable seizures in TSC, having another pharmacological option available for seizure control is always a welcome contribution.

1.1.4.3 Resective surgery

As previously mentioned, brain surgery is advised in TSC patients with symptomatic or fast-growing SEGA, where the risk of hydrocephalus is high. The total removal of the SEGA mass is determinant for a positive surgical outcome, as regrowth has been reported in patients where complete removal was not achieved[190,191]. Resective brain surgery is also a treatment option for patients that do not respond to AED and in whom it is possible to identify one or more clearly defined epileptogenic foci. These are usually associated with the presence of cortical tubers[62,81,192,193]. Patients with generalized discharges, high frequency of seizures or multiple foci are usually considered unsuitable surgical candidates[47,62,194,195]. Resective surgery promotes complete seizure remission in 57-75% of patients[18,55,196]. In the remainder, it also allows a reduction in the number of AED necessary for seizure control, a factor shown to increase QoL in epilepsy patients[47,81,197–199].

However, despite the relatively successful rate of resective surgery in managing selected SEGA and intractability cases, the procedure itself is highly invasive. Additionally, pre- and post-operative examinations present with elevated financial costs for both institutions and patients, which can limit surgery availability depending on health care system and country[62,200,201]. Furthermore, resective surgery is not without risks. In a cohort of 37 patients who underwent resective surgery, Arya and colleagues reported a 13.5% incidence of postoperative complications in TSC patients, all transient and usually involving infection[202]. The rate of complications in TSC patients undergoing

resective surgery is similar to the rate observed in the general population, with a similar trend found in respect to mortality as well. This is estimated to be up to 2% with permanent sequelae associated with the resected brain area of up to 10%[194,202–204].

1.1.5 TSC genetics and epidemiology

As seen so far, TSC affects many organs and systems with different degrees of severity. To a certain extent, the type of mutation present and the gene affected (*TSC1* or *2*) account for this variability. However, considerable data is missing on the relationship between the genotype and the phenotype of TSC patients. Before discussing the molecular pathways altered due to TSC mutations (Section 1.1.5), this section will present an overview of disease inheritance and how distinct mutations contribute to such vast phenotypical heterogeneity.

1.1.5.1 Types of mutations

The incidence of TSC is of approximately 1:6000[15] people, classifying it as a rare disease according to both the European Medicines Agency (EMA) (*5:10 000*) and the Food and Drugs Administration (FDA) (*less than 200 000 people in the United States*) definitions.

Mutations in the *TSC1* or the *TSC2* genes can be organized in two main groups: spontaneous mutations, or *de novo,* are present in 60-70% of patients and arise from an error in DNA replication that was propagated during development[60,205,206]. Mutations can also be inherited, or *familial*, present in 20-30% of TSC patients, and transmitted through generations of the same family[60,205,206]. In the case of spontaneous mutations, the parents of the new-born with TSC will not exhibit mutations in their *TSC* genes while, in the second case, one of the parents will be the carrier of the mutated allele. Mutations in the *TSC2* gene have a higher prevalence among mutation-diagnosed patients (83%) and also occur more often as *de novo* mutations[35,207,208].

Around 20% of the total number of TSC patients meet the clinical diagnosis criteria but belong to a third genetic group denominated *no-mutation-identified* (NMI)[35,41,96]. In these patients, although genetic testing has been conducted, no pathogenic mutations were detected in neither the *TSC1* nor the *TSC2* genes. The absence of genetic findings in the NMI group led to the hypothesis that a third TSC gene might exist[60,207]. However, this is now thought to be an unlikely hypothesis and that technical limitations are the most likely reason for the lack of mutation identification[28,209]. The most readily available method to detect TSC mutations is the exon-based Sanger sequencing method. However, if mutations are present in non-coding sequences (introns) or exist only in specific populations of somatic cells (i.e. when mosaicism occurs[210]), conventional diagnosis methods will not easily detect these mutations[211,212]. With the increasing availability of next-generation sequencing (NGS), mutation detection is less limited by technical methodology. In 2015,

Tyburczy and colleagues showed that, by using NGS in saliva and blood samples of 53 TSC patients previously classified as NMI, genetic diagnosis was increased by 85%. In this cohort, a 58% rate of mosaicism was present while 40% of patients were carriers of intronic mutations[213].

With the increased availability of genetic testing, predicting a patient's phenotype based on mutation became one of the goals of TSC research. However, the high number of reported *TSC1* and *TSC2* mutations made this task a difficult one to address. In the LOVD (Leiden Open Variation TSC database), 3212 different mutations were reported for the *TSC1* gene and 7456 were reported for *TSC2*. The two most mutated exons are also the largest ones of each protein, exons 15 and 33, respectively[28]. However, no preferential mutation sites, also called *hotspots*, have been found so far[23].

All types of mutations have been reported for *TSC1* and *2* including rearrangements, deletions and insertions, the outcome of which includes both missense and nonsense mutations[23,28,35,41,206,207]. In general, mutations that originate truncated proteins, hence inactive or highly limited in function, induce a more severe phenotype. On the other hand, missense and small in-frame mutations originate milder phenotypes as their product, although a dysfunctional protein that is rapidly degraded, still exhibits some residual function minimizing the effect of the genetic mutation[214]. Of note, genetic modifications of greater impact such as rearrangements and large deletions, are more frequent in the *TSC2* gene. This is likely due to the higher number of splicing events occurring in *TSC2* which increase the probability of genetic error[215]. The genetic severity of *TSC2* mutations also predicts increased disease burden of these patients when compared to the *TSC1* group[23,216].

1.1.5.2 Genotype-Phenotype relationship

In 1999, the first comprehensive study looking at the relationship of specific TSC mutations with phenotypic presentation was published[206]. In a cohort of 150 patients, intellectual disability was reported in 57% of the individuals, 67% of these carriers of a *TSC2* mutation[206]. In a larger, more recent study, van Eeghen and colleagues analysed the IQ (or developmental quotient (DQ), when appropriate) of 377 TSC patients. The total mean IQ was scored at 71.1, but when split by mutation, scores of 83 for *TSC1*- and 64 for *TSC2*-mutation carriers were observed. Additionally, intellectual disability was present in 23% and 57% of *TSC1* and *TSC2* mutation carriers, respectively[214]. In patients with *TSC1* mutations, alterations in the tuberin-interacting domain of hamartin led to lower mean IQ when compared to all other *TSC1* mutations (66 vs 83). Conversely, for *TSC2*, the lowest mean IQ was also present in patients with a mutation in the hamartin-interacting domain of tuberin (51 vs 64). Interestingly, this mean IQ was lower than the mean IQ of patients with mutations in tuberin's functional GAP domain[214], suggesting that the interaction between hamartin and tuberin, and not only tuberin's enzymatic function, was crucial for the correct

function of the complex. *TSC2* mutated patients exhibited a much higher prevalence of IS (1% for *TSC1* mutations vs 59% for *TSC2* mutations)[214], a relationship that has now been found in several other studies[35,91,217]. In fact, *TSC2* mutations were associated with a higher risk of epilepsy development, in particular when this form of childhood seizures had been present before[35,218,219]. In accordance, history of IS contributed for cognitive impairment in 74% of patients, while only 39% with no seizure history were cognitively impaired[35]. Importantly, IS are also a major predictor of AED resistance. 75.4% of patients with IS develop intractable seizures contrasting with a 39.8% rate of resistance in patients without IS[35].

In another study, Sancak and colleagues identified 60% of TSC patients with intellectual disability, 98% of these with epilepsy. This contrasted with the 59% rate of epilepsy in patients of normal IQ[216]. Intellectual disability was also more prevalent in patients with a *TSC2* mutation (49% for *TSC1* vs 83% for *TSC2*)[216]. Additionally, lower IQ was found to be inversely related to tuber load[36,220].

While there are reports of non-significant differences regarding tuber load between *TSC1* and *TSC2* patients[216], others have identified higher tuber counts in *TSC2* patients[23,207,221]. Moreover, cyst-like tubers, a type of tuber associated with increased seizure incidence, are also more prevalent in *TSC2* patients[41]. Similarly, studies have also reported a higher frequency of SEN and SEGA in *TSC2* patients[23,207,219,221].

Regarding ASD, although still a relatively new field in TSC research, studies so far seem to suggest a higher prevalence of ASD in patients with *TSC2* mutations, compared with *TSC1*[115–117]. Nonetheless, a recent study from Capal and colleagues reported that, in their cohort of 77 individuals, mutation did not correlate with the presence of ASD or the performance in the ADOS, although a higher incidence of neuropsychiatric disfunction in *TSC2* patients predicted an increased risk of neurological pathology[110].

Altogether, *TSC2* mutations predict a more severe phenotype compared to the one observed in *TSC1* or NMI patients. However, it is clear that mutation is not the sole contributor to TSC pathology. Other aspects, such as the loss of heterozygosity discussed in the next section, can contribute to the development of a complex disease profile.

1.1.5.3 Loss of heterozygosity

A classic feature of TSC is the phenotypical variability present across patients. In fact, even intrafamilial cases of TSC can show distinct symptomatology[208,222]. As an example, Lyczkowski and colleagues, in a study of 5 families with TSC, reported one pair of monozygotic twins that presented with similar peripheral manifestations, such as cardiac rhabdomyomas and renal angiomyolipomas, but exhibited very distinct neurocognitive profiles. In fact, while one of the twins

required resective surgery to attempt seizure control, the other had only recorded three episodes of febrile seizures[220].

One explanation for these differences is the Knudson, or two-hit, hypothesis. In specific types of cancer, such as retinoblastoma, loss of heterozygosity (LOH), the loss of the only functional or normal existing allele in tumour suppressor genes, is necessary for tumorigenesis to occur. In LOH, an individual who already has a higher predisposition for cancer development (first-hit), undergoes an additional mutation (second-hit), losing its only functional gene. Homozygosity for the tumour-prone genotype occurs and tumorigenesis progresses[223]. If this second-hit mutation was essential for the development of a TSC phenotype, that would explain why some patients present with a more aggressive disease progression than others: these would be the ones who underwent a second mutation in their functional *TSC1* or *TSC2* gene, in addition to the germline mutation already carried[208].

Supporting the second-hit hypothesis, LOH was found in some clinical manifestations of TSC, such as SEGA[60,78], renal angiomyolipomas and lymphangioleiomyomatosis[224–227]. Until recently, however, LOH had not been found in tuberal tissue, a pathological hallmark of TSC, questioning the role of LOH in TSC-associated tumour development[60,228,229]. However, in 2010, work by Crino and colleagues further described the relationship between LOH and tubers. In this study, tubers from 6 different TSC patients were collected. Instead of using whole tuberal tissue to detect LOH, genetic analysis was conducted specifically on giant cells that had been previously stained for phosphorylated rpS6. In these cells, evidence for a second mutation in the *TSC1* or the *TSC2* genes was present, reigniting the debate on the requirement for LOH in TSC hamartoma development[230].

Despite this evidence, TSC tumour progression can still exist if LOH is not present, as shown by Ma and collegues[231]. This work postulated the possibility of a "functional" second-hit where, instead of a true loss of heterozygosity in the *TSC1* or *TSC2* genes, alterations in the regulation of other pathway-intervening molecules could lead to mTOR hyperactivation and abnormal proliferation and growth[231]. In this *in vitro* and *in vivo* study, it was shown that, despite lack of LOH, tumour progression could still be promoted by constitutive activation of ERK. This kinase upstream of the TSC complex would in turn promote the inhibition of the TSC complex and allow the downstream activation of mTOR.

Regardless of how the heterogeneous phenotypes in TSC appear, the variability between patients contributes greatly to the difficulty in managing this pathology. Each individual requires a multi-professional team and a treatment plan specifically designed for their personal needs, reflecting the complexity of TSC.

1.1.6 Molecular Biology

As mentioned before, TSC is caused by a mutation in one of the tumour suppressor genes *TSC1* or *TSC2*. Pathological mutations in either of the resultant proteins, that alter the normal function of the downstream mTOR pathway, lead to multiple organ dysfunction, abnormal cell growth and proliferation[232–234]. In this section, more detail on the structure and function of the TSC1 and 2 genes and proteins, and on the mTOR pathway, will be described to better understand the pathological features present in TSC and how to target them.

1.1.6.1 TSC1-TSC2 Complex

The *TSC1* gene consists of 53 284 nucleotides located on chromosome 9q34, organized in 23 exons, and whose product is TSC1 or hamartin, a 130 kDa protein with different functional domains in its structure (Figure 1.3)[13,235–237]. The N-terminal domain is located around amino acids 1 to 350 of hamartin. This has the primary function of stabilizing the protein and, curiously, the vast majority of *TSC1* missense mutations are located in this region[237–240]. Amino acid residues 145 to 510 comprise a Rho GTPase activating domain, while residues 674 to 1164 and 881 to 1084 interact with neurofilament L (NF-L) and ezrin-radixin-moezin (ERM) actin-binding proteins, respectively[235,238,241].

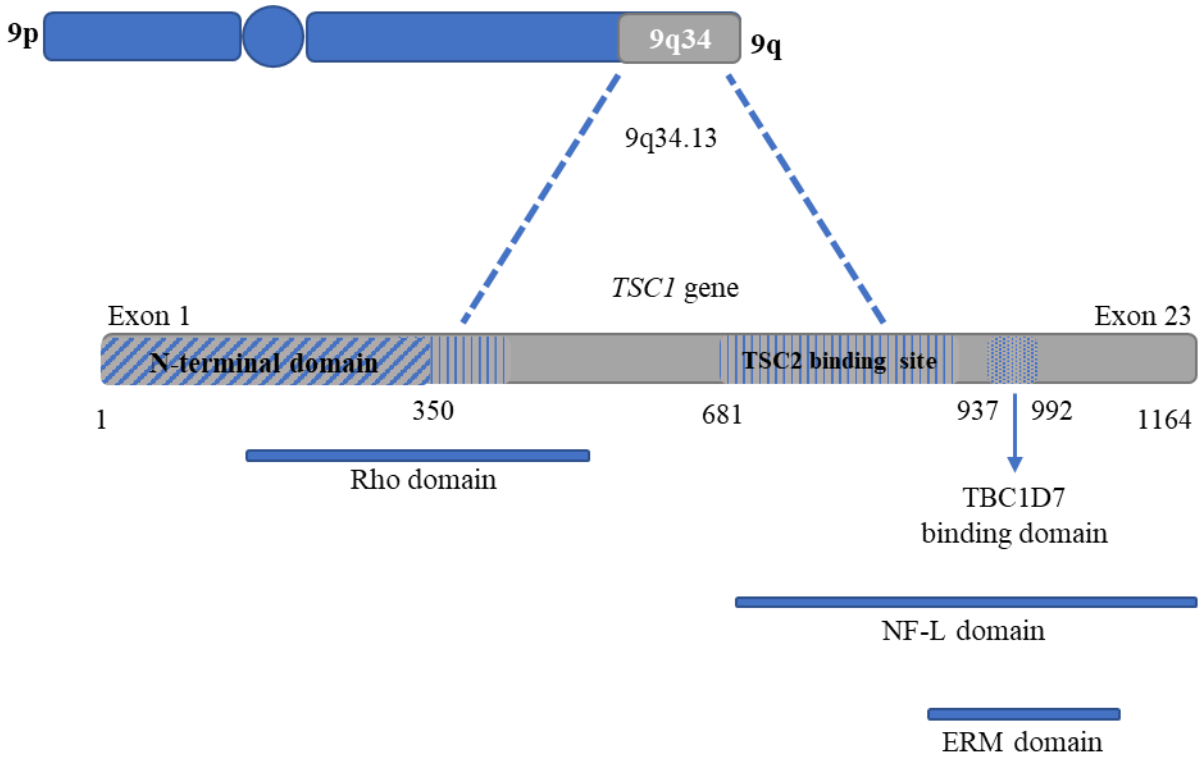

Figure 1.3: *TSC1 structure*. A schematic representation of the *TSC1* human gene is presented, together with its chromosomal location, exon distribution and main functional domain aposition. Adapted from reference 221.

Amino acids 939 to 992 exhibit a binding site for Tre2-Bub2-Cdc16 (TBC) 1 domain family, member 7 (TBC1D7), while amino acids 302 to 430 and 681 to 937 correspond to the binding site of tuberin[235,236,239,240]. Regarding the TSC1-2 complex, hamartin's main function is to be a scaffold for TSC2, stabilizing and preventing its ubiquitin-mediated degradation[236,241,242].

TSC2 (also known as tuberin) is coded by the *TSC2* gene, located on chromosome 16p13.3. *TSC2* is smaller than *TSC1*, consisting on 40 723 nucleotides, organized in 42 exons (Figure 1.4)[8,12]. Although smaller in genetic sequence, tuberin is a bigger protein than hamartin, as a 198 kDa protein. Tuberin interacts with hamartin through amino acids 1-418[238] but this is not the only functional domain it exhibits. Important interactions are made with Akt, AMP-activated protein kinase (AMPK), Erk and GSK3-β, kinases that phosphorylate TSC2 residues, an important activation and deactivation switch in signalling cascades[236,243–246]. Additionally, tuberin has several binding sites for proteins of the 14-3-3 family, important regulators in signal transduction and cell proliferation[247–249]. Finally, one of the most relevant functional domains of TSC2 is its GTPase-activating protein (GAP), between amino acids 1517-1674[12,250]. This domain is responsible for converting active GTP-bound Ras homologue enriched in brain (Rheb) into inactive GDP-bound Rheb (Figure 1.5)[251–253]. This step is crucial for the integration of the tumour suppressor complex function with the mTOR pathway[235,254]. Alternative splicing forms of both *TSC1* and *TSC2* have been reported although these do not seem to have major effect in the function of neither protein[255,256].

The previously mentioned TBC1D7 protein is a recently found third subunit of the TSC complex[257]. This protein was shown to bind preferentially to the TSC1-2 complex, rather than the individual free proteins, and to associate with the complex through TSC1[239,240,257,258]. Although further studies are needed to address the full function of this third subunit, it seems that binding of TBC1D7 to TSC1 stabilizes TSC1 homodimers and the TSC complex itself, aiding the oligomerization of multiple TSC1-TSC2 units[239,240,258,259]. So far, there is no evidence for the direct interaction of TBC1D7 with TSC2[239]. The effect of TBC1D7 mutations towards TSC pathology is still unknown. A small cohort of 12 NMI patients was screened for mutations in this gene and no mutations were identified[257]. However, one case report of two consanguineous siblings with mild intellectual disability and megalencephaly, but without tubers, SEN or other TSC manifestations, revealed a truncating mutation in the *TBC1D7* gene, absence of TBC1D7 protein, and high levels of mTORC1 activity. This indicated a potential but still unclear role of TBC1D7 in disease[260].

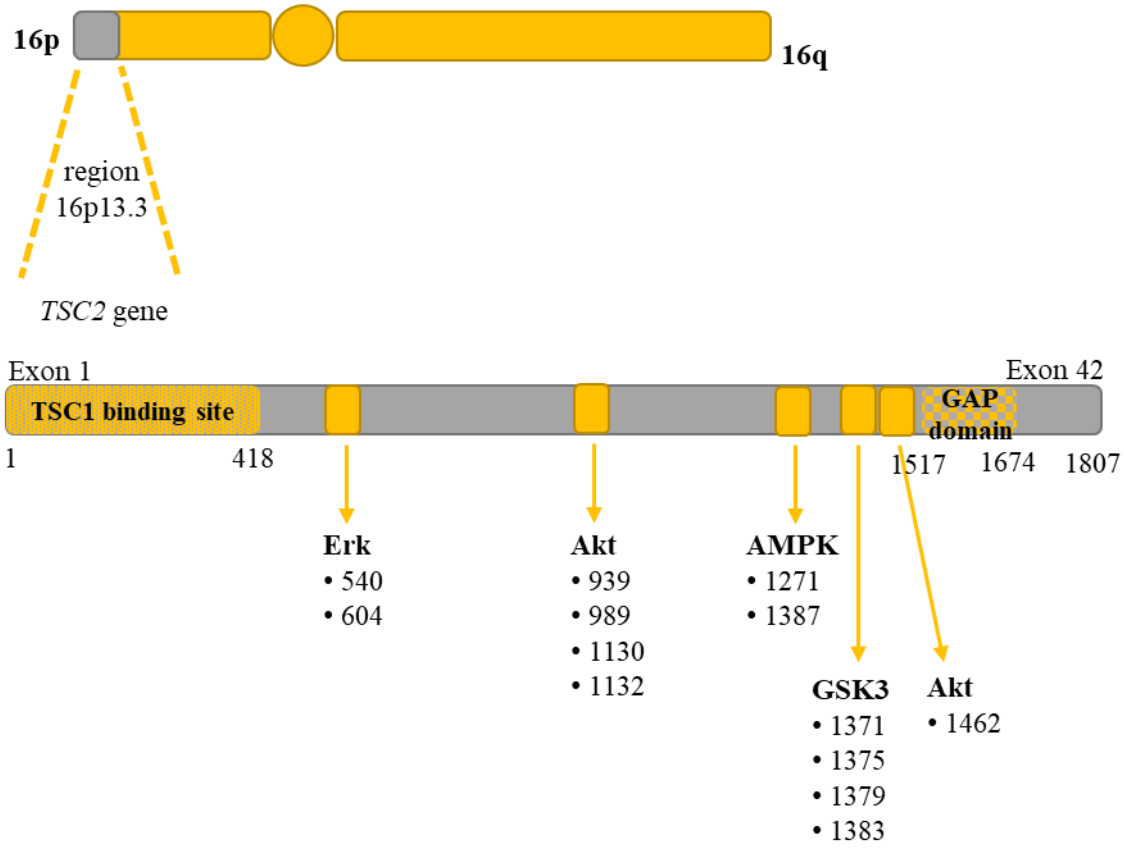

Figure 1.4: *TSC2 structure*. A schematic representation of the *TSC2* human gene is presented, together with its chromosomal location, exon distribution and main functional domain aposition. Adapted from references 221 and 230.

Some evidence suggests that the TSC1 and TSC2 proteins can have mTOR independent actions, namely concerning centrosome-related structures, cytoskeleton and VEGF regulation[261–264]. Nonetheless, the main reported and studied function of this complex is to be an intracellular switch controlling the activation and deactivation of mTOR[251,265–268]. Therefore, given the wide distribution of mTOR throughout different tissues, it is with no surprise that also TSC1 and TSC2 are ubiquitously distributed in different cell types and organs[269–272]. Regarding the subcellular localization of the TSC complex, first reports indicated that tuberin and hamartin colocalized predominantly in the cytosol, with small fractions associated with other structures such as the Golgi apparatus, endosomes and cytoskeleton[235,273]. However, more recent studies have not replicated these findings. Instead, these suggested that under unstimulated conditions, increased concentrations of TSC1 and TSC2 are found in the lysosomal surface, where they co-localize with Rheb[267]. When TSC2 is phosphorylated, the complex moves away from the lysosome and distributes through the cytoplasm[239,267,274,275]. This enables the interaction between Rheb and mTOR, as it will be explained in the following section.

1.1.6.2 TSC complex and mTOR

The first studies indicating a relationship between TSC and mTOR were done in *Drosophila* in 2001, when genetic screenings of *TSC1* and *2* orthologue mutants, *dTsc1* and *dTsc2* respectively, revealed increased total organ size due to increased cell size and proliferation[236]. Before this, it was already known that both in *Drosophila* and in higher eukaryotes the presence of amino acids could activate mTOR and promote downstream phosphorylation of ribosomal protein S6 kinase (S6K) and eukaryotic initiation factor 4E-binding protein (4E-BP1). This process was reversed by starvation conditions[276]. Additionally, the association between S6K and ribosomes had also been reported, suggesting a potential role in protein synthesis and cell growth. In 1999, this was confirmed by Montagne and colleagues, when S6K *Drosophila* mutants were found to present with growth delays. Furthermore, most flies would die in a larval stage without reaching adulthood, and had reduced body size compared to wild-type flies. Interestingly, it was also observed that all systems appeared to be affected equally, a detail that suggested the ubiquity of S6K (and mTOR) in the organism[277]. However, there was still a missing explanation as to how amino acids regulated this process and how mTOR controlled S6K. Therefore, the discovery that *TSC* genes controlled cell size in *Drosophila*, implied that these proteins could also be present along the mTOR pathway. Together with S6K, these could contribute to the regulation of mTOR signalling.

In 2002, the link between TSC, mTOR and cell size was published by Gao and collegues[276]. Although they observed premature death in *dTsc1*-null flies, viability was extended when uni-allelic deletion of *mtor* was also performed. Moreover, this deletion was enough to reduce photoreceptor size, increased in the d*Tsc1* mutants. d*Tsc1-mtor*-null flies had similar cell size to their wild-type counterparts, only 0.25 times bigger than the latter. To confirm mTOR regulation by TSC and knowing that S6K activation was an output of mTOR, S6K activity was analysed. Following the knock down of d*Tsc1* and d*Tsc2*, increased S6K activity was detected[276]. This indicated that the TSC complex was involved in mTOR and S6K regulation.

Also in 2002, Kwiatkowski and colleagues reported the development of a Tsc1 mouse model whose phenotype resembled *Drosophila*'s[278]. Lethality was present in the $Tsc1^{-/-}$ but not in $Tsc1^{+/-}$ embryos, and abnormal cell growth was present in the form of liver and kidney tumours. Using embryonic tissue (murine embryo fibroblasts, MEF), increased expression of phosphorylated S6K, phosphorylated rpS6 and p4E-BP1 was observed[278]. This indicated that, similar to the Drosophila mutants, mice also presented with a link between TSC-mTOR-rpS6. In the *Tsc2* rat model of TSC, the Eker rat (described in detail in Section 1.1.5.4.2)[279–281], increased expression of phosphorylated rpS6 and p4E-BP1 was also found in renal lesions[282]. Furthermore, increased mTOR and S6K phosphorylation was also detected in renal tumours and angiomyolipoma tissue from TSC patients[282]. Altogether, these studies suggested a strong similarity between the functions

of the mTOR pathway in different species, as well as an important contribution of the TSC-mTOR pathway to TSC pathology.

As previously mentioned, the TSC complex is present in the lysosomal surface, together with Rheb. On the other hand, the subcellular location of mTOR can change depending on its association as mTOR complex 1 (mTORC1) or as mTOR complex 2 (mTORC2) (Section 1.1.5.3).

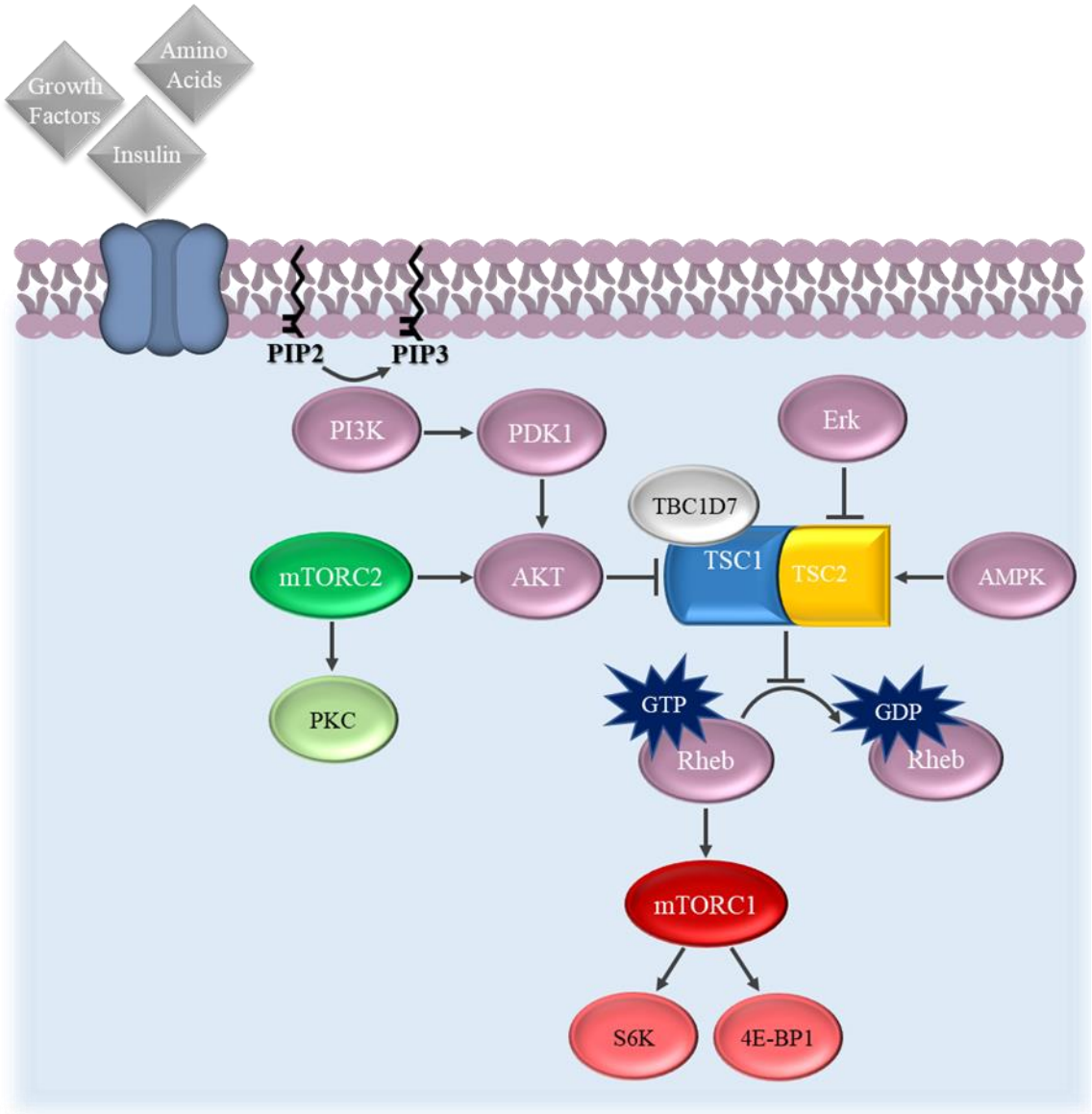

Figure 1.5: *The mTOR pathway*. A simplified scheme of the TSC-mTOR pathway is represented in this diagram, based on references 14, 37, 164 and 216.

In a general, although mTOR seems to associate with different organelles, the translocation from the cytoplasm to the lysosomal surface, and from an inactive to active state, respectively, has now been replicated several times[244,267,274,283–285]. This proximity to the lysosomal surface, physically approximates the TSC complex, Rheb and mTOR, allowing the interaction between the different

components. In an unstimulated basal state, TSC2's GAP domain promotes the hydrolysis of the GTP-bound Rheb to GDP, maintaining it in an inactive state (Figure 1.5)[251,252,286]. Following extracellular growth factor or amino acid stimulation (with insulin being one of the most studied components), distinct signalling cascades lead to the phosphorylation of TSC by kinases such as Erk or Akt[175,205,267,268]. This induces the translocation of the TSC complex with dissociation of TSC1 and 2. The movement to the cytoplasm, away from the lysosomal surface, separates TSC1-TSC2 from Rheb and mTOR[175,274,275,287]. This activates the mTOR kinase and its downstream targets (Section 1.1.6.3). Although indirect methods of activation of mTOR have also been proposed[245,251], the direct activation method has been strongly supported and comprehends the binding of GTP-bound Rheb to mTOR, leading to an enhancement of the activity of this kinase[288].

1.1.6.3 mTOR and its downstream effects

As previously described, the TSC complex negatively regulates mTOR and, upon amino acid or growth factor stimulation, tuberin is phosphorylated and its GAP function inactivated. This allows phosphorylation of Rheb and activation of the serine-threonine kinase mTOR (Section 1.1.5.2) (Figure 1.5)[79,289]. In the following section, the consequences of this activation will be described, with focus on those most important for TSC CNS pathology.

The functions of mTOR, first and foremost, depend on mTOR's organization which, although we have been describing mTOR as a single unit, comprises two different forms, mTORC1 or mTORC2 (Figure 1.6). To date, most functions attributed to mTOR refer to when mTOR is in its C1 configuration, whilst the functions of mTORC2 are not as well understood[236]. The study of mTORC1 has been facilitated by the existence of the specific mTORC1 inhibitor, rapamycin. Rapamycin, like its analogues, complexes with the FK506-binding protein (FKBP12) and binds mTOR through its FKBP12-rapamycin binding (FRB) domain. This decreases the binding affinity of substrates to mTORC1 therefore inhibiting its activity[175,177,289]. Although prolonged exposure to rapamycin has been shown to promote mTORC2's inhibition in some cell types[79,290,291], this complex is usually considered to be insensitive to rapamycin. As a consequence, fewer studies exist on the specific actions of mTORC2.

The mTOR complexes are assembled with other subunits. mTORC1 comprises mTOR, Raptor (rapamycin-associated protein of TOR), mLST8 (also called GβL; mammalian lethal with SEC13 protein 8), PRAS40 (proline-rich Akt substrate 40 kDa) and DEPTOR (DEP domain-containing mTOR interacting protein)[177,245], while mTORC2 is composed of mTOR, Rictor (rapamycin-insensitive companion of mTOR), mLST8, mSin1 (stress-activated protein kinase interacting protein 1) and DEPTOR[175,292]. Raptor is involved in mTORC1 assembly and substrate recognition, facilitating mTOR's access to downstream components. Rictor has an equivalent function in mTORC2[175,289]. Raptor and Rictor are specific for each complex and ablation of these

constituents impairs the function of the respective complexes[175,293–295]. The function of mLST8 is not yet fully understood but it appears to positively regulate mTOR by stabilizing its active site. At least during development, mLST8 seems to be more relevant for mTORC2's function than mTORC1's[295–298]. mSin1 acts as a scaffold for mTORC2 and as an Akt substrate[299], while both DEPTOR and PRAS40 are negative modulators of the complexes' activity (Figure 1.6)[175,300,301].

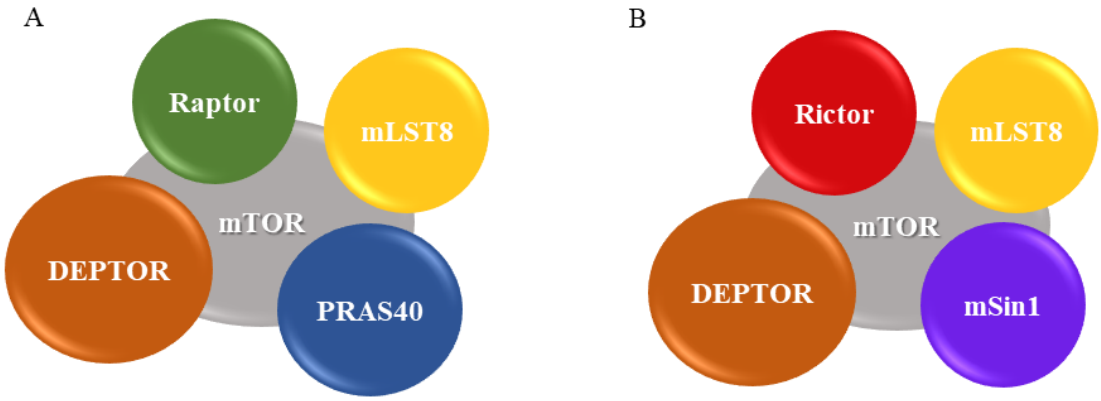

Figure 1.6: *mTOR complexes*. The mTOR kinase associates with different protein components to originate complex 1 (mTORC1) (A) and complex 2 (mTORC2) (B), which exhibit different targets and biological functions.

mTORC1's main function relates to protein translation and transduction[173,175], but it also mediates the synthesis of other macromolecules such as lipids and nucleic acids[175,245,292]. The two most studied downstream effectors of mTORC1 are S6K and 4E-BP1[79,175,292]. In contrast, mTORC2 phosphorylates several kinases primarily involved in cell survival and cytoskeleton actin regulation[79,175,283]. Indirectly, mTORC2 controls mTORC1 as it phosphorylates Akt on serine 473, promoting its full activation and inducing further inhibitory phosphorylation of TSC2[15,292,293,302,303].

Of note, although a lysosomal location for mTOR was previously described, this is actually the main site for mTORC1 docking. When mTOR is functioning under its complex 2 organization, several intracellular locations have been reported, one of these being the plasma membrane where mTORC2 would be physically closer to Akt[283,299].

Following mTORC1 activation, S6K is phosphorylated on threonine 389. S6K phosphorylates and activates several other substrates that contribute to the initiation and elongation of protein translation and ribosome biogenesis[175,292,304]. One of these substrates is 40S ribosomal protein S6 (rpS6), located in the interface between the large 60S ribosomal subunit and the small 40S ribosomal subunit[304,305]. rpS6 is phosphorylated by S6K on Ser235/236 and Ser240/244, a phosphorylation commonly used as a readout of mTORC1 activity. However, other enzymes such as ERK can also promote rpS6 phosphorylation[306]. The exact effect of rpS6 phosphorylation is still under investigation. While initial studies suggested that this process regulated mRNA binding to

ribosomes and the initiation of protein translation this has recently been proposed to be an area-dependent regulation, rather than global[304,305].

In addition to protein synthesis, S6K also promotes the synthesis of lipids through sterol regulatory element-binding protein activation 1 (SREBP1)[306–308]. mTORC1 also phosphorylates 4E-BP1, inducing the release of eukaryotic initiation factor 4E (eIF4E). Free eIF4E recognizes and binds to the 5′ mRNA cap, promoting mRNA translation[51,289,292]. As a result of these anabolic downstream mTORC1 functions, in a TSC status, overactivation of this pathway leads to an abnormal production of biomass, cell growth and division.

The consequences of the abnormal activation of mTOR are varied and vast. Specifically, in the CNS, proper regulation of the mTOR pathway is crucial for brain development[205]. During embryonic stages, mTOR is involved in the proliferation, migration and differentiation of neuronal stem cells and radial glia cells. Together with the unviability of homozygous *Tsc1* or *Tsc2* mutants, this suggests a crucial role of the TSC-mTOR axis in development[173,175,292,309,310]. Likewise, in non-dividing post-mitotic neurons, alterations to the regulation of the mTOR pathway can induce structural modifications. In fact, mTOR signalling has been shown, *in vitro* and *in vivo*, to control neuronal soma size, axon growth, and Schwann cell-mediated myelination[173,289,311–313].

Cell size modulation is regulated by several TSC-mTOR axis downstream mechanisms. On one hand, the phosphorylation and activation of mTOR by growth factors or deficient TSC repression induces nuclear accumulation of the previously mentioned SREBP[314]. This induces the *de novo* synthesis of lipids, crucial for construction of new plasma and organelle membranes, enabling cell growth[175]. Additionally, mTOR induces the activation of S6K and 4E-BP1, two main regulators of protein translation and transduction. In TSC, the unregulated activation of protein synthesis machinery increases protein production, specially of ribosomal-related proteins, which promotes the increase of overall cell volume and size[315].

The alteration of soma size due to mTOR overactivation is particularly important in neurons given the contribution of size to cell apposition, and capacitance and membrane resistance[173]. While macroscopical changes in size alter the physical organization and contact between neurons, electrophysiological alterations contribute to the establishment of abnormal neurotransmitter responses and release mechanisms[316,317]. Both modification types ultimately lead to the development of altered neuronal networks and response to stimuli.

Particular consideration has been given to the impact of conditional *Tsc1* or *Tsc2* deletions on neurons' finer morphology with the analysis of dendritic spines. In a very elegant work, Tavazoie and colleagues showed that both shape, size and number of dendritic spines were altered in *Tsc1* or *Tsc2* deficient pyramidal neurons. Loss of *Tsc1* or *Tsc2* induced changes from spherical head spines with thin necks into enlarged bulbous spines with elongated necks, as well as decreased spine density[313].

In addition to neuronal size and structure, the synthesis mechanisms altered due to increased mTOR signalling in TSC, also promote increased glia growth, namely of astrocytes. In tubers and perituberal tissue from TSC patients, astrocytes were shown to present in increased numbers and size compared to control tissue samples[318]. This hypertrophic astrocyte status, commonly associated with a reactive phenotype, is predominant in acute traumatic states, such as localized brain injuries or ischaemia[319,320]. However, in conditions were chronic brain injury is present, such as epilepsy, highly prevalent in TSC patients, this hypertrophic and reactive phenotype is detrimental for brain function. Instead of contributing for lesion healing, astrocytes promote increased tissue degradation and scarring due to the unregulated release of pro-inflammatory mediators, such as chemokines[321,322].

This simplified description of the consequences of abnormal TSC-mTOR signalling predict alterations concerning cell number, migration and shape. This suggests the macroscopical presence of dysplasias and augmented cell masses, which are indeed present in the TSC population[44,173,323]. At a microscopical and functional level, structural alterations can also have an impact on cellular physiology. Abnormal placement of neurons can lead to altered synaptogenesis and neurotransmitter release[79,313]. Changes in neuronal size predict alterations in input resistance and capacitance[173], as well as a modified electrophysiological response[51,149,324,325]. Overall, these macroscopic and microscopic changes, together with the alterations of GABA and glutamate receptor expression in tuber samples[57,326], support the concept that abnormal mTOR signalling contributes to the development of both an epileptogenic phenotype and behavioural manifestations seen in TSC[79,140].

1.1.6.4 Experimental *in vivo* models of TSC

Research towards the understanding of TSC has highlighted the importance of animal models for the investigation of the underlying mechanisms causing pathological manifestations. However, given the complexity of this pathology, and the variability and unpredictability of phenotypes, it is no surprise that no single animal model carries all features of TSC.

In the human presentation of TSC, *TSC1* or *TSC2* mutations are present in one single allele. Mutational homozygosity is not observed in humans and it has been shown to be embryonically lethal in animal models[278,327–329]. Yet, contrasting with the human form of TSC, the study of heterozygote models has been hindered by the absence of severe disease-like manifestations, especially CNS hamartomas and seizures[232,330,331]. Heterozygote models have, however, been particularly useful in the study of renal manifestations and dysfunctional behaviour[324,329,332–335]. One of the proposed reasons for this phenotypical variation, besides the obvious difference in organism complexity, was the possible lack of LOH in heterozygote animals that could prevent the development of certain hamartomas[310]. To overcome this limitation, conditional knockout models

have emerged, where deletion of both *Tsc1* or *Tsc2* alleles occurs in a time- and cell-specific manner (Table 1.2).

To date, a number of animal models of TSC have been found and developed (Table 1.2). As no single model displays all the characteristic features of TSC, the use of several animal models in research is key. This enables a better understanding of different TSC manifestations and allows the investigation of therapeutic interventions that could potentially modify disease progression. With this in mind, this work presents experimental data involving two different animal models of TSC, the *tsc2*^{vu242} zebrafish model and the *Tsc2*$^{+/-}$ (Eker) rat model. The following sections describe both models in more detail, together with their relevance for the study of TSC.

1.1.6.4.1 Zebrafish as a research, and TSC, model

In the "*An account of the fishes found in the river Ganges and its branches*" (1822), Francis Hamilton described a fish with "*several blue and silver stripes on each side; with the body much compressed, and with four tendrils, of which two are a little longer than the head*". Called *Cyprinus rerio* at the time, this was the first description of the zebrafish (now known as *Danio rerio*), a tropical fish native to southeast Asia, specially Bangladesh, India, Nepal and Pakistan[336,337]. However, it was not until the 1960s that this animal was first used in scientific research[338].

George Streisinger was a geneticist whose work focused on vertebrate development and regressive mutations. As a fish enthusiast, he knew zebrafish were easy to raise and maintain, even in the large numbers required for scientific research, given that adult fish reach a maximum of 6 cm in length[336]. Although no previous work had been conducted with this organism, Streisinger decided to use it as his own research model and, in 1981, the first zebrafish paper was published[339,340]. Here, the development of homozygote zebrafish maintaining solely maternal DNA was described. This novel technique allowed the development of mutated homozygotes and the study of mutations that would otherwise be lost in heterozygosity. After this publication, the use of zebrafish as an animal model in research grew quickly. This was particularly true in the genetics and development fields, as genetic knockdown or overexpression in zebrafish was, and is, considered a relatively accessible technique[337,341,342].

In addition to the maintenance benefits already mentioned, zebrafish are also exhibit high fecundity when mated. Sexual maturation can be achieved as early as 2 months and females can produce 200 to 300 eggs a week[338,343–345]. This allows rapid experiment turnover and data collection. Additionally, larvae develop *ex utero* and both eggs and embryos are transparent. This easy visualization of internal structures facilitates experimental manipulation. Moreover, compounds and drugs, if of appropriate solubility, can be added directly to the swimming medium, easing pharmacological delivery. Altogether, these characteristics transformed zebrafish into a medium to high throughput screening model for drug development[342,346,347].

Model		Genetic Mutation	Reference
Tsc1	Zebrafish		
	tsc1a	Global loss of *Tsc1a*	DiBella *et al.* 2009
	Mouse		
	$Tsc1^{+/-}$	Global loss of *Tsc1*	Goorden *et al.* 2007
	$Tsc1^{Nestin}$	Loss of *Tsc1* in SVZ neural stem cells	Zhou *et al.* 2011
	$Tsc1^{fl/mut}$	Loss of *Tsc1* in single cells during corticogenesis	Feliciano *et al.* 2011
	Tsc1-SynI^{Cre}	Loss of *Tsc1* under synapsin promotor	Meikle *et al.* 2007
	$Tsc1^{GFAP}$	Loss of *Tsc1* in GFAP-positive astrocytes	Uhlmann *et al.* 2002
	$Tsc1^{Emx1}$	Loss of *Tsc1* in embryonic neural progenitor cells	Magri *et al.* 2011
	Tsc1-L7^{Cre}	Loss of *Tsc1* in Purkinje cells	Tsai *et al.* 2012
	Tsc1-Lhx^{Cre}	Loss of *Tsc1* in eye-committed neural progenitor cells	Jones *et al.* 2015
Tsc2	Zebrafish		
	$tsc2^{vu242}$	Global loss of *tsc2*	Kim *et al.* 2011
	Mouse		
	$Tsc2^{+/-}$	Global loss of *Tsc2*	Ehninger *et al.* 2008
	$Tsc2^{f36-37}$ *Emx1*	Loss of *Tsc2* in embryonic neural progenitor cells	Ess *et al.* 2013
	$Tsc2^{GFAP}$	Loss of *Tsc2* in GFAP-positive astrocytes	Zeng *et al.* 2011
	Tsc2-Pcp2^{Cre}	Loss of *Tsc2* in Purkinje cells	Reith *et al.* 2011
	Rat		
	$Tsc2^{+/-}$	Global loss of *Tsc2*	Yeung *et al.* 1994

Table 1.2: *Animal models of TSC*. A number of spontaneous and genetically-modified animal models of TSC are presented, together with mutation target and outcome. References are not exhaustive and indicate representative work for each model.

Following Stresinger's work, zebrafish were soon accepted as a model organism to study embryogenesis and development, especially in the CNS[340]. However, a model organism is only valuable as such if findings can be translated to other species. To assess similarities between zebrafish and rodent and human pathology, the Wellcome Trust Sanger Institute (Cambridge, UK) initiated in 2001 the zebrafish genome sequencing project. The Tubigen strain was used as reference given that it had been the most widely used zebrafish strain to date[341]. With this pioneering study, it

was possible to obtain comparative genetic data between zebrafish and other species, allowing for a more accurate validation of this animal's model status.

Although it was first proposed that zebrafish had 24 pairs of chromosomes[336], they were later discovered to exhibit 25; humans, on the other hand, have 23 chromosomal pairs[336]. Nonetheless, the zebrafish genome was estimated to be half the size of the human one[343], with 26 206 protein coding genes, a great part of them species-specific and without orthologues to human, mouse or chicken[341]. Importantly, 71.4% of human genes have an orthologue in the zebrafish genome and, of these, 84% can be associated with pathological conditions[337]. Despite genomic similarity, it is important to acknowledge that, as in another fish species, zebrafish genome has undergone significant processes of gene duplication. As a consequence, regardless of a similar number of chromosomes compared to humans, some zebrafish genes can be expressed differently[337,348,349]. This is particularly important when knockout or overexpression of genes is being considered. One example of gene duplication in zebrafish is actually the *tsc1* gene, where *tsc1a* and *tsc1b* genes are present[327,350].

The first use of zebrafish for the study of TSC was conducted by DiBella and colleagues in 2009. Because cilia, a cell organelle, appeared to be essential for kidney cyst prevention, and PKD was highly prevalent in TSC patients, they hypothesised that cilia would be related to the *tsc* genes. In this first description of *tsc1* in zebrafish, two *tsc1* genes were found, *a* and *b*, which had a 36% and 44% homology to the human gene, respectively. Additionally, single zebrafish homologues to the human *TSC2* and *RHEB* genes were also identified. In accordance to human studies, zebrafish *tsc1* knockdown induced growth of kidney cysts and increased mTOR pathway activation. Cilia growth was also increased in mutants compared to controls, supporting a relationship between cilia, mTOR and *tsc1*, as well as pathway homology to mammalian models[23,350,351]. Two years later, Kim and colleagues examined the role of tuberin in zebrafish, this time coded by a single *tsc2* gene and with a 73% homology to its human counterpart[327,350]. Using the Targeting-Induced Local Lesions IN Genomes (TILLING) technique, a mutant harbouring a *tsc2* mutated gene (the $tsc2^{vu242}$ mutant) was identified. This mutant carried a cytosine to adenine transversion which originated a stop codon. As a consequence, tuberin was without its GAP domain and was functionally inactive[327,352]. Characterization of the $tsc2^{vu242}$ mutant showed common features with other TSC models[209,278,317,324,328,353], including homozygous lethality by 11 days post-fertilization (dpf), increased mTOR signalling, as seen by rpS6 and 4E-BP1 phosphorylation, and enlarged hepatocytes and neurons. Importantly, rapamycin administration reduced phosphorylated rpS6 immunoreactivity and cell size, evidencing once again the similarities between the zebrafish and mammalian TSC-mTOR axis[327]. Using this same model, Scheldeman, in collaboration with myself and others, showed increased brain to body ratio in $tsc2^{-/-}$ zebrafish as well as decreased exploratory behaviour and startle response. Furthermore, local field potential recordings revealed the presence of epileptiform-like activity in $tsc2^{-/-}$ mutants[354].

In summary, these studies indicate that the *tsc2*^{vu242} model replicates some of the disease features present in human TSC, while also exhibiting additional species-specific behavioural alterations, such as reduced swimming behaviour. These are desirable characteristics that make this model useful for novel drug screening. With this in mind, the *tsc2*^{vu242} zebrafish model was used in this thesis to address the possible effects of CBD on behaviour and molecular characteristics modified by *tsc2* mutation (Chapter 2). The experimental work presented in Chapter 2 was published in *Behavioural Brain Research* (2019) 363:135-144 and partially features the patent "Use of cannabidiol in the treatment of tuberous sclerosis complex" (WO2018234811).

1.1.6.4.2 The Eker rat as a TSC model

As previously mentioned, several animal models of TSC are available (Table 1.2), each replicating different manifestations of disease. In this thesis, in addition to the zebrafish model described above, a rodent model of TSC, the Eker rat, was also used (Chapters 3 to 5).

In 1954, Reidar Eker published "*Familial renal adenomas in wistar rats: a preliminary report*" where he reported a generation of rats with high incidence of renal adenoma[355]. Interestingly, although this disease was already known in humans, it had never been reported in other mammals. This motivated Eker to keep and maintain the colony, later used to establish a model of genetic familial cancer[8,280,356]. In 1983, the Eker rat caught the attention of Alfred Knudson. Now considered one of the most important researchers in the cancer genetics field[357], Knudson had proposed, in 1971, the previously mentioned two-hit hypothesis (Section 1.1.4.3). However, this concept had been conceived solely based on epidemiological and statistical data from retinoblastoma patients[358]. To test his hypothesis experimentally, Knudson was searching for an animal model of hereditary cancer. Therefore, the finding of the Eker rat allowed his group to explore with practical methodology, and for the first time, the hereditary characteristics of tumour inheritance.

In 1993, Hino and colleagues confirmed the predisposition of the Eker rat to renal tumours. More importantly, they showed that a second hit (ionizing radiation) increased the number of tumours in the Eker group but not in wild-types. This confirmed that Ekers exhibited an unknown mutation that predisposed them to renal carcinoma. Additionally, this study also revealed that homozygosity for this unknown mutation was lethal, as it produced unviable embryos at around embryonic day 10[359]. These results further suggested that the mutated gene in the Eker rat was critical for cell division and migration, and that mutations in both alleles did not allow progression of intra-uterine development[359,360]. Also this year, the same group demonstrated with linkage analysis that the mutation responsible for the Eker phenotype was located in the chromosome band 10q12. Furthermore, they showed that loss of heterozygosity was present in renal tumours[360]. Following this work, Yeung and colleagues linked the mutation responsible for the Eker rat

pathology to its human homologue located on chromosome 16p13.13, where the *TSC2* gene, already known as a tumour suppressor at the time, was located[12,356]. In 1995, the exact mutation product was found to be a 5kb insertion that rendered Tsc2 inactive[361]. This inactivation was caused by an intracisternal-A particle transposition into codon 1272 that generated a longer, and therefore prone to degradation, tuberin. Additionally, this insertion prevented the formation of the GAP domain, essential for tuberin's function[361].

The molecular and phenotypical consequences of the Eker mutation soon lead to its investigation as a possible model of TSC. The renal epithelial tumours exhibited by the Eker rat have a penetrance of 100% by the age of 12 months[362], although these were observed in animals as young as 4 months old[8]. Because TSC patients have a 2 to 4% higher probability of exhibiting renal cell carcinoma (RCC) than general population[19], this was a desirable property of this model. In addition, renal disease is the major cause of disease-related mortality in TSC patients[363]. However, it is important to acknowledge that other types of renal manifestations common in TSC patients, like cysts and angiomyolipoma (Table 1.1), are not exhibited by the Eker rat model[280].

Regarding its neurological profile, the Eker rat does not show major gross morphological alterations[45,232,364–366]. In a comprehensive study by Yeung and colleagues, only small brain lesions were found in the Eker rat brain[364]. Using 18 to 24-month-old rats from the Fisher background, small lesions with large cells next to the ventricles were found, which were proposed to resemble human subependymal lesions. However, these did not protrude into the ventricles, as is usually seen in patients. Occasional cortical lesions were also reported, although no tubers nor alterations of the cortical layer organization were detected[364]. Yet, it is important to acknowledge that this study used rather old animals and that 43 Ekers vs only 4 controls were analysed. It is plausible that this age and group imbalance could contribute to the difference in results between this and other studies in the literature[45,232,364,366]. A similar study by Mizuguchi and colleagues also supported the absence of gross morphological brain abnormalities in 17 to 24-month-old Ekers from the Long-Evans background. Here, for the first and only time, one cortical tuber was reported in one single animal, in addition to the presence of few subcortical and subependymal lesions with large GFAP positive cells in 2/14 Ekers[367]. Again, the imbalance between control and Eker animals could impact data interpretation as 14 Ekers were compared to only 6 controls. Furthermore, when younger animals were used, neurological pathology seemed to be even scarcer. Waltereit and colleagues analysed the brains of 15 male Ekers of the Long-Evans background, aged 8 months old, and found one single subependymal lesion in one animal alone, with no cortical tubers evident[232]. This study supported a previous report suggesting that, although a second hit such as radiation could increase the number of abnormal cells Eker brains, these were absent in young non-irradiated animals[45,232]. Overall, evidence indicates that the Eker rat brain does not seem to mimic the human presentation of TSC, although the presence of CNS pathology may be increased in older animals.

The lack of neurological features does not necessarily exclude the presence of behavioural comorbidities. Epilepsy is one of the most common neurological presentations in TSC (Table 1.1)[14,16,18]. The Eker rat does not exhibit spontaneous seizures. However, a few studies evaluated its propensity to develop seizures when challenged with convulsive compounds. Wenzel and colleagues measured the latency to tonic-clonic (TC) seizure development in 3-month-old Ekers and control rats, using the flurothyl inhalation method. Here, no difference was found in the latency to develop TC seizures[45]. Using intraperitoneally administered pentylenetetrazole (PTZ), a $GABA_A$ receptor antagonist that inhibits chloride currents and increases neuronal activity, Waltereit and colleagues also failed to find differences in seizure susceptibility in 3 to 6-month old Ekers[232,368,369]. However, when a kindling protocol was used, Eker rats developed Racine's scale stage 5 seizures, defined as "loss of posture or death", earlier than wild-types[232]. Therefore, it is possible that the Eker rat exhibits altered susceptibility to seizures. However, given that seizures manifest early in patients with TSC, more data using younger Eker rats would be valuable to understand if this model could better elucidate seizure development in TSC.

Another highly relevant feature of TSC is ASD (see Table 1.1). A common symptom in ASD is the difficulty in interacting socially or in social environments. Evidence seems to indicate that the Eker rat mimics some of these TSC features, although few studies have been published to date. Using 3 to 6-month old males, Waltereit and colleagues analysed the behaviour of wild-type and Eker rats, when faced with an unknown social partner ("stranger rat"). Ekers showed reduced social exploration, which comprised ano- and non-anogenital exploration, as well as approaching and/or following the social partner[370]. Furthermore, when epilepsy was chemically induced in these rats, social evasion was accentuated[370]. In a follow-up study, Schneider and colleagues proposed that treatment with the mTOR inhibitor Everolimus would reverse some of the previously observed interaction deficits[371]. After induction of an epilepsy paradigm using kainic acid, a glutamate analogue, three intraperitoneal injections with 1 mg/kg Everolimus reversed social impairments to control levels[371]. However, it is important to note that this study used only two experimental groups, one naïve control and one Eker with epilepsy. No other comparator control groups were tested. Although this does not invalidate the obtained data, it would be interesting to investigate whether effects of treatment on social behaviour could also be observed in non-epileptic Eker rats.

Although seizure and ASD-like features appear to be in some way present in the Eker rat, other behavioural features, such as memory, learning and anxiety behaviours, seem to be similar to wild-type rats (Table 1.3)[232,370]. The literature on the Eker rat is not extensive but, overall, only mild neurological and behavioural phenotypes are consistently presented. On the other hand, the development of kidney tumours seems to follow quite closely the human presentation of disease[372]. Nonetheless, given the complexity of this model compared to others (rat *vs* mouse), the Eker rat is a valuable organism to address behavioural aspects of TSC.

Experimental task	Behaviour assessed	Difference to wild-type rats (Y/N)	Reference
Water maze	Spatial learning and memory	N	Waltereit *et al.* 2006; 2011
Delayed water maze	Spatial learning and memory	Y Faster platform finding during trial 2 only	Waltereit *et al.* 2006
Light/dark box	Unconditioned anxiety response	N	Waltereit *et al.* 2006; 2011
Conditioned taste aversion	Learning memory	N	Waltereit *et al.* 2006
Radial maze	Working and reference memory	Y Fewer trial errors	Waltereit *et al.* 2006
Open field	General activity level	N	Waltereit *et al.* 2011
PTZ acute	Seizure susceptibility	N	Waltereit *et al.* 2006
PTZ kindling	Epileptogenesis	Y Increased stage 5 susceptibility	Waltereit *et al.* 2006
Fear conditioning	Associate learning	N	Waltereit *et al.* 2011
Novel object recognition	Recognition memory	N (similar recognition of novel object) Y Less time exploring objects	Waltereit *et al.* 2011
Social interaction	Interest in social novelty	Y Reduced social exploration	Waltereit *et al.* 2011

Table 1.3: *The Eker rat behavioural profile*. A summary of the different behavioural experiments and their simplified results is presented in this table together with the reference work.

1.2 Cannabidiol

1.2.1 *Cannabis*, THC and CBD- an overview

Cannabis is a plant from the Cannabaceae family, indigenous to the south and centre of Asia[373,374], comprising one main species, *Cannabis sativa* (Figure 1.7A). *Cannabis indica* and

Cannabis ruderalis are often reported as two other species from this genus of plant. However, it is now more accepted that these are variations or subspecies of *C. sativa* rather than individual species in their own right [374–378]. Although the use of the *Cannabis* plant for medicinal purposes was first documented circa 2900 BC by the Chinese Emperor Fu His and then by the Emperor Shen Nung around 2700 BC[379,380], the main uses of the plant were as a source of fibre, oil and food[373]. *Cannabis* contains over 400 different compounds, including flavonoids, alkaloids and terpenoids, with ratios depending on the subspecies and strain of plant[373]. Around 60 to 80 of these compounds belong to a *Cannabis* specific class of terpenophenolic structures denominated cannabinoids, primarily stored in the plant's trichomes (Figure 1.7B)[373,374,381,382].

Figure 1.7: *The* Cannabis *plant*. Photograph of an indoor grown *Cannabis* plant (A) and of trichomes in a *Cannabis* bud (B), both taken at the Cannabis Museum (6 Damstraat, Amsterdam, Netherlands).

The two most abundant cannabinoids in *Cannabis* are Δ-9-tetrahydrocannabinol (THC) and cannabidiol (CBD)[383,384]. THC, the main psychoactive component of *Cannabis*[385], was first isolated and structurally described by Gaoni and Mechoulam in 1964, through the use of chromatography on an hexane extract of *C. sativa* hashish[386]. THC is often associated with the recreational use of *Cannabis*, as its psychoactive properties are greatly responsible for the "high" felt after *Cannabis* consumption. However, THC has also been proposed to possess relevant medical properties, mainly via the partial agonism of both the CB1 and CB2 receptors[387–390]. These include the control of spastic disorders, pain and emesis[388,391,392]. Nevertheless, due to its psychotropic effects, the use of THC in medical formulations, especially in infantile pathologies, is highly limited[393,394]. CBD is the second most abundant compound in *Cannabis* and, as opposed to THC, it does not exhibit psychotropic properties. CBD does not bind to CB1 and CB2 receptors in physiological concentrations[374,395,396]. CBD was first isolated in 1940 from a red oil from Minnesota wild hemp[397]. Preliminary structural suggestions were made in this same year by two different research groups[397–399]. However, the actual correct structure of CBD was only published in 1963 and 1964, with the use

of nuclear magnetic ressonance[400,401]. Given the absence of a psychotropic profile, CBD has been assessed for several different medicinal uses as an anti-epileptic[402–404], anxiolitic[405–408], anti-psychotic[374,409,410] and anti-tumoural compound[411–414]. Presently, CBD is commercialized as an FDA-approved medication by GW Pharmaceuticals in two different formulations: in a 1:1 ratio combination with THC (Sativex®), for multiple sclerosis spasticity; and in isolation (Epidiolex®) for the treatment of seizures in Lennox-Gastaut syndrome (LGS) and in Dravet syndrome (DS).

In the *Cannabis* plant, the synthesis of THC and CBD begins with identical precursors (Figure 1.8). Both compounds exhibit very similar chemical structures, distinguished by the presence of a closed pyran ring in THC, opened in CBD (Figure 1.8)[401,415]. Note that the natural biosynthesis of THC and CBD originates the carboxylated forms Δ-9-tetrahydrocannabinolic acid (THCA) and cannabidiolic acid (CBDA), respectively. In fact, only when exposed to increased levels of light, heat or drying conditions, does the non-enzymatic decarboxylation of THCA and CBD occur, leading to the accumulation of THC and CBD *per se* in the plant's trichomes[377,415,416].

Because of the similarities between the structure and biosynthesis of THC and CBD, and given the increasing research into CBD's use as a medical treatment, concerns were raised regarding the possibility of *in vivo* conversion of CBD into THC, which could hypothetically promote unwanted psychotropic effects. To address this issue, Merrick and colleagues analysed the presence of CBD and its metabolites, after 75 minutes of exposure to simulated gastric fluid. Using compound separation with ultra-performance liquid chromatography and detection by ultraviolet and mass spectrometry, this work revealed the presence of both Δ^9-THC and Δ^8-THC, suggesting the conversion of CBD into THC[417]. This was however a conversion of unknown biological significance. Although an interesting result, the simulated gastric fluid used in this study consisted of 0.1M HCl and 0.2% NaCl only, omitting the contribution that other gastric components, such as trypsin, pepsin and gastricsin, have on metabolism, and nutrient and compound availability[418,419].

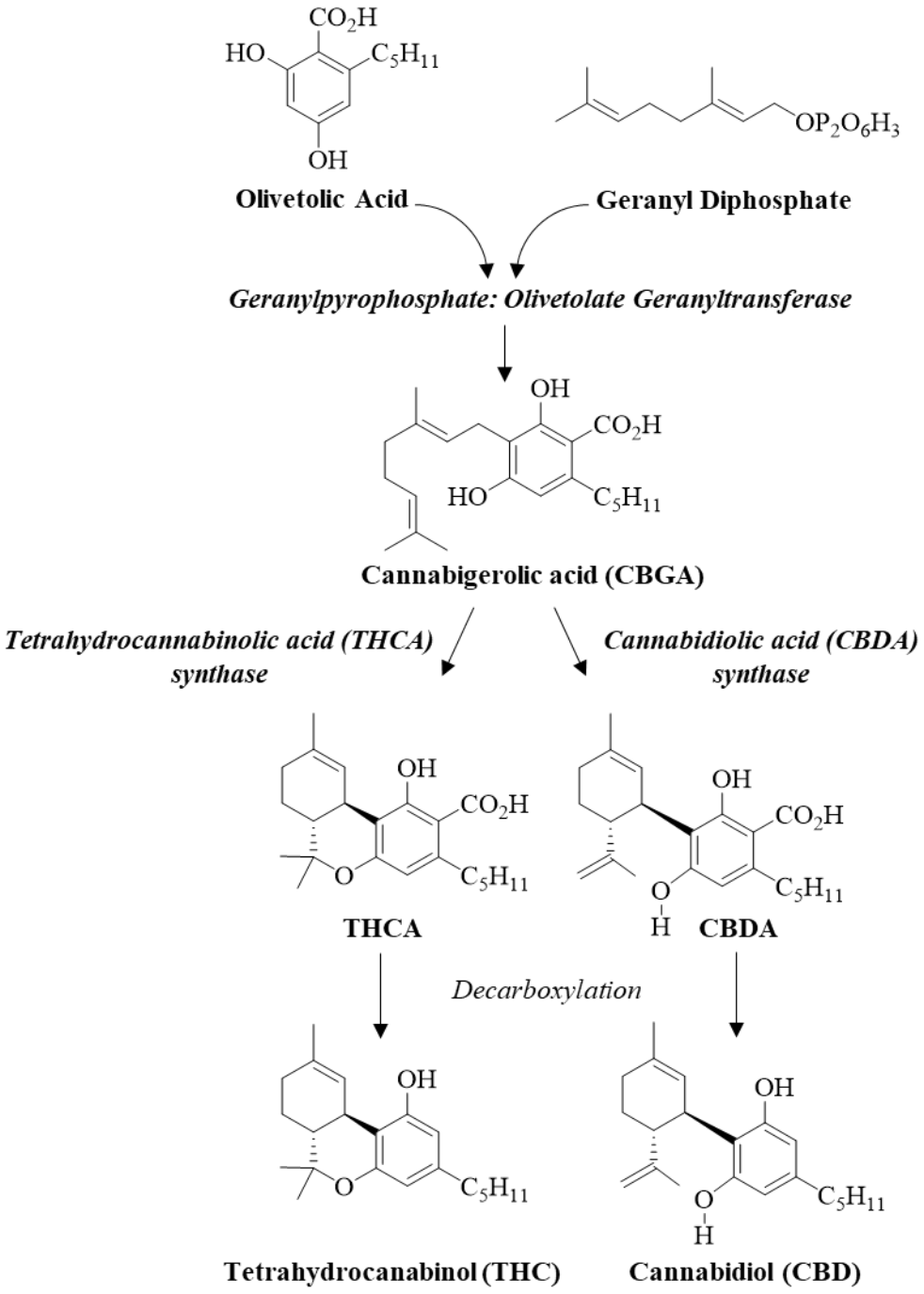

Figure 1.8: *Biosynthesis of THC and CBD.* In the *Cannabis* plant, olivetolic acid and geranyl diphosphate are alkylated by the enzyme Geranylpyrophosphate: Olivetolate Geranyltransferase, originating CBGA. Among other compounds, CBGA is the precursor of THC and CBD, following the action of the oxidocyclases THCA synthase and CBDA synthase, respectively[366,380]

Although the work by Merrick and colleagues was contested by experts in the CBD field[416,420], the suggestion of an *in vitro* conversion of CBD into THC led to further experimental work evaluating this possibility *in vivo*. Hlozek and colleagues administered 10 mg/kg CBD by oral

gavage or subcutaneous injection to Wistar rats and measured THC levels in the serum. THC was detected varying between 2 to 30% of the initially concentration of administered CBD. However no THC was detected in brain tissue making it unclear if the amount of THC detected could have an effect on the CNS and behaviour[421]. In contrast with this study, when Pallazoli and colleagues administered 50 mg/kg of CBD by oral gavage to Sprague Dawley rats, no THC or metabolites were detected in blood, 3 and 6 hours after treatment. This detection was limited by the limit of quantitation of the liquid chromatography-mass spectrometry (LC-MS) of 0.5 to 5 ng/mL, depending on compound[422]. In a study with minipigs, a model with a more comparable diet and gastrointestinal metabolism as humans[423,424], Wray and colleagues administered 15 mg/kg of CBD by oral gavage. Both blood and gastrointestinal fluid were analysed by LC-MS and no trace of THC or 11-OH-THC was found, despite the lower limit of quantitation of this study (0.5 ng/mL for both compounds)[425].

In vivo data seems to suggest that the conversion of CBD into THC is unlikely, although clinical data would be necessary to support this claim. One double-blind, placebo-controlled, randomized crossover clinical study evaluated the presence of THC in Huntigton's patients, following a 6-week treatment with 10 mg/kg/day CBD in sesame oil. Gas chromatography and mass spectrometry were used on blood samples to detect both CBD and THC, but no THC was detected throughout the study. Although in line with previous reports, it is still important to consider the detection limits of this work, as only 60% of the compounds could be retrieved from the samples[426].

Finally, when used in clinical settings, commonly reported adverse effects following CBD administration include somnolence, decreased appetite, diarrhoea and fatigue[402–404,427]. These symptoms are quite distinct from what has been reported for THC which includes relaxation, anxiety and euphoria[428–430]. This indicates that it is unlikely that patients are experiencing THC-dependent effects. In conclusion, although there are few reports of CBD conversion into THC, it is improbable that this is the case in humans or that the hypothetically achievable concentrations of THC would originate CNS or behavioural effects.

1.2.2 The role of CBD in epilepsy treatment

CBD exists in two approved medications, Sativex® and Epidiolex®. However, despite regulatory approval, the exact mechanism of action of CBD is still uncertain. As a consequence of the vast array of proposed targets and effects for CBD (such as 5-HT, TRPV1 or adenosine receptor activation; antagonism of GPR55; or inhibition of the ENT1 transporter[374,396,416]), its potential application in a plethora of medical conditions has been investigated. One of the fields in which there has been great focus regarding CBD use is epilepsy, and this will be the focus of the next section.

Until the 19th century, *Cannabis* was considered an official medicine, featuring in several European and American Pharmacopoeias in the form of oils and tinctures[431,432]. However, a prohibition period in the late 19th and beginning of the 20th century led to a new classification of *Cannabis* as a Schedule 1 drug classifying it as "*(drugs) with no currently accepted medical use and a high potential for abuse*", therefore hindering its use in medicine[379,384,433–435]. This however did not impede the illegal use of *Cannabis* in recreational and medical cases. Early anecdotal reports suggested that patients with epilepsy benefited well from the drug[436,437], although cases of increased seizure frequency due to drug intake were also reported[431,437]. This reignited the study of *Cannabis* extracts and of CBD for seizure control. CBD has now been extensively tested in *in vitro* models of epileptiform-like activity[438–440] and in *in vivo* models, where it was shown to have anti-convulsive properties in rodents in common seizure models such as the maximal electroshock[441–444], PTZ[444,445], pilocarpine[446] and penicillin[446], among others[447,448]. Importantly, as opposed to THC, there is no pre-clinical evidence for a pro-convulsant action of CBD[447,449].

The overall positive results obtained in pre-clinical research led to the authorization of CBD use in expansion and small open-label trials. These in turn allowed the development of large-scale clinical trials where CBD was administered in better controlled cohorts and conditions. In an open-label, multicentre study, 137 patients with intractable epilepsy, aged 1 to 30 years old, were given 25 or 50 mg/kg/day of CBD orally. After 12 weeks, a reduction in the median frequency of seizures from 30.0 to 15.8 was seen, together with seizure freedom in 5/137 patients with motor seizures. Two patients were free of all seizure types[402]. Regarding two forms of severe childhood epilepsy, DS and LGS, a significant monthly median reduction of seizure frequency was seen for DS patients (49.8% reduction in motor seizures and 42.7% in all seizure types), while a lower but significant reduction was also observed for LGS (36.8% decrease in the median frequency for motor seizures and 35.5% for all types of seizures)[402]. As an open-label trial, this study lacked the proper placebo and experimental ("blind") controls. Nonetheless, it still suggested a possible beneficial role of CBD as an add-on therapy for intractable patients.

More reliable data on the anti-epileptic action of CBD was obtained in subsequent randomized, double-blind, placebo-controlled studies for DS and LGS. In 2017, results from a clinical trial with DS patients were published. Here, 120 individuals between the ages of 2.5 and 18 years old were given a maximum of 20 mg/kg/day CBD for 14 weeks. Following this treatment period, reduction of seizure frequency was observed in the CBD group (38.9% vs 13.3% in the placebo group). A significant difference favouring CBD treatment in the caregiver Global Impression of Change (GIC) scale, concerning patient's overall condition, was also found. No differences were detected regarding the effect of CBD on sleep disturbances nor on the Vineland Adaptative Behaviour Scales (VABS)[427], which evaluates communication, socialization and daily living domains[450]. For the investigation of CBD in LGS, two cohorts of patients were used. In one of these, 225 individuals aged 2 to 43 years old received 10 or 20 mg /kg CBD orally. Median

reductions in drop seizures of 41.9% in the 20 mg/kg dose, 37.2% in 10 mg/kg and 17.2% in placebo group were observed, with CBD exhibiting similar results for total seizure type reduction. A small but significant improvement in patients' QoL and overall physical and cognitive condition favoured the 10mg/kg CBD dose (66% patients were reported to exhibit improvements with the Patient or Caregiver GIC vs 44% in the placebo group)[451]. Another trial recruited 171 patients between the ages of 2 and 39, who were treated with 20 mg/kg CBD for 14 weeks. Again, a significant median reduction in drop seizures was observed (43.9% in the CBD vs 21.8% in the placebo group), together with a reduction in the frequency of all seizure types (reduction of 41.2% in the CBD vs 13.7% in the placebo group). Similar to the previous study, patient and caregiver GIC scale indicated improvements in the overall condition of patients who received CBD (58% vs 34% in the placebo group)[404].

Overall, clinical trials suggest that CBD improves seizure profile particularly in refractory populations, while having tolerable adverse effects. Importantly, significant improvements in QoL were seen after CBD treatment, although these results were based on carers' and parents' assessments rather than patient reports. Both these characteristics, i.e. improving seizure profile and QoL, would also be of great value to the TSC population. Currently, two clinical trials assessing the use of CBD in TSC are underway, both sponsored by GW Research Ltd. One of these trials is a double-blind, placebo-controlled, randomized study in recruitment phase to "*Investigate the Efficacy and Safety of Cannabidiol (GWP42003-P, CBD) as Add-on Therapy in Patients With Tuberous Sclerosis Complex Who Experience Inadequately-controlled Seizures"* (NCT02544763). The other is an open-label extension trial (NCT02544750). While completion of the first study is expected by September 2018, data will not be available for several months after the trial has been completed. However, a previous open-label trial with TSC patients suggested that, like in DS and LGS, CBD might have a beneficial effect on this population[403]. Here, 18 TSC patients aged 2 to 31 years old received a maximum of 25 mg/kg/day of CBD for at least 6 months. During this period, the median number of seizures per week decreased from 22 to 9.7. Twelve patients, parents or physicians reported cognitive gains, although the method for this analysis was not described in the study. Additionally, from the 9 patients who had reported behavioural difficulties, 6 described improvements in this parameter, again suggesting that CBD could be an useful add-on therapy for this patient group[403].

1.2.3 CBD and the mTOR pathway

Seizures are an integral feature of TSC (Section 1.1.3.4) and data so far suggests that CBD might be a viable pharmacological option for TSC patients, although results are still required from randomized, double-blind, placebo-controlled trials. Most pathological manifestations in TSC develop due to mTOR over-activation (Section 1.1.5.3). Consequently, it would be advantageous if

CBD also acted along this pathway, in addition to its anti-seizure profile. Although clinical data is not available on this matter, a number of *in vitro* and *in vivo* studies have analysed this signalling pathway after CBD treatment. Overall, results summarized below suggest that CBD might exert some direct and indirect actions along the mTOR pathway.

Using different cell lines derived from human breast cancer cells (both oestrogen-receptor positive and negative), Shrivastava and colleagues analysed the effect of a 24-hour incubation of increasing CBD concentrations (0–10 μM). Starting at 5 μM, CBD reduced cell viability and decreased the expression of pAKT (Ser473), p4E-BP1 (Ser65), cyclin D1 and pmTOR (Ser2448) in a concentration-dependent manner[412]. These western blot results indicated that CBD reduced mTOR pathway activation and some of its downstream targets, which are increased in several types of cancer[452]. Also in breast cancer cells, Sultan and colleagues suggested a CBD-induced concentration-dependent (1-7 μM) reduction in pmTOR and cyclin D1[413], although only qualitative information was presented and no western blot quantification was given. Furthermore, in the Jurkat leukaemic T-cell line, 2 hours of 10 μM CBD incubation lead to a decrease in phosphorylated rpS6[411]. Despite phosphorylation sites not being given, this suggests a possible contribution of the Erk or mTOR pathway to this change, as both kinases phosphorylate S6K. Contrasting with the previous studies, in a rat model of schizophrenia (amphetamine-induced sensitization), intracerebral injection of 100 ng/0.5μL CBD over 5 days resulted in a reduction of pGSK3β (Ser9) and pAKT (Ser473) and increased pmTOR (Ser2448) and pS6K (Thr389)[410]. Giacoppo and colleagues also found increased mTOR pathway activation after CBD administration to a mouse model of autoimmune encephalomyelitis (EAE). Analysis of western blot data after daily intraperitoneal injections of 10 mg/kg CBD across 28 days demonstrated increased pAKT, pmTOR and pS6K[453], although specific phosphorylation sites of action were not provided.

The effects of CBD on the mTOR pathway have also been analysed indirectly through the co-administration of rapamycin. In a model of cocaine-induced seizures, CBD reduced seizure duration across different concentrations (15-90 mg/kg), but this effect was prevented by pre-treatment with rapamycin[448]. Moreover, when exposed to the forced swim test, mice receiving 10 nmol/0.2μL of CBD into the dorsal hippocampus presented with reduced immobility time, an effect that was absent from mice pre-treated with rapamycin[406]. These results were replicated in a separate study using the forced swim test in rats[454].

The previously described actions of CBD along the mTOR pathway, and the effect of the latter on cell size regulation, suggest that CBD could also modulate size. Indeed, Kalenderoglou and colleagues reported that the treatment of Jurkat lymphoblastic T cells with 10 μM CBD lead to a decrease in cellular volume[411]. In this work, mTOR pathway inhibition by CBD was suggested given that a decrease in phosphorylated rpS6 and phosphorylated mTOR was observed after compound incubation[411]. Likewise, the incubation of T-47D and MDA-MB-231 breast cancer cells with 7 μM CBD was also reported to reduce mTOR phosphorylation and cell size[413]. Astrocytic hypertrophy, an important indicator of inflammation and

putative brain damage, was also shown to be reduced in the hippocampus after a 10 mg/kg or 30mg/kg CDB treatment[455,456]. Despite the fact that mTOR involvement was not explored in these last studies, agonism of peroxisome proliferator-activated receptor gamma (PPARɣ) was suggested as a potential mechanism of action of CBD. Interestingly, PPARɣ induction was shown to reduce mTOR signalling albeit in a mouse model of osteoarthritis[457]. Nonetheless, it is important to acknowledge that both the effects of PPARɣ in the TSC brain and the effects of CBD on neuronal size remain unexplored.

Altogether, reports on CBD's mechanism of action present conflicting results that include both decreased and increased activation of the mTOR pathway. The effects of CBD on mTOR signalling originated not only molecular changes but also behavioural modifications that appeared to be largely disease-dependent. Therefore, given this action along the mTOR pathway, it is possible to hypothesize that CBD may contribute towards mTOR regulation in TSC, ultimately aiding disease management beyond seizure control.

1.3 Aims and objectives

Cannabidiol has been widely investigated in our research group regarding its anti-epileptic properties in different *in vivo* models of seizures and epilepsy. In itself, this is a therapeutic property that could be highly beneficial for TSC patients given the high prevalence of epilepsy in this population. However, other neurological and neuropsychiatric manifestations are present in TSC. The main goal of this project was to explore potential new properties of CBD. I investigated if this compound could provide specific therapeutic contributions towards TSC, with regards to the mTOR pathway, central molecular alterations and behavioural modulation. To explore these research questions, two different animal models of TSC, the *tsc2*^{vu242} zebrafish and the *Tsc2*$^{+/-}$ Eker rat, were used and, with these, I attempted to answer the following:

<u>What is the effect of short- or long- term CBD treatment on:</u>

1) phosphorylated rpS6, a readout of mTOR activity?

2) cerebellar morphology and ASD-like molecular markers?

3) TSC-mutation-induced aberrant behaviour?

Chapter 2: Cannabidiol modulates phosphorylated rpS6 signalling in a zebrafish model of Tuberous Sclerosis Complex

The chapter presented here is the final manuscript version submitted to **Brain Behavioural Research**, *later published as* 363:135-144 (2019) *under the authorship of* ***Ines Serra***, *Chloë Scheldeman, Michael Bazelot, Benjamin J. Whalley, Mark L. Dallas, Peter A. M. de Witte and Claire M. Williams. The work presented in this chapter is also partially described in the patent "Use of Cannabidiol in the treatment of tuberous sclerosis complex"* (*WO/2018/234811). Alterations were performed to comply with the structure and layout of this thesis.* All experiments described in this chapter were performed by myself with the exception of the chronic CBD treatment, performed by Chloë Scheldeman.

2.1 Abstract

Tuberous sclerosis complex (TSC) is a rare disease caused by mutations in the *TSC1* or *TSC2* genes and is characterized by widespread tumour growth, intractable epilepsy, cognitive deficits and autistic behaviour. CBD has been reported to decrease seizures and inhibit tumour cell progression, therefore we sought to determine the influence of CBD on TSC pathology in zebrafish carrying a nonsense mutation in the *tsc2* gene.

CBD treatment from 6 to 7 days post-fertilization (dpf) induced significant anxiolytic actions without causing sedation. Furthermore, CBD treatment from 3 dpf had no impact on *tsc2*$^{-/-}$ larvae motility nor their survival. CBD treatment did, however, reduce the number of phosphorylated rpS6 positive cells, and their cross-sectional cell size. This suggests a CBD mediated suppression of mechanistic target of rapamycin (mTOR) activity in the *tsc2*$^{-/-}$ larval brain.

Taken together, these data suggest that CBD selectively modulates levels of phosphorylated rpS6 in the brain and additionally provides an anxiolytic effect. This is pertinent given the alterations observed in mTOR signalling in experimental models of TSC. Additional work is necessary to identify upstream signal modulation and to further justify the use of CBD as a possible therapeutic strategy to manage TSC.

2.2 Introduction

Tuberous sclerosis complex (TSC) is a rare genetic disease caused by a mutation in the *TSC1* or *TSC2* genes, coding for the proteins hamartin and tuberin, respectively[15]. TSC1 and TSC2 form an inhibitory complex with GTPase-activating protein (GAP) activity. This keeps Ras homolog enriched in brain (Rheb) bound to GDP and in an inactive form, preventing downstream phosphorylation of mechanistic target of rapamycin (mTOR). In humans and animal models of

TSC, mutations in TSC1 or TSC2 impair the inhibitory function of the complex, allowing activation of Rheb by GTP and constitutive activation of mTOR[257,458].

mTOR is a major convergence point for extracellular signalling, through regulation of anabolic processes such as transcription and translation[267]. This regulation of protein synthesis by mTOR extends throughout the mammalian lifespan and is crucial for central nervous system (CNS) development, where it controls soma size, dendritic arborisation, cortical lamination, and plasticity[289,459].

Overactivation of mTOR is evident in the majority of TSC patients that present with benign tumours in several organs, such as skin, kidneys and brain[16,459]. These often require surgical treatment and are a major source of morbidity for patients[23]. Furthermore, disruption of mTOR function in TSC also leads to neurological and neuropsychiatric complications in 85% of patients. Brain lesions such as cortical dysplasia, subependymal nodules and tubers are present in 70-90% of these patients[15]. Importantly, tubers and the perituberal tissue have long been associated with epilepsy, the most common neurological manifestation in TSC. In fact, 80-96% of patients have epilepsy with two thirds refractory to existent therapies[15,18]. Failure to control seizures in TSC patients is highly correlated with an early onset of seizures, before the age of 1 year old, in the form of focal epilepsy and infantile spasms[82]. Epilepsy is frequently associated with tuberous sclerosis associated neuropsychiatric disorders (TAND), such as autism spectrum disorder, present in 40-50% of patients, and intellectual disability, present in 30%[18,205]. The importance of seizure control is further reinforced by its positive impact on developmental outcomes and QoL assessments[172,460]. Nonetheless, despite the availability of some treatment options, due to the high heterogeneity of manifestations and TSC phenotype, not all individuals respond to the currently available therapies and new options are needed to attend to the patients' needs[81,82,89].

Given that a vast array of different systems and organs are affected by TSC, treatment typically requires a poly-pharmacological approach. mTOR inhibitors, such as rapamycin and everolimus, are current first-line treatments to control the growth of asymptomatic lesions. Epilepsy treatment can include one or multiple anti-epileptic drugs (AEDs), especially if resistance is present. Vigabatrin, which has been proposed to modulate both GABA levels and the mTOR pathway[153], displays good efficacy in TSC and is the most commonly used AED in these patients[14,18]. Regarding TAND, no specific therapies are yet approved, although early-intervention neuropsychiatric programmes, seizure control and mTOR inhibition have shown to contribute to cognitive improvement[18,92].

There is growing evidence to support the use of cannabidiol (CBD), the most abundant non-euphoric phytocannabinoid derived from *Cannabis sativa*[396], in the management of seizures[374]. Previous *in vitro* and *in vivo* studies have demonstrated the efficacy of CBD in reducing the frequency and severity of seizures, in different models of epilepsy[461,462]. More recently, two clinical trials provided evidence of a CBD induced reduction in the median frequency of convulsive

seizures and of drop seizures, in Dravet Syndrome (DS) and Lennox-Gastaut Syndrome, respectively[404,427]. Additionally, an expanded-access study of CBD for patients with TSC also suggested an effect of CBD in reducing seizure frequency in this population[403]. CBD has also shown beneficial effects in tumour studies. *In vitro* reduction of cellular viability and proliferation was demonstrated in both tumour cell lines[412,414,463–466] and primary tumour cells[463], whilst reducing tumour volume[414,463,465] and metastasis *in vivo*[414,467,468]. Importantly, CBD has been shown to modulate some components of the mTOR pathway[410–412,414,448,453,454], however there is a divergence in the reported effects with evidence from the cancer field supporting a CBD inhibition of mTOR, while epilepsy studies indicate an activation of mTOR. Therefore, in the complex pathology of TSC, the modulation of mTOR signalling via CBD is unclear.

Several animal models are available for the study of TSC, although none of these fully replicates all features of the human disease[60]. Mammalian models include the Eker rat, with a spontaneous *Tsc2* mutation, and several conditional knockout mice which allow biallelic inactivation of *Tsc1* or *Tsc2* in a cell specific manner[60,469]. Non-mammalian models are also widely used, as it is the case of *Saccharomyces cerevisiae, Drosophila* and zebrafish[470]. The zebrafish model of TSC used here carries the nonsense *vu242* mutation in the *tsc2* gene[327]. This renders tuberin inactive as it lacks the functional GAP domain. Several human-like disease features, such as increased phosphorylation of rpS6, a protein downstream of mTOR and often used as a readout of mTORC1's activity[177,306], increased cell size and early death of homozygotes, are present in this model[327]. More recently, an mTOR-dependent disruption of locomotor behaviour was also demonstrated in homozygous tcs2$^{-/-}$ larvae[354]. Here we use a zebrafish model of TSC to examine the effects of CBD on the pathogenesis of TSC, including behavioural effects and ribosomal protein 6 phosphorylation. Our data highlights that CBD can modulate the mTOR pathway, through regulating the phosphorylation status of ribosomal protein 6 in a relevant model of TSC.

2.3 Materials and methods

2.3.1 Zebrafish Husbandry

Zebrafish embryos, heterozygous for the *tsc2*^{vu242} mutation backcrossed with Tupfel longfin wild-type fish, were a generous gift of Malgorzata Wiweger, head of the Zebrafish Core Facility of the International Institute of Molecular and Cell Biology (Warsaw, Poland). The zebrafish model of TSC with a *tsc2* nonsense mutation (*tsc2*$^{+/-}$) was previously described[327,354]. For this study, heterozygous (*tsc2*$^{+/-}$) zebrafish were interbred to generate a mixture of wild-type (*tsc2*$^{+/+}$), heterozygous (*tsc2*$^{+/-}$) and homozygous (*tsc2*$^{-/-}$) larvae. Adult zebrafish were maintained at 28.5 °C in UV-sterilized water on a 14 h light/10 h dark cycle under standard aquaculture conditions. Fertilized eggs were collected via natural spawning. Embryos and larvae (*tsc2*$^{+/+}$, *tsc2*$^{+/-}$ and *tsc2*$^{-/-}$)

were raised in embryo medium, containing 1.5 mM HEPES, pH 7.6, 17.4 mM NaCl, 0.21 mM KCl, 0.12 mM $MgSO_4$ and 0.18 mM $Ca(NO_3)_2$ in an incubator on a 14 h light/10 h dark cycle at 28.5 °C. For all experiments described, larvae from 0 to 10 days post-fertilization (dpf) were used. All zebrafish experiments were approved by the Ethics Committee of the University of Leuven (Ethische Commissie van de KU Leuven, approval number 061/2013) and by the Belgian Federal Department of Public Health, Food Safety and Environment (Federale Overheidsdienst Volksgezondheid, Veiligheid van de Voedselketen en Leefmilieu, approval number LA1210199).

2.3.2 Maximum tolerated concentration (MTC)

6 dpf larvae were placed in a 24 well-plate (Corning Inc., New York, USA) and incubated with 396 µL of swimming medium (Danieau's) and 4 µL DMSO (0.1 or 1%) or CBD (GW Pharmaceuticals, Cambridge, UK) dissolved in DMSO, directly added to the swimming media. CBD was serial diluted and tested in concentrations ranging from 0.3 µM to 125 µM. Plates were then transferred to a 37 ˚C incubator, in the dark, and larvae touch-response was tested after 1 and 24 hours of incubation. The MTC was defined as the highest concentration of CBD in DMSO that did not induce any observable signs of toxicity, such as necrosis, abnormal heart beat or loss of posture[471].

2.3.3 Locomotor assay

The locomotor assay was performed as previously published[354]. 6 dpf larvae were placed in a 24 well-plate and treated with Danieau's (called *naïve* larvae in the text), 0.1% DMSO or 1.25 µM CBD in 0.1% DMSO, by adding compounds directly to the swimming media. The larvae were incubated in the plate in dark for 24 hours in a 37ºC incubator. After 24 hours, the plates were removed from the incubator and placed in a ZebraBox (ViewPoint, Behaviour Technology, USA). Here, the movement of the larvae was automatically tracked in both light and dark conditions (see below) and expressed in "*actinteg*" units (which is the sum of pixel changes detected during tracking). In the ZebraBox, fish were first habituated for 10 minutes under both light and dark conditions before being tracked for 5 minutes in both the light and dark conditions. To measure anxiogenic or anxiolytic effects due to compound administration, changes in the startle response upon light to dark transition were measured as previously published[472,473]. Touch response (TR) can be used to corroborate the MTC data for toxicity as it is also a measure of larval peripheral reflexes[474]. Therefore, the touch-response of the larvae was also tested, by touching the larvae's tail with a blunt needle, before and after tracking. The number of responding and non-responding larvae was registered. All researchers were blinded to genotype throughout behavioural testing and data analyses.

2.3.4 Chronic treatment and survivability assay

Larvae were incubated in 200 µl of Danieau's, in a 96-well plate, and observed daily from 3 dpf until 10 dpf. The swimming medium was changed every other day and 0.1% DMSO or 1.25 µM CBD in 0.1% DMSO added to each larva's well. During this period of observation, the number of dead larvae was counted. At the end of the assay, when larvae were 10 dpf, the surviving larvae underwent the previously described locomotor assay (Section 2.3.3).

2.3.5 Genotyping

Genotyping was conducted as previously published[354].After the locomotor assay, larvae were sacrificed in ice cold water. Larvae were placed under a stereo microscope (Leica) and zebrafish tails were dissected. Tails were lysed in 10 mM Tris-EDTA pH 8, 2 mM EDTA 0.5 M pH 8, 0.2% Triton-X-100 and 200 µg/ml Proteinase K in MilliQ water for 3 hours, at 55 ˚C, followed by 10 minutes at 95 ˚C. PCR was performed on the lysates using *Pfu* polymerase (Thermo Scientific, UK), and the primers GTAACACAGAATCAGTGAATCGGA (forward primer) and CACACACAGAAAACACTTGAAGC (reverse primer), amplifying a 500 bp DNA fragment. After PCR, samples underwent digestion with the restriction enzyme *HpyCh4 IV* (New England Biolabs, UK), for 1 hour, at 37 ˚C, followed by fragment separation on a 2% agarose/0.5 µg/mL ethidium bromide gel, for 1 hour, at 110 V. Due to post-mortem genotyping, and because a smaller ratio of *tsc2*$^{-/-}$ larvae is obtained compared to *tsc2*$^{+/+}$ and *tsc2*$^{+/-}$, variation in group sizes exists throughout experiments.

2.3.6 Immunohistochemistry (IHC)

After completion of the locomotor assay, 7 dpf zebrafish larvae were sacrificed in ice cold water. Heads were dissected under a stereo microscope (Leica) and placed in 4% PFA for 48 hours, at 4 ˚C, and then transferred into a 30% sucrose in PBS solution, at 4 ˚C. Zebrafish heads were then briefly dried, embedded in optimum cutting temperature (OCT) compound, frozen in dry ice and stored at -80 ˚C until sectioned.

For IHC, 10 µm sections were cut and collected onto microscope slides (SuperFrost Plus, Thermo Fisher Scientic, UK) and stored at -80 ˚C until used. On the first day of IHC, sections were incubated for 2 hours, at room temperature, in a 2% BSA, 10% horse serum and 0.05% TX-100 buffer, followed by an overnight incubation with a primary antibody against phosphorylated rpS6 (Ser235/236) (1:500; 2211 New England Biolabs, lot 0023, UK), in a 1 % BSA and 0.05% TX-100 buffer, at 4 ˚C. The next day, slides were rinsed 3 x 10 minutes in Tris-buffered saline (TBS) and incubated for 2 hours, at room temperature, with a goat anti-rabbit Alexa Fluor-647 secondary

antibody (1:1000; A-21245 Thermo Fisher Scientific, lot 1805235, UK). After 3 further TBS rinses, each of 10 minutes, sections were counterstained with DAPI (1:10 000; D1306 Thermo Fisher Scientific, UK) during a 10-minute incubation. At the end of this stage, slides were rinsed in TBS, dried at room temperature, and mounted in DPX.

For TUNEL staining (1:10; 12156792910 Roche, lot 26320800, Sigma, UK), slides underwent the same buffer incubation procedure explained above, excluding antibody incubation. After the final rinsing step, sections were incubated with TUNEL solution according to manufacturer's instructions, in the dark, for 1 hour, at 37 ˚C. A negative control slide was obtained by omitting the enzyme solution from incubation, while positive control was performed by previous incubation of sections with 5 mg/mL DNAse, for 10 minutes, at 37 ˚C.

2.3.7 Imaging and image quantification

After IHC or TUNEL stain, non-consecutive brain sections were imaged using a Zeiss AxioImager microscope. Exposure time was constant during image acquisition and background fluorescence was measured in sections from slides where the primary antibody or enzyme solution was omitted. Pictures were taken with a 20x objective using the AxioVision software. The obtained original images were processed on Fiji Image J[475]. First, a region of interest (ROI) was freehand defined around the brain outline. Then, the average intensity value for each previously defined ROI, in each picture, was measured as Intensity Arbitrary Units (IAU), following background subtraction for each picture. For cell counting, cells were considered positive for the rpS6 antibody if staining for both phosphorylated rpS6 and DAPI were clearly present. To measure cell size, a similar procedure was used, except five cells per picture were randomly selected and its cross-sectional area measured. A minimum of three animals per group and genotype were used, and 3-9 sections per animal were imaged and counted.

2.3.8 Statistical analysis

Statistical analysis was performed in SPSS (IBM SPSS Statistics 22) and GraphPad Prism 5. Repeated measures two-way ANOVA was used to analyse data from the locomotor assay (genotype x treatment x exposure to light/dark) and phosphorylated rpS6 positive cell number (genotype x treatment x number positive cells/section), while a three-way ANOVA was used to analyse cell size (genotype x treatment x area of cells). Touch response (TR) (yes x no) was analysed by chi-square test and TUNEL positive cells with the Kruskal- Wallis test. Normality was assessed with the D'Agostino-Pearson omnibus test. Statistical testing was followed by Tukey or Bonferroni post-hoc tests.

Data are expressed as mean ± SEM unless stated otherwise, and significant values were considered when $p \leq 0.05$. All graphs were prepared with GraphPad Prism 5.

2.4 Results

2.4.1 CBD safety profile

To determine the maximum tolerated concentration (MTC) to be used in further experiments, CBD and DMSO were tested at different concentrations, ranging from 0.3 µM to 125 µM CBD in DMSO, and 0.1% to 1% respectively.

Concentrations from 5 to 125 µM CBD in 1% DMSO, induced varying levels of toxicity in the larvae, manifested by slow heartbeat, loss of posture and death. We then compared lower CBD concentrations (0.3 to 2.5 µM) in 0.1 or 1% DMSO. Here, the toxicity of CBD was reduced with the decrease in DMSO concentration from 1% to 0.1%. 1.25 µM CBD in 0.1% DMSO was the highest CBD concentration in which all animals were alive after 24 hours and showed no signs of gross morphological abnormalities.

At a cellular level, toxicity signs were absent from the central nervous system, as indicated by a non-significant difference ($p=1.0$) in the number of apoptotic cells, as indicated by positive TUNEL staining (Fig. 2.1A-C).

Regarding touch-response, compared to both the Danieau's and 0.1% DMSO treated groups, administration of CBD from 6 to 7 dpf did not affect the percentage of responders to touch ($\chi^2(2)=2.51$, $p=0.3$; 98.0% for Danieau's, n=155; 95.8% for 0.1% DMSO, n=166; 94.7% for CBD, n=171), as manifested by a non-significant difference in the TR of treated larvae (Fig.2.2A).

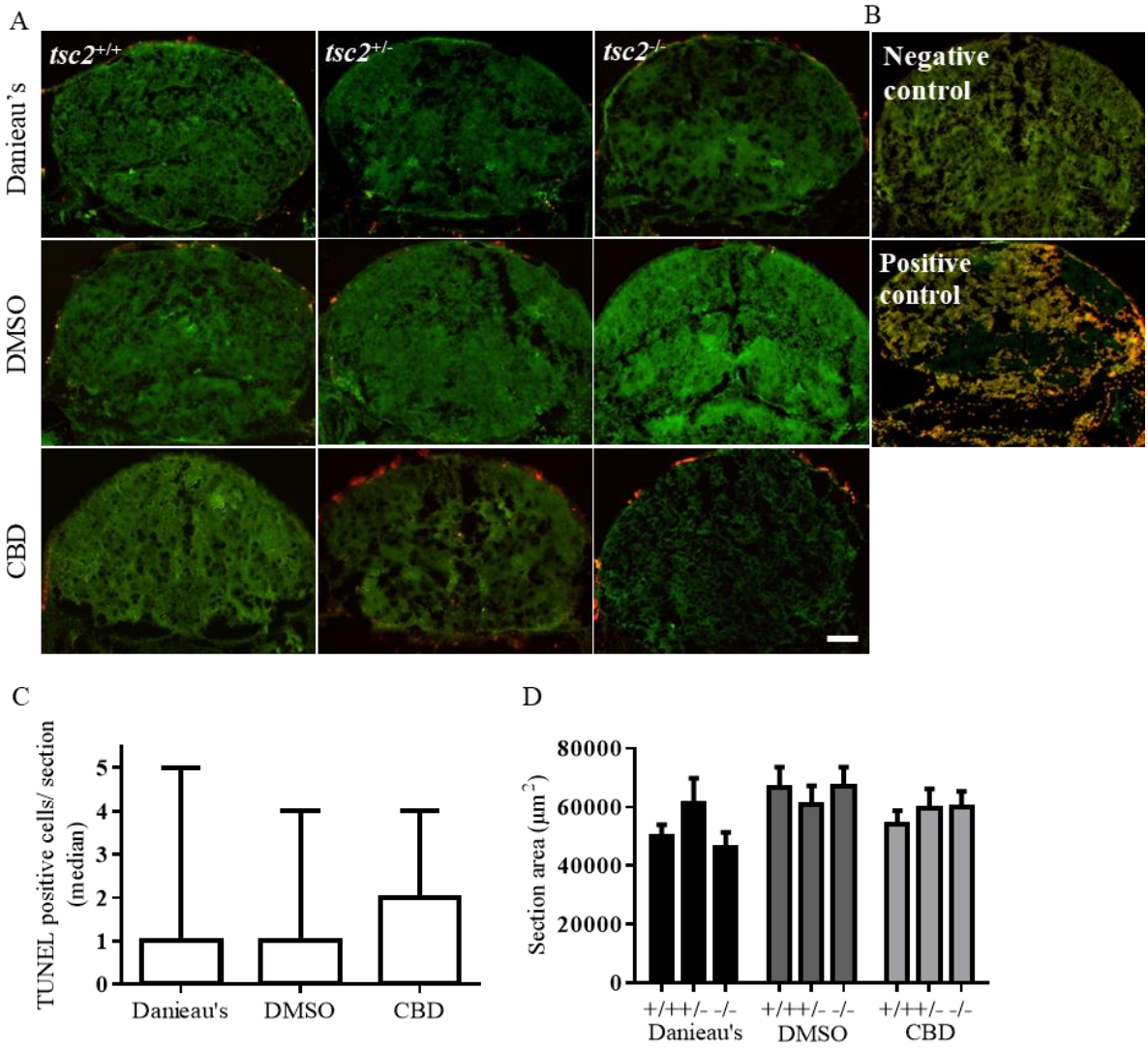

Figure 2.1: TUNEL labelling in the larval brain. (A) Representative pictures of the midbrain, for each treatment (Danieau's, 0.1% DMSO and 1.25 µM CBD) and genotype (*tsc2*$^{+/+}$, *tsc2*$^{+/-}$ and *tsc2*$^{-/-}$), showing TUNEL positive cells in red and tissue autofluorescence in green. (B) Representative pictures of negative control, where enzyme solution was omitted, and of positive control, incubated with DNAse. (C) The median number of TUNEL positive cells in each section was analysed and revealed no statistical differences between treatment groups. (n=3 animals per group; p=1.0. Data shown as median and minimum to maximum values) (D) Measurement of brain sections' area showed no significant differences in the mean cross-sectional size, regardless of genotype ($F(2,209)=0.30$, $p=0.7$) or treatment ($F(2,209)=2.92$, $p=0.06$) (n= 3-4 animals per group, 15-30 sections per group measured). Scale=50 µm.

2.4.2 Behavioural effects of CBD

2.4.2.1 CBD does not induce sedation in this zebrafish TSC model

Next, we analysed larvae locomotor behaviour. To test the reported sedative properties of CBD[403,427], we quantified the average swimming movement of larvae during the light period, as a reduction of overall exploratory movement can be used as a measure of sedation[476,477]. There were no statistically significant differences in the baseline behavioural exploration, between vehicle (0.1% DMSO, 24h incubation) and CBD (1.25 µM, 24 hour incubation) treated larvae ($F(1,322)=2.28$, $p= 0.1$), in the *tsc2*$^{+/+}$ (2275.9 ± 190.3 *actinteg* units, n=63 vs 1914.7 ± 289.1 *actinteg* units, n=49, p=0.873), *tsc2*$^{+/-}$ (2349.3 ± 241.7 *actinteg* units, n=76 vs 1907.3 ± 158.2 *actinteg* units, n= 92, p=0.338) and *tsc2*$^{-/-}$ (906.1 ± 208.3 *actinteg* units, n=26 vs 732.5 ± 159.1 *actinteg* units, n=22, p=1.00) groups, indicating that, under these conditions, CBD does not induce sedation (Fig. 2.2B).

2.4.2.2 CBD reduces startle response of larvae during the dark period

Zebrafish larvae respond to changes in light beginning from 5 dpf[478,479], and sudden changes from light to dark induce a startle response. Decreased locomotion after a startle stimulus is indicative of an anxiolytic effect[477,478,480–482]. Here, CBD (1.25 µM, 24 hour incubation) treatment significantly reduced dark-induced movement compared to 0.1% DMSO ($F(1,322)=7.26$, $p=0.01$) (Fig.2.2C).

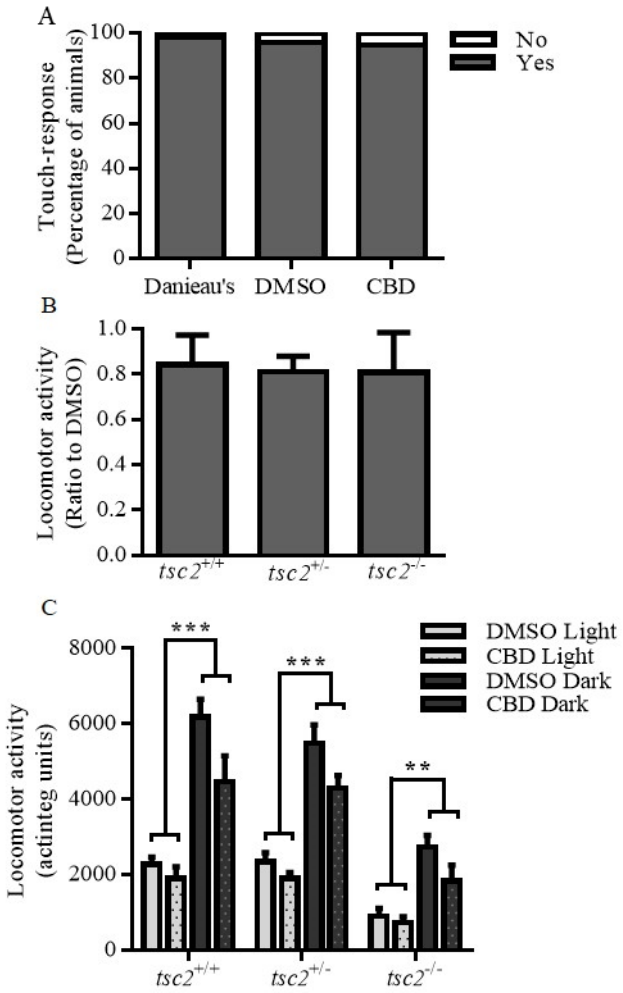

Figure 2.2: Treatment and genotype effects on larval locomotor behaviour. (A) Zebrafish touch-response was tested after compound incubation and is not altered by the presence of 0.1% DMSO nor CBD. Pooled data demonstrating no significant differences ($\chi^2(2)=2.5$, p= 0.3) between the percentage of zebrafish responding to touch in each treatment group (n=152 for Danieau's, n=165 for 0.1% DMSO, n=163 for CBD). Values are shown as percentage of "Yes" or "No" response. (B) CBD has no effect on locomotor activity during light phase. *Actinteg* units normalised to vehicle (0.1% DMSO) values demonstrate lack of effect on swimming activity under light (F(1,322)=2.28, p= 0.1), following exposure to CBD, indicating the absence of sedating properties (n= 49-63 for *tsc2*$^{+/+}$, n=76-92 for *tsc2*$^{+/-}$, n= 22-26 for *tsc2*$^{-/-}$). (C) CBD reduces zebrafish locomotor activity after a dark startling stimulus. Exposure to CBD during the light period (light bars) did not alter the average larval movement in any genotype. In the presence of a dark startling stimulus (dark bars), CBD induced a reduction of the average swimming activity (F(1,322)=7.26, p=0.01). Values are shown as mean *actinteg* units ± SEM, ***p<0.001, **p<0.01, *p<0.05.

2.4.2.3 CBD does not rescue homozygote behavioural phenotype

One of the features of this model is early death of *tsc2*$^{-/-}$ homozygotes, between 9 and 11 dpf[327,354]. This can also be seen in other TSC model organisms, such as mice and rats, which typically die at embryonic day 10-10.5[233,281,359]. Additionally, reduced overall locomotion was recently shown in *tsc2*$^{-/-}$ larvae[354]. We therefore assessed the effects of long-term CBD incubation, from 3 to 10 dpf, on survivability and locomotion. No difference in the survival of *tsc2*$^{-/-}$ larvae ($\chi^2(1)=0.27$, p=0.6; n= 72 per group) (Fig.2.3A) nor swimming ability (t(1)=3.06, p=0.2; 1459.8 ± 366.8 *actinteg* units, n=28, vs 2875.6 ± 520.1 *actinteg* units, n=27) (Fig.2.3B) was found between 0.1% DMSO and CBD treated groups.

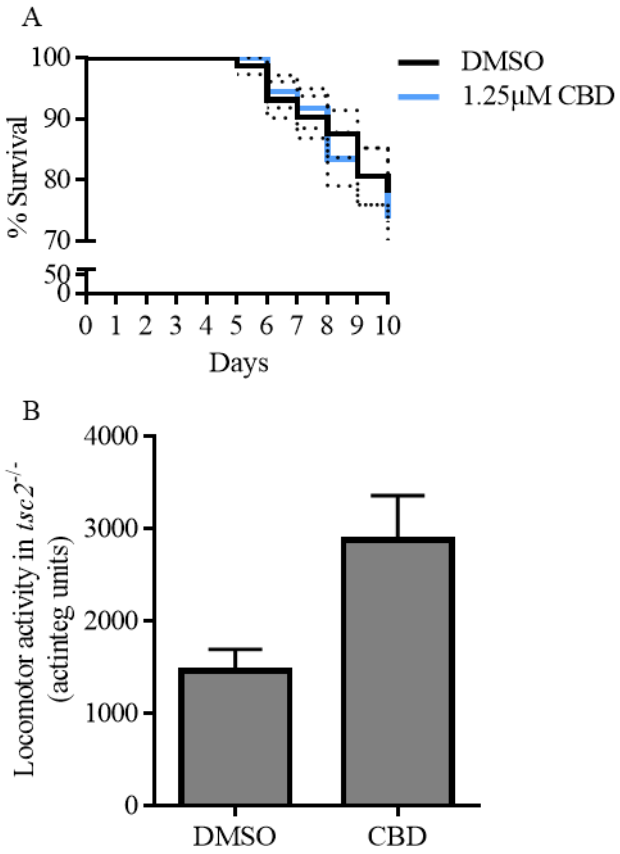

Figure 2.3: *CBD does not improve tsc2*$^{-/-}$ *larvae survival nor rescues movement deficits.* (A) Daily incubation of larvae with 1.25 µM CBD, from 3-10 dpf, did not alter *tsc2*$^{-/-}$ larvae survival compared to the vehicle DMSO (n=72 per group). (B) Daily incubation of larvae with CBD treatment from 3-6 dpf CBD did not modulate movement deficits in *tsc2*$^{-/-}$ larvae (t(1)=3.06, p=0.2; 1459.8 ± 366.8 vs 2875.6 ± 520.1 *actinteg* units, n= 28 for 0.1% DMSO and n=27 for CBD, data presented as mean ± SEM) (Data collected by Chloë Scheldeman).

2.4.3 CBD modulates phosphorylated rpS6

2.4.3.1 CBD reduces the number of phosphorylated rpS6 positive cells in *tsc2*$^{+/+}$, *tsc2*$^{+/-}$ and *tsc2*$^{-/-}$ larvae

We subsequently assessed the impact of CBD treatment upon rpS6 phosphorylation, which is increased in *tsc2*$^{-/-}$ zebrafish[327,354]. In the Danieau's group, we observed increased phosphorylated rpS6 immunofluorescence in *tsc2*$^{-/-}$ zebrafish brains (18.0 ± 2.0 IAU), compared to the *tsc2*$^{+/+}$ (8.0 ± 1.1 IAU) and *tsc2*$^{+/-}$ (8.4 ± 1.3 IAU) groups, confirming what others had previously shown[327,354]. Unexpectedly, an overall increase in phosphorylated rpS6 intensity was also observed in sections from 0.1% DMSO incubated larvae (10.72 ± 1.7, for *tsc2*$^{+/+}$, 6.0 ± 0.6, for *tsc2*$^{+/-}$, 12.1 ± 1.4 IAU, for *tsc2*$^{-/-}$), while reduced immunofluorescence was found in the CBD groups (4.5 ± 0.6, for *tsc2*$^{+/+}$, 6.0 ± 0.9, for *tsc2*$^{+/-}$, 11.09 ± 1.2, for *tsc2*$^{-/-}$ IAU) (Fig.2.4A).

Section size was accounted for by prior analysis of total brain section size. This revealed no significant differences between genotypes or treatments (Fig.2.1D).

Quantification of phosphorylated rpS6 positive cells revealed a significant main effect of treatment, indicating that 0.1% DMSO on its own increased the number of phosphorylated rpS6 positive cells per section (187.1 ± 13.6 cells per section) compared to Danieau's (116.1 ± 11.7 cells per section) and to CBD (42.8 ± 13.0 cells per section). Considering genotype-specific effects, further analysis revealed that 0.1% DMSO significantly increased the number of phosphorylated rpS6 positive cells in the *tsc2*$^{+/+}$ group, while this increase was not evident in the *tsc2*$^{+/-}$ and *tsc2*$^{-/-}$ group. CBD suppressed the DMSO-induced increase in the number of phosphorylated rpS6 positive cells across all genotypes (184.1 ± 26.0, n=12 vs 10.7 ± 19.6, n=21, $p<0.001$; 97.7 ± 23.2, n=15 vs 3.2 ± 26.0, n=12, $p=0.03$; 279.3 ± 21.2, n=18 vs 114.7 ± 21.2, n=18 $p<0.001$; for *tsc2*$^{+/+}$, *tsc2*$^{+/-}$ and *tsc2*$^{-/-}$ larvae, respectively) (Fig.2.4C).

Taken together, this data suggests that CBD led to a reduction of phosphorylated rpS6 immunoreactivity in larval brain.

2.4.3.2 CBD reduces the size of phosphorylated rpS6 positive cells in *tsc2*$^{+/+}$, *tsc2*$^{+/-}$ and *tsc2*$^{-/-}$ larvae

The phosphorylation status of rpS6 has been correlated with cell size[411,483], therefore we measured the cross-sectional area of phosphorylated rpS6 positive cells in the brain (Fig.2.4B).

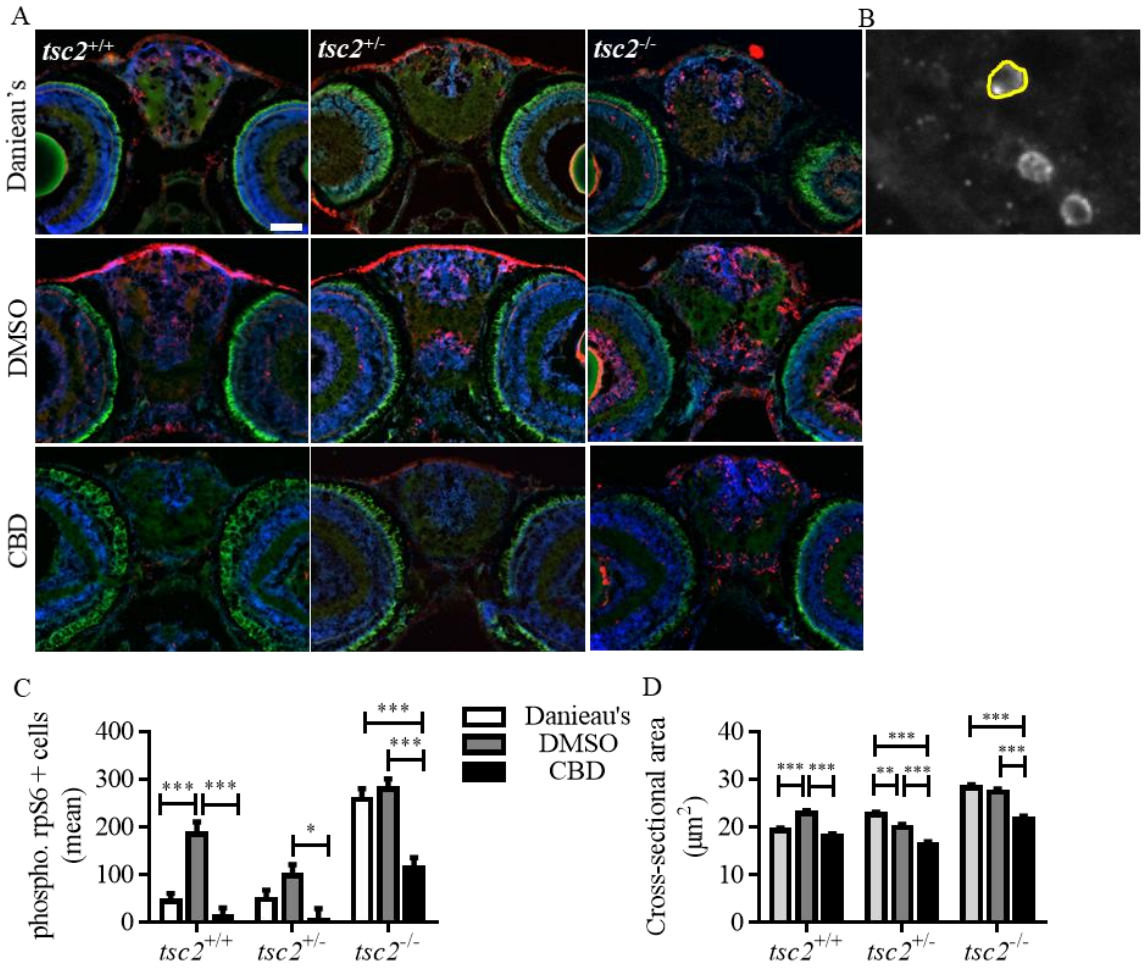

Figure 2.4: *CBD reduces the number and size of phosphorylated rpS6 (Ser235/236) positive cells.* (A) Representative immunohistochemistry pictures of the forebrain of Danieau's, 0.1% DMSO and CBD incubated larvae of the three genotypes. Blue represents DAPI, green tissue autofluorescence and red phosphorylated rpS6 (Ser235/236) positive cells. (C) Quantification of the number of phosphorylated rpS6 (Ser235/236) positive cells in larval brain sections reveals that 0.1% DMSO incubation increased the number of phosphorylated rpS6 (Ser235/236) positive cells in the $tsc2^{+/+}$ group. CBD reduced the number of positive cells in all genotypes compared to 0.1% DMSO but only in the $tsc2^{-/-}$ group, compared to the Danieau's incubated larvae ($F(4,44)=3.14$, $p=0.02$; n= 3-9 sections analysed, from 3-4 animals per group). (B) Magnification of a 0.1% DMSO-treated $tsc2^{+/+}$ brain section exemplifying how the cross-sectional area of phosphorylated rpS6 (Ser235/236) positive cells was measured. (D) The cross-sectional area of rpS6 (Ser235/236) positive cells was measured and CBD incubation induced a reduction of the average cross-sectional area of phosphorylated rpS6 (Ser235/236) positive cells in all genotypes, compared to 0.1% DMSO ($F(4,1050)=9.06$, $p<0.001$; n= 77-115 cells per genotype and treatment from 3-4 animals per group). Values are shown as mean ± SEM. ***$p<0.001$, *$p<0.05$. Scale=50 µm.

A genotype dependent increase in cell area was seen in the naïve group. That is, cells from *tsc2*$^{+/-}$ sections were larger than *tsc2*$^{+/+}$ (22.5 ± 0.6 μm^2, n=133 vs 19.3 ± 0.5 μm^2, n=165; p<0.001), while *tsc2*$^{-/-}$ cells were also larger compared to *tsc2*$^{+/-}$ (28.3 ± 0.6 μm^2, n=105 vs 22.5 ± 0.6 μm^2, n=133; p<0.001) (Fig. 2.4D). Therefore, while a difference in the number of phosphorylated rpS6 positive cells between the naïve *tsc2*$^{+/+}$ and *tsc2*$^{+/-}$ larvae was absent, here, the area of cells from heterozygote and wild-type animals did differ. Regarding CBD incubated larvae, these had smaller phosphorylated rpS6 positive cells than the ones present in the 0.1% DMSO group (Fig.2.4C). This effect was seen across *tsc2*$^{+/+}$ (22.8 ± 0.7 μm^2, n= 95 vs 18.0 ± 0.6 μm^2, n=129; p<0.001), *tsc2*$^{+/-}$ (19.9 ± 0.6 μm^2 n=115 vs 16.3 ± 0.6 μm^2 n=77; p=0.001) and *tsc2*$^{-/-}$ larvae (27.4 ± 0.6 μm^2, n=115; 21.7 ± 0.6 μm^2, n=144; p<0.001) (Fig.2.4D). Similar to results seen for cell number, where an effect of 0.1% DMSO was reported, a DMSO-driven increase in cell size was also observed here (Fig.2.4D). This was also significantly supressed by CBD incubation. Altogether, these data indicate that CBD reduces genotype and DMSO- induced increase of size in *tsc2*$^{+/-}$ and *tsc2*$^{-/-}$ zebrafish brain cells.

2.5 Discussion

CBD is a non-psychoactive component of *Cannabis*, that has increasingly been recognised as the basis for pharmacology intervention in a host of diseases[374,396,484]. Here we examine the effects of CBD to modulate aberrant mTORC1 signalling in zebrafish carrying a *tsc2* mutation.

Anxiety is a TSC-associated neuropsychiatric disorder and evidence indicates altered serotonin signalling as a biological mechanism[234,485–487]. One of the proposed targets for CBD is the 5-HT$_{1A}$ receptor, where it has been shown to bind and to have agonist functions *in vitro*[488,489]. Several serotonin receptors, orthologues to human receptors, have been shown to be expressed in zebrafish larvae, including the 5-HT$_{1A}$ receptor[349,490]. This is pertinent to the current study with the 5-HT$_{1A}$ receptor a proposed site of action for CBD[488,489]. However, contrasting with the function of mammalian 5-HT$_{1A}$ receptors, the role of these receptors on anxiety behaviour in zebrafish is less defined. For example, extracellular serotonin content has been reported to have contrasting effects on anxiety in the same adult zebrafish species[490,491]. Larvae, in contrast to their adult counterparts, exhibit a transient elevation in motor activity in response to sudden onset of darkness[347,478,492]. Dark avoidance was shown to be modulated by anxiolytic drugs such as the 5-HT$_{1A}$ agonist, buspirone, which increased dark preference patterns in zebrafish larvae[347].

Here we demonstrate a CBD induced reduction in startle response across genotypes. However, a limitation of this model is that *tsc2*$^{-/-}$ larvae do not reach adulthood and, therefore, later behavioural testing cannot be performed to confirm an anxiolytic effect of CBD in this genotype. Nonetheless, further studies in *tsc2*$^{+/-}$ larvae could still be beneficial to elucidate possible effects of CBD in TSC, given the clinical TSC population are heterozygous[16].

Several molecular processes have been proposed to modulate CBD actions[396]. The serotonergic system is one such example and modulation here could provide control of other TSC features such as epilepsy, highly prevalent in TSC patients[14]. Evidence from epilepsy studies indicates that a reduction in serotonin concentration promotes seizures, while reduced serotonin binding to the 5-HT_{1A} receptor has been reported in epileptogenic foci[493,494]. Studies also indicate that TSC patients present with increased tryptophan uptake localised to epileptic foci[495]. Given that CBD has been shown to reduce seizures in pathologies with different aetiologies[403,427,496], and that *tsc2*$^{-/-}$ zebrafish, and other TSC models, have been shown to exhibit abnormal brain activity[331,353,354,497], it would be relevant to further study its role in the serotonergic system of TSC models.

A hallmark of TSC across all experimental models is an increase in mTOR activity[15,289,327,458,459,498]. Activation of mTOR leads to an increase in the ratio of downstream targets phosphorylated rpS6 /total rpS6, both in *in vitro* and *in vivo* models[53,63,324,331]. Therefore, phosphorylated rpS6 is often used as a read out of mTOR activation[176,313,499]. The reduction of rpS6 phosphorylation presented here is in line with published work where CBD treatment was found to modulate the mTOR pathway. In breast cancer cells, incubation with CBD has been observed to modulate Akt, a kinase upstream of mTOR, as well as 4E-BP1 and cyclin D[412,414]. Another study also reported the reduction of ERK phosphorylation, a kinase upstream of mTOR[414]. The effects observed here with 0.1% DMSO may indicate a proinflammatory response[500–502] with subsequent activation on mTOR[503,504].

The mTOR-S6K-rpS6 axis is also known to have a major role in controlling cell size[304,313]. In fact, we saw that Danieau's incubated animals showed a mutation-dependent increase in cell size, with *tsc2*$^{-/-}$ brain cells bigger than *tsc2*$^{+/-}$, followed by *tsc2*$^{+/+}$. These results are similar to previous work on this model, where a difference in size was found between *tsc2*$^{+/+}$ and *tsc2*$^{-/-}$, in liver, brain, and spinal cord cells[327]. In accordance with a reduction in phosphorylated rpS6 positive cells there was a corresponding CBD effect on the cross-sectional area of brain cells. A comprehensive analysis of mTOR activity in phosphorylated rpS6 cells through enzymatic assay would definitely link the disruption in phosphorylated rpS6 to mTOR activity which remains unresolved in this current study.

However, contrasting effects on the mTOR signalling pathway by CBD have also been reported. For example, in amphetamine-sensitized rats, CBD reduced levels of pGSK-3β and pAkt, but importantly it induced an increase of pmTOR and pS6K[410]. To further demonstrate the effect of CBD on mTOR specifically, this effect was reversed with the mTOR inhibitor, Torin 2[410]. Additionally, administration of 10 mg/kg CBD to a mouse model of multiple sclerosis revealed increased pPI3K, pAkt, pmTOR and pS6K in spinal cord tissue. Importantly, in this model, basal levels of mTOR pathway activation were shown to be decreased[453]. Regarding the zebrafish model used here, we observed a decrease in phosphorylated rpS6, which could result from a reduction in

mTOR activation. However, the survival and locomotion data regarding the chronically CBD-treated *tsc2*$^{-/-}$ larvae highlight that this modulation of mTOR was insufficient to impact these whole system outputs.

2.6 Conclusion

In the current study, using a TSC zebrafish model, we demonstrate that CBD was tolerable, while behavioural testing showed that CBD exhibited an anxiolytic profile without sedative effects. Additionally, we showed modulation of rpS6 manifested by the reduction of the number and size of phosphorylated rpS6 positive cells in the brain. Altogether, these data demonstrate that CBD modulates aberrant mTOR signalling in a model of TSC. It provides a rationale for further investigation into CBD as a therapeutic agent in diseases where mTOR signalling is disrupted.

Chapter 3: The Eker rat cerebellum: ASD-like marker characterization and effects of CBD treatment

3.1 Introduction

TSC1 and 2, together with TBC1D7, form a complex that prevents GTP binding to Rheb, maintaining it in an inactive form[253,257,274,505]. In TSC, dysfunction of this complex allows Rheb to constitutively activate mTOR[251,253,267,284,289,506]. As a consequence of this overactivation, phosphorylation of downstream markers such as S6K and rpS6 ultimately leads to widespread tumour growth[16,289,304]. The brain is predominantly affected in TSC[3,18,24,351,507]. Neuropsychiatric dysfunction is present in TSC, with one of the most prevalent features being ASD, present in 20-60% of patients[14,94,112,113,115,117] (Section 1.1).

ASD is characterized by social communication impairments, restricted and repetitive behaviour, and inflexibility to change (Section 1.1.3.5). All of these symptoms have a major impact on QoL[508,509]. While psychosocial interventions are useful in managing ASD-associated symptoms and are included in European treatment guidelines, evidence for beneficial pharmacological treatments is not yet ascertained[114,510].

A vast array of drugs has been trialled towards the management of core and associated ASD features. However, there are no current pharmacological options specifically approved for use in ASD and, ultimately, careful examination of each individual is required to evaluate the benefit of drug prescription[114,511]. Commonly prescribed drugs for the management of ASD symptoms include antipsychotics (aripiprazole and risperidone), used to control irritability and repetitive behaviour; melatonin, prescribed in situations of insomnia, especially in paediatric settings; and methylphenidate, a dopamine and norepinephrine transporters' inhibitor recommended for ADHD symptoms[511–514]. Given the great variation of effects between the administration of these compounds to paediatric and adult populations, evidence for specific clinical benefit of these agents in ASD is limited and usually inconsistent among studies[114,511,515,516]. Non-pharmacological interventions, such as the ketogenic diet, show poor relief of ASD-associated symptoms despite providing seizure relief in TSC patients[155]. In one single clinical study, compliance to therapy proved to be low (18 out of 30 patients) with only 2/30 patients reporting significant improvements on the CARS[517].

mTOR inhibitors were recently proposed as an option to address ASD in TSC (Section 1.1.3.4.2), and are currently being evaluated in two clinical trials (NCT01289912 and NCT01954693)[518]. Yet, a few studies suggested that the use of mTOR inhibitors in TAND might be limited. Initially, small clinical studies suggested parent- and clinician-reported improvements in psychiatric symptoms and social cognition after short-term everolimus treatment (1-6 months)[94,172]. However, clinical data from long-term treatment periods (6-48 months) suggested that these

improvements might not persist over longer periods of time[186,519], implying a loss of treatment efficacy. mTOR inhibitors have been trialled for chemotherapy resistance due to mTOR hyperactivation in certain cancers[520–522]. In these cases, the development of mTOR inhibitor resistance has also been observed and, in some reports, shown to be mediated by a shift towards mTORC2 activation[523,524], which is not the primary target of mTOR inhibitors (Section 1.1.5.3).

The complexity of phenotypes and lack of biological markers hinder the study of ASD in TSC. However, cerebellar alterations have often been observed in individuals with ASD (Section 1.1.3.5)[106,124–126,147]. Alterations in PC number[127,135,525] and cross sectional area[526] have been reported, and PC loss has also been found in TSC cerebella[334]. Changes in cerebellar volume have also been reported[527] and MRI studies with children have detected reduced cerebellar grey matter volume[139,528–530]. In adults, reduced[122] or no change[531] in cerebellar volume was reported, although area-specific analysis of grey matter volume indicated a reduction of this parameter in the left side crus I area, progressive with age. Functional MRI revealed decreased connectivity between PC and the dentate nuclei in ASD patients[128]. Cerebellar-specific alterations in the GABAergic system have also been found, together with modifications in microglia morphology (Section 1.1.3.5). Finally, motor skill impairments, recognized in the diagnosis and treatment guidelines for ASD, also suggest a cerebellar role in its development, although movement coordination is not exclusive to cerebellar control[114,532]. Altogether, evidence suggests that structural and molecular alterations are indeed present in the cerebella of individuals with ASD and TSC-ASD, and that these may contribute to the behavioural and cognitive manifestations exhibited by the patients.

Strengthening the hypothesis of the role of the cerebellum in the development of ASD in TSC, are two conditional mice models *Tsc1*-L7^{Cre} and *Tsc2*-Pcp2^{Cre}, with *Tsc* deletions exclusive to PC[324,333,334]. In both these models, PC loss was observed together with increased phosphorylated rpS6 immunoreactivity[324,333,334]. Furthermore, social interaction and novelty preference deficits were found, behaviours that are classified as ASD-like behaviours[324,333]. Therefore, evidence suggests the possibility of cerebellar alterations contributing to the behavioural deficits seen in TSC-ASD patients. Further studies with additional animal models would be welcome to ascertain the role of the cerebellum in this matter.

The Eker rat was shown to present with reduced social interaction when exposed to a novel unknown rat[370] (Section 1.1.5.4.2). However, the cerebellum of the Eker rat has been poorly explored. Only one study reported on the cerebellum, focusing on the presence of tumours between the cerebellum and brainstem of 4/9 18-24 month-old Ekers, although no comparison with wild-type animals was performed[366]. Here, by characterizing the Eker rat cerebellum I hypothesized that, if conditional cerebellar models of TSC exhibit cerebellar pathology and ASD-like behaviours, the Eker rat could also carry molecular and/or cellular changes in cerebellar tissue. Therefore, the first objective of this work was to 1) compare the Eker rat cerebellum to wild-type littermates. To allow translatability of results, I analysed features previously reported to be changed in human ASD

samples, such as cerebellar morphology and cellular density, GABAergic system and inflammatory responses; secondly, using these same markers, I 2) investigated whether treatment with CBD induced any morphological or molecular changes to the cerebellum.

3.2 Methods

3.2.1 Breeding and animal groups

Adult male Eker rats from the Long-Evans background were kindly provided by Dr. Robert Waltereit (Technical University of Dresden, Dresden, Germany). Both wild-type (WT; *Tsc2*$^{+/+}$) and Eker (Heterozygote; *Tsc2*$^{+/-}$) animals were bred at the University of Reading Bioresource Unit, where they were group housed and kept at room temperature on a 12:12-h day/night cycle (dark/red light 7pm – 7am, normal light 7am – 7pm). Food and water were given *ad libitum*. At P14, male animals were ear-notched and genotyped, as described in section 3.2.2. After genotyping, animals were assigned to one of four experimental groups: 7 animals to the WT-vehicle group, 7 animals to the WT-CBD group, 7 animals to the Eker-vehicle group and 7 animals to the Eker-CBD group. Animals in each group were derived from different litters and different cages always housed animals from different groups. All experiments were approved by the University of Reading Ethics Board and the UK Home Office (PPL 70/8974) and carried out in accordance with UK Home Office regulations (Animals (Scientific Procedures) Act, 1986) and the ARRIVE guidelines.

3.2.2 Genotyping

Genotyping was performed based on previously described protocols[232,328]. After ear notch collection, DNA was extracted using the PCRBio Rapid Extract PCR kit (PCR Biosystems, UK) according to manufacturer instructions. After extraction, 0.5 µL of DNA lysate were mixed with 10 µL of PCRBio HS Taq Mix Red (PCR Biosystems, UK), 8.2 µL of ddH_2O and 0.4 µL of the primers (5'-GTCTAATGCCCTTATGGCTG-3') and (5'-TCCTCCTGAAGCTGAAGAGT-3')[328] (Sigma, UK), which target intron 31, where the Eker rat mutation is inserted (Section 1.1.5.4.2). The following thermal cycle (T100™, Bio-Rad, UK) was used: 94 ˚C for 2 minutes for the initial denaturation step; 30 cycles of 94 ˚C for 1 minute for denaturation, 60˚C for 1 minute and 68 ˚C for 54 seconds for annealing, and 72 ˚C for 7 minutes for the extension step. At the end of the PCR protocol, products were cooled down to 4°C and kept at this temperature until analysed. Analysis of PCR products was conducted together with positive (original Eker notch, collected *in house* after animal reception) and negative (water) controls, as well as with an Exact gene 100bp ladder (Fisher Scientific, UK). Products were separated by electrophoresis at 70V for 45 minutes in a 2% (w/v) agarose gel in tris-acetate-EDTA buffer and visualized in a Syngene U:Genius 3 (Syngene, UK) gel

imaging system. Eker rats were identified by the presence of a DNA band, absent in wild-type samples (Figure 3.1).

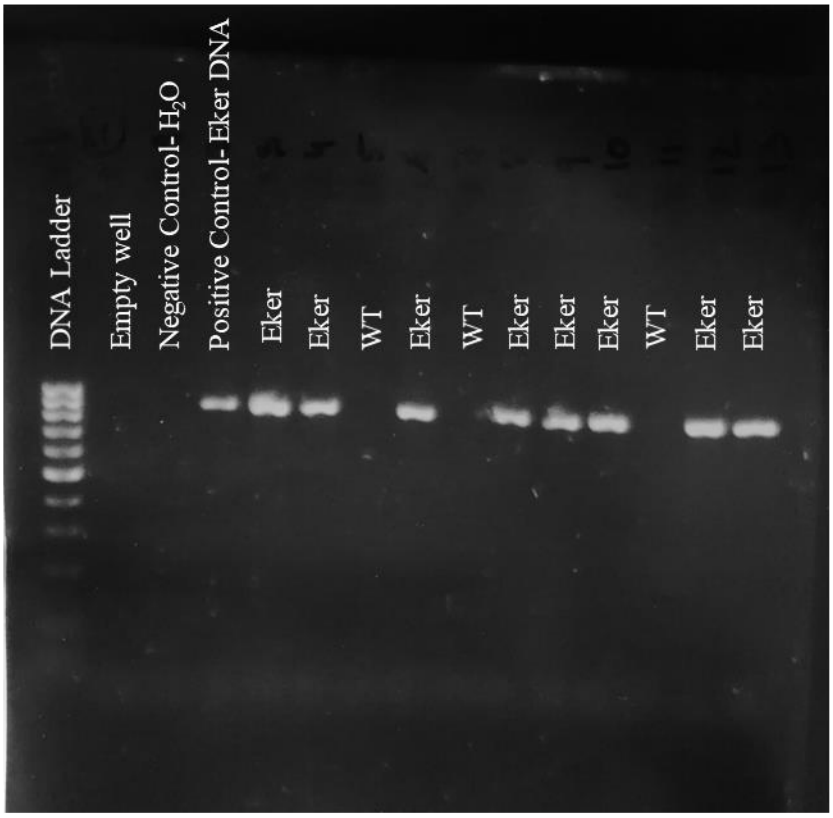

Figure 3.1: *Genotyping of WT and Eker rats*. An example of a gel visualization image is presented here, showing the detection of WT and Eker DNA, together with the DNA ladder, positive and negative controls. As Eker rats exhibit an insertional mutation (Section 1.1.5.4.2), a visible band indicates a *Tsc2*$^{+/-}$ sample while the absence of a band represents a WT sample.

3.2.3 Pharmacological treatment

From P18 to P24, male WT and Eker rats (7 animals per group, n= 28) were weighed twice daily before each subcutaneous injection. The injected compounds, vehicle (2:1:17 EtOH: Cremophor: 0.9% saline) (Ethanol 32221, Merck) (Kolliphor®HS 15, 42966, Sigma) or 100mg/kg of CBD (GW Pharmaceuticals, Cambridge, UK), were prepared at the beginning of the treatment week and kept in glass vials, protected from light at 4°C. During treatment, animals were always handled by familiar experimenters to prevent effects resulting from unknown handlers.

3.2.4 Immunohistochemistry

At P24, animals were anesthetised with gaseous isoflurane and, when absence of righting and paw withdrawal reflexes was confirmed, decapitated. The brain was rapidly removed and the cerebellum dissected through an incision in the transverse fissure. Tissue was washed in PBS, transferred to a 4% PFA solution and weighed. After 24 hours, brains were transferred into a 30% sucrose in 4% PFA solution and, the next day, into a 30% sucrose solution. Samples were embedded in OCT compound (CellPath™, UK) and stored at -80°C until used.

12 µm sagittal sections were obtained with a 5040 Bright cryostat and mounted onto microscope slides (SuperFrost Plus, Thermo Fisher Scientific, UK). Slides were incubated for 2 hours in a 2% BSA, 10% horse serum and 0.05% TX-100 buffer, at room temperature, followed by an over-night incubation with primary antibodies (Table 3.1) in a 1% BSA and 0.05% TX-100 buffer, at 4°C. The next day, slides were rinsed 3 times in TBS, for 10 minutes, followed by secondary antibody (Table 3.1) incubation for 2 hours at room temperature. After further rinsing in TBS, sections were counterstained with DAPI (1:10 000; D1306, Thermo Fisher Scientific, UK) or Nissl (1:500, N21480, lot 931328, Life Technologies) and finally rinsed again. For TUNEL-incubated sections (1:10; 12156792910 Roche, lot 26320800, Sigma, UK), the same treatment was applied to the slides, omitting primary and secondary antibody incubation. Sections were incubated with TUNEL reaction for 1 hour at 37 °C, together with a negative control, omitting the enzyme solution, and positive control, incubated with DNase. All slides were left to dry and mounted using DPX Mountant (44581, Sigma).

3.2.5 Imaging and Image analysis

Three randomly selected images for each animal (n=5 animals per group) were acquired from different sections of the posterior cerebellum, using a Zeiss AxioImager microscope with the AxioVision software. Image analysis was undertaken using Fiji Image J[475].

Cerebellar layer thickness was measured in µm on Nissl stained sagittal sections, as published elsewhere[533] (Figure 3.3A). Cell density in the molecular layer (ML) and in the granular cell layer (GCL) was analysed on DAPI stained sections. For the ML, cells were automatically counted using the "*Analyse particle*" function in Fiji Image J. For the granular cell layer (GCL), given the high density of cells, pictures were converted to a binary picture using the *Huang* threshold filter on Fiji Image J, and the mean intensity quantified and used as a measure of cell density (measured in arbitrary density units, ADU). The number of Purkinje cells (PC) was manually counted using Nissl stained sections.

For antibody fluorescence intensity analysis, measured in arbitrary intensity units (AIU), squared ROI were defined in the molecular (200 x 200) and granular cell layers (250 x 250) and kept constant for all pictures. For Purkinje cell layer (PCL) analysis, a ROI was manually defined around the layer and mean fluorescence intensity was divided by the total area of the selection.

For PC structure analysis, measurements were done as previously published[534] and as illustrated in Figure 3.4A, using SMI311 stained sections (number of analysed cells: n=23 PC for WT, n=20 PC for Eker, n=23 PC for vehicle and n=20 PC for CBD). Cross sectional area was obtained by drawing a line around the cell body. Length of the main dendrite was measured until first branching, starting in the middle of the cell body, and the thickness of the main dendrite was measured in its mid-point. For Iba1-positive cell analysis, the total number of cells with a clearly visible nucleus was counted in each picture, together with the number of round cells, classified as the ones with an ameboid morphology lacking visible processes[409,535,536].

For quantification of TUNEL positive cells, slides from 5 animals per group were visualized under the microscope and the number of positive cells counted in each section.

	Target	Dilution	Host	Supplier	Reference	Lot
Primary	GAD-67	1:500	Mouse	Millipore	MAB5406	2972846
	Iba1	1:500	Goat	Abcam	ab5076	GR245353-2
	Neurofilament (pan neuronal SMI311)	1:500	Mouse	BioLegend	837801	B204317
	Parvalbumin	1:2000	Rabbit	Abcam	ab11427	GR296273-5
	rpS6 (235/236)	1:500	Rabbit	Cell Signalling	2211L	0023
Secondary	Anti- goat 594	1:1000	Donkey	Life technologies	A11058	1736986
	Ant- rabbit 647	1:1000	Donkey	Life technologies	A31573	1693297
	Anti- rabbit 647	1:1000	Goat	Invitrogen	A21245	1805235
	Anti- mouse 594	1:1000	Goat	Invitrogen	A11032	748192
	Anti- mouse 647	1:1000	Goat	Invitrogen	A21236	1156622

Table 3.1: *Antibody list.* The following primary and secondary antibodies were used at the dilutions described above. Different antibodies were used in combination to obtain co-labelling in the same microscope slide.

3.2.6 Statistical Analysis

Data was analysed using IBM SPSS Statistics 22 and graphs produced using GraphPad Prism 6. Normality was assessed using the Shapiro-Wilk test and homogeneity with the Levene's test. Outliers were detected with the Grubbs test. *Genotype* (wild-type or Eker, n=5 per group) and *Treatment* (vehicle or CBD, n=5 per group) were defined as independent variables. Cellular density,

body and brain weight, weight gain, number of Iba1-positive cells and % of round Iba1-positive cells were analysed using a two-way ANOVA. The immunofluorescence of phosphorylated rpS6, GAD-67 and PV, as well as the weight ratios and layer thickness, were analysed with repeated-measures ANOVA, taking into account the different cerebellar layers. The PC parameters, mid-point thickness of the main dendrite, length of the main dendrite until first branching point and soma area were individually analysed. Thickness was analysed with a two-way ANOVA, while length and area were analysed with a robust two-way ANOVA using the bootstrapping method, as both parameters did not follow normality nor homogeneity[537,538]. Post-hoc analysis was done using the Bonferroni test adjusted for multiple comparisons. Results were considered statistically significant when the *p* value was less than 0.05.

3.3 Results

3.3.1 Gross body and brain morphology are not affected by genotype nor CBD

After the 7-day treatment period, weight was used as a measure to analyse gross morphology. Across the treatment week, average group weight progressed similarly in all four groups (Figure 3.2A). Weight gain analysis revealed a main effect of treatment ($F(1,24)=9.773$, $p=0.005$), but not of genotype ($F(1,24)=0.060$, $p=0.809$) nor interaction ($F(1,24)=0.578$, $p=0.454$), indicating that overall CBD-treated animals showed decreased daily weight increments compared to vehicle-treated animals (3.83 g/day ± 0.18 for vehicle vs 3.04 g/day ± 0.18 for CBD) (Figure 3.2B). At the end of the study, there were no significant differences in average body weight in any of the groups (genotype: $F(1,24)=0.226$, $p=0.610$; treatment: $F(1,24)=2.927$, $p=0.100$; genotype*treatment: $F(1,24)=0.042$, $p=0.840$; Figure 3.2C). No significant effects of treatment or genotype were found regarding the average weight of the cortex and cerebellum (Figure 3.2C). Similar results were seen for the cortex/body, cerebellum/body, whole brain/body and cerebellum/whole brain weight ratios (genotype: $F(1,24)=0.025$, $p=0.877$; treatment: $F(1,24)=0.054$, $p=0.819$; genotype*treatment: $F(1,24)=0.210$, $p=0.651$; Table 3.2).

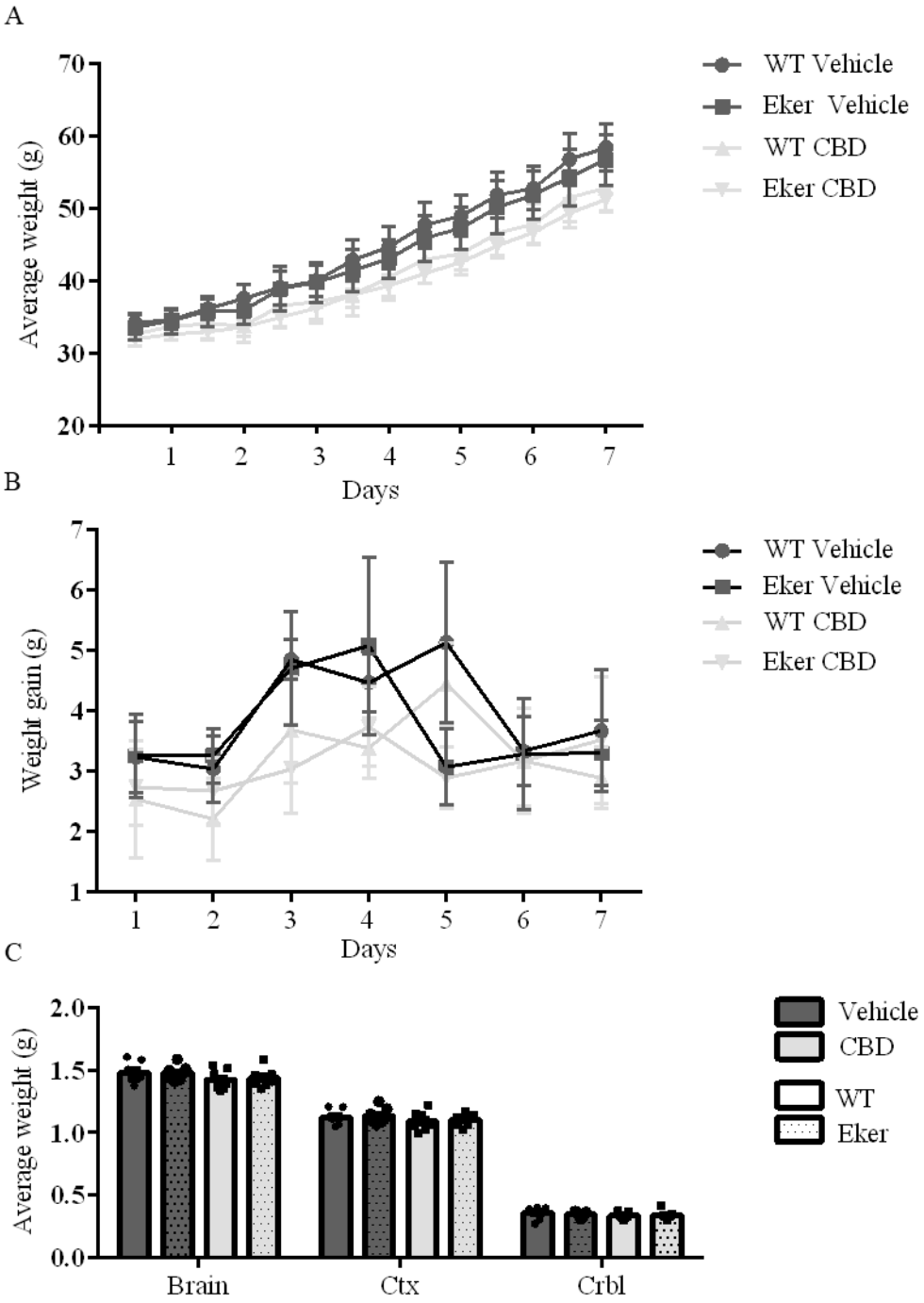

Figure 3.2: *CBD altered weight gain, but body and brain gross morphology were unaffected by Tsc2 mutation or treatment*. (A) Monitoring of weight progression over the 7-day treatment period for wild-type and Eker animals revealed a steady increase in weight during treatment. (B) Analysis of the weight gained per day revealed a main effect of treatment ($F(1,24)=9.773$, $p=0.005$) indicating decreased weight gain in CBD-treated animals. (C) Data from the final brain weight revealed no effect of genotype (WT vs Eker: $F(1,24)=0.226$, $p=0.610$) or CBD (100 mg/kg) treatment ($F(1,24)=2.927$, $p=0.100$) on whole brain, cortical (Ctx) nor cerebellar (Crbl) weight. Data is presented as mean ± SEM, n=7 animals per group.

Ratio	WT(g)		Eker (g)	
	Vehicle (n=7)	CBD (n=7)	Vehicle (n=7)	CBD (n=7)
Cortex/ Body	1.84 ± 0.08	1.98 ± 0.08	1.94 ± 0.08	2.03 ± 0.08
Cerebellum/ Body	0.58 ± 0.04	0.61 ± 0.04	0.59 ± 0.04	0.62 ± 0.04
Whole Brain/ Body	2.42 ± 0.10	2.59 ± 0.10	2.52 ± 0.10	2.65 ± 0.10
Cerebellum/ Whole Brain	23.93 ± 0.83	23.37 ± 0.83	23.16 ± 0.83	23.54 ± 0.83

Table 3.2: *Brain to body weight ratios*. After one week of treatment, body, whole brain, cortex and cerebellum weight was measured. Data are presented in grams as mean ± SEM, n=7 animals per group.

3.3.2 CBD treatment alters cerebellar layer thickness and Purkinje cell area

Brain sections were used to assess alterations in cerebellar structure due to treatment or genotype. Consistent with previous literature for the cerebellum[539,540], few TUNEL positive cells (0 to 2) were found (data not shown), indicating no CNS degeneration nor abnormal developmental cell death.

Alterations in mTOR signalling and autism have been associated with changes in cerebellar thickness[132,310,541–543]. Therefore, we next measured cerebellar layer thickness (Figure 3.3A). We found no main effect of genotype on thickness ($F(1,15)=0.002$, $p=0.969$) (Figure 3.3B). However, a significant main effect of treatment ($F(1,15)=5.104$, $p=0.039$) and genotype*treatment interaction ($F(1,15)=6.123$, $p=0.026$), together with a significant effect of layer ($F(2,30)=442.38$, $p=0.000$) and a layer*genotype*treatment ($F(2,30)=4.482$, $p=0.020$) interaction were present. Post hoc analysis revealed a change located in the GLC with CBD significantly increasing layer thickness in the wild-type CBD-treated group, compared to the wild-type vehicle-treated group (147.86 ± 11.31 µm for the vehicle vs 207.26 ± 12.64 µm, for the CBD group, $p=0.003$; Figure 2B). Additionally, in the PCL, the CBD-treated Eker group also exhibited increased layer thickness compared to the vehicle-treated Eker group (25.17 ± 1.12 µm for the CBD vs 21.78 ± 1.12 µm for the vehicle group, $p=0.048$; Figure 3.3B).

We next analysed cellular density in each layer. There was no effect of treatment ($F(1,15)=0.777$, $p=0.392$), genotype ($F(1,15)=0.132$, $p=0.721$) nor genotype*treatment ($F(1,15)=0.168$, $p=0.687$) regarding the ML density (Figure 3.3C). This layer is mainly composed of stellate and basket cell bodies, and the dendritic tree of PC[539]. Therefore, the lack of difference seen here, together with the absence of layer thickness alterations, suggest that neither interneuron number nor PC dendritic tree were altered by genotype or treatment[544–546]. In the GCL, a main effect of genotype ($F(1,15)=6.708$, $p=0.021$) but not of treatment ($F(1,15)=0.106$, $p=0.750$) nor interaction (genotype*treatment: $F(1,15)=0.001$, $p=0.975$) was found, indicating that Eker rats exhibited an

overall higher cellular density in this layer when compared to WT rats (1.01×10^{-3} ADU ± 1.36×10^{-4} for WT vs 1.22×10^{-3}ADU ± 1.82×10^{-4} for Eker, p=0.02) (Figure 3.3D).

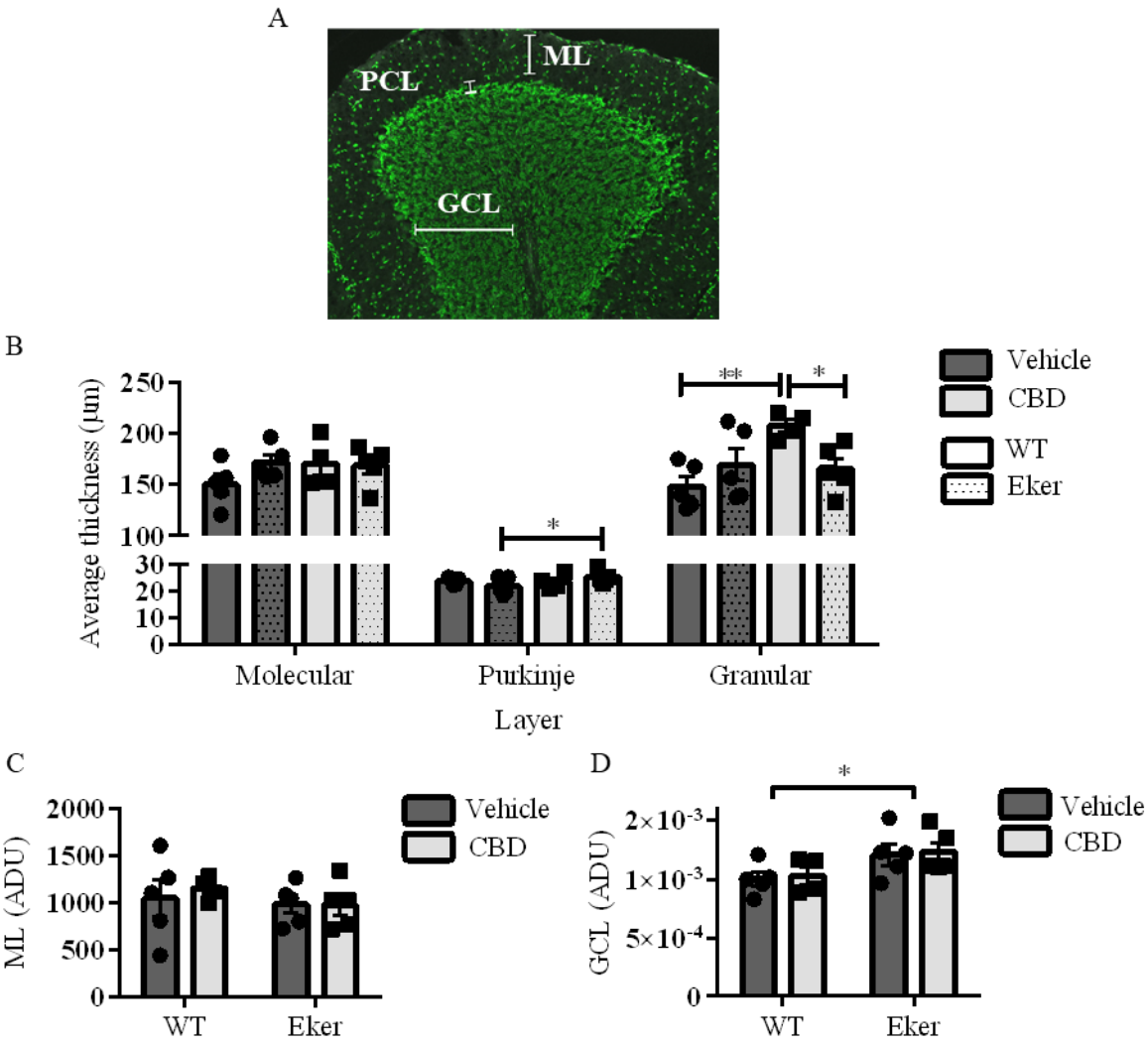

Figure 3.3: *Treatment and Tsc2 mutation dependent changes on cerebellar layer thickness and cellular density*. After IHC, the thickness of the three cerebellar layers was measured as in (A). (B) Thickness measurements revealed a significant effect of CBD (F(1,15)=5.104, p=0.039), increasing both GCL and PCL average thickness. (C-D) Cell density values were also quantified, using arbitrary density units (ADU). No alterations were detected in the molecular layer (F(1,15)=0.777, p=0.392) (C), while in the granular layer, an effect of mutation revealed that Ekers rats had increased cellular density (F(1,15)=6.708, p=0.021) (D). Data is presented as mean ± SEM, n=5 animals per group, 3 pictures per animal. *p<0.05; **p<0.01.

Alterations in the GCL can reflect changes in the PCL[547]. Given the alteration in PCL thickness found, PC were analysed in more detail (Figure 3.4A). There was no difference in the number of PC in the different genotypes (F(0,15)=0.008, p=0.928) or following CBD treatment (F(1,15)=3.806, p=0.070), and no interaction between genotype and treatment (F(1,15)=0.175,

p=0.681) (Figure 3.4B). Additionally, no difference was found for the average length of the main dendrite (genotype: F(1,39)=3.746, bootstrapping p=0.071 (p=0.060 without bootstrapping); treatment: F(1,39)=1.149, bootstrapping p=0.293 (p=0,290 without bootstrapping; genotype*treatment: F(1,39)=0.017, p=0.897) (Figure 3.4C), nor regarding the thickness at its mid-point (genotype: F(1,38)=1.639, p=0.208; treatment: F(1,38)=1,316, p=0,259; genotype*treatment: F(1,38)=2.254, p=0.142) (Figure 3.4D). A significant difference was found regarding the average PC area. In this case, a significant main effect of genotype (F(1,39)=9.711, bootstrapping p=0.003 (p=0.003 without bootstrapping) revealed that WT animals had an overall bigger PC area than Ekers (385.79 μm^2 ± 20.20 for WT vs 296.21 ± 20.27 μm^2 for Ekers). Additionally, a main effect of treatment was also found (F(1,39)=8.833, bootstrapping p=0.009 (p=0.005 without bootstrapping)), indicating that vehicle-treated animals presented with smaller PC cross-sectional area than CBD-treated animals (289.28 μm^2 ± 13.93 for vehicle vs 383.72 μm^2 ± 24.92 for CBD). The interaction between genotype and treatment was not statistically significant (F(1,39)=0.079, p=0.781) (Figure 3.4E-F).

3.3.3 GAD-67 and PV immunofluorescence is similar between WT and Ekers, irrespective of CBD treatment

GABAergic neurons are abundant in the cerebellum, including PC in the PCL, stellate and basket cells in the MCL and Golgi cells in the GCL[539,548]. We therefore explored if other alterations in GABAergic neurons were present, especially following the previously reported changes in the PC and the PCL. To this effect, we first looked at the immunoreactivity of glutamic acid decarboxylase 67 (GAD-67), an enzyme responsible for GABA synthesis, abundant in the cytoplasm of cerebellar cells[549]. As expected[550,551], we found GAD-67 positive cells in all three layers (Figure 3.5A). Quantification of the fluorescent signal revealed a similar distribution of GAD-67 across the different genotypes (F(1,15)=0.005, p=0.946) and treatments (F(1,15)=0.079, p=0.782), and no interaction between these variables was found (F(1,15)=0.004, p=0.950) (Figure 3.5B). GAD-67 sections were also co-stained with a parvalbumin (PV) antibody. PV is a calcium binding protein that contributes to the regulation of synaptic plasticity[552–554]. GAD-67 and PV stain appeared to overlap, as seen by the yellow stain resulting from the merge of the two antibody images, indicating a colocalization of the two markers (Figure 3.5A- fourth column). PV stain was detected in the cell bodies of PC and cells from the ML, while no specific PV positive stain was seen in cell bodies from the GCL, albeit diffuse background fluorescence was present[553,555,556] (Figure 3.5A- third column). Fluorescence quantification of PV intensity did not differ between experimental groups (genotype: F(1,15)=0.119, p=0.735; treatment: F(1,15)=0.147, p=0.707; genotype*treatment: F(1,15)=0.229, p=0.639) (Figure 3.5C).

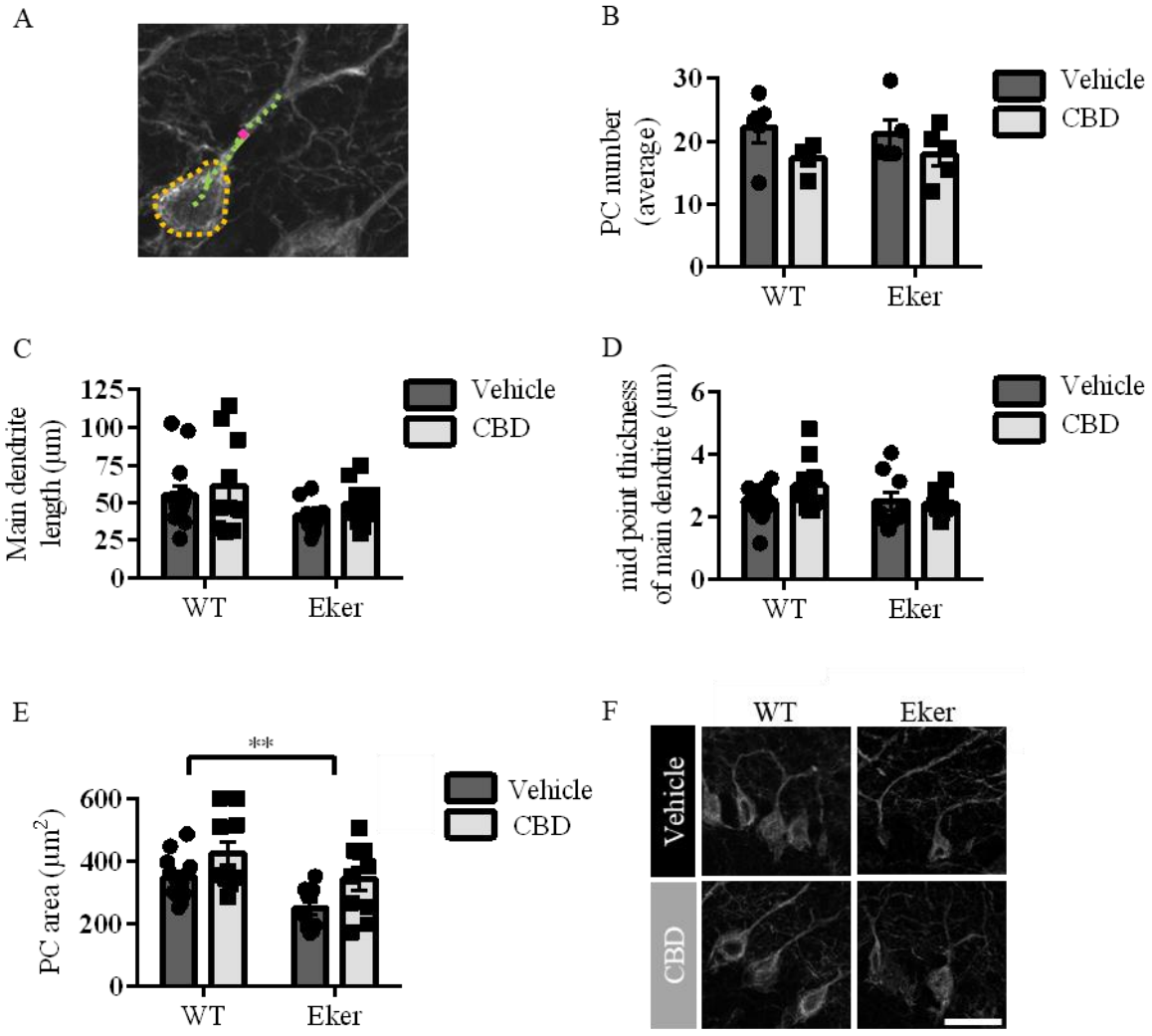

Figure 3.4: *Purkinje cell area is modified by both TSC2 mutation and CBD treatment.* (A) Schematic example of the measurement of Purkinje cell parameters with *area* shown in yellow, *main dendrite length* in green and *mid point thickness of the main dendrite* in magenta. (B) The cellular density of PC was manually analysed by counting the number of cells in each section. No effect of genotype ($F(0,15)=0.008$, $p=0.928$) nor treatment ($F(1,15)=3.806$, $p=0.070$) was observed. (C-E) Values for main dendrite length (genotype: $F(1,39)=3.746$, $p=0.071$; treatment: $F(1,39)=1.149$, $p=0.293$ (C) and mid-point thickness of the main dendrite (genotype: $F(1,38)=1.639$, $p=0.208$; treatment: $F(1,38)=1,316$, $p=0,259$) did not differ between groups (D). Purkinje cell area was decreased in the Eker group ($F(1,39)=9.711$, $p=0.003$) and increased by CBD treatment ($F(1,39)=8.833$, bootstrapping $p=0.009$)(E). (F) Representative pictures of Purkinje cells from both genotypes and treatments. Data are presented as mean ± SEM. *$p<0.05$; **$p<0.01$. n= 20-23 PC per group. Scale= 50µm.

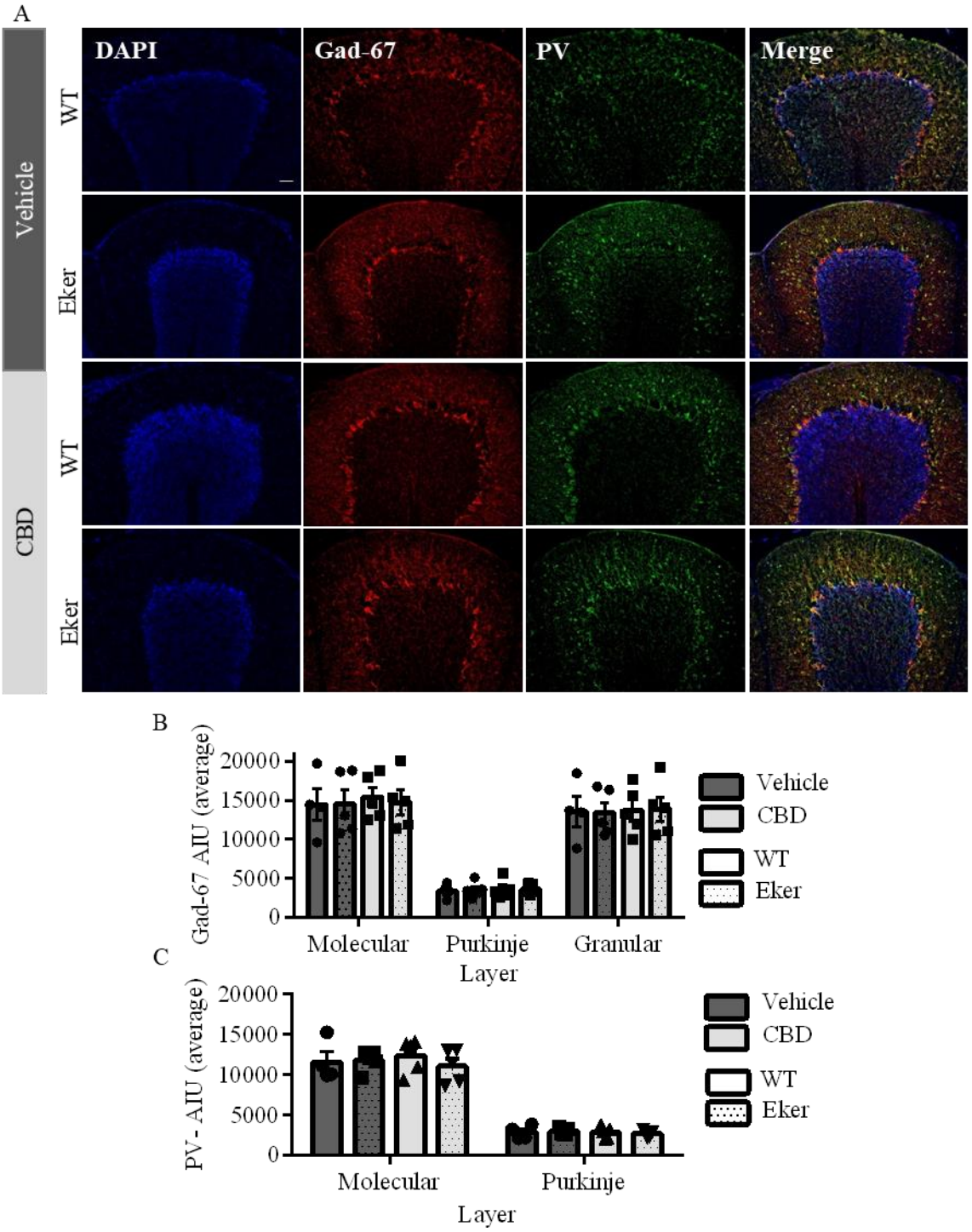

Figure 3.5: *GAD-67 and PV labelling is preserved in the Eker rat and not modified by CBD treatment*. (A) Cerebellar sections were stained with DAPI (blue), and GAD-67 (red) and a PV antibodies (green). Merged pictures reveal co-labelling of both GABAergic markers on the cerebellum. (B-C) The average immunofluorescence of each marker was quantified in arbitrary intensity units and found to be similar between groups for both GAD-67 (genotype: ($F(1,15)=0.005$, $p=0.946$); treatment ($F(1,15)=0.079$, $p=0.782$)) (B) and for PV labelling (genotype: $F(1,15)=0.119$, $p=0.735$; treatment: $F(1,15)=0.147$, $p=0.707$) (C). Data presented as mean ± SEM. n=5 animals per group, 3 pictures per animal. Scale=50µm.

3.3.4 Phosphorylated rpS6 and Iba1 immunoreactivity remain unaltered by the Eker mutation or CBD treatment

Phosphorylated rpS6 is commonly used as a readout of mTOR activity[362,557] and its expression is increased in both animal models and human samples of TSC[53,209,313,331,498,558]. CBD treatment has been shown to reduce rpS6 phosphorylation levels and the total number of Iba1-positive cells, including the ones with a reactive phenotype (Section 2)[409,411,559]. Iba1 is a calcium binding protein present in microglia cells that can be used to count and visualize the shape of microglia cells[560,561]. Therefore, in addition to phosphorylated rpS6 fluorescence, to explore the numbers and shape of microglia in the Eker rat cerebellum, an Iba1 antibody was also used[562,563]. Phosphorylated rpS6 staining was similar across all groups and predominantly localized to PC (Figure 3.6A- second column). Sporadic phosphorylated rpS6 positive cells were also found in the GCL (Figure 3.6A- second column, arrow heads). Quantification of the fluorescence intensity in the different layers revealed no significant differences in phosphorylated rpS6 immunofluorescence between any groups (genotype: $F(1,15)=0.757$, $p=0.398$; treatment: $F(1,15)=1.747$, $p=0.206$; genotype*treatment: $F(1,15)=0.014$, $p=0.908$) (Figure 3.6B). Iba1 positive cells were homogenously scattered throughout the cerebellar layers, as previously reported regarding this brain area[562,564], and they exhibited a morphology with few visible primary branches (0 to 5 visible branches per cell, mode=1) (Figure 3.6A- forth column). The total number of Iba1 positive cells per field/ per animal was similar in all four groups, as we found no effect of genotype ($F(1,16)=1.105$, $p=0.309$), treatment ($F(1,16)=0.909$, $p=0.355$) nor interaction ($F(1,16)=1.215$, $p=0.287$) between groups (Figure 3.6C). Additionally, no main effect of genotype ($F(1,16)=0.320$, $p=0.579$), treatment ($F(1,16)=0.061$, $p=0.809$) nor interaction ($F(1,16)=0.927$, $p=0.350$) was observed regarding the percentage of round Iba1 positive cells (Figure 3.6D). Finally, the number of cells positive for both phosphorylated rpS6 and Iba1 were counted. In all acquired images, the number of double positive cells was 12. In total, 1 ramified cell was found in the WT-vehicle group, 2 round cells in the WT-CBD group, 4 ramified and 1 round cells in the Eker-vehicle group and 4 ramified cells in the Eker-CBD group.

3.4 Discussion

We sought out to characterize for the first time the cerebellum of the Eker rat, a heterozygous model of TSC proposed to exhibit autism-like behaviour[370]. Additionally, we also explored the effect of a 7-day CBD treatment on the cerebellum, a compound proposed to modulate social behaviour[565,566].

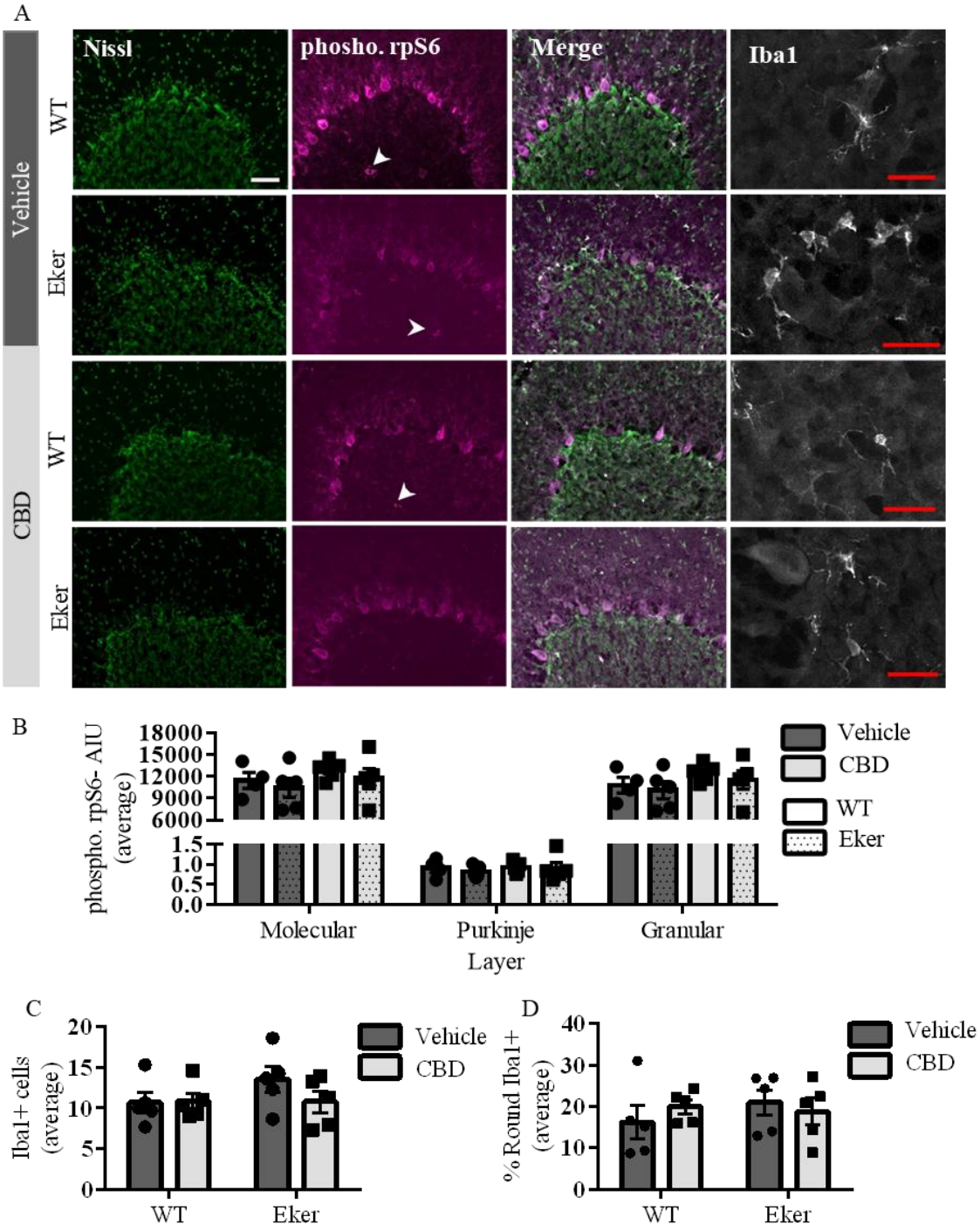

Figure 3.6: *Phosphorylated rpS6 immunoreactivity and microglia structure are unchanged by the Eker mutation and by CBD treatment.* (A) Cerebellar sections were stained with Nissl (green), phosphorylated rpS6 (magenta) and Iba1 (grey). Arrowheads in the phosphorylated rpS6 panel indicate pS6+ cells in the molecular layer. (B) Quantification of phosphorylated rpS6 immunofluorescence indicated no differences between groups (genotype: $F(1,15)=0.757$, $p=0.398$; treatment: $F(1,15)=1.747$, $p=0.206$). (C-D) The average number of Iba1+ cells per field and the percentage of round Iba1+ cells were quantified and found to be similar between treatment and genotype groups. Data is presented as mean ± SEM. Scale= 50 µm on panel images and 25 µm in the Iba-1 magnification column. n=5 animals per group, 3 pictures per animal.

3.4.1 Effects of the *Tsc2*$^{+/-}$ mutation on the Eker rat cerebellum

Previous studies with the Eker rat have indicated no changes in whole brain and cortex weight in adults compared to WT[45,232,364,365,567]. This was consistent with the findings reported here. In addition, no gross alterations in cerebellar morphology or weight were observed. More severe models of TSC carrying conditional homozygous deletions show poor weight gain and increased brain weight[153,317,568–570]. For example, both the *Tsc1*^{GFAP}cKO and the *Tsc2*^{GFAP}cKO exhibit weight changes compared to WT by post-natal weeks 7-8[153,353,568]. In the *Tsc2*^{hGFAP}cKO and *Tsc1*$^{Emx\text{-}1}$cKO, weight changes are visible from post-natal weeks 2 and 3, respectively[310,571]. Altogether, the lack of body and brain weight alterations seen here is in line with results from other heterozygous models of TSC[324,330,335,572].

Analysis of the finer structure of the cerebellum revealed no changes in layer thickness. However, Ekers exhibited increased cellular density in the GCL. This could be indicative of increased proliferation of *Tsc2*$^{+/-}$ GC. Work with the TSC2-RGΔ model has shown that GC precursors exhibited increased proliferation compared to WT cells after Sonic Hedgehog (SHH) treatment[573]. Additionally, human induced pluripotent stem cells from *TSC2* mutated patients expressed increased levels of Ki67, a proliferation marker[149]. A clinical study also revealed that cerebellar lesions in TSC have a higher incidence in patients with *TSC2* mutations and it was hypothesised that the high capacity of GC proliferation increases the probability of a second mutation and subsequent lesion development[574]. Because of this high capacity for proliferation compared to other cerebellar populations[575], it is possible that the Eker mutation promotes increased cell division in the GCL, detected earlier due to the increased number of cells in this layer compared to others. GC are the main excitatory neurons in the cerebellum and act on PC, the sole output of the cerebellar cortex. Consequently, GC dysfunction can have major impact on downstream cerebral substrates. Analysis of proliferation markers, such as Ki67, could help clarify if these density changes are GCL-specific or present throughout the cerebellum.

Changes in cellular number could also be due to cell migration alterations. During embryonic development, GC precursors undergo mitosis and accumulate in a layer parallel to the pial surface (external granule layer, EGL)[576,577]. Postnatally, GC exit cell cycle and migrate inwards[576,577]. This process is finalized in rodents between P21-P24, matching the disappearance of the EGL[539,576–579]. Here, no traces of EGL were visible indicating proper migration. This contrasts with data from the TSC2-RGΔ model which exhibits residual EGL cells[573]. This discrepancy may arise from the less severe phenotype of the Eker rat. Although both models exhibit defective GAP activity, the Eker rat mutation affects exon 30 while the RGΔ affects the genomic DNA between exons 8 and 9, differences that can contribute to the establishment of different phenotypes[279,580]. Further studies with different time points, and with neuronal-specific markers, such as NeuN[581,582], could provide valuable insight to whether changes in cell number and/or delays in granule cell

migration could also be present in the Eker rat. Likewise, timed studies could indicate if increased cellular density was induced by reduced developmental apoptosis although, at this age, we found no difference in the number of TUNEL-positive cells.

Adult male rats are estimated to have around 10.72×10^6 cerebellar glia cells[583]. Thus, glia alterations could also contribute to increased cell density[584]. Studies with the microglia marker HLA-DR and with the *in vivo* tracer [^{11}C](*R*)-PK11195 have reported increases in microglia numbers in the cerebellum of TSC[228], as well as of ASD, patients[585,586]. Here, we used the marker Iba1 and found no difference between groups. Although this suggests it is unlikely that density changes are due to microglia number alterations, it is also important to consider other microglial markers. In fact, work by Hendrickx and colleagues revealed that, in human brain tissue, although overlapping immunoreactivity was seen in some microglial cells with the use of Iba1, HLA-DR and CD68 antibodies, other cells would only express one or two of these markers[587]. This suggests the presence of different microglia populations which we did not address in this work. Likewise, reports from human TSC cases have described changes in the astrocyte population in the cerebellum[228,588,589], and *Tsc1*$^{+/-}$ and *Tsc2*$^{+/-}$ mice were shown to exhibit increased numbers of GFAP-positive astrocytes compared to control brains[590]. Therefore, increased astrogliosis could contribute to changes in the GCL. Further studies with astrocyte markers, such as GFAP, glutamine synthase or S100B[591–594] could help understand the possible contribution of these cells to the GCL changes reported here.

An overall decrease in PC cross-sectional area was also observed in the Eker group. This has also been reported in human cases of ASD[526], although data is inconsistent[143,146]. This decrease in size was unexpected as it is in contrast to the understanding that *TSC* mutations promote mTORC1 activation and increases in cell size[60,304]. Furthermore, as opposed to conditional homozygous TSC models, work with heterozygous models has shown no alterations in cellular size[324,330]. However, one other model in which reduction in PC soma size has been reported was in mice with a conditional knockout of rictor (RibKO)[595]. Rictor, which is highly expressed in PC[596], is essential for the formation of mTORC2 (Section 1.1.5.1; Figure 1.6)[24,595,597–599]. This suggests that proper mTORC2 function is necessary for the development of a correct PC size.

The relationship between mTORC2 and the TSC complex has been poorly explored and is still not fully understood. Work by Huang and colleagues demonstrated that the presence of a functional Tsc1-Tsc2 complex was required for correct mTORC2 assembly and function, and that this effect was independent of Tsc2's GAP function[505]. A physical interaction between the Tsc1-Tsc2 complex and mTORC2 was also observed. This was later determined to be dependent on the N-terminal region of Tsc2 (amino acids 1-1530)[505,600]. This domain of interaction could be impaired in the Eker rat as its mutation modifies Tsc2 around amino acid 1229[601]. Furthermore, the Eker mutation has also been shown to affect the number of Tsc1-Tsc2 complexes, as co-immunoprecipitation revealed a lower complex yield in cells with the Eker mutation than in wild-

type cells[602]. Therefore, it could be possible that the magnitude of the Tsc1-Tsc2 interaction reduction in the Eker rat is greater than its GAP activity dysfunction. In this case, the *Tsc2* mutation would be sufficient to trigger a decrease in mTORC2 activity, but not a significant reduction in mTORC1 signalling, thereby leading to an overall reduction in PC size. In line with this hypothesis, we found no difference in phosphorylated rpS6 stain between genotypes. To further explore these intriguing possibilities, the analysis of molecules that provide a readout of mTORC2 activity, such as the expression of PKCγ or phosphorylated Akt (Ser473)[505,603,604], would provide valuable information on the possible dysfunction of mTORC2 in the Eker cerebellum.

3.4.2 Effects of CBD treatment on the Eker rat cerebellum

The second objective of this work was to investigate the effects of CBD on the cerebellum of the Eker model. We first observed decreased weight gain in CBD-treated animals. This effect has been previously reported albeit using a different animal cohort (10 week-old Wistar rats) treated with comparatively low doses of CBD (2.5 or 5 mg/kg/day)[605]. This action of CBD on weight was attributed to agonism of the CB2 receptor, given that CBD's effect was absent when co-administered with the CB2 antagonist AM630. We cannot ascertain if this was the mechanism of action by which CBD induced the reduction in weight gain observed here. However, it would be important to further study this effect given the proposed applications of CBD in paediatric populations who are still growing and developing.

Another effect of CBD was the increase in the thickness of the GCL in the wild-type group. As previously explained, increases in layer thickness could potentially be due to increased cell proliferation, altered developmental migration, decreased developmental apoptosis or increased cell size[606]. Given the different proposed actions of CBD in the CNS[402,405,438,440,456,607–609], one that could be highlighted here is CBD's capacity to increase survival and neurogenesis[405,456,609,610]. This could potentially lead to increased layer thickness due to cellular proliferation. However, although the effects of CBD on cerebellar development are not know, we initiated treatment at P18, well past the EGL proliferation peak[547,579,611]. Therefore, it is unlikely that treatment would induce an increase in neuronal cell number and layer thickness. Increased glia numbers, rather than neurons, could also contribute to increased layer thickness[319,612]. However, although it has been reported that CBD treatment could increase the number of astrocytes in piglets exposed to an ischaemic insult[613], a greater number of publications suggest that CBD reduces the number of both GFAP and Iba1 positive cells, albeit in models of ischemia, Alzheimer's and schizophrenia[409,455,456,608,614]. Therefore, based on the available literature, it is unlikely that CBD is inducing an increase in cellular number. Finally, we cannot discard that CBD might cause an increase in cell size, as seen for PC (see below), leading to increased layer thickness, but not density. This would contrast with previous work where CBD treatment was shown to reduce cell size (Chapter 2)[411,615,616]. However, due to

technical considerations, the high density of cells in the GCL did not allow for individual measurements of size. Future work focusing on individual cell analysis and glia-specific markers, as mentioned before, could help understand if CBD modifies the proliferative capacity of cells in the cerebellum.

Contrasting with the GCL experiments, we could indeed measure and confirm an increase in PC cross-sectional area due to CBD treatment. Particularly in the Eker group, this was also accompanied by an increase in PCL thickness. This is pertinent given that we found that Eker rats exhibited smaller PC size compared to WT animals. One of the proposed actions of CBD is the promotion of autophagy[412,617–619]. Autophagy, in turn, was shown to induce mTORC2 signalling independently of mTORC1 activity[620,621]. Although this relationship was shown in fibroblasts and colorectal cancer cells, if mTORC2 dysfunction is indeed present in the Eker rat, as we previously hypothesized, and is responsible for altered PC size, this could be a potential mechanism of action by which CBD is correcting for this defect.

From a functional point of view, PC size regulation is of particular importance given that cell size is one of the determinants of input resistance and ion channel distribution, which further impacts on type and timing of PC discharges[324,622,623]. Physiologically, these alterations can potentially be of great importance as changes in PC response have been found in animal models of TSC and autism-like behaviour[324,624].

3.5 Conclusion

This work revealed mild phenotypical alterations in the Eker rat cerebellum. Eker rats exhibited increased cell density in the GCL, which could possibly be attributed to an increased proliferation rate, and a decrease in PC size, which could potentially be associated with mTORC2 signalling deficits. We also found that CBD increased layer thickness and cell area, opposing the effect of the *Tsc2*$^{+/-}$ mutation in PC size. This could possibly be accomplished by the modulation of mTORC2. Pharmacological targeting of PC size alterations could have potential therapeutic value thus, further studies with CBD focusing on its cerebellar mechanism of action could help understand its possible role in ASD-like behaviours.

Chapter 4: The effect of CBD on Eker rat behaviour: a focus on locomotor, repetitive- and anxiety-like, social interaction and memory outputs

4.1 Introduction

TSC is a genetic disease with significant neurological and neuropsychiatric involvement. Despite phenotypical variability between patients, CNS dysfunction is present in up to 90% of individuals, not only in the form tubers and SEGAs, but also in the form of TAND, such as increased levels of anxiety, memory deficits and high ASD prevalence (Section 1.1.3)[14,18,95,97]. Consequently, alongside the pharmacological treatment of tumours and epilepsy (Section 1.1.3.4), TSC patients often require additional therapy to manage their neuropsychiatric symptoms. This polypharmacological approach is far from optimal, with unwanted interactions, resistance to treatment, relapse following cessation of therapy and unknown effects of long-term treatments documented in the literature (Section 1.1.3.4.2). The use of multiple drugs and therapies has also been shown to contribute to disease burden, decreasing QoL as well as school and work productivity, while simultaneously increasing patient- and government-supported medical expenses[34,152,625].

Typically, the treatment of symptoms such as anxiety, attention deficit or sleep difficulties in TSC follows treatment and prescription guidelines for the general population[92,98]. Behavioural difficulties, often associated with the ASD comorbidity, are highly prevalent in TSC[14,110,113,117]. A number of drugs are available for their management, albeit addressing a limited range of behavioural features such as aggressive behaviour and irritability (Section 3.1)[626,627]. However, evidence for the efficacy of these compounds is scarce and, especially in children and young adults, side effects of long-term treatment are considerable, including metabolic syndrome, tachycardia, increased irritability or increased frequency of suicidal thoughts[511,626–628]. Therefore, careful individual evaluation of the risk versus benefit of pharmacological treatment is needed before prescription. Given the burden of neuropsychiatric dysfunction to individuals, and the significant impact behavioural alterations have on the QoL of both patients and carers[508,509,629–632], research into new therapeutic options that can aid TAND management is crucial.

In the search for new compounds that could benefit TSC patients, this thesis has focused on the evaluation of CBD for different pathological features present in TSC. We have previously reported that, in a zebrafish model of TSC, a one-day treatment with 1.25 μM CBD induced a reduction in the number and size of phosphorylated rpS6 positive cells, while also reducing anxiogenic-like responses (Chapter 2)[615,616]. In the Eker rat, we showed that mutation-induced reductions in PC cross-sectional area were increased by a twice daily administration of 100 mg/kg CBD for 7 days (Chapter 3).

In pre-clinical studies, CBD administration was shown to ameliorate a number of symptoms relevant to TAND. These include the reduction of anxiety- and depression-like behaviours and the improvement of social interaction deficits[405,406,565,633]. Clinical work has also suggested a possible beneficial role of CBD in improving behavioural features altered in TSC. For example, 66.7% TSC patients with refractory epilepsy, treated for 12 months with 5-50 mg/kg/day CBD, reported (by either parents and physicians) behavioural improvements[403]. Together, this body of work suggests beneficial contributions of CBD towards the behavioural alterations typically presented by TSC patients. Seminal work by Waltereit and colleagues reported that 3-6 month old Ekers exhibited social interaction deficits and reduced object exploration, both representative of ASD-like features[370,634]. However, limited work has been done on the possible ASD-like phenotype of the Eker rat[232,370]. Therefore, we hypothesised that this model could exhibit other behavioural dysfunctionalities in addition to the ones reported thus far, similar to what is reported by TSC patients, and that CBD could potentially reverse these alterations.

To test which behaviours might be modified and, conversely, which of these could be changed by CBD administration, a battery of behavioural tasks was designed aimed at screening different neuropsychiatric symptoms reported by TSC patients. As already mentioned, one of these is social interaction impairment (Section 1.1.3.5)[111,112,115]. Here, we addressed these social deficits by studying the interaction between the Eker rat and a stranger (unknown, novel) rat. Social engagement is a typical rodent behaviour. Both rats and mice tend to engage in contact with novel partners, displaying increased investigation and play behaviour with unknown animals[370,635]. Thus, the social interaction task can be used to detect deficits in social behaviour which correlate to those observed in some TSC-ASD patients[634]. Reduced interest in new environments and experiences is also a common feature of TSC-ASD as well as nsASD patients[115,117,636]. In rodents, this behaviour can be evaluated indirectly by measuring the time spent exploring old and new objects, as rodents exhibit a preference for objects that are unknown to them[637,638]. As a measure of this, the novel object recognition task directly assesses working memory deficits. Animals must recognize and distinguish a previously presented object[638–640], a valuable output given that memory deficits have also been observed in TSC patients[95,641].

Anxiety disorders are a common comorbidity in TSC[94,96,98,642]. Additionally, the high prevalence of ASD in this population itself predicts a higher incidence of anxiety in these individuals[94–97,643,644]. We then studied if the Eker rat exhibited increased anxiety levels by quantifying the time spent exploring the inner area of an open-field arena. Rats preferentially ambulate in areas where at least one wall is present, hence avoiding open and exposed spaces[645–648]. Therefore, increased time spent in the inner area of the open-field is interpreted as an anxiolytic-like state, which can be modulated by compounds and mutations[648–652]. Furthermore, grooming behaviour during open-field exploration was also quantified as, although not a marker of anxiety in itself, this innate repetitive behaviour can likewise be potentiated or decreased depending on the

stressful stimuli presented[653–656]. Higher levels of anxiety have also been associated with the presence of repetitive behaviours[657,658]. In TSC, these are also part of the identified TAND[95,659–661], although typical of the TSC-ASD population rather than the TSC-no ASD one[642,662]. To assess the presence of perseverative behaviours in TSC, Eker rats were also exposed to the marble burying task, as excessive digging has been shown to translate into obsessive-like behaviour[663–665].

Finally, decreased gross and fine motor control were detected with the MSEL in children with TSC as young as 9 months old[113]. Furthermore, atrophy and death of PC, which contributes to altered motor function and gait[539,666], have also been found in *post-mortem* cerebella of TSC patients[228,334]. Therefore, we assessed motor performance by analysing spontaneous locomotion in the open-field and footprint patterning on the gait apparatus.

The present work 1) explored the presence of behavioural alterations in the Eker rat analogous to TAND manifestations and 2) investigated the effect of an 8-week CBD treatment on behaviour. We hypothesized that the Eker rat would exhibit additional behavioural deficits to the ones reported in previous work and that long-term CBD treatment would ameliorate these features.

4.2 Methods

4.2.1 Breeding and animal groups

Wild-type (WT; *Tsc2*$^{+/+}$) and Eker rats (heterozygotes; *Tsc2*$^{+/-}$) from the Long-Evans background were kindly provided by Dr. Waltereit (Technical University of Dresden, Dresden, Germany) and bred in-house, group-housed at room temperature on a 12:12 hour day/night cycle and with food and water provided *ad libitum*. Genotyping of male rats was conducted during post-natal week 2 (see below; Section 3.2.2). Once finalized, animals were assigned to one of four groups, each containing 9 animals: WT-vehicle, WT-CBD, Eker-vehicle and Eker-CBD. In total, 36 male rats were used for this study. From post-natal week 3 to 10, animals underwent vehicle or CBD treatment (see below, Section 4.2.3), with behavioural testing conducted during post-natal weeks 9 and 10 (see below, Section 4.2.4) (Figure 4.1). Animals undergoing treatment were handled twice daily by the researchers conducting the behavioural experiments to ensure familiarity of the animals with the handlers. Habituation to handling for the unfamiliar rats used in the social interaction task (see below, Section 4.2.4.2) was done at least twice a week. All animal experiments were approved by the University of Reading Ethics Board and the UK Home Office (PPL 70/8974), and carried out in accordance with UK Home Office regulations (Animals (Scientific Procedures) Act, 1986) and the ARRIVE guidelines.

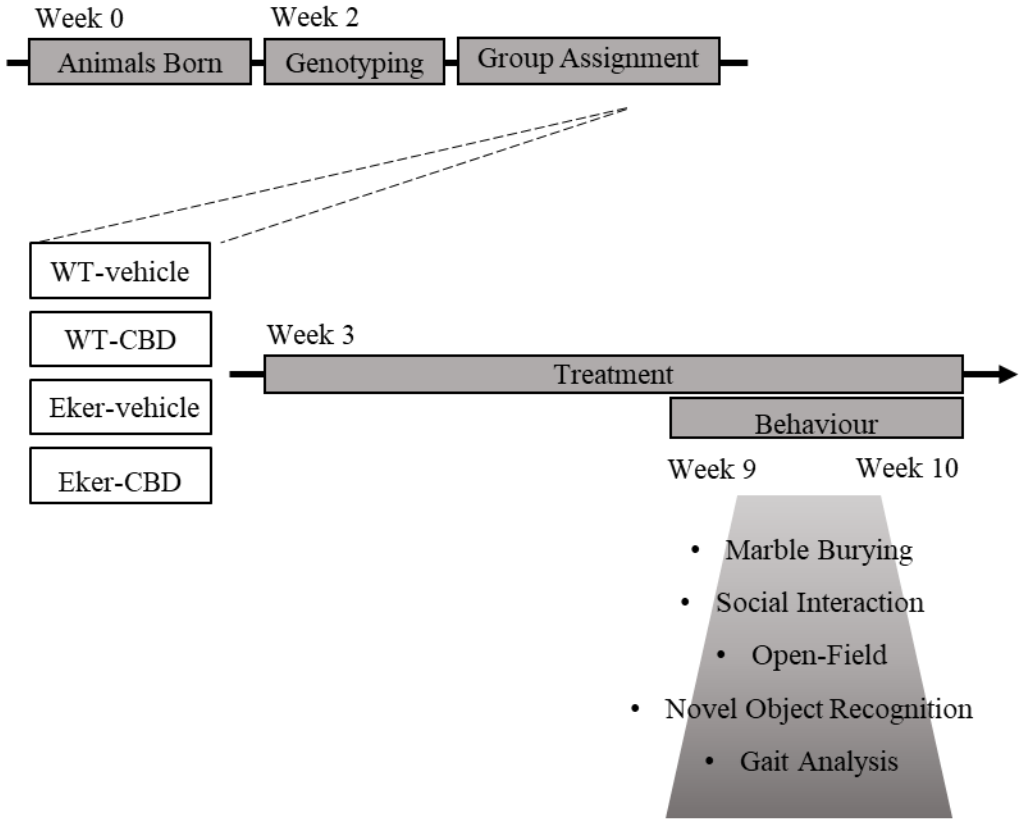

Figure 4.1: *Treatment timeline*. Animals were genotyped during post-natal week 2 and assigned into four different treatment groups. Treatment was initiated on week 3 and continued for 6 weeks. A behavioural test battery was initiated on week 9 and treatment continued until testing was concluded.

4.2.2 Genotyping

Genotyping was performed as described in Section 3.2.2. Briefly, at post-natal day 14, animals were ear-notched and DNA was extracted. PCR was conducted using previously published primers that target the Eker mutational insertion[328], together with positive (original Eker DNA) and negative (water) controls. PCR products were analysed in a 2% agarose gel in tris-acetate-EDTA buffer and visualized in a Syngene U:Genius 3 gel imaging system (Syngene, UK).

4.2.3 Pharmacological treatment

From post-natal weeks 3 to 10, animals were weighed prior to injection (i.e., twice daily) and their weights recorded and monitored. Weight values were used to calculate the average weight gain per week (*weight gain)* and the average body weight at the end of the experimental period (*final weight*). After calculation of the required injection volume, based on each animal's weight, rats were injected subcutaneously with either vehicle (2:1:17 EtOH: Cremophor: 0.9% saline)

(Ethanol 32221, Merck) (Kolliphor®HS 15, 42966, Sigma) or 100 mg/kg CBD (GW Pharmaceuticals, Cambridge, UK), twice daily, until the last day of behavioural experiments (Figure 4.1). Vehicle and CBD formulations were prepared and aliquoted in glass vials and kept at 4°C protected from light. Prior to injection, both formulations were warmed to room temperature.

4.2.4 Behavioural tasks

All behavioural tasks were conducted in the light phase, between 10:00 and 16:00, during post-natal weeks 9 and 10 (Figure 4.1). All behavioural tasks and animal weighing were conducted in the same room, except for the gait task. Animals were left to acclimatize to the behavioural testing room for at least one hour after the morning injection of the last rat, and all behavioural tasks were initiated after this period. This allowed for the maximal concentration of CBD to be achieved in the brain before behavioural tasks were initiated[607]. For the gait task, animals were moved to the test room after weighing and drug administration, before being left to habituate for at least one hour prior to task initiation. All apparatus and equipment were thoroughly cleaned with 70% ethanol between each individual animal and at the end of each experimental day. Except for the marble burying and gait tasks, all experiments were recorded with a video camera and behavioural parameters (outlined below) were coded with Noldus The Observer® XT, Version 9 (Noldus Information Technology b.v., Wageningen, The Netherlands).

4.2.4.1 Marble burying

To study the presence of obsessive-compulsive-like and repetitive behaviours, the number of buried marbles was quantified in the marble burying task[607,667]. In summary, standard 32 x 50 x 18 cm rat cages were filled with 5 cm of bedding and 5 rows of 4 marbles were set on the surface of the bedding. Animals were then placed in the cage facing a corner and the cage lid closed. Rats were left undisturbed for 30 minutes and returned to their home cage at the end of this period. A photo of each cage was acquired before and after the task took place (Figure 4.2A) and the number of marbles that had been buried was calculated (maximum score= 20). For analysis of the number of buried marbles, the surface area of each individual marble was measured with Fiji Image J[475] in both before and after task photos. Comparing the area of exposed marble in both pictures, marbles were considered buried if two thirds or more of their surface was covered by bedding material[607].

4.2.4.2 Social interaction

The social interaction task, aimed at studying the interaction between the test animal and an unfamiliar strange rat, was performed as previously described[370,668]. To habituate the animals to the

test arena, the day before the test trial, animals were individually placed into a 52 x 52 x 45 cm Perspex arena and allowed to freely explore for 5 minutes. On the test day, each animal was placed individually in the centre of the arena. After one minute, an unfamiliar rat was added to the arena facing a corner. Unfamiliar rats were age- and weight-matched male Long-Evans which belonged to a different litter than the test animal. Each unfamiliar rat interacted individually with 3-5 test rats. After three minutes of interaction, both test animal and stranger rat were returned to their home cages. The latency to first contact between test and unfamiliar animals, the time the test animal spent interacting with the unfamiliar rat and the total number of interactions were coded and quantified. An event was coded as an interaction if the test rat was grooming, sniffing, crawling under or over, or play fighting with the unfamiliar rat. Data for each group of animals (WT-vehicle, WT-CBD, Eker-vehicle and Eker-CBD) was pooled together to yield a mean frequency and duration of interaction, as previously published[370].

4.2.4.3 Open-field

The open-field task was performed as published elsewhere[669] aiming at quantifying spontaneous locomotor activity. Here, the 52 x 52 x 45 cm Perspex arena was divided into 4 x 4 squares, as illustrated in Figure 4.2B. Animals were placed in the centre of the arena, left to explore for 5 minutes, and the total time each animal spent moving was quantified. A moving event was coded when the animal was traversing across squares of the arena. Additionally, to measure anxiety-like behaviour, the time each animal spent in the inner squares of the arena, as well as the time spent grooming and the number of grooming events, were also coded and quantified. A grooming event was considered when the animal was licking or chewing its fur.

4.2.4.4 Novel object recognition

To evaluate memory impairments and the distinction between known and unknown stimuli, the novel object recognition task was performed as previously published[370,670]. Each individual animal was placed in a 52 x 52 x 45 cm Perspex arena and allowed to explore an unknown object for 3 minutes (Phase 1). These consisted of hard plastic, geometric, three-dimensional shapes, such as cones, triangular and squared pyramids. After Phase 1, each animal was returned to its home cage. Following a 15-minute interval, a copy of the object used in Phase 1 was placed in the arena, together with a new unknown object. This should be recognized as novel and, therefore, preferentially explored (Phase 2) (Figure 4.2C). After 3 minutes of exploration, rats were again returned to their home cage. The time spent exploring the object during Phase 1 and the time spent exploring either object during Phase 2 were coded and quantified. Exploration of the object was considered when the animal was touching, sniffing or biting the object. Standing on top of the

object was not considered object exploration, unless the animal was sniffing or biting the object specifically[671,672].

4.2.4.5 Gait analysis

Locomotor symmetry and motor coordination was evaluated with the gait test. The protocol used here was adapted from previously published work[673–675]. A transparent Perspex apparatus consisting of a 100 x 13 x 11 cm corridor attached to a 31 x 31 x 11 cm dark box was used. Animals were habituated to the apparatus and task for two consecutive days, by performing the task as described below but using water instead of ink. On the third day, the hind paws of each rat were coloured with blue tattoo ink and the animal was placed at the entrance of the corridor, lined with a white paper strip (uncoated Inkjet Printer Roll, 610 mm x 45 m, 90 gsm, Office Depot), and allowed to run along the corridor to the dark box. After crossing into the dark box, the rat was returned to its home cage and, 5 minutes later, a second trial was repeated. The right side stride length (the distance between two right foot strikes, measured from the mid-point between the central foot pad print and the proximal toe print), left side stride length (the distance between two left foot strikes, measured from the mid-point between the central foot pad print and the proximal toe print) and stride width (the midpoint distance between consecutive left and right strikes, obtained by the measurement parallel to the mid-point distance between the central foot pad and the proximal toe print) were measured in centimetres as shown in Figure 4.2D. The results of the two gait runs were averaged for each animal.

4.2.5 Western Blot

To assess mTORC1 pathway alterations due to genotype or treatment, phosphorylated rpS6 (235/236) and total rpS6 proteins were quantified using western blot. All chemicals were purchased from Sigma unless stated otherwise.

Following completion of behavioural tasks, animals were sacrificed with CO_2 and brains were rapidly removed and washed in PBS. Samples were flash frozen and kept at -80° C until used. For western blot, 3 brains from the WT-Vehicle, 3 brains from the WT-CBD, 3 brains from the Eker-Vehicle and 3 brains from the Eker-CBD group were used.

For sample lysate preparation, brains were first homogenized using an electronic homogenizer, 3 times for 30 seconds each time. The Bradford assay was used to quantify the total protein content of each sample using NanoDrop™ (Thermo Fisher, UK), according to manufacturer instructions. Samples were diluted with sample buffer (150 mM Tris-HCl (pH 6.8), 300 mM DTT, 6% SDS, 0.3% bromophenol blue, and 30% glycerol) to achieve a 5 µg/µl concentration and boiled at 95º C for 5 minutes.

Proteins in the lysate were separated by electrophoresis using a Mini-PROTEAN® II electrophoresis cell (Bio-Rad, UK). First, a 10% separating gel was prepared, consisting of 5 ml of H_2O, 2.5 ml of separating buffer (0.75 mM Tris base, 0.4% SDS; pH 8.8), 2.5 ml of 40% acrylamide, 60 µl of 10% ammonium persulfate and 6 µl of TEMED. After the separating gel settled, a 5% stacking gel consisting of 1.85 ml of H_2O, 0.75 ml of stacking buffer (0.25 mM Tris base, 0.4% SDS; pH 6.8), 0.375 ml of 40% acrylamide, 40 µl of 10% ammonium persulfate and 4 µl of TEMED was prepared and poured over the separating gel. Once the stacking gel was settled, the first well was loaded with the protein molecular weight marker Precision Plus Protein™ (1610374, Bio-Rad, UK). The subsequent wells were loaded with 10 µL of sample lysate, each in duplicate. The gel was covered with running buffer (48 mM Tris base, 384 mM glycine, 0.1% SDS) and ran for 30 minutes at 80V and then for 100-120 minutes at 110 V.

Once the gel run was finished, proteins were transferred to an Immun-Blot® PVDF (polyvinylidene difluoride) Membrane (1620177, Bio-Rad, UK), using a Trans-Blot® SD Semi-Dry Transfer Cell (1703940, Bio-Rad, UK). To prepare the transfer, PVDF membranes were activated in absolute methanol for 30 seconds and in distilled H_2O for 2 minutes. Membranes were soaked in transfer buffer (25 mM Tris base, 250 mM glycine, 25% methanol) for 10 minutes. Filter papers (Whatman, UK) were soaked for 10 to 15 minutes solely in transfer buffer. A transfer "sandwich" was prepared by stacking the transfer membrane and the gel between two layers of filter paper and ran at 15V for 1 hour.

After the transfer, membranes were blocked by incubation with a 2.5% non-fat milk, TBS-0.1% Tween 20 (TBST) buffer for 1 hour, at room temperature, in an orbital shaker. After this step, membranes were incubated with primary antibodies targeting phosphorylated rpS6 (Ser 235/236) (1:800, rabbit anti-phospho S6 Ribosomal Protein (Ser235/236), #2211, Cell Signalling) or total rpS6 (1:1000, rabbit anti-S6 Ribosomal Protein, #2217, Cell Signalling), and with a primary antibody against glyceraldehyde-3-phosphate dehydrogenase (GAPDH) (1:5000, mouse anti-GAPDH, monoclonal GA1R, MA5-15738, Thermo Fisher, UK), used as a loading control. Antibodies were diluted in 2.5% non-fat milk in PBS and left overnight in an orbital shaker at 4º C. On the following day, membranes were brought up to room temperature and placed in the orbital shaker for another hour. Membranes were then washed in TBST, TBS and finally in PBS for 3 x 10 minutes. After this step, membranes were incubated for 2 hours at room temperature, with the corresponding horseradish peroxidase (HRP)-conjugated secondary antibodies (Goat anti-rabbit IgG (H+L), HRP (474-1506), 5450-0010, SeraCare KPL, USA; Goat anti-mouse IgG (H+L), Human Serum Adsorbed, HRP (474-1806), 5450-0011 SeraCare KPL, USA), diluted in 2.5% non-fat milk in PBS. At the end of the two-hour incubation, membranes were washed again in TBST, TBS and PBS for 3 x 10 minutes.

To reveal protein bands, membranes were incubated with Clarity™ Western ECL Substrate (Bio-Rad, UK) and bands detected with a BioSpectrum® AC Imaging System (UVP, UK). A picture

of each membrane was acquired after a 1-minute exposure and the optical density of each band was analysed with Image J[475] as described below.

4.2.5.1 Optical Density Measurement

Protein bands detected in the western blot membrane were analysed with the densitometry method[676,677]. Membrane images were loaded into the Image J software and bands were horizontally aligned, when necessary, with the *Image → Transform → Rotate* command. A ROI was defined around the protein bands and, using the command *CTRL1 + CTRL3*, a histogram of each band was obtained. The area of each histogram, proportional to the band's intensity, was selected and measured using the *Wand* tool. A normalization factor was determined by dividing the highest GAPDH optical density value (ODV) by the remaining GAPDH values. The ODV obtained for each sample was then divided by the corresponding normalization factor to obtain a normalized experimental signal (NES) for each experimental sample[678]. As each sample was loaded in the gel in duplicate, two NES were obtained per sample. These were averaged to obtain one single NES value per sample, i.e. per animal.

4.2.6 Statistics

All datasets were analysed with IBM SPSS Statistics 22 and graphs were designed with GraphPad Prism 6. Prior to data analysis, data was scanned for outliers using the Grubbs test. The following outliers were found and removed: one value in *object recognition Phase 1* ($z = 3.708$, $p<0.05$); one value in *object recognition Phase 2* ($z = 4.113$, $p<0.05$); one value in *inner squares exploration* ($z = 4.733$, $p<0.05$); and one value in *weight gain* ($z=3.0215$, $p>0.05$). An initial exploratory analysis revealed a significant difference between the weights of the different groups. Therefore, in all further statistics, *weight* was used as a covariate except with *weight gain*, *final weight* and the western blot data. Normality and homogeneity were tested with the Shapiro-Wilk and Levene's tests, respectively. All data was analysed with a two-way ANCOVA using *treatment* and *genotype* as independent variables and *weight* as a covariate. *Weight gain* was analysed with repeated-measures, taking into account the average weight gain per animal during each treatment week. A two-way ANOVA was used to analyse western blot data with *treatment* and *genotype* as independent variables and *normalized experimental signal (NES)* as the dependent variable. Post hoc analysis was performed using the Bonferroni test corrected for multiple comparisons. Where assumptions of normality and homogeneity were not met, bootstrapping was performed, to account for the unequal distribution of data and variance[537,538]. This was the case for *inner squares exploration* (Open-field task), *time spent grooming* (Open-field task), *grooming frequency* (Open-field task) and *time to first approach* (Social interaction task). Additionally, as weight was a

significant covariate in *inner square exploration* (p=0.049) and approached significance in the *open-field locomotion* (p=0.052), a correlation was also conducted between these variables, using the Pearson correlation coefficient.

4.3 Results

4.3.1 Weight progression and phenotypic observations during the 8-week drug treatment

During the treatment period, no changes in response to handling or any atypical behaviour were observed for any group. Animals were well habituated to handlers, did not show any aggressive reactions and exhibited a standard play behaviour and posture in the cage[679]. With repeated CBD injections some animals exhibited subcutaneous lumps at the injection site despite injection site rotation. These persisted for a few days but did not appear to be painful, as animals did not react aggressively to touch on the affected areas nor exhibited increased scratching behaviour, with exception of one single animal. Therefore, these did not require any additional treatment or veterinary intervention. These lumps were not present in the vehicle-treated group.

As expected for this age range, a gain in weight was present across all groups (effect of week: F(3.274, 52.388)=90.113, p=0.000) (Figure 4.3A). Significant weight increments were found from the first to the last treatment weeks, with exception of weeks 4 and 5 where weight gain was constant between weeks. No weight loss was observed across the 8-week treatment period (Figure 4.3B). No significant interactions between *week* and other variables were observed. Further analysis of the weekly weight gain revealed a main effect of treatment (F(1,16)=30.42, p=0.000) and a significant treatment x genotype interaction (F1,16)=4.89, p=0.042). This showed that while WT CBD-treated animals constantly gained less weight than WT vehicle-treated rats (average weight gain: 40.98 g ± 1.16 for WT-vehicle vs 31.97 g ± 1.05 for WT-CBD; p=0.000), this effect of CBD was more pronounced in the Eker group, where the magnitude of weight gain was lower (37.55 g ± 1.29 for Eker-vehicle vs 33.70 g ± 1.16 for Eker-CBD; p=0.041) (Figure 4.3B). There was no significant effect of genotype on weight gain (F(1,16)=0.533, p=0.476).

Analysis of the final weight at the end of the 8-week treatment period revealed a significant effect of treatment (F(1,32)=7.692, p=0.009; 314.98 g ± 8.69 for vehicle vs 280.88 g ± 8.69 for CBD), but no effect of genotype (F(1,32)=0.026, p=0.873; 296.94 g ± 8.69 for WT vs 298.92 ± 8.69 for Eker) or treatment x genotype interaction (F(1,32)=2.319, p=0.138) were detected (Figure 4.3C). These results indicate that, overall, CBD-treated animals gained less weight than vehicle-treated animals although no weight loss was observed.

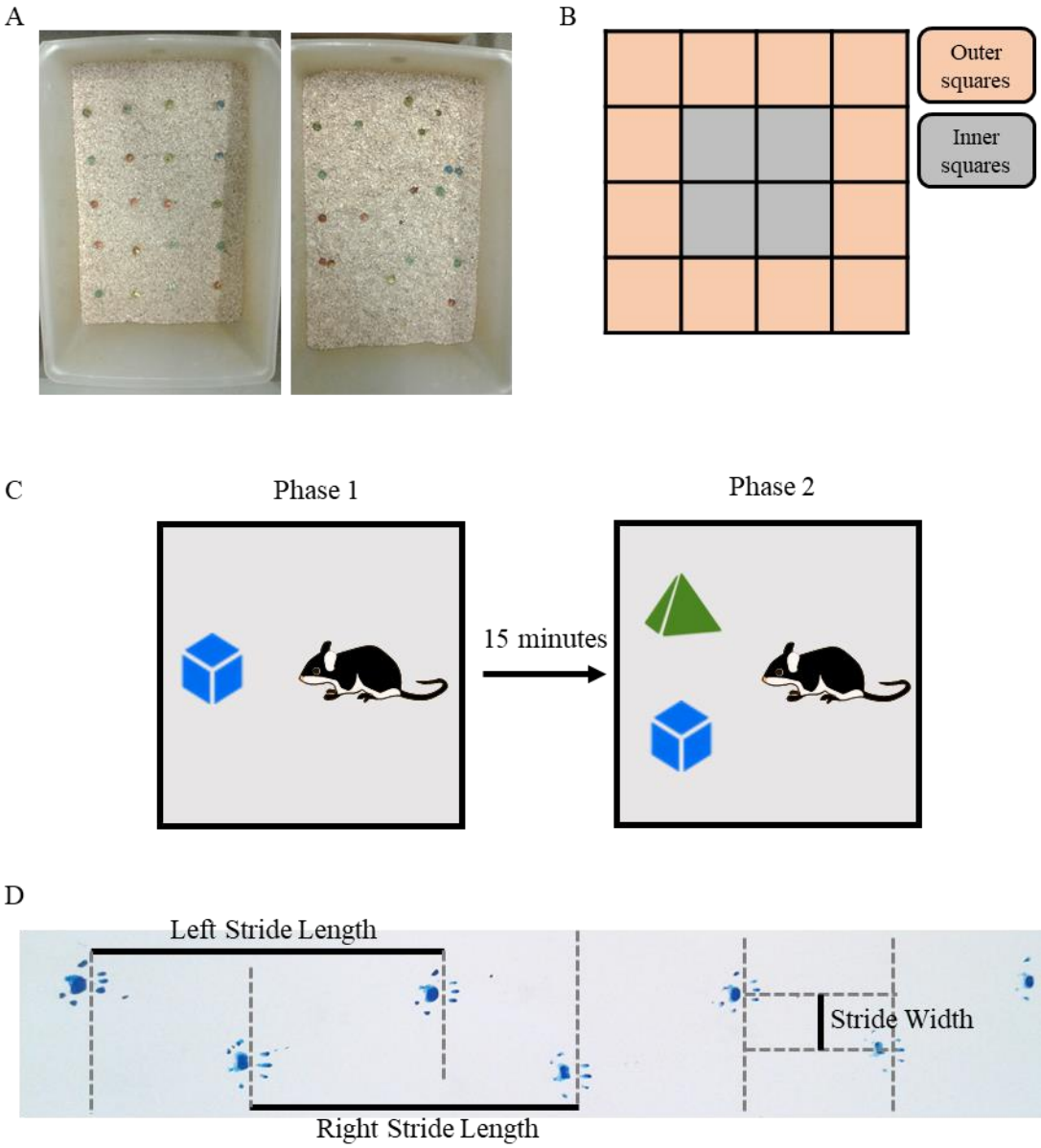

Figure 4.2: *Experimental set-up for behavioural testing.* (A) Representative photos of the marble burying task, with the left panel showing the marble set up before the test and the right panel showing the result of the task after 30 min of animal exposure. (B) During the open-field task, the test arena was divided in 4 x 4 squares and an inner and outer area was defined. (C) In the novel object recognition task, animals were presented with an unknown object in Phase 1 (C, left panel), and a copy of that same object, together with a novel object, during Phase 2 (C, right panel). (D) An example of a gait task output is presented with indication on the measuring method for the left side stride length, right side stride length and stride width. Parallel lines between the central foot pad print and the proximal toe print were designed to guide the measurement of the three parameters.

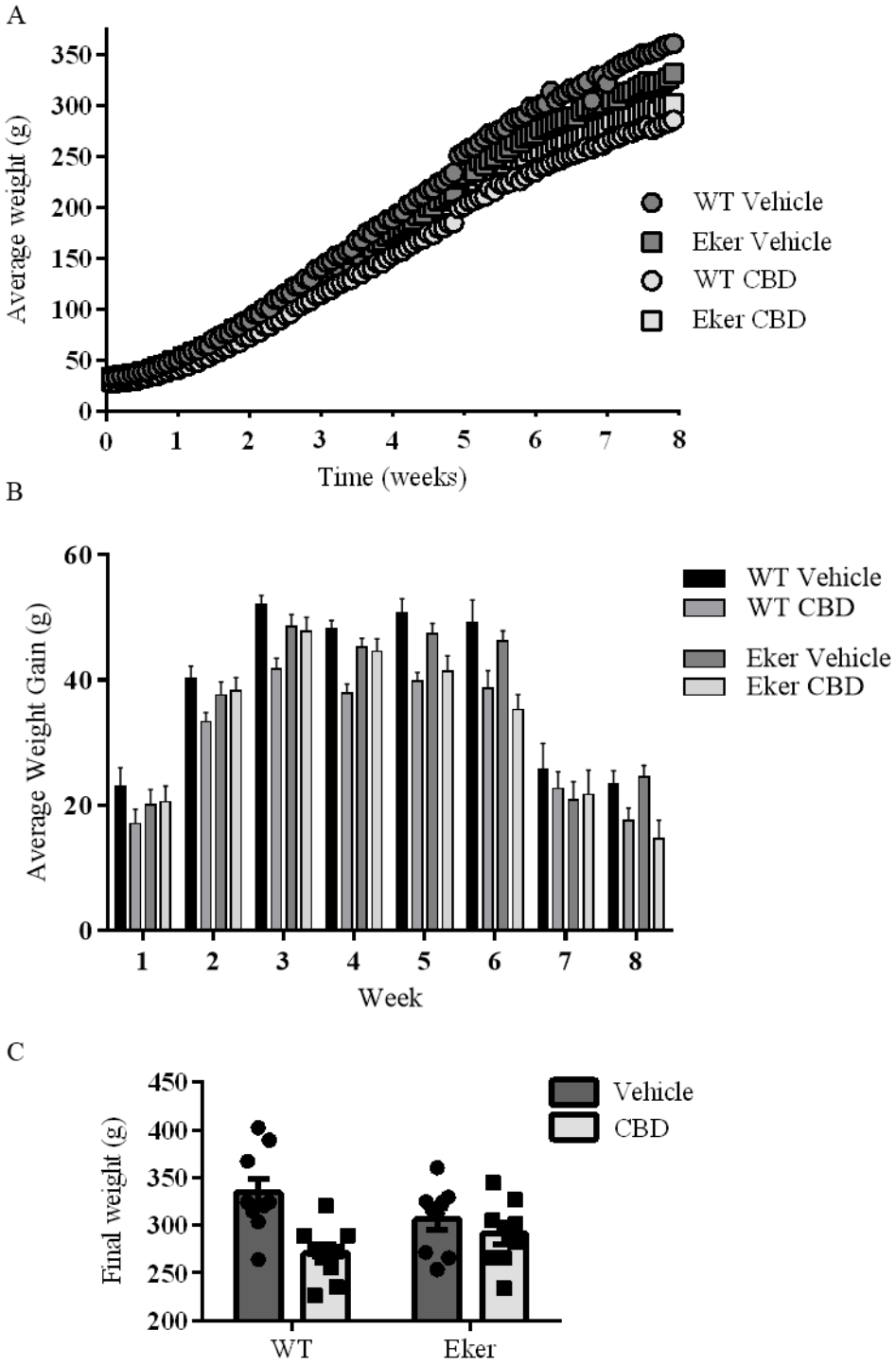

Figure 4.3: *Weight progression during the 8-week treatment is changed by CBD administration.* (A) During the treatment period, all animals increased in total body weight regardless of group. (B) However, a main effect of treatment was observed ($F(1,16)=30.42$, $p=0.000$), indicating that CBD-treated animals gained less weight than vehicle-treated ones. (C) At the end of the study, a significant difference in weight was found between the vehicle and CBD-treated groups ($F(1,32)=7.692$, $p=0.009$), with the latter exhibiting lower weight than the former. Data are presented as mean. SEM was excluded from (A) for clarity but is present in (B) and (C). n= 9 animals per group.

4.3.2 Eker rats exhibit reduced locomotor exploration in the open-field whilst CBD treatment reduces gait width in Ekers and WT

Spontaneous locomotor activity was analysed with the open-field apparatus. No significant main effect of treatment ($F(1,31)=0.153$, $p=0.699$; 36.86 ± 4.08 % time for vehicle vs 34.46 ± 4.08 % time for CBD) nor interaction between variables ($F(1,31)=0.08$, $p=0.779$) was observed for the time spent moving (Figure 4.4A). However, in contrast to previous reports[232,370], a significant main effect of genotype was found ($F(1,31)=8.076$, $p=0.008$) with Ekers spending less time exploring the open-field arena (43.30 ± 3.80 time for WT vs 28.02 ± 3.80 % time for Eker; Figure 4.4A). As the covariate *weight* approached significance ($F(1,31)=4.068$, $p=0.052$), a correlation between *weight* and the *time spent moving* was performed. A significant and positive correlation was found between the two variables indicating that heavier animals spent more time moving that lighter ones ($r=0.384$, $p=0.021$) (Figure 4.4B).

Next, we analysed performance on the gait apparatus (Figure 4.2D). Footprint analysis demonstrated that both right and left strides presented with a similar distribution in all groups highlighting symmetry of stride. This indicates a lack of central and peripheral motor deficits[680]. These parameters were also similar between groups, suggesting the preservation of a typical stride rhythm in all groups[680,681]. There was no main effect of genotype on the right stride length ($F(1,31)=0.112$, $p=0.740$; 12.74 ± 0.39 cm for WT vs 12.92 ± 0.40 cm for Eker) nor on the left stride length ($F(1,31)=0.196$, $p=0.661$; 12.86 ± 0.42 cm for WT vs 13.12 ± 0.42 cm for Eker) (Figure 4.4C-D). Additionally, no main effect of treatment was found for the right stride length ($F(1,31)=1.230$, $p=0.276$; 13.21 ± 0.44 cm for vehicle vs 12.45 ± 0.44 cm for CBD) nor for the left stride length ($F(1,31)=0.347$, $p=0.560$; 13.20 ± 0.47 cm for vehicle vs 12.78 ± 0.47 cm for CBD) (Figure 4.4C-D). There were no statistically significant interactions between treatment and genotype for either stride length (right: $F(1,31)=10.065$, $p=0.069$; left: $(1,31)=1.807$, $p=0.189$). Analysis of the stride width revealed a main effect of treatment ($F(1,31)=7.262$, $p=0.011$) with CBD-treated animals presenting with a reduction in stride width irrespective of genotype (3.72 ± 0.12 cm for vehicle vs 3.23 ± 0.12 cm for CBD; Figure 4.4E). No effects on width were cause by genotype ($F(1,31)=2.218$, $p=0.146$; 3.58 ± 0.11 cm for WT vs 3.36 ± 0.11 cm for Eker) nor was there a significant interaction between variables ($F(1,31)=0.039$, $p=0.844$).

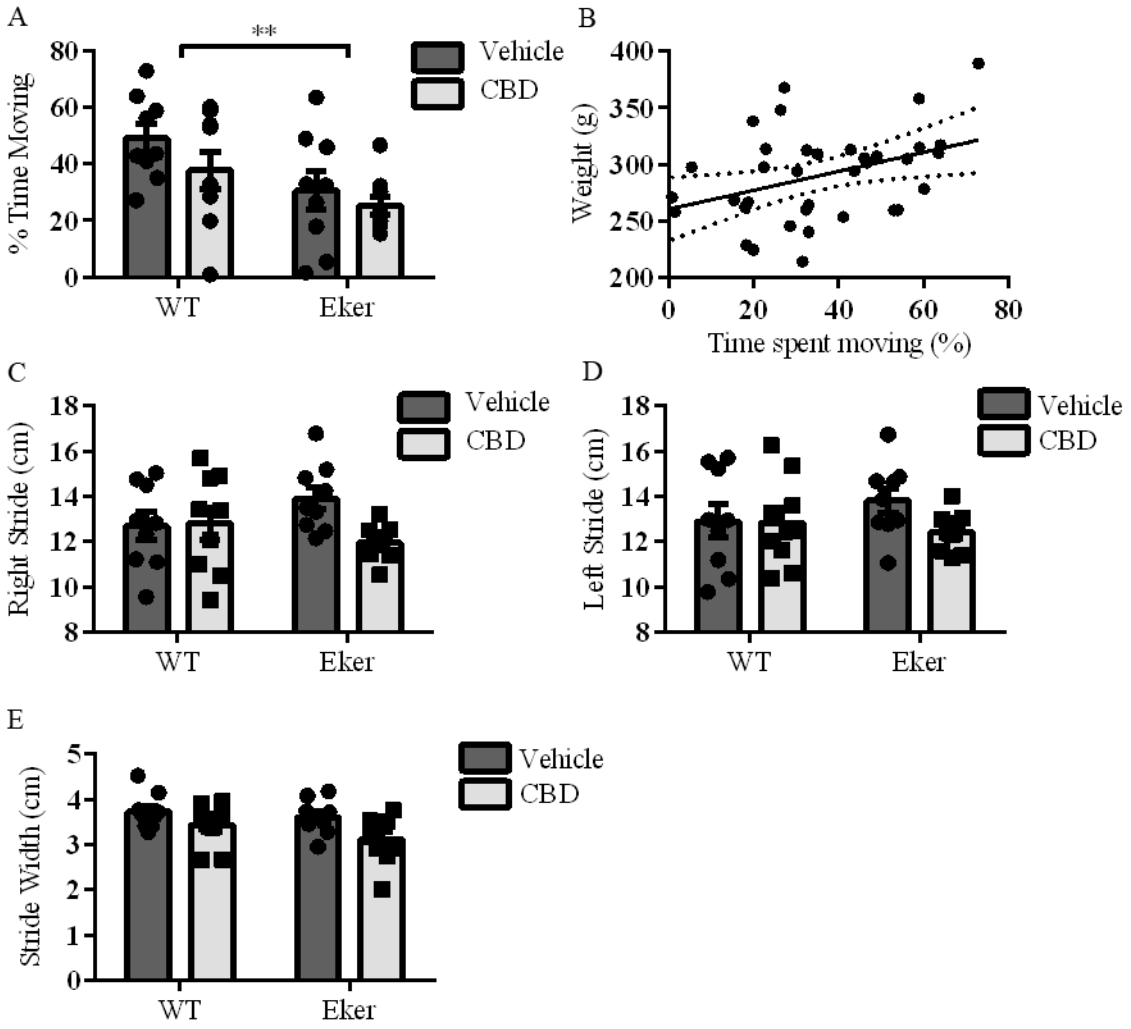

Figure 4.4: *Open-field exploration and gait analysis*. (A) Spontaneous locomotor activity was measured in the open-field arena and found to be reduced in Eker rats ($F(1,31)=8.076$, $p=0.008$). (B) This locomotor activity was also found to be positively correlated with total body weight, i.e. that heavier rats spent more time moving ($r=0.384$, $p=0.021$; curve of best fit with 95% confidence band). (C-E) Average gait measurements for each animal were also obtained for the right stride (C), left stride (D), and stride width (E), revealing that CBD administration reduced stride width in both genotypes ($F(1,31)=7.262$, $p=0.011$) (gait experiment performed by Leo Geng and Elena Serafeimidou). Data is presented as mean ± SEM; n= 9 animals per group; **$p<0.01$.

4.3.3 Repetitive and anxiety-like behaviours are absent in the Eker rat and are unchanged by CBD treatment

The marble burying test was used to evaluate the presence of perseverative behaviours[103,663,667] (Figure 4.2A). There were no effects of treatment on marble burying ($F(1,30)=1.506$, $p=0.229$; 10.09 ± 1.53 marbles for vehicle vs 7.30 ± 1.47 marbles for CBD), nor any significant interaction between treatment and genotype ($F(1,30)=0.036$, $p=0.852$) regarding the

number of buried marbles. However, there was a trend for Ekers to bury more marbles than WT animals (6.91 ± 1.41 buried marbles for WT; 10.48 ± 1.37 buried marbles for Ekers) but this did not reach statistical significance (F(1,30)=3.288, p=0.080) (Figure 4.5A).

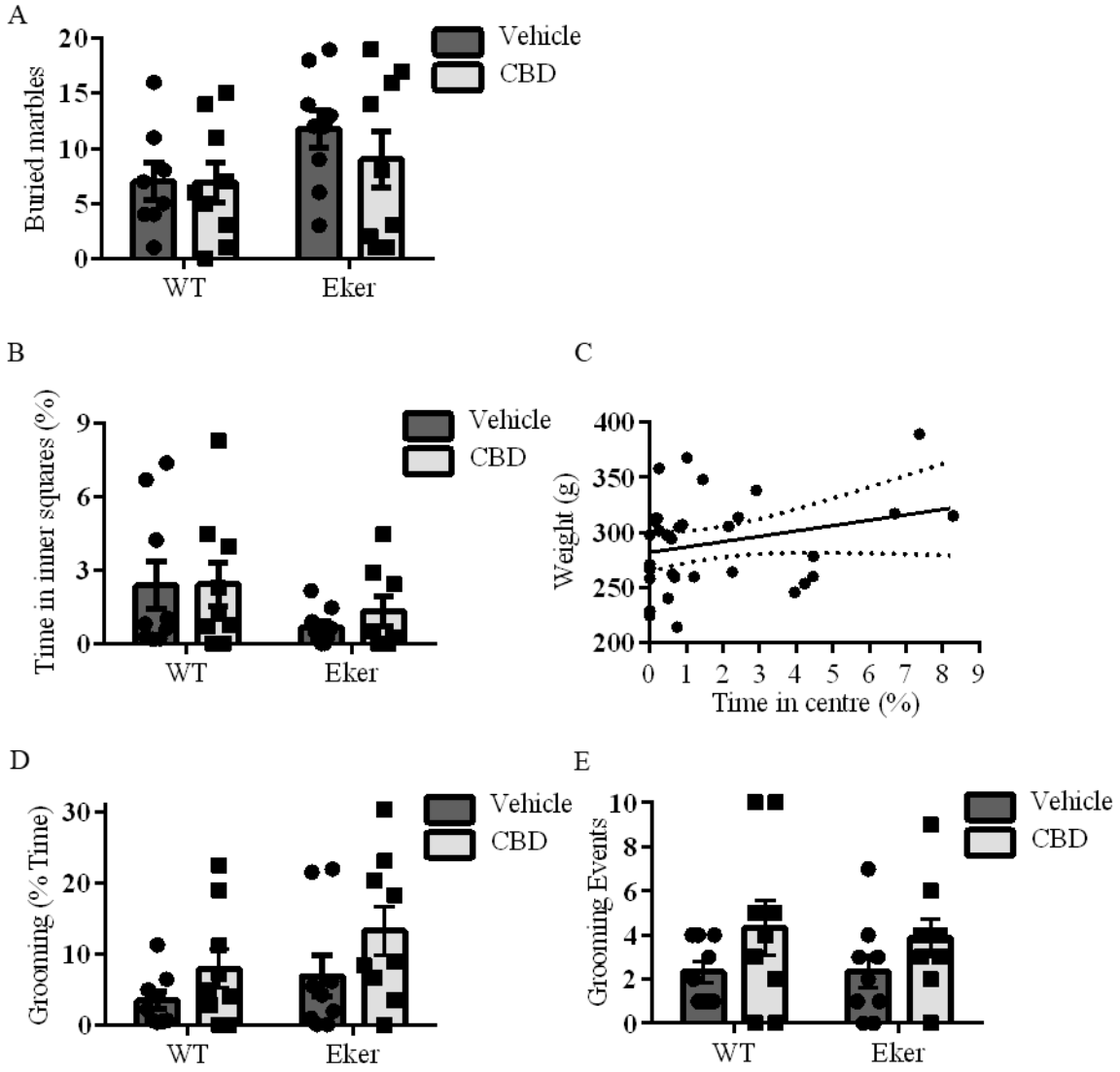

Figure 4.5: *Repetitive behaviours and anxiety-like features are absent from Eker rats and not modified by CBD treatment*. (A) Repetitive-like behaviours, analysed with the marble burying task by the quantification of the number of buried marbles, revealed no differences between experimental groups. (B) Likewise, anxiety-like behaviours, analysed in the open-field apparatus and with time spent in the inner squares of the arena, were quantified and found to be similar between groups. (C) A correlation analysis between weight and the time spent in the central area revealed a non-significant relationship between weight and time spent in the inner squares (r=0.268, p=0.120; curve of best fit with 95% confidence band). (D-E) Grooming behaviour quantification revealed no genotype (F(1,31)=2.754, p=0.109) nor treatment-induced changes (F(1,31)=0.903, p=0.284) in the time nor the number of grooming events. Data are shown as mean ± SEM; n= 9 animals per group.

The presence of anxiety-like behaviour was investigated with the quantification of the time spent in the inner squares of the open-field arena (Figure 4.2B). We found that both WT and Eker animals spent a similar amount of time in the inner area of the arena, although a tendency for higher avoidance of inner squares was observed in the Eker group but this did not reach statistical significance ($F(1,30)=3.528$, $p=0.087$ ($p=0.070$ without bootstrapping); 2.37 ± 0.61 % time for WT vs 1.02 ± 0.32 % time for Eker). Treatment had no effect on inner square exploration ($F(1,30)=1.985$, $p=0.201$ ($p=0.169$ without bootstrapping); 1.12 ± 0.50 % time for vehicle vs 2.27 ± 0.58 % time for CBD), and there was no significant interaction between the two variables ($F(1,30)=0.150$, $p=0.701$) (Figure 4.5B). A significant effect of the covariate *weight* was found regarding central exploration ($F(1,30)=4.225$, $p=0.049$) but the correlation between both variables was not statistically significant ($r=0.268$, $p=0.120$) (Figure 4.5C). As we previously observed a correlation between weight and general locomotion, this is likely a reflection of that effect.

Finally, we quantified grooming behaviour during the open-field exploration. Both the time spent grooming and the number of grooming events, behaviours that engage distinct central mechanisms, were quantified[653]. Here, no differences were found regarding genotype ($F(1,31)=2.754$, $p=0.109$ ($p=0.107$ without bootstrapping); 5.75 ± 1.46 % time for WT vs 10.03 ± 2.04 % time for Eker) nor treatment ($F(1,31)=0.903$, $p=0.284$ ($p=0.349$ without bootstrapping); 6.49 ± 1.74 % time for vehicle vs 9.29 ± 1.83 % time for CBD) for the time spent grooming (Figure 4.5D). The number of grooming events was also similar between groups irrespective of genotype ($F(1,31)=0.073$, $p=0.791$ ($p=0.789$ without bootstrapping); 3.34 ± 0.66 events for WT vs 3.10 ± 0.52 events for Eker) or treatment ($F(1,31)=2.121$, $p=0.145$ ($p=0.155$ without bootstrapping); 2.50 ± 0.51 events for vehicle vs 3.95 ± 0.72 events for CBD) (Figure 4.5E). There were no significant interactions between treatment and genotype for the time spent grooming ($F(1,31)=1.120$, $p=0.298$) nor for the number of grooming events ($F(1,31)=0.001$, $p=0.977$). Overall, these data indicate that the anxiety and repetitive behaviour profile of the Eker rat, at this age, is similar to WT and that these features were not modified by CBD treatment.

4.3.4 Object, but not stranger rat, exploration is reduced in the Eker rat, and both parameters are modified by CBD treatment

The latency and length of interaction between test animal and an unfamiliar stranger animal was quantified in the social interaction task. We first quantified the latency, in seconds, for the first approach between the test rat and the unfamiliar rat. A main effect of treatment was found ($F(1,31)=9.105$, $p=0.011$ with bootstrapping [$p=0.005$ without bootstrapping]) with CBD-treated animals taking more time to initiate contact with the stranger rat compared to animals in the vehicle-treated group (vehicle: 3.07 s ± 0.71; CBD: 6.13 s ± 0.73). Contrastingly, there was no significant effect of genotype ($F(1,31)=0.347$, $p=0.539$ ($p=0.560$ without bootstrapping)) nor

treatment x genotype interaction ($F(1,31)= 0.599$, $p=0.445$) on the time to initiate contact (Figure 4.6A). Similarly, we found no effect of genotype on the total time spent interacting with an unfamiliar animal ($F(1,31)=0.002$, $p=0.964$; 30.83 ± 2.44 % time for WT vs 30.67 ± 2.44 % time for Eker), contrasting with previously published data for this model[370]. There were also no genotype-induced changes in the number of interaction events ($F(1,31)=0.475$, $p=0.496$; 14.61± 0.97 events for WT vs 15.56 ± 0.97 events for Eker). Treatment with CBD did not alter the total time spent interacting ($F(1,31)=2.861$, $p=0.101$; 27.28 ± 2.68 % time for vehicle vs 34.22 ± 2.68 % time for CBD) nor the number of interaction events ($F(1,31)=0.139$, $p=0.712$; 15.78 ± 1.07 events for vehicle vs 15.39 ± 1.07 events for CBD) (Figure 4.6B-C). The interaction treatment x genotype was also not significant in relation to the time spent interacting ($F(1,31)=1.219$, $p=0.278$) and the number of interactions ($F(1,31)=1.115$, $p=0.299$). Overall, these results indicate no deficits in social behaviour across genotypes, with CBD treatment increasing the time to first approach.

Memory was assessed with the novel object recognition task. During Phase 1 of the task, Ekers spent significantly less time exploring the object than wild-type animals ($F(1,30)=5.928$, $p=0.021$; 11.22 ± 0.96 % time for WT vs 7.88 ± 0.99 % time for Ekers), indicating decreased interest for novel stimuli, supporting previously published data[370] (Figure 4.6D). Exploration was unaffected by treatment ($F(1,30)=1.835$, $p=0.186$; 10.62 ± 1.06 % time for vehicle vs 8.48 ± 1.03 % time for CBD) and no significant interaction between treatment and genotype was found for the object exploration in Phase 1 ($F(1,30)=0.293$, $p=0.593$; Figure 4.6D). During Phase 2, when a new object was presented together with a copy of the previous object, no main effect of genotype was observed ($F(1,30)=2.644$, $p=0.114$; 62.54 ± 2.47 % time for WT vs 68.32 ± 2.55 % time for Eker) (Figure 4.6E). There was a trend for an effect of treatment on novel object exploration ($F(1,30)=3.454$, $p=0.073$) with vehicle-treated animals spending slightly more time exploring the new object compared to the CBD-treated animals (69.22 ± 2.67 % time for vehicle; 61.64 ± 2.74 % time for CBD). There was no significant interaction between genotype and treatment ($F(1,30)=0.756$, $p=0.391$) (Figure 4.6E). Finally, given the reduction in exploration observed in Phase 1 for the Eker group, Phase 2 exploration was also analysed using the percentage of time spent exploring in Phase 1 as a covariate. When this parameter was introduced in the analysis, a main effect of treatment was observed ($F(1,29)=4.858$, $p=0.036$), while no effect of genotype ($F(1,29)=1.255$, $p=0.272$) nor treatment x genotype interaction ($F(1,29)=0.853$, $p=0.363$) were found. This indicated that, while Ekers explored the first object less, compared to wild-type animals, when taking into account the time spent exploring the object in Phase 1, overall in Phase 2 CBD-treated animals spend less time exploring the novel object than vehicle-treated animals (69,42 ± 2.57 % time for vehicle vs 61.35 ± 2.58 % time for CBD). These data indicate that Ekers explore objects less than wild-types, with CBD treatment impairing the exploration of novel, but not old, objects. Nonetheless, all groups preferentially explored the new object when given a choice, rather than the previously explored object from Phase 1.

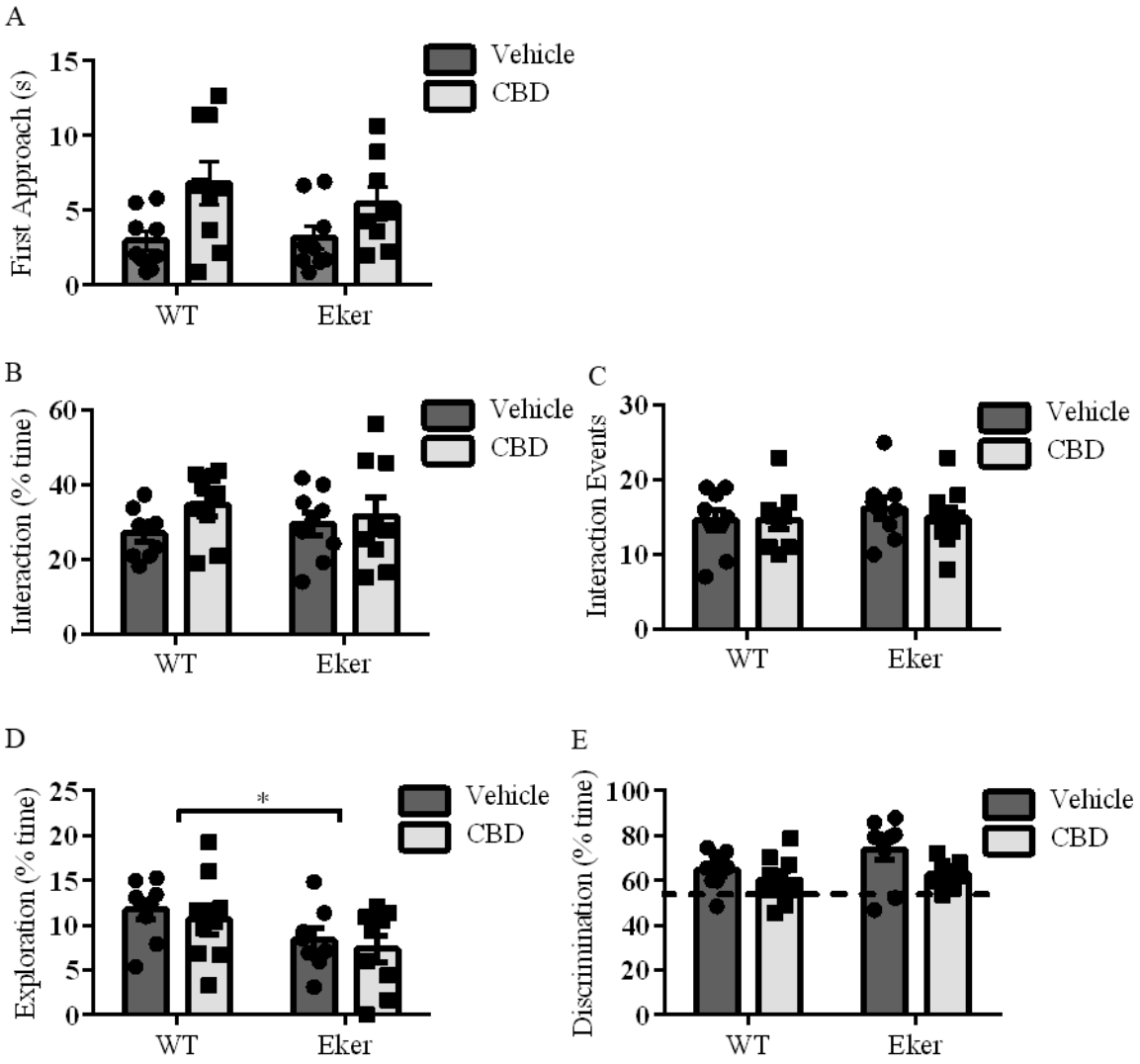

Figure 4.6: *CBD treatment increases the time to first social approach while the Eker rat mutation decreases object exploration.* (A) During the social interaction task, CBD treatment increased the latency for social approach in both WT and Eker animals ($F(1,31)=9.105$, $p=0.011$) . (B-C) Nonetheless, no differences were found regarding the time spent interacting with an unfamiliar rat (B) nor the number of interaction events (C) during the social interaction task. (D-E) Memory function was evaluated with the novel object recognition task. Eker rats spent less time exploring the object presented during Phase 1 ($F(1,30)=5.928$, $p=0.021$) (D) but all experimental groups preferentially explored the novel object presented in Phase 2 (genotype: $F(1,30)=2.644$, $p=0.114$; treatment: $F(1,30)=3.454$, $p=0.073$) (E). Data are presented as mean ± SEM; n= 9 animals per group; *$p<0.05$.

4.3.5 Phosphorylated rpS6 is unaffected by treatment and genotype and total rpS6 is decreased by CBD treatment

Western blot was conducted on whole brain tissue to evaluate mTORC1 signalling in the different genotype and treatment groups. There was no main effect of genotype ($F(1,8)=1.544$, $p=0.249$) or of treatment ($F(1,8)=0.830$, $p=0.389$) on phosphorylated rpS6 expression. The interaction between genotype and treatment was also not statistically significant ($F(1,8)=3.964$, $p=0.082$), although there was a tendency for CBD to increase phosphorylated rpS6 expression in WT animals while reducing it in Ekers (Figure 4.7A). Total rpS6 levels were also quantified and no effect of genotype ($F(1,8)=0.604$, $p=0.459$) or treatment ($F(1,8)=3.616$, $p=0.094$) was observed. A significant interaction between genotype and treatment ($F(1,88)=7.272$, $p=0.027$) indicated that while CBD administration had no effect on WT animals, it reduced total rpS6 levels specifically in the Eker group (WT-vehicle 19418,43± 1998.388, WT-CBD 21007.423 ± 1998.388, Eker-Vehicle 23254.100 ± 1998.388, Eker-CBD 14065,097 ± 1998.388) (Figure 4.7B).

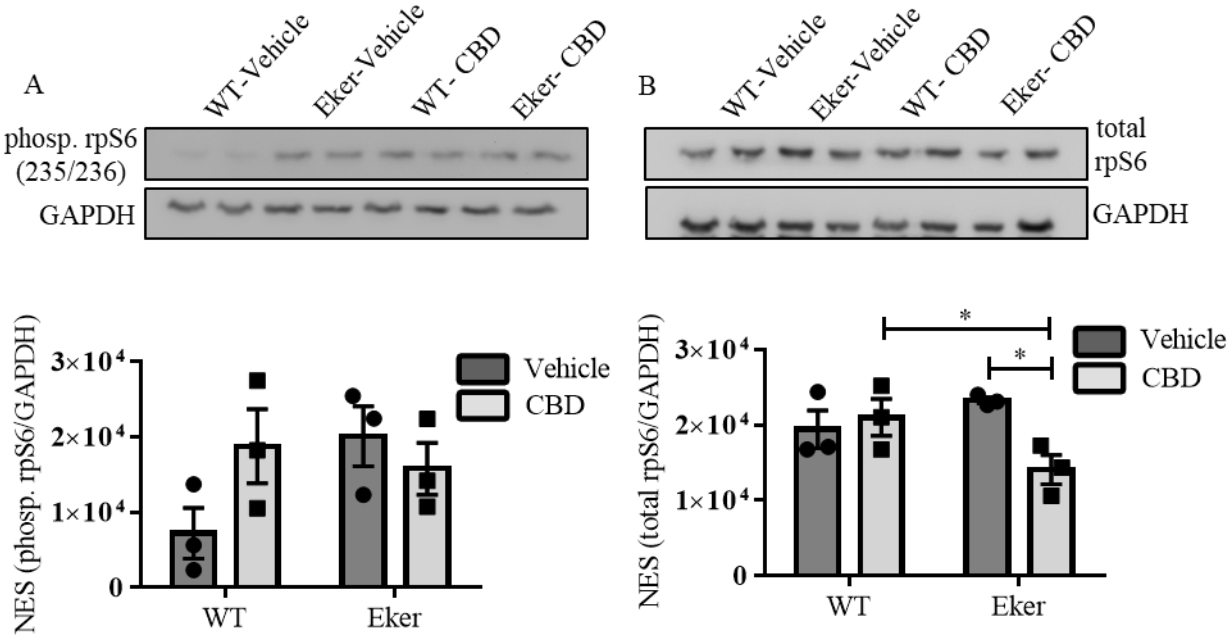

Figure 4.7: *CBD treatment has no effect on phosphorylated rpS6 but reduces total rpS6 expression levels*. (A) Western blot was performed to quantify the expression of phosphorylated S6 levels. This were found to be similar across genotypes ($F(1,8)=1.544$, $p=0.249$) and treatments ($F(1,8)=0.830$, $p=0.389$). (B) On the other hand, CBD administration changed total S6 expression in the Eker group ($F(1,88)=7.272$, $p=0.027$) (experiment performed by Leo Geng). Data are presented as mean ± SEM; NES= normalized experimental signal; n=3 animals per group; *$p<0.05$.

4.4 Discussion

In this work, a battery of behavioural tasks was conducted to further understand the TSC-like neuropsychiatric phenotype exhibited by the Eker rat and to explore the effect of an 8-week CBD treatment regimen.

During treatment, weight was monitored and all animals exhibited a time-dependent increase in body mass. Interestingly, CBD-treated animals displayed smaller increments of weight-gain, regardless of genotype, such that by the end of the treatment period, animals receiving CBD presented with lower body weight compared to vehicle-treated animals. This finding is consistent with a previous report where 10-week old male Wistar rats treated intraperitonially with 2.5 mg/kg or 5 mg/kg CBD for 14 days, exhibited reduced weight gain compared to the ones injected with an ethanol, cremophor, saline (1:1:18) solution[605]. Contrastingly, when 30-day old Wistar rats were injected with intraperitoneal 0.5, 1 or 5 mg/kg CBD for 30 days, no changes in body weight were observed[682]. Our study and these two others use distinct doses and durations of CBD treatment, as well as different rat strains. Given that weight progression is both age- and strain- dependent[682,683], this could explain the variability of results. As trials with CBD often target infantile pathologies, it is possible that CBD administration accompanies decisive periods of growth in these patients[684]. Hence, it would be important to further understand and monitor possible effects of CBD on weight and development, that could potentially translate into a significant impact on children's growth.

Impairments in fine and gross motor skills can be found in TSC patients from as early as 9 months, with lower fine motor scores potentiated by the presence of the ASD comorbidity[113,685,686]. A number of TSC models also exhibit motor impairments, with abnormal gait and rotarod performance reported in homozygote animals[324,333,687]. However, motor function appears to be preserved in heterozygote TSC models[107,333,572]. Accordingly, we found no genotype-induced gait alterations. Therefore, although we previously reported a PC area reduction in Eker cerebella (Section 3.3.2) which could suggest cerebellar atrophy and ataxic movement[334,666,688–691], behaviourally this was not observed in older Eker rats. CBD did induce a decrease in stride width in both WT and Ekers which correlates with the reported effect of CBD on weight, as these two parameters have been shown to increase in a curvilinear manner[690,692]. Furthermore, no effect of CBD was found on locomotor activity supporting previous pre-clinical work with this compound[669,693–695]. However, Ekers did exhibit decreased spontaneous locomotor exploration compared to WT animals, supporting previous work with this model[370]. This result contrasts with locomotion data from other heterozygote models of TSC, where no changes in ambulatory movement have been reported[324,333,335,572]. One of the reasons for this inconsistency could be the parameters measured as *time spent moving* was used here, whilst other studies have reported *total distance travelled*[324,335,572] or *average speed values*[333]. Furthermore, species-related differences could also contribute to the changes observed between TSC mice and rats. Mice stop more frequently and move slower compared to rats during open-field exploration[696], which could also account for the different results between models. Decreased ambulation in the open-field could also be indicative of motor deficits although, as previously mentioned, these would likely be independent of cerebellar dysfunction[697,698]. To further clarify possible motor impairments in the Eker rat, further work should include muscle strength tests, such as the grip strength test[699].

Focusing on motor-specific tasks would allow a better differentiation between motor symptoms and other confounding behaviours present in the open-field task such as anxiety- or depression-like manifestations. Indeed, decreased open-field exploration has also been associated with increased immobility time in the forced swim test, a task that analyses depressive-like behaviours[700]. Additionally, comparison between adult Wistar and Long-Evans rats reported that the latter exhibited increased depressive-like behaviour in both the forced swim and sucrose preference tests[701]. Thus, it is possible that the Eker rat exhibits an increased depressive-like phenotype, relevant for TSC pathology. In fact 19-43% of TSC patients are reported to exhibit depression[96,98,642,702], while the latest World Health Organization report estimates the prevalence of depression for the general population in 4.4%[703].

CBD was previously reported to modify repetitive behaviours[607,664,704]. This contrasts with the data presented here. One major difference between this and other studies is treatment duration, with previous reports describing the effects of a single CBD injection or a 7-day treatment. In work by Casarotto and colleagues, an average of 5/25 marbles were buried after a single CBD injection. After 7 days of treatment however, this number had increased to 10/25, with the naïve group burying 19/25 marbles[664]. This suggests there may be a loss of CBD effect on the marble burying task with repeated treatment. Therefore, although CBD has been proposed as a possible alternative to address perseverative behaviours[705], treatment might not promote long-term benefits. Although a significant effect of genotype was not present, Ekers did exhibit a tendency to bury more marbles than WT animals, which could be reminiscent of an increased repetitive-like behaviour. However, this was not supported by our measures of grooming behaviour, which failed to show differences between genotypes, irrespective of treatment. No changes in anxiety-like behaviours were seen, although a tendency for increased avoidance of the inner squares was seen in the Eker group. A similar propensity for inner area avoidance was also reported in the Tsc2-DN model. Nevertheless, the overall lack of an anxiety-like phenotype in Eker rats is in line with previous work using the light/dark box task, where no differences were observed between WT and Ekers[232,370].

CBD had an effect on both genotypes in the latency to first approach. As diazepam was shown to also increase latency in Wistar rats[706], the effect seen here could indicate an anxiolytic action of CBD. However, we did not observe any other effects of CBD in the remaining anxiety-like behaviour paradigms used in this study (grooming frequency and duration; time spent exploring the inner squares). Alternatively, this increased latency to approach a novel animal could suggest a reduction in interest of the experimental rodent towards the new partner. If translated to a TSC clinical setting, this would be an unwanted effect of CBD given the already existent and highly impactful psychosocial difficulties faced by these individuals, especially by TSC-ASD patients[98,150]. Overall evidence suggests that, at this age, the Eker rat does not exhibit repetitive nor anxiety-like behaviours and, therefore, does not replicate this feature of TSC. As CBD was previously shown to modulate anxiety-like behaviours (Section 2.3.2.2)[405,407,615,707], it would be valuable to investigate its

effect in models of TSC that do exhibit an increased anxiety phenotype. This would clarify its possible role in the modulation of these features[333,572].

The Eker rat has been proposed as a model of ASD-like behaviour, as it displayed social interaction dysfunction at 12-24 weeks[370]. Using 9-week-old Ekers, we found no evidence of social interaction deficits. The data presented here therefore suggests that these deficits in the *Tsc2*$^{+/-}$ rats may be exacerbated by age. For example, while Sprague-Dawley rats aged 4 to 10 weeks presented with similar social interaction patterns[708], 10 week-old Wistar rats were shown to have increased interaction time compared to 19 and 25 week-old animals[709]. Furthermore, 6-week old Fischer 344 male rats exhibited increased social interaction compared to 12 and 72 week rats[710]. Thus, it is possible that the discrepancy of results between this and previous work with the Eker rat may be due to an age-dependent effect. Younger Ekers exhibit typical social interaction behaviours whilst social differences in older animals are potentiated by age and the *Tsc2* mutation.

Although no differences in social exploration were found, object exploration was altered in the Eker group, replicating previous work with this model[370]. Laboratory rats are naturally inquisitive and preferentially explore novel environments and objects rather than previously known ones[711–713]. Preference for an object is also dependent on the memory of previous exposures, which ultimately makes the novel object recognition task a memory test[638,714]. In this regard, no memory deficits have been previously reported with the Eker rat[232]. Reduced object exploration can be associated with increased levels of anxiety-like behaviour[715,716], which were not observed in these experiments. Alternatively, reduced levels of exploration suggest decreased novelty seeking behaviour, a characteristic of TSC-ASD and nsASD individuals[713,717–719]. CBD treatment reduced object exploration in the discrimination phase, when the time spent exploring during the acquisition phase was taken into account. This could be due to an effect of CBD on memory retention. Indeed, this compound has been shown to improve[566,669,720], impair[721–723] or have no effect[566,669,724] on memory retention in naïve animals and disease models. With the present data it is not possible to discern what would be a memory deficit from an alteration in innate novelty exploration. Thus, further behavioural tasks focused on memory, such as the T-maze, would enable a better differentiation of these effects[714,725].

rpS6 is a ribosomal protein that shuttles between the cytoplasm and the nucleus[304]. Although phosphorylation of rpS6 is frequently used as a readout of mTOR activity, the exact function of rpS6 is still debated. Previous work with CBD reported decreased phosphorylated rpS6 after compound administration[411,615]. This was not observed in this work. While here an 8-week CBD treatment was administered to rats, prior studies have used incubations overnight in zebrafish (Chapter 2)[615,616] or of 2 hours in Jurkat cells[411]. Thus, it is possible that the discrepancies in effects are due to model-specific mechanisms of action or to the attenuation of the effect of CBD on phosphorylated rpS6 over long periods of treatment time. Clinically, CBD appears to maintain a sustained effect after 48 weeks of treatment albeit concerning seizure control[726,727]. Further studies

with a timed evaluation of CBD's effect on phosphorylated rpS6 would enable clarification of its role on the mTOR pathway. This could provide valuable information to elucidate possible contributions of this compound to the specific treatment of TSC manifestations where rpS6 phosphorylation is increased.

Interestingly, we did observe a CBD-induced reduction in total rpS6 expression specifically in the Eker group. Mutant mice with rpS6 haploinsufficiency present with impaired mitosis and decreased rRNA, indicating alterations in protein synthesis[728]. *S6*$^{flox/cre+}$ mice exhibit altered 40S biogenesis and cell cycle arrest due to lack of cyclin E[729]. Furthermore, total rpS6 was shown to be increased in several types of tumours and its expression was indicative of a poor prognosis[730]. Thus, the reduction in total rpS6 expression seen in the CBD-treated Eker group suggests a potential beneficial effect of CBD on the abnormal cell growth.

Finally, an injection-induced effect was observed in this study. This was manifested by the presence of skin abnormalities in the form of small subcutaneous lumps in a number of CBD-injected rats, regardless of genotype. Previous work with Long-Evans has reported that daily subcutaneous injections with peanut oil led to the appearance of subcutaneous lumps, after a 21-day treatment[731]. These had no effect on behavioural testing[731]. Here, a different vehicle was used. However, we did not find evidence of these lumps in vehicle-treated animals suggesting that, as opposed to peanut oil, in this case we were in the presence of a CBD rather than a vehicle effect. These lumps suggest an accumulation of CBD under the skin, which has also been previously described with transdermal CBD delivery[732]. Other reports of subcutaneous CBD treatment have not stated the presence of these abnormalities, although these comprehended single CBD administrations instead of long-term treatments[421,607]. Although this subcutaneous reaction can be a previously unknown side effect of repeated CBD injections, clinical treatment with CBD often follows an oral route[402–404,427,733]. Therefore, this effect would unlikely be found in CBD-treated patients.

4.5 Conclusion

In TSC, behavioural alterations in nonverbal IQ and visual reception can be detected in patients as young as 6 months old[113]. Despite the burden that these alterations have on patients' lives, the vast majority of them remains untreated. This in part reflects the complexity of behavioural presentations but also the difficulty in addressing specific behavioural components of disease[93,95,98,150]. Therefore, research with models that mimic behavioural aspects of TSC is of great need and importance to the TSC population. Here, exploring the behavioural profile of the young Eker rat, we confirmed its mild phenotypical profile. Although interesting differences in exploratory behaviour were found, no other changes representative of the behavioural profile of TSC patients were observed. Furthermore, although CBD did not greatly affect animal behaviour, it did promote

a reduction in weight gain, changes in memory retention and increased contact latency that could be relevant to the TSC population. Hence, to better evaluate behavioural changes, the use of animal models of TSC with a more human-like phenotype could prove beneficial. For example, the *Tsc2*-DN model which exhibits increased anxiety levels, decreased social behaviour and novelty preference, deficient memory and reduced motor coordination. Administration of CBD to other models could help clarify its long-term effects and safety. This is crucial to the TSC population given their complex symptomatology and associated comorbidities. The use of CBD to manage behavioural TSC symptoms is therefore still to be resolved.

Chapter 5: The effect of CBD administration on PTZ-induced tonic-clonic seizures and mortality in the Eker rat model of TSC

5.1 Introduction

Epilepsy is highly prevalent in TSC patients, present in 80 to 96% of individuals[18], with 30 to 50% of these exhibiting first seizures before the age of one, in the form of IS[14,35,82,83,88,91,460] (see also Section 1.1.3.4.; Table 1.1). While some TSC patients achieve seizure freedom with pharmacological treatment[90,91,734,735], one to two thirds develop refractory epilepsy. Anti-epileptic drugs are the therapeutic approach most likely to induce seizure freedom. In TSC, vigabatrin is the compound most often prescribed as the first AED treatment, followed by valproate, carbamazepine and levetiracetam[82,735]. Besides pharmacological treatment, resective surgery can also provide a seizure-free prognosis, with the ketogenic diet and vagus nerve stimulation reducing seizure frequency but often failing to promote complete seizure remission[201,735,736].

The development of epilepsy in TSC has a significant impact on the QoL of patients. This is a combination of the inherent disease burden, caused by the direct presence of seizures and AED-related side effects, its economic cost[34,737], and the impact of seizures on cognitive and mental health (Section 1.1.3.5)[83,217,460,738]. This is evident in TSC, where there is a close relationship between epilepsy, cognitive delay and autism. Decreased cognitive function is observed in patients with ASD, with epilepsy, and with both conditions combined[97,116,739]. More importantly, reducing seizure frequency has been shown to positively contribute to the QoL of TSC patients[83]. Altogether, given the number of TSC patients that do not currently achieve seizure freedom, the development of new anti-epileptic therapies is crucial for the improvement of seizure control and for improved health and QoL of patients.

Recently, CBD has shown potential as a new anti-epileptic medication especially in the management of treatment-resistant epilepsies[402] (Section 1.2.2). Preclinical studies first reported the effectiveness of CBD in reducing seizure frequency in a plethora of systems. These included acute seizure models, such as PTZ, penicillin and maximal electroshock[443,445,446], acquired models of epilepsy, like corneal kindling and the reduced intensity status epilepticus-spontaneous recurrent seizure (RISE-SRS) model[675], and a genetic model of DS[565].

In clinical populations, a randomized, double-blind, placebo-controlled trial for LGS has shown a 37 to 41% dose-dependent reduction in drop seizure frequency following 14 weeks of CBD treatment. In DS, convulsive seizure frequency was reduced in 39% after CBD administration, and 62% of caregivers reported improved overall condition after treatment. Seizure freedom was reported by 5% of individuals receiving CBD[404,427]. Furthermore, in an open-label trial with TSC patients with refractory epilepsy, addition of CBD to the AED treatment schedule induced a 48.8%

median percent change in seizure frequency[403]. Thus, although only a limited number of clinical trial results are available, the current clinical evidence supports the preclinical data suggesting a positive effect of CBD in reducing the frequency of drug-resistant seizures.

To date, no studies have investigated the possible anti-seizure actions of CBD in the *Tsc2*$^{+/-}$ animal model, the Eker rat. This TSC model does not exhibit spontaneous seizures itself and therefore, to explore seizure physiology, seizures must be evoked through chemical induction (Section 1.1.5.4.2). One way to achieve this is through the acute administration of PTZ, an experimental method considered to be a gold-standard in the field of AED research and development[740,741]. PTZ's convulsive action derives from its antagonism of $GABA_A$ receptors (Section 1.1.6.4.2)[369,741]. In AED discovery, the assessment of novel compounds against a 50-100 mg/kg PTZ challenge is a widely accepted screening assay to assess the anticonvulsant potential of novel compounds[445,742–745]. Furthermore, a number of currently approved AED, such as ethosuximide, vigabatrin and valproate, were first selected due to their efficacy against PTZ-induced seizures[746,747].

Using an acute PTZ administration paradigm, Waltereit et al. (2006) showed that 10 to 14 week-old Eker rats did not show increased susceptibility to 30, 40 or 50 mg/kg PTZ, when compared to wild-type animals[232]. Although no changes in susceptibility were observed, this model did shown a convulsive response to PTZ administration, indicating that this can be a valuable platform to investigate the effect of antiepileptic compounds, such as CBD[748].

Age is also an important variable regarding seizure development, as susceptibility to PTZ has been shown to be modulated by the age of exposure[745,749–751]. For example, Kliouéva and colleagues injected intraperitoneal 25 mg/kg PTZ in WAG/Rij and Wistar male rats. At P10, tonic-clonic (TC) seizures were present in 7 and 31% of the animals, respectively. This incidence increased to 40 and 33% at P26, and to 100% in both strains from P70[749]. In contrast, Sircar and colleagues reported that administration of 100 mg/kg PTZ to male and female Sprague-Dawley rats induced 100% incidence of tonic-clonic seizures in animals aged P21, but in only 64% and 20% of the animals aged P40 and P60, respectively[745]. This suggests that age may influence the development of PTZ-induced seizures, although the exact relationship between these two variables is still to be ascertained. Thus, using the PTZ acute seizure model I 1) hypothesized that using younger rats (P24-P28) compared to Waltereit's study (P70-P98) would modify the Eker's response to the PTZ challenge and 2) investigated the anti-convulsant ability of CBD in the Eker rat.

I first piloted this protocol on P24 to P28 wild-type male rats to optimize the PTZ dose to be used in further experiments. Subsequently, wild-type and Eker animals were treated with vehicle or CBD, prior to administration of the piloted dose of PTZ. The effects of genotype and CBD treatment on the development of TC seizures and mortality were measured.

5.2 Methods

5.2.1 Breeding and animal groups

Male wild-type (*Tsc2*$^{+/+}$) and Eker (*Tsc2*$^{+/-}$) Long-Evans rats, from our in-house colony at the University of Reading Bioresource Unit facilities, were maintained at room temperature, on a 12:12 hour day/night cycle and with access to food and water *ad libitum*. At P14, animals were ear-notched and genotyped as described in detail in Section 3.2. Briefly, following DNA extraction and PCR, the obtained PCR products were separated in a 2% agarose gel and visualized with a Syngene U:Genius 3 (Syngene, UK) gel imaging system. Eker DNA was identified by a visible band around the 892-bp ladder reference band, representative of the mutational insertion in the *Tsc2* gene (Figure 3.1; Section 1.1.5.4.2). For the experiments in this chapter, an initial pilot study was designed to ascertain the PTZ dose to be used in subsequent experiments. Here, 19 wild-type male animals aged P24 to P28 were used. In the experimental study, 40 male animals (20 wild-type and 20 Eker) aged P24 to P28 were used with 10 animals assigned to the WT-vehicle group, 10 to the WT-CBD group, 10 to the Eker-vehicle group and 10 to the Eker-CBD group. All experiments were approved by the University of Reading Ethics Board and the UK Home Office (PPL 70/8974) and carried out in accordance with UK Home Office regulations (Animals (Scientific Procedures) Act, 1986) and the ARRIVE guidelines.

5.2.2 Compound and drug preparation

Before each round of PTZ sessions, vehicle with a ratio of 2:1:17 EtOH: Cremophor: 0.9% saline (Ethanol 32221, Merck) (Kolliphor®HS 15, 42966, Sigma) and CBD (GW Pharmaceuticals, Cambridge, UK) in a concentration of 35mg/mL were freshly prepared and stored at 4°C, in individual glass vials and protected from light. On the morning of each experiment, a fresh solution of 30 mg/mL PTZ (P6500-100G, Sigma-Aldrich) was prepared in saline, and stored in individual glass vials protected from light.

5.2.3 Pilot protocol for PTZ dose optimization

Using a protocol adapted from previously published work[438,445,745], 90 mg/kg and 95 mg/kg concentrations of PTZ were selected and administered to 9 and 10 wild-type male animals, respectively[742]. On the morning of each pilot, animals were moved to the observation room, weighed and placed in a transparent, 15 x 15 x 24 cm plastic observation arena with a lid, where they were left to acclimatize for 120 minutes until 10:00hrs. After this time, animals were injected intraperitonially (ip) with vehicle (2:1:17 EtOH: Cremophor: 0.9% saline), and returned to their

observation arena for a further 60 minutes, mimicking the experimental protocol (described below)[607]. At 11:00 hrs, each animal was injected with either 90 or 95 mg/kg PTZ, according to a pseudo-randomised design, and immediately placed back in their observation arena for 30 minutes. The presence of TC seizures, defined by a prolonged contraction of muscles with loss of posture and righting reflex[752,753], as well as mortality, were visually recorded. After 30 minutes of observation, animals were euthanized by carbon dioxide exposure followed by neck dislocation.

5.2.4 Experimental Protocol

To test the effect of genotype and CBD on PTZ-induced seizures, P24-28 male wild-type and Eker rats were injected (i.p.) with 90 mg/kg PTZ, based on the pilot results. The protocol used for the experimental rounds was similar to the one described above for the pilot round. Twenty wild-type rats and 20 Ekers were moved into the experimental room 2 hours before first injection, after their weight was measured. Subsequently, animals were allocated to the vehicle or CBD group and, two hours after acclimatization, injected with either vehicle or 200 mg/kg CBD (Figure 5.1), the suggested dose by the sponsors of this work, GW Pharmaceuticals[675]. One hour after vehicle or CBD administration, animals were injected with 90 mg/kg PTZ and observed for 30 minutes. Whilst in the observation arenas, animals were continuously visually monitored for the development of TC seizures and for the occurrence of mortality, as well as for the latency of these events.

5.2.5 Data analysis and statistics

Statistical analysis of the collected data was performed in IBM SPSS Statistics 22 and graphs were produced using GraphPad Prism 6. Due to the small sample size of this study and violation of normality in some data sets (see below), the presence of outliers was analysed using the ROUT test[754,755]. One outlier was identified in the *latency to first TC seizure* variable and consequently removed from statistical analysis.

For the analysis of the pilot data, *PTZ dose* was the independent variable, with *weight*, recorded in grams, *TC seizures* and *mortality*, recorded as the number of animals exhibiting each feature, as dependent variables. *Weight* was analysed with a one-way ANOVA, as data followed normality under the Shapiro-Wilk test and only wild-type and vehicle-treated animals were used. *TC seizures* and *mortality* was plotted in a "Yes/No" variable format and analysed with the Chi-square test of independence.

For the analysis of the data obtained in the experimental rounds, *genotype* and *treatment* were the independent variables. *Weight*, in grams, was analysed with a two-way ANOVA with bootstrapping, following a statistically significant Shapiro-Wilk normality test result. The number of animals exhibiting *TC seizures* and *mortality* (Yes/No) was analysed with the Chi-square test of

independence. The *latency to first TC seizure*, recorded in minutes, was analysed with a two-way ANOVA with bootstrapping, as normality was violated.

All data are presented as mean ± SEM, unless stated otherwise and the *p* value for significance was set at 0.05.

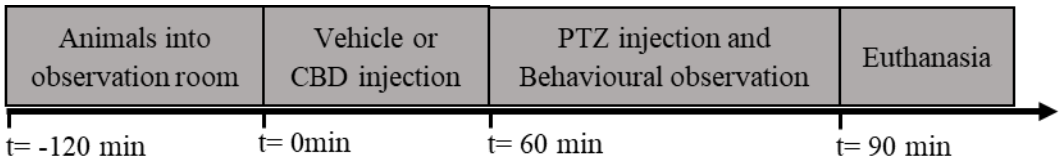

Figure 5.1: *PTZ acute seizure model.* Animals were placed in the observation room two hours before injection of vehicle or CBD. One hour later, PTZ was injected and behavioural observation was conducted for 30 minutes. At the end of the observation period, animals were euthanized.

5.3 Results

5.3.1 Pilot results for the PTZ dose optimization

A pilot round was performed to determine the optimal PTZ dose to be used in further experiments, using wild-type males injected with vehicle (at the time point when CBD will be administered during the experimental phase) and 90 mg/kg or 95 mg/kg PTZ. Both the 90 mg/kg group and the 95 mg/kg group presented with similarly distributed weights (85.156 ± 2.0 g for the 90 mg/kg group vs 84.590 ± 1.898 g for the 95 mg/kg group; $F(1,17)= 0.042$, $p= 0.840$) (Figure 5.2A). Following PTZ administration, all animals exhibited TC irrespective of the administered PTZ dose (Figure 5.2B). Significant differences in mortality between the two doses were seen ($\chi^2(1)= 4.866$, $p=0.027$). One in nine animals died in the 90 mg/kg group and 6/10 animals in the 95 mg/kg group (Figure 5.2C).

Previous data comparing Eker rats with wild-type animals indicates a mild seizure phenotype, suggesting that mutation-induced differences between wild-type and Eker in response to PTZ and CBD could be subtle[232]. Furthermore, as the intensity and speed of progression of PTZ seizures is dose-dependent[756–759], these small differences could, in turn, be obscured by high doses of PTZ[758,760,761]. Therefore, to avoid masking genotype or drug-induced effects, the lower 90 mg/kg dose was selected for use in the experimental phase.

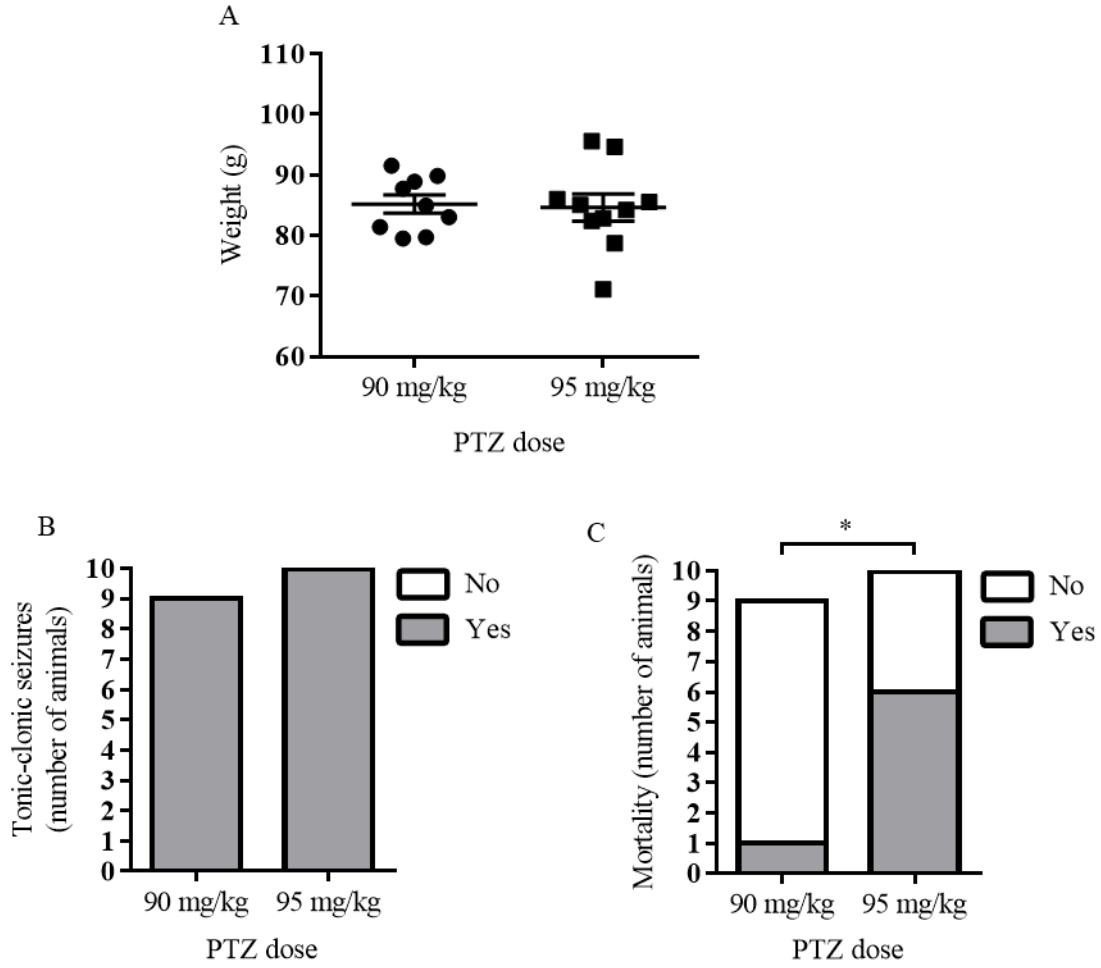

Figure 5.2: *PTZ dose pilot in WT animals*. A pilot experiment was performed using 90 mg/kg and 95 mg/kg PTZ doses in two different male WT cohorts. (A) The weight distribution of the animals, presented as mean ± SEM, was similar between groups, (B) as was the proportion of animals exhibiting TC seizures. (C) The mortality rate was significantly higher in the 95 mg/kg group ($\chi^2(1)= 4.866$, p=0.027); n=9 for the 90 mg/kg group and n=10 for the 95 mg/kg group; * p< 0.05.

5.3.2 Animal weight variation between groups during experimental rounds

Animals used for the experimental rounds of PTZ were randomly allocated to vehicle or CBD treatment groups. Despite randomization, a significant main effect of treatment was found ($F(1,36)= 6.865$, p= 0.013 (0.013 without bootstrapping)), with animals allocated to the vehicle group being heavier than those allocated to the CBD group (90.725 ± 5.368 g for vehicle vs 71.620 ± 4.219 g for CBD). There was no significant main effect of genotype (82.510 ± 4.864 g for WT vs 79.835 ± 4.954 for Eker; $F(1,36)= 0.135$, p= 0.735 (0.716 without bootstrapping)) nor any significant genotype x treatment interaction ($F(1,36)= 0.008$, p= 0.931) (Figure 5.3A).

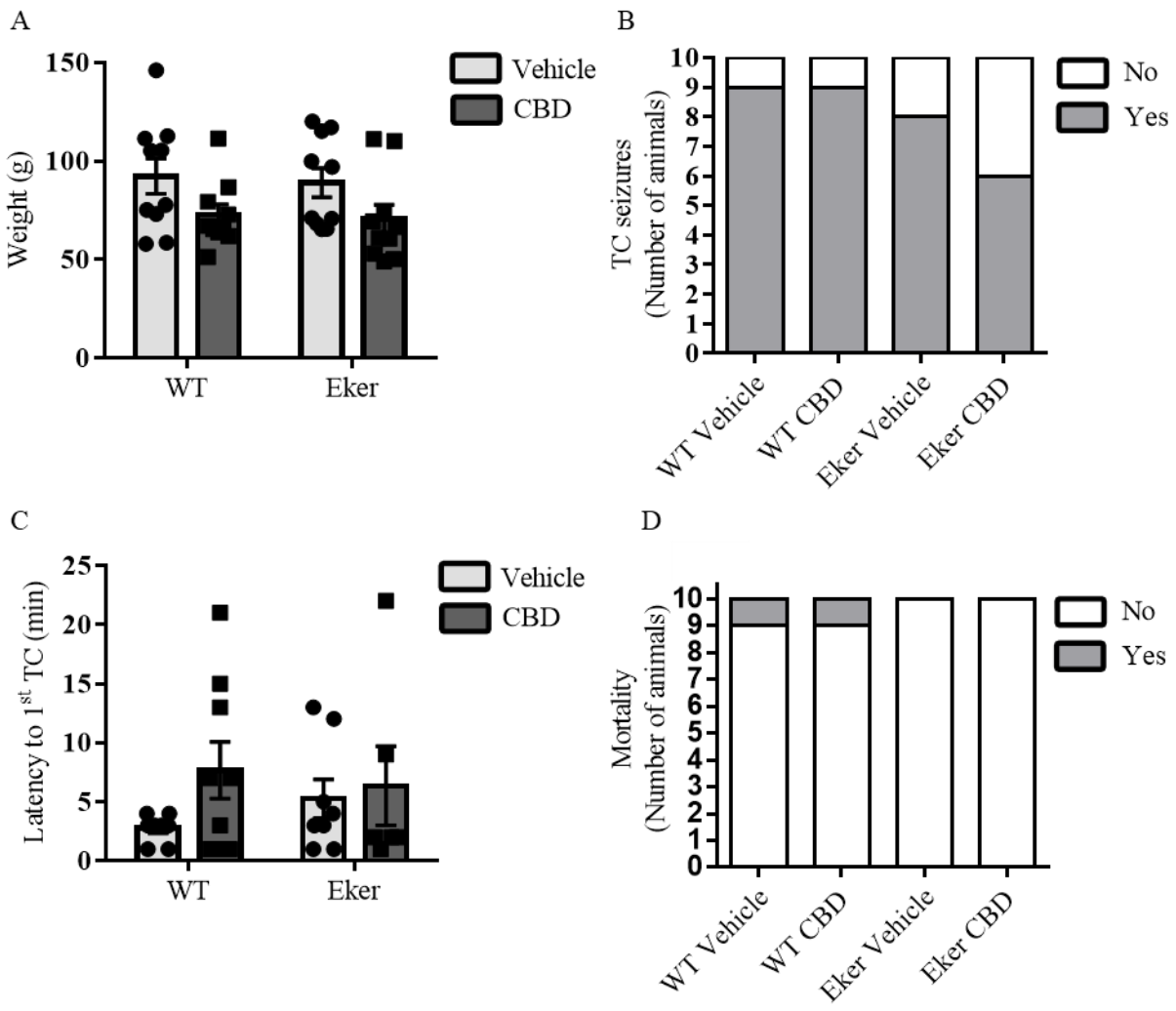

Figure 5.3: *The effects of CBD after a 90 mg/kg acute dose of PTZ*. During experimental rounds, a 90 mg/kg dose of PTZ was used. (A) Animals allocated to the CBD-treated group presented with lower weight compared to the ones in the vehicle-treated group ($F(1,36)= 6.865$, $p= 0.013$). (B-C) Tonic-clonic seizures were analysed by visual recording. (B) Their presence (Yes/No) was similar between groups, as was (C) their latency, presented in minutes. (D) The mortality rate in each treatment and genotype was also recorded as a Yes/No variable. Data for *weight* and *latency* is presented as mean ± SEM; n=10 animals per group.

5.3.3 CBD-treated Eker rats present with the lowest TC seizure frequency

Both the frequency and latency to TC seizures were visually monitored. WT animals exhibited the highest rate of TC, with 9/10 animals exhibiting at least one episode of this type of seizure irrespective of treatment. Eight in ten vehicle-treated Eker rats presented with TC seizures while CBD-treated Eker rats presented with the lowest TC rate (6/10) (Figure 5.3B). Chi-square analysis of the presence of TC seizures revealed a non-significant association between the presence

of TC and treatment ($\chi^2(1)=0.625$, p= 0.429) and between the presence of TC and genotype ($\chi^2(1)=2.5$, p=0.114). In both cases the two variables were weakly associated (Cramer's V=0.125 for treatment; Cramer's V=0.250 for genotype). The latency to first TC seizure was not different between genotypes (5.208 ± 1.415 min for WT vs 5.792 ± 1.573 min for Eker; F(1,27)= 0.076, p= 0.793 (0.785 without bootstrapping)) nor treatments (4.0 ± 1.456 min for vehicle vs 7.0 ± 1.535 min for CBD; F(1,27)= 2.010, p= 0.212 (0.168 without bootstrapping)) (Figure 5.3C). There was no interaction between genotype and treatment (F(1,27)=0.820, p=0.373).

5.3.4 Mortality was consistent across all experimental groups

Mortality following PTZ administration was also analysed. Consistent with the pilot data, a low incidence of mortality was found following the administration of 90 mg/kg PTZ. By the end of the 30-minute observation period, only 2 animals had died during the procedure: one from the WT-vehicle group, 5 min after PTZ injection and one from the WT-CBD group, 12 min after PTZ injection. No Eker rats died during these experiments (Figure 5.3D).

5.4 Discussion

CBD has been shown to have anti-epileptic properties in several *in vivo* animal models[447] and in human trials[404,427,451]. Data from an open-label trial also suggests CBD has efficacy to treat seizures in TSC[403], although controlled clinical data is still needed (Section 1.2.2). To further understand the possible role of CBD in TSC, we examined the Eker rat, a *Tsc2*$^{+/-}$ model, following an acute dose of PTZ. Overall, we found no major differences between vehicle and CBD treatment on the presence and latency of TC seizures or mortality in both genotypes.

In the pilot round, 95 mg/kg PTZ induced the development of TC seizures in WT animals followed by a relatively high mortality (6/10) in comparison to the 90 mg/kg dose (1/9). As no differences in susceptibility to seizure were found between WT and Eker rats in previous work[232], only the possibility of modest differences in relation to PTZ susceptibility were expected in this study, despite higher doses of PTZ being used. The 90 mg/kg dose was chosen to facilitate the detection of subtle differences in TC seizure development due to either the *Tsc2* mutation and/or CBD treatment. This is a dose that falls well within the range of PTZ doses previously used for the assessment of CBD in this model, although it should be noted that considerable variation in PTZ doses during antiepileptic compound assessment is found between studies[444–446,742,744,762].

Given the role of the PTZ acute paradigm as a gold-standard screening tool for novel AED compounds, it is of great importance that a balanced group assignment is properly achieved for robust and comprehensive compound investigation. Differences in litter size, and consequent feeding, can lead to distinct rates of growth and physiological maturation between litters[763–766], a

factor that can itself contribute to differences in drug response[767,768]. Therefore, the use of animals of similar weights across groups can help reduce variability in response due to experimental design. Given the positive results with pseudo-random allocation obtained in the pilot round, a similar procedure was used in the experimental round. However, despite this approach, we detected a difference in weight between the animals that were allocated to the vehicle and CBD groups. Importantly, this was not a drug-induced effect as animals were weighed prior treatment administration. It is still unclear if weight could have had an impact on the effect of CBD. For example, CBD is a lipophilic compound that can accumulate in adipose tissue[769]. Consequently, rats with different weights and percentage of fat mass could have different rates of absorption and distribution of CBD. Therefore, to avoid the contribution of confounding factors to drug response, further work should proceed with allocations to each experimental group after weight measurements have been taken[752]. This will allow an even distribution of weight throughout the different groups and minimize the effect of heterogenous populations to the final results.

Regarding seizure development, we examined TC seizures which resemble the generalized myoclonic seizures present in the TSC population[18,35,746]. These are also the most important risk factor for sudden unexpected death in epilepsy (SUDEP)[770,771]. No statistically significant differences were found for the latency to TC seizure development nor for the presence (yes/no) of TC seizures. Given the *Tsc2* mutation present in the Eker rat, increased susceptibility to chemically-induced seizures was expected for the this group. Indeed, previous work with other TSC models has shown that mutations in the *TSC* genes increased neuronal excitability and the susceptibility for seizure development (Section 1.1.3.4)[53,331,354,569]. However, in line with previous work with this model[232], WT-vehicle animals exhibited a similar TC frequency to Eker-vehicle animals (9/10 vs 8/10). This was unexpected since the susceptibility to PTZ-induced TC seizures has been shown to decrease with age in pre-pubescent and young adult rats[745,749,772], increasing again in older animals[749,751]. Therefore, as this work used P24-28 rats, contrasting with the 3 to 6-month-old rats previously used by Waltereit and colleagues, an increased frequency of TC was expected in the Eker group. However, the absence of significant TC frequency differences does not preclude changes in other types of PTZ-induced seizure behaviours. In this sense, it would be interesting to record more detailed seizure information following PTZ treatment. For instance, tracking seizure development using the modified Racine scale, which grades seizure severity from 0 to 5, would provide a more complete evaluation of seizure progression following the PTZ challenge[742,773]. This includes the recording of other seizure types besides TC (a score 5 in the Racine scale), to better evaluate the susceptibility of the Eker rat to PTZ convulsions at this age. For example, myoclonic jerks (a score 1 in the Racine scale) can also be seen with PTZ administration, and translate into human motor seizures without loss of awareness, also present in TSC patients[232,773]. Therefore, the evaluation of seizure development using the complete Racine scale could be of value to the TSC population. Other factors may have also contributed to the lack of effect of mutation on PTZ-

induced seizures. The Eker rat does not exhibit major signs of TSC-related brain pathology (Section 1.1.5.4.2). This might impact the rate and severity of seizure development as both tubers and perituberal tissue have been shown to be major contributors to seizures[31,36,41,47,50,326], and both of these features are absent from the Eker rat at the different ages analysed.

The group with the lowest incidence of TC was the CBD-treated Eker group, suggesting that CBD might impact the frequency of TC seizures, specifically in the presence of mutation. In TSC models with spontaneous seizures, mTORC1 signalling was shown to be increased with seizures, and administration of rapamycin was shown to decrease seizure frequency[103,153,568,569]. Furthermore, phosphorylated rpS6 levels increased in 6-week-old Sprague Dawley rats following 75 mg/kg PTZ (ip) treatment. Phosphorylated rpS6 Ser240/244 and Ser235/236 expression was detected, indicating an induction of the mTOR pathway, 5 minutes and 1 hour post-injection, respectively[743]. Furthermore, after acute PTZ administration to both zebrafish and rats, rapamycin treatment was shown to increase the latency of seizures[774,775], suggesting that PTZ treatment increased mTORC1 activation and that reduction of this activation through mTOR-inhibitor treatment exhibited protective effects. Therefore, given the *Tsc2* mutation present in the Eker rat, PTZ could further potentiate mTORC1 activation in these animals compared to wild-types. We found that short- (Chapter 2)[615,616] but not longer-term (Chapters 3 and 4) CBD treatment decreased phosphorylated rpS6 levels. Thus, this could potentially be a mechanism by which CBD could induce a reduction in TC frequency, specifically in the Eker group. Interestingly, Talos and colleagues observed that mTORC2 activation in temporal lobe epilepsy was responsible for improved neuronal survival[776]. In Chapter 3 we hypothesized that a possible mTORC2 induction was present after CBD treatment. Although just a theory, if proven to be the case, this could further contribute to a beneficial action of CBD on TSC seizures. However, given the relatively similar frequency values of TC seizures in all groups and the small effect sizes detected, additional experiments with larger cohorts and quantification of time spent in TC would be required to clarify the effect of CBD on Eker seizures. Overall, additional molecular biology experiments including the quantification of S6K, phosphorylated rpS6 (Ser240/244), phosphorylated rpS6 (Ser235/236) or pAkt (Ser473), throughout different experimental time points, would be valuable to investigate if CBD exhibits modifying actions in the mTOR pathway during PTZ-induced seizures.

Finally, despite the presence of a high incidence of TC seizures in the experimental rounds, only a low mortality rate was present. Although 2/20 WT animals died, in contrast with 0/20 animals from the Eker group, the low mortality rate does not allow for detailed interpretation of the role of genotype or treatment on this parameter. In this case, given the high mortality rate seen with the 95 mg/kg PTZ dose, it might be necessary for future work to increase mortality rate or treatment group size to fully understand the effect of CBD on mortality.

5.5 Conclusion

No substantial changes were found between groups regarding the effects of genotype or treatment on response to PTZ-induced TC seizures and mortality. Considering the previously referred limitations of this study, more data is necessary to investigate the effects of CBD in chemically-induced seizures with TSC models. Further research into these effects may be able to clarify if CBD has a TSC-specific effect, beyond its known seizure reduction action, through modulation of the mTOR pathway. If shown to be true, this would provide TSC patients with an alternative AED not only to control severe seizures but also to manage other epilepsy-associated symptoms.

Chapter 6: General Discussion and Conclusion

CBD is a non-euphoric phytocannabinoid from *Cannabis sativa* that has been shown to reduce seizure frequency. In the work described in this thesis, I explored the hypothesis that CBD could exert beneficial effects in TSC, using two different animal models of this pathology, the *tsc2*^{vu242} zebrafish and the *Tsc2*$^{+/-}$ Eker rat. CBD received FDA approval under the designation of Epidiolex® to treat seizures associated with two forms of childhood epilepsy syndromes, DS and LGS[427,451]. More recently, CBD was also used in a randomized placebo-controlled trial towards seizures in TSC (NCT02544763). Therefore, I sought out to investigate the effect of this compound in addition to its seizure component in a TSC specific context, by analysing its effect on mTOR readouts, brain structure and behaviour.

Throughout the years, the study of TSC as a disease has been strongly associated with the study of *TSC1* and *2* as biochemical tumour suppressors, and with the mTOR kinase and pathway[12,13,268,276,777,778]. The discovery that functional mutations in these tumour suppressors induced mTOR overactivation, and that this potentiated the growth of TSC-associated tumours[278,282,779], led to the hypothesis that inhibition of mTOR would be beneficial in the treatment of TSC-associated lesions. Rapamycin and Everolimus are currently prescribed mTOR inhibitors that show efficacy in reducing tumour volume in TSC patients. However research into the effect of these mTOR inhibitors on other TSC features, such as TAND and epilepsy, has so far been limited[169,186,519,780]. Thus, although mTOR inhibitors revolutionized the treatment of TSC, they do not address all features of disease and the study of novel compounds that fill this therapeutic gap is necessary. With this in mind, this project evaluated the administration of CBD in two distinct animal models of TSC to address what possible effects CBD could have on different features of TSC. The use of different models is advantageous as they possess distinct characteristics, allowing the study of different facets of the disease and possible CBD effects.

In the zebrafish *tsc2*^{vu242} model, I analysed the effect of the *tsc2* mutation and CBD on mTORC1 activation, by quantifying the number and size of brain cells expressing phosphorylated rpS6. I also investigated changes in anxiety-like and swimming behaviour by evaluating the response to a light-dark startling stimulus and locomotion (Chapter 2). Here I demonstrated that mutations in *tsc2* induced an increase in mTOR activation, as assessed by the number of cells with phosphorylated rpS6 fluorescence. Therefore, this model allowed for an assessment of the effect of CBD on this molecule. We indeed saw a reduction of rpS6 phosphorylation and cell size, indicating an action of CBD along the mTOR pathway. This was consistent with previous literature[411–413], albeit some authors have also observed an induction of the mTOR pathway following CBD administration, as seen by increased expression of the phosphorylated forms of mTOR and S6K[410,453]. Although the mechanism of action of CBD was not explored thoroughly in this work, the

data obtained does suggest that short-term CBD treatment decreases mTORC1 activation in this model. If this was also proven to be the case in TSC patients, this effect would be highly beneficial in a clinical setting. Furthermore, in this zebrafish model, I also observed an anxiolytic action of CBD, supporting previous literature using rodent and clinical populations[405,407,633,781], although this seems to be a dose- and pre-condition-dependent effect[633,707]. If, again, this effect were to be translated into the human population, given the high level of anxiety in TSC patients across different age groups[98], this could provide beneficial effects to patients receiving CBD. Overall, this multi-effect action of CBD would be advantageous over mTOR inhibitors, enabling a reduction of the pharmacological burden of patients and of the potential side effects and interactions associated with complex treatment schedules.

A mammalian model of TSC, the Eker rat, was then used. Its brain homology with primates benefits the study of the neuroanatomy and behaviour changed in TSC[782,783]. The Eker rat has been known to have a mild phenotype regarding both behavioural and neurological TSC-like manifestations[232,364,367]. However, this model has been reported to exhibit autistic-like features[370], representing an opportunity to study not only ASD but possibly other neuropsychiatric aspects characteristic of TSC. I first focused on the cerebellum, a rather overlooked structure in this model, that has been shown to be involved in autism-like behaviour[106,126,130]. Changes in cerebellar weight and layer thickness were investigated, together with alterations in cell morphology and in the expression of different disease markers (Chapter 3). Four main findings were reported on the cerebellum, namely that the Eker rat presented with increased cellular density in the granular cell layer and exhibited a reduction in the cross-sectional area of PC, while CBD treatment increased GCL thickness and increased PC cross-sectional area. These are relevant findings as they suggest that the Eker rat might have altered cerebellar development and that CBD partially corrected for this defect. In humans, as in rodents, a great part of the cerebellar structure develops post-natally which could provide a good window for CBD therapy initiation[622]. PC soma maturation was altered in this work and CBD administration promoted an increase in the cross-sectional area of the PC. However, this is a seemingly contradictory effect on size to the one reported previously with the zebrafish model. Hence, how could CBD have two apparently opposing actions in different models of the same pathology? One important note to be made at this point is that, in the zebrafish model, increased mTOR signalling through phosphorylated rpS6 (235/236) was detected, while this was not the case for the Eker rat cerebellum. This possible bidirectional action of CBD is suggestive of a homeostatic, disease-, and state-dependent role, which has previously been reported in other experimental conditions such as regarding the regulation of intracellular calcium levels in a physiological vs hyper-excitable state[784,785], or in relation to the viability of tumoural vs non-tumoural cell lines[412,786]. Furthermore, distinct mutations or models, as used in this study, could elicit different compensatory mechanisms that would differentially alter the expression of CBD targets and hence, its activity and outcome. More importantly, mTORC1 and mTORC2, which can

have opposite effects in cell size regulation (Chapter 3), have been shown to negatively regulate each other. This would allow the simultaneous activation of one complex and the inhibition of the other[787]. Once again, a deeper look into the mechanism of action by which CBD is modulating both complexes of the mTOR pathway would be crucial to fully understand its role in TSC.

The molecular changes seen in the Eker rat cerebellum suggested possible future modifications in behaviour. Therefore, I analysed motor, anxiety and ASD-like behaviour in the Eker rat upon CBD treatment. I also investigated this model's response to an acute convulsant dose of PTZ to understand the effect of mutation and treatment in the presence of seizures. Few neuropsychiatric changes were observed in the Eker rat and following CBD treatment, in agreement with previous literature (Chapters 4 and 5)[232,370]. Our PTZ trial results contrasted with data from human trials, as we found no significant effect of mutation nor of CBD on the response to PTZ-induced seizures, although a lower number of animals exhibited TC seizures in the Eker-CBD group. The animals used in these studies presented a younger age compared to previous work with this model, which I hypothesized would translate better into the age at which TAND and seizures manifest in TSC patients. However, this difference in age profile did not accentuate the behavioural phenotype of the Eker rat as anticipated. Instead, overall, it led to a more typical behavioural profile compared to previous reports[232,370]. This is of crucial importance as manifestations of epilepsy and TAND start very early in the life of TSC patients[35,113]. Consequently, the models used to study the effect of pharmaceutical interventions to be administered in this population should present TSC-like features at early ages as well. Therefore, this work suggests that the Eker rat is not a good model to address the early development of neuropsychiatric and neurological manifestations in TSC and, consequently, to study their management. The pharmacology of TSC would benefit from more studies where models with TSC-like manifestations are used with young ages. This would provide a better match to the age at which human manifestations occur, and potentially reveal novel information on how to manage young TSC patients[788]. Although I did not evaluate if the cerebellar changes reported in Chapter 3 were still present during behavioural testing (Chapter 4), a lack of alterations in cerebellar-dependent tasks was observed. This apparent discrepancy suggests that either initial cerebellar changes were not of sufficient magnitude to impact future behaviour or that alternative mechanisms contributed to a compensation for this developmental change, culminating in behavioural adjustment. Additionally, it is possible that the cerebellar alterations detected in Chapter 3 represented immature, rather than atrophic, cells and that these modifications were corrected by the time of behavioural testing. These are interesting considerations because they indicate that, although the Eker rat may not be a suitable model to study TAND and therefore, by extension, to investigate possible therapies to manage the patients' neuropsychiatric phenotypes, it might instead be an interesting model to understand how other signalling mechanisms compensate for modifications to the mTOR pathway. In this case, comparing the development of the Eker rat with other models of TSC, with a more evident behavioural phenotype, could provide valuable

insight on the modifications that occur between patients that lead to such a vast heterogeneity of neurological and neuropsychiatric phenotypes in TSC.

Considering the impact of CBD on behaviour and seizures, treatment did not affect the majority of the parameters analysed. However, a possible contribution of CBD towards the management of TAND and epilepsy cannot be excluded, as the lack of an evident neuropsychiatric-like phenotype in the Eker rat did not allow a conclusive evaluation of possible treatment effects. To ascertain whether this is true, it is crucial that further work considers more severe models of TSC, where behaviour and its pharmacological modulation can be properly addressed. This is especially important given that we found an effect of CBD on total rpS6 expression after an 8-week treatment, which may reflect modifications in protein translation (Chapter 4). This, together with the reduction in phosphorylated rpS6 found after an overnight CBD treatment (Chapter 2) suggests that CBD may alter mTOR signalling in a time-dependent manner. Given the overactive mTORC1 present in TSC, these properties might prove clinically relevant for the TSC population. Once again, a timed analysis of CBD's effect would benefit further work on its mechanism of action.

One aspect that was changed by CBD administration, both in the short-term 1-week treatment and in the long-term 8-week treatment, was weight gain, which was used as a measure of growth[789]. Therefore, it is important to consider how this could translate into a human population. Clinical trials with CBD have often reported vomiting, decreased appetite and diarrhoea as side effects[402,403,427,451,790], but they have focused heavily on seizure progression measures and scarcely report other clinical parameters such as weight progression[402]. As CBD has been widely proposed as a drug to address childhood epilepsy syndromes, it is indeed important to include, in current and follow-up studies, a progressive assessment of, not only the neurological, but also the physical and motor profile of patients. This will ensure the detection of significant alterations to a typical development upon CBD treatment, as childhood is a highly sensitive period of growth. Another important implication of this finding relates to the fact that CBD is often seen as the innocuous sibling of THC, that presents no psychotropic nor adverse effects. Furthermore, although CBD is becoming a widely accessible product, available in many main stream market contexts, long-term studies with CBD treatment are scarce, both in pre-clinical and clinical models[790–792]. Hence, it is important to be aware of the differences between anecdotal reports of CBD's benefits and the actual scientific evidence available, remembering that there are still a considerable number of unknowns in relation to this compound.

One of the limitations of this work was indeed the lack of a marked behavioural component in the Eker rat model, which did not allow absolute conclusions regarding the effect of CBD on TSC-specific behavioural alterations. These results reinforce the notion that the Eker rat is not the most appropriate model to study the establishment of TAND or infantile epilepsy in the TSC population. Another important limitation was that each experiment analysed the effect of CBD on single time points. This methodology does not allow the detection of possible progressive or time-

limited effects of CBD. This is particularly important to address given that we found effects of short-term but not of long-term treatment on the status of phosphorylated rpS6. Finally, the mechanism of action of CBD on the mTOR pathway was only briefly investigated in this work. This was mainly accomplished with the use of phosphorylated rpS6. Given that this marker can also be modified by other signalling pathways and feedback regulation, the observations collected should also be interpreted with care.

Presently, the mechanism of action of CBD is highly debated. Contradictory results are not rarely reported, especially between *in vitro* and *in vivo* results[396,793], and this work was no exception. This could be due to the use of different models and therefore, to an altered expression and distribution of target receptors or enzymes throughout the different systems. Furthermore, different preparations, vehicles, doses and routes of administration of CBD have been used in *in vitro* and *in vivo* studies, which could further elicit these distinct results[396]. Therefore, further *in vivo* research, where increasing doses of CBD are administered, would allow to properly build a dose-response curve on the effect of CBD along the mTOR pathway. Furthermore, as this is a very complex signalling system, with the convergence of different signalling pathways into mTOR, it would also be important to consider different downstream targets, not only phosphorylated rpS6 (235/236) used in this work as a readout of this pathway. Therefore, in order to properly clarify the role of CBD in TSC, future work should focus on two specific areas: 1) experimental sampling during different time points of CBD administration, so that acute and chronic effects of CBD treatment in TSC could be evaluated; 2) exploring the exact mechanism of action of CBD on the mTOR pathway. In this case, the use of high throughput screening (for example, an mTOR signalling pathway array) would be crucial to efficiently identify CBD's targets. These experiments would enable a better understanding of which targets would more likely be changed by CBD treatment and at which treatment timepoint. Importantly, these questions should be addressed in different models of TSC in which disease features are present, namely in conditional knockout murine models.

To a certain extent, the experimental method applied in this work moves in the opposite direction of the conventional drug discovery process. Instead of the pre-clinical work leading to the development of clinical trials, here, results from clinical studies inspired the investigation of the role of CBD in TSC[403]. Large clinical trials are currently undergoing to assess the effect of CBD in TSC-derived seizures (NCT02544763), and data from previous smaller scale studies seem promissing[402,403]. However, could CBD have any other action besides aiding seizure control? Ultimately, the goal with TSC treatment would be to have a single drug that could eventually address tumour growth, seizures and neuropsychiatric dysfunction. This would enable a reduction of the number of prescribed drugs, minimizing adverse effects and pharmacological interactions. However, CBD is also often portrayed as a *silver bullet*, with a plethora of effects that are often anecdotal[781]. Therefore, it is important to acknowledge that considerable data is still lacking for this compound, primarily regarding its mechanism of action.

In TSC, there is great urgency for compounds that address TAND. Furthermore, research in TAND development and management has been rather overlooked compared to our understanding of the underlying processes regulating seizures and tumours. For the progress of TSC research, it is crucial to focus efforts into the understanding of its neurodevelopment and of how *TSC* mutations impact CNS maturation and behaviour establishment. The TSC field would progress drastically with the investigation of novel compounds that could aid neurodevelopment and TAND management, whilst also being safe to allow early interventions. This knowledge would be of great value to improve the quality of life of TSC patients and provide them with the independence they so much deserve.

In sum, this work adds to the existent literature information regarding the actions of CBD on the mTOR signalling cascade, brain structure and behaviour. Importantly, this new knowledge regarding CBD is relevant not only for the TSC population but also to all patients that are increasingly recommended the use of this compound for vastly distinct pathologies. This work provides the bases for further research into the value of CBD as a clinical product to tackle neurological conditions, which may contribute to the development of a novel therapeutic entity for currently poorly addressed pathologies.

Bibliography

1. Rayer, P. F. O. Traité théorique et pratique des maladies de la peau, avec un atlas in 4 contenant 400 figures gravées et coloriées. (1835). Available at: https://archive.org/details/traitthoriqu01raye.

2. Bourneville, D. M. Sclérose tubéreuse des circonvultions cérébrales: idiotie et épilepsie hémiplégique. *Arch. Neurol.* **1,** 81–91 (1880).

3. Krueger, D. A. & Northrup, H. Tuberous Sclerosis Complex Surveillance and Management : Recommendations of the 2012 International Tuberous Sclerosis Complex Consensus Conference. *Pediatr. Neurol.* **49,** 255–265 (2013).

4. Pellizzi, G. B. Contributo allo studio dell'idiozia. *Riv. Sper. Freniatr. Med. Leg. Alien. Ment.* **27,** 265–269 (1901).

5. Perusini, G. Uber einen Fall von Sclerosis Tuberosa hypertrophica. *Monatsschr Psychiatr Neurol* **17,** 69–225 (1903).

6. Roach, E. S. Are Diagnostic Criteria for Tuberous Sclerosis Still Relevant? *Pediatr. Neurol.* **49,** 223–224 (2013).

7. Moolten, S. E. Hamartial nature of the tuberous sclerosis complex and its bearing on the tumor problem: Report of a case with tumor anomaly of the kidney and adenoma sebaceum. *Arch. Intern. Med.* **69,** 589–623 (1942).

8. Whittemore, V. H. in *Tuberous Sclerosis Complex* (eds. Kwiatkowski, D. J., Whittemore, V. H. & Thiele, E. A.) 1–9 (Wiley-VCH Verlag GmbH & Co. KGaA, 2010). doi:10.1002/9783527630073.ch1

9. Fryer, A. E. *et al.* Evidence that the gene for Tuberous Sclerosis is on chromosome 9. *Lancet* **21,** 659–661 (1987).

10. Northrup, H. *et al.* Evidence for Genetic Heterogeneity in Tuberous Sclerosis: One Locus on Chromosome 9 and at Least One Locus Elsewhere. *Am. J. Hum. Genet.* **51,** 709–720 (1992).

11. Kandt, R. *et al.* Linkage of an important gene locus for tuberous sclerosis to a chromosome 16 marker for polycystic kidney disease. *Nat. Genet.* **2,** 37–41 (1992).

12. Consortium, E. C. 16 T. Identification and Characterization of the Tuberous Sclerosis Gene on Chromosome 16. *Cell* **75,** 1305–1315 (1993).

13. Slegtenhorst, M. Van *et al.* Identification of the Tuberous Sclerosis Gene TSC1 on Chromosome 9q34. *Science (80-.).* **8,** 805–808 (1997).

14. Kingswood, J. C. *et al.* TuberOus SClerosis registry to increase disease Awareness (TOSCA) - baseline data on 2093 patients. *Orphanet J. Rare Dis.* **12,** 1–13 (2017).

15. Curatolo, P. Mechanistic Target of Rapamycin (mTOR) in Tuberous Sclerosis Complex-Associated Epilepsy. *Pediatr. Neurol.* **52,** 281–289 (2015).

16. Curatolo, P., Bombarderi, R. & Jozwiak, S. Tuberous sclerosis. *Lancet* 657–68 (2008).

17. Aronow, M. E., Nakagawa, J. A., Gupta, A., Traboulsi, E. I. & Singh, A. D. Tuberous Sclerosis Complex: Genotype/Phenotype Correlation of Retinal Findings. *Ophthalmology* **119,** 1917–1923 (2018).

18. Curatolo, P., Moavero, R. & de Vries, P. J. Neurological and neuropsychiatric aspects of tuberous sclerosis complex. *Lancet. Neurol.* **14,** 733–745 (2015).

19. Yang, P. *et al.* Renal cell carcinoma in tuberous sclerosis complex. *Am. J. Surg. Pathol.* **38,** 895–909 (2014).

20. Jó, S. & Sadowski, K. Liver Angiomyolipomas in Tuberous Sclerosis Complex- Their Incidence and Course. *Pediatr. Neurol.* **78,** 20–26 (2018).

21. Gupta, N. & Henske, E. P. Pulmonary manifestations in tuberous sclerosis complex. *Am. J. Med. Genet.* 1–12 (2018). doi:10.1002/ajmg.c.31638

22. Sparling, M. A. J. J. D., Hong, C.-H., Brahim, J. S., Moss, J. & Darling, T. N. Oral Findings in 58 Adults with Tuberous Sclerosis Complex. *J. Am. Acad. Dermatol.* **56,** 786–790 (2007).

23. Curatolo, P., Moavero, R., Roberto, D. & Graziola, F. Genotype/Phenotype Correlations in Tuberous Sclerosis Complex. *Semin. Pediatr. Neurol.* **22,** 259–273 (2017).

24. Caban, C., Khan, N., Hasbani, D. M. & Crino, P. B. Genetics of tuberous sclerosis complex: implications for clinical practice. *The Application of Clinical Genetics* **10,** 1–8 (2017).

25. Switon, K., Kotulska, K., Janusz-Kaminska, A., Zmorzynska, J. & Jawroski, J. Critical Review Tuberous Sclerosis Complex : From Molecular Biology to Novel Therapeutic Approaches Clinical Manifestations of TSC. *IUBMB Life* **68,** 955–962 (2016).

26. Wortmann, S. B., Reimer, A., Creemers, J. W. T. & Mullaart, R. A. Prenatal diagnosis of cerebral lesions in Tuberous sclerosis complex (TSC). Case report and review of the literature. *Eur. J. Pediatr. Neurol.* **12,** 123–126 (2008).

27. Saada, J., Dumez, Y. & Benachi, A. Prenatal diagnosis of cardiac rhabdomyomas: incidence of associated cerebral lesions of tuberous sclerosis complex. *Ultrasound Obstet. Gynecol.* **34,** 155–159 (2009).

28. Rosset, C., Netto, O. & Ashton-Prolla, P. TSC1 and TSC2 gene mutations and their implications for treatment in Tuberous Sclerosis Complex : a review. *Genet. Mol. Biol.* **40,** 69–79 (2017).

29. Institute, N. C. NCI Dictionary of Cancer Terms. Available at: https://www.cancer.gov/publications/dictionaries/cancer-terms/def/hamartoma?redirect=true.

30. Francis X. McCormack, M.D., Yoshikazu Inoue, M.D., Ph.D., Joel Moss, M.D., Ph.D., Lianne G. Singer, M. D. *et al.* Efficacy and Safety of Sirolimus in Lymphangioleiomyomatosis. *N. Engl. J. Med.* **364,** 1595–1606 (2011).

31. Pascual-Castroviejo, I. *et al.* Significance of tuber size for complications of tuberous sclerosis complex. *Neurología* **28,** 550–557 (2013).

32. Crino, P. B. Molecular Pathogenesis of Tuber Formation in Tuberous Sclerosis Complex. *J. Child Neurol.* **19,** 716–725 (2004).

33. Eijkemans, M. J. C., Wal, W. Van Der, Reijnders, L. J., Roes, K. C. B. & Doorn-khosrovani, S. B. V. W. Van. Long-term Follow-up Assessing Renal Angiomyolipoma Treatment Patterns, Morbidity, and Mortality: An Observational Study in Tuberous Sclerosis Complex Patients in the Netherlands. *Am. J. Kidney Dis.* **66,** 638–645 (2015).

34. Rentz, A. M. *et al.* Tuberous Sclerosis Somplex: A Survey of Health Care Resource Use and Health Burden. *Pediatr. Neurol.* **52,** 435–441 (2015).

35. Chu-Shore, C. J., Major, P., Camposano, S., Muzykewicz, D. & Thiele, E. A. The natural history of epilepsy in tuberous sclerosis complex. *Epilepsia* **51,** 1236–1241 (2010).

36. Kaczorowska, M. *et al.* Cerebral tuber count and its impact on mental outcome of patients with tuberous sclerosis complex. *Epilepsia* **52,** 22–27 (2011).

37. Jülich, K. & Sahin, M. Mechanism-Based Treatment in Tuberous Sclerosis Complex. *Pediatr. Neurol.* **50,** 290–296 (2014).

38. Mous, S. E. *et al.* Cortical dysplasia and autistic trait severity in children with Tuberous Sclerosis Complex : a clinical epidemiological study. *Eur. Child Adolesc. Psychiatry* **27,** 753–765 (2017).

39. Crino, P. B. Evolving neurobiology of tuberous sclerosis complex. *Acta Neuropathol.* **125,** 317–332 (2013).

40. Grajkowska, W., Kotulska, K., Jurkiewicz, E. & Matyja, E. Brain lesions in tuberous sclerosis complex. Review. *Folia Neuropathol.* **48,** 139–149 (2010).

41. Chu-Shore, C. J., Major, P., Montenegro, M. & Thiele, E. Cyst-like tubers are associated with TSC2 and epilepsy in tuberous sclerosis complex. *Neurology* **72,** 1165–1169 (2009).

42. Goodman, M. *et al.* Cortical Tuber Count: A Biomarker Indicating Neurologic Severity of Tuberous Sclerosis Complex. *J. Child Neurol.* **12,** 85–90 (1997).

43. Park, S.-H. *et al.* Tuberous sclerosis in a 20-week gestation fetus: immunohistochemical study. *Acta Neuropathol.* **94,** 180–186 (1997).

44. Mühlebner, A. *et al.* Specific pattern of maturation and differentiation in the formation of cortical tubers in tuberous sclerosis complex (TSC): evidence from layer-specific marker expression. *J. Neurodev. Disord.* **8,** 9 (2016).

45. Wenzel, H. J. *et al.* Morphology of cerebral lesions in the Eker rat model of tuberous sclerosis. *Acta Neuropathol.* **108,** 97–108 (2004).

46. Meng, X., Yu, J., Song, J., Chi, S. & Tan, L. Role of the mTOR signaling pathway in epilepsy. *J. Neurol. Sci.* **332,** 4–15 (2013).

47. Major, P. *et al.* Are cortical tubers epileptogenic? Evidence from electrocorticography. *Epilepsia* **50,** 147–154 (2009).

48. Doherty, C., Goh, S., Poussaint, T. Y., Erdag, N. & Thiele, E. A. Prognostic Significance of Tuber Count and Location in Tuberous Sclerosis Complex. *J. Child Neurol.* **20,** 837–841 (2005).

49. Mühlebner, A., Scheppingen, J. Van & Hulshof, H. M. Novel Histopathological Patterns in Cortical Tubers of Epilepsy Surgery Patients with Tuberous Sclerosis Complex. *PLoS One* **11,** 1–15 (2016).

50. Sosunov, A. A. *et al.* Epileptogenic but MRI-normal perituberal tissue in Tuberous Sclerosis Complex contains tuber-specific abnormalities. *Acta Neuropathol. Commun.* **3,** 1–15 (2015).

51. Crino, P. B. mTOR Signaling in Epilepsy : Insights from Malformations of Cortical Development. *Cold Spring Harb. Perspect. Med.* **5,** 1–17 (2015).

52. Mizuguchi, M. Abnormal giant cells in the cerebral lesions of tuberous sclerosis complex. *Congenit. Anom. (Kyoto).* **47,** 2–8 (2007).

53. Talos, D. M., Kwiatkowski, D. J., Cordero, K., Black, P. M. & Jensen, F. E. Cell-specific alterations of glutamate receptor expression in tuberous sclerosis complex cortical tubers. *Ann. Neurol.* **63,** 454–465 (2008).

54. Wong, M. Mechanisms of epileptogenesis in tuberous sclerosis complex and related malformations of cortical development with abnormal glioneuronal proliferation. *Epilepsia* **49,** 8–21 (2008).

55. Kannan, L., Vogrin, S., Bailey, C., Maixner, W. & Harvey, A. S. Centre of epileptogenic tubers generate and propagate seizures in tuberous sclerosis. *Brain* **139,** 2653–2667 (2016).

56. Cepeda, C. *et al.* Morphological and electrophysiological characterization of abnormal cell types in pediatric cortical dysplasia. *J. Neurosci. Res.* **72,** 472–486 (2003).

57. White, R. *et al.* Selective Alterations in Glutamate and GABA Receptor Subunit mRNA Expression in Dysplastic Neurons and Giant Cells of Cortical Tubers. *Ann. Neurol.* **49,** 67–78 (2001).

58. Barker-Haliski, M. & White, H. S. Glutamatergic Mechanisms Associated with Seizures and Epilepsy. *Cold Spring Hrbor Perspect. Med.* **5,** 1–15 (2015).

59. Callaghan, F. J. K. O. *et al.* The relation of infantile spasms, tubers, and intelligence in tuberous sclerosis complex. *Arch. Dis. Child.* **89,** 530–534 (2004).

60. Holmes, G. L. & Stafstrom, C. E. Tuberous sclerosis complex and epilepsy: recent developments and future challenges. *Epilepsia* **48,** 617–630 (2007).

61. Jarrar, R. G., Buchhalter, J. R. & Raffel, C. Long-term outcome of epilepsy surgery. *Neurology* **62,** 479–481 (2004).

62. Shahid, A. Resecting the epileptogenic tuber: What happens in the long term? *Epilepsia* **54,** 135–138 (2013).

63. Ruppe, V. *et al.* Developmental brain abnormalities in tuberous sclerosis complex : A comparative tissue analysis of cortical tubers and perituberal cortex. *Epilepsia* **55,** 539–550 (2014).

64. Tee, A. R., Sampson, J. R., Pal, D. K. & Bateman, J. M. The role of mTOR signalling in neurogenesis, insights from tuberous sclerosis complex. *Semin. Cell Dev. Biol.* **52,** 12–20 (2016).

65. Siedlecka, M., Szlufik, S., Grajkowska, W., Roszkowski, M. & Jóźwiak, J. Erk activation as a possible mechanism of transformation of subependymal nodule into subependymal giant cell astrocytoma. *Folia Neuropathol.* **53,** 8–14 (2015).

66. Campen, C. J. & Porter, B. E. Subependymal Giant Cell Astrocytoma (SEGA) Treatment Update. *Curr Treat Options Neurol* **13,** 380–385 (2012).

67. Tubbs, R. S., Oakes, P., Maran, I. S., Salib, C. & Loukas, M. The foramen of Monro: a review of its anatomy, history, pathology, and surgery. *Child's Nerv. Syst.* **30,** 1645–1649 (2014).

68. Tully, H. M. & Dobyns, W. B. Infantile hydrocephalus: a review of epidemiology, classification and causes. *Eur. J. Med. Genet.* **57,** 359–368 (2014).

69. Jozwiak, S., Nabbout, R. & Curatolo, P. Management of subependymal giant cell astrocytoma (SEGA) associated with tuberous sclerosis complex (TSC): Clinical recommendations. *Eur. J. Paediatr. Neurol.* **7,** 348–352 (2013).

70. Brat, D. J. & Perry, A. *Chapter 5 - Astrocytic and Oligodendroglial Tumors*. *Practical Surgical Neuropathology: A Diagnostic Approach* (Elsevier Inc.). doi:10.1016/B978-0-443-06982-6.00005-5

71. Kim, S. *et al.* Biological behavior and tumorigenesis of subependymal giant cell astrocytomas. *J. Neurooncol.* **52,** 217–225 (2001).

72. Mizuguchi, M. & Takashima, S. Neuropathology of tuberous sclerosis. *Brain Dev.* **23,** 508–515 (2001).

73. Sheperd, C. Subependymal Giant Cell Astrocytoma: A Clinical, Pathological, and Flow Cytometric Study. *Neurosurgery* **28,** 864–868 (1991).

74. Chan, D. L., Calder, T., Lawson, J. A., Mowat, D. & Kennedy, S. E. The natural history of subependymal giant cell astrocytomas in tuberous sclerosis complex: a review. *Rev. Neurosci.* **29,** 295–301 (2017).

75. Mei, G., Liu, X., Zhou, P. & Shen, M. Clinical and imaging features of subependymal giant cell astrocytoma: report of 20 cases. *Chinese Neurosurg. J.* **3,** 1–7 (2017).

76. Zordan, P. *et al.* Tuberous sclerosis complex – associated CNS abnormalities depend on hyperactivation of mTORC1 and Akt. *J. Clin. Invest.* **128,** 1688–1706 (2018).

77. Roth, J., Koenig, M. K., Weiner, H. L., Franz, D. N. & Wang, H. Z. Subependymal Giant Cell Astrocytoma : Diagnosis , Screening , and Treatment . Recommendations From the International Tuberous Sclerosis Complex Consensus Conference 2012. *Pediatr. Neurol.* **49,** 439–444 (2013).

78. Chan, J. A., Ieslawa, G. R. W., Owalik, J. O. L. E., Otulska, K. A. K. & Wiatkowski, D. A. J. K. Pathogenesis of Tuberous Sclerosis Subependymal Giant Cell Astrocytomas : Biallelic Inactivation of TSC1 or TSC2 Leads to mTOR Activation. *J. Neuropathol. Exp. Neurol.* **63,** 1236–1242 (2004).

79. Wong, M. Mammalian Target of Rapamycin (mTOR) Pathways in Neurological Diseases. *Biomed J* **36,** 1–17 (2013).

80. Krueger, D. A. Management of CNS-related Disease Manifestations in Patients With Tuberous Sclerosis Complex. *Curr. Treat. Options Neurol.* **15,** 618–633 (2013).

81. Saxena, A. & Sampson, J. R. Epilepsy in Tuberous Sclerosis: Phenotypes, Mechanisms, and Treatments. *Semin. Neurol.* **35,** 269–76 (2015).

82. Jeong, A., Nakagawa, J. A. & Wong, M. Predictors of Drug-Resistant Epilepsy in Tuberous Sclerosis Complex. *J. Child Neurol.* **32,** 1092–1098 (2017).

83. Capal, J. K. *et al.* Influence of seizures on early development in tuberous sclerosis complex. *Epilepsy Behav.* **70,** 245–252 (2017).

84. Chen, Z., Brodie, M. J., Liew, D. & Kwan, P. Treatment Outcomes in Patients with Newly Diagnosed Epilepsy Treated With Established and New Antiepileptic Drugs: A 30-Year Longitudinal Cohort Study. *JAMA Neurol.* **75,** 279–286 (2017).

85. Kwan, P. *et al.* Definition of drug resistant epilepsy: Consensus proposal by the ad hoc Task Force of the ILAE Commission on Therapeutic Strategies. *Epilepsia* **51,** 1069–1077 (2010).

86. D'Alonzo, R., Rigante, D., Mencaroni, E. & Esposito, S. West Syndrome: A Review and Guide for Paediatricians. *Clin. Drug Investig.* **38,** 113–124 (2018).

87. Nelson, G. R. Management of infantile spasms. *Transl. Pediatr.* **4,** 260–270 (2015).

88. Shields, W. D. & Angeles, L. Infantile Spasms: Little Seizures, BIG Consequences. *Epilepsy Curr.* **6,** 63–69 (2006).

89. Vignoli, A. *et al.* Epilepsy in TSC : Certain etiology does not mean certain prognosis. *Epilepsia* **54,** 2134–2142 (2013).

90. Cusmai, R., Moavero, R., Bombardieri, R., Vigevano, F. & Curatolo, P. Long-term neurological outcome in children with early-onset epilepsy associated with tuberous sclerosis. *Epilepsy Behav.* **22,** 735–739 (2011).

91. Muzykewicz, D. A., Costello, D. J., Halpern, E. F. & Thiele, E. A. Infantile spasms in tuberous sclerosis complex: Prognostic utility of EEG. *Epilepsia* **50,** 290–296 (2009).

92. Gipson, T. T. & Johnston, M. V. New insights into the pathogenesis and prevention of tuberous sclerosis-associated neuropsychiatric disorders (TAND) [version 1 ; referees : 3 approved] Referee Status : *F1000Research* **6,** 1–7 (2017).

93. Leclezio, L., Jansen, A., Whittemore, V. H. & de Vries, P. J. Pilot Validation of the Tuberous Sclerosis-Associated Neuropsychiatric Disorders (TAND) Checklist. *Pediatr. Neurol.* **52,** 16–24 (2015).

94. Chung, T., Franz, D. N. & Krueger, D. A. Psychiatric comorbidity and treatment response in patients with tuberous sclerosis complex. *Ann. Clin. Psychiatry* **23,** 263–269 (2011).

95. Leclezio, L., Gardner-Lubbe, S. & de Vries, P. J. Is It Feasible to Identify Natural Clusters of TSC-Associated Neuropsychiatric Disorders (TAND)? *Pediatr. Neurol.* **81,** 38–44 (2018).

96. Muzykewicz, D. A., Newberry, P., Danforth, N., Halpern, E. F. & Thiele, E. A. Psychiatric comorbid conditions in a clinic population of 241 patients with tuberous sclerosis complex. *Epilepsy Behav.* **11,** 506–513 (2007).

97. de Vries, P. J., Hunt, A. & Bolton, P. F. The psychopathologies of children and adolescents with tuberous sclerosis complex (TSC) A postal survey of UK families. *Eur. Child Adolesc. Psychiatry* **16,** 16–24 (2007).

98. Vries, P. J. De *et al.* TSC-associated neuropsychiatric disorders (TAND): findings from the TOSCA natural history study. *Orphanet J. Rare Dis.* **13,** 1–13 (2018).

99. Bandelow, B. & Michaelis, S. Epidemiology of anxiety disorders in the 21st century. *Dialogues Clin. Neurosci.* **17,** 327–335 (2015).

100. Kelleher, R. J. & Bear, M. F. The Autistic Neuron: Troubled Translation? *Cell* **135,** 401–406 (2008).

101. Subramanian, M., Timmerman, C. K., Schwartz, J. L., Pham, D. L. & Meffert, M. K. Characterizing autism spectrum disorders by key biochemical pathways. *Front. Neurosci.* **9,** 1–18 (2015).

102. Peters, J. M. *et al.* Brain functional networks in syndromic and non-syndromic autism: a graph theoretical study of EEG connectivity. *BMC Med.* **11,** 1–16 (2013).

103. McMahon, J. J. *et al.* Seizure-dependent mTOR activation in 5-HT neurons promotes autism-like behaviors in mice. *Neurobiol. Dis.* **73,** 296–306 (2015).

104. Kreiser, N. L. & White, S. W. ASD in Females: Are We Overstating the Gender Difference in Diagnosis? *Clin. Child Fam. Psychol. Rev.* **17,** 67–84 (2014).

105. Bozzi, Y., Provenzano, G. & Casarosa, S. Neurobiological bases of autism-epilepsy comorbidity: a focus on excitation/inhibition imbalance. *Eur. J. Neurosci.* **47,** 534–548 (2018).

106. Crippa, A. *et al.* Cortico-cerebellar connectivity in Autism Spectrum Disorder: What do we know so far? *Front. Psychiatry* **7,** 1–7 (2016).

107. Sato, A. *et al.* Rapamycin reverses impaired social interaction in mouse models of tuberous sclerosis complex. *Nat. Commun.* **3,** 1292–1299 (2012).

108. National Institute of Mental Health. Autism Spectrum Disorder. *March* (2018). Available at: https://www.nimh.nih.gov/health/topics/autism-spectrum-disorders-asd/index.shtml.

109. Association, A. P. *Diagnostic and statistical manual of mental disorders : DSM*-5. (2013).

110. Capal, J. K. *et al.* Utility of the Autism Observation Scale for Infants in Early Identification of Autism in Tuberous Sclerosis Complex. *Pediatr. Neurol.* **75,** 80–86 (2017).

111. Richards, M., Mossey, J. & Robins, D. L. Parents' concerns as they relate to their child's development and later diagnosis of autism spectrum disorder. *J. Dev. Behav. Pediatr.* **37,** 532–540 (2016).

112. McDonald, N. M. *et al.* Early autism symptoms in infants with tuberous sclerosis complex. *Autism Res.* **10,** 1981–1990 (2017).

113. Jeste, S. S. *et al.* Early developmental trajectories associated with ASD in infants with tuberous sclerosis complex. *Neurology* **83,** 160–168 (2014).

114. National Institute for Health and Care Excellence. Autism: The management and support of children and young people on the autism spectrum. *Nice Guideline 170* (2016). Available at: https://www.nice.org.uk/guidance/cg170/evidence/autism-management-of-autism-in-children-and-young-people-full-guideline-248641453. (Accessed: 1st August 2018)

115. Jeste, S. S. *et al.* Symptom profiles of autism spectrum disorder in tuberous sclerosis complex. *Neurology* **87,** 766–772 (2016).

116. Numis, A. L. *et al.* Identification of risk factors for autism spectrum disorders in tuberous sclerosis complex. *Neurology* **76,** 981–987 (2011).

117. Vignoli, A. *et al.* Autism spectrum disorder in tuberous sclerosis complex: Searching for risk markers. *Orphanet J. Rare Dis.* **10,** 1–9 (2015).

118. Curatolo, P., Porfirio, M. C., Manzi, B. & Seri, S. Autism in tuberous sclerosis. *Eur. J. Paediatr. Neurol.* **8,** 327–332 (2004).

119. Werling, D. M. & Geschwind, D. H. Sex differences in autism spectrum disorders. *Curr. Opin. Neurol.* **26,** 146–153 (2013).

120. Ospina, M. B. *et al.* Behavioural and Developmental Interventions for Autism Spectrum Disorder: A Clinical Systematic Review. *PLoS One* **3,** (2008).

121. Sparks, B. F. *et al.* Brain structural abnormalities in young children with autism spectrum disorder. *Neurology* **59,** 184–192 (2002).

122. Hallahan, B. *et al.* Brain morphometry volume in autistic spectrum disorder: A magnetic resonance imaging study of adults. *Psychol. Med.* **39,** 337–346 (2009).

123. Wang, S. S., Kloth, A. D. & Badura, A. The Cerebellum, Sensitive Periods, and Autism.

Neuron **83,** 518–532 (2014).

124. Amaral, D. G., Schumann, C. M. & Nordahl, C. W. Neuroanatomy of autism. *Trends Neurosci.* **31,** 137–145 (2008).

125. Bauman, M. L. & Kemper, T. L. Neuroanatomic observations of the brain in autism: a review and future directions. *Int. J. Dev. Neurosci.* **23,** 183–187 (2005).

126. D'Mello, A. M. & Stoodley, C. J. Cerebro-cerebellar circuits in autism spectrum disorder. *Front. Neurosci.* **9,** 1–18 (2015).

127. Whitney, E. R., Kemper, T. L., Bauman, M. L., Rosene, D. L. & Blatt, G. J. Cerebellar Purkinje cells are reduced in a subpopulation of autistic brains: A stereological experiment using calbindin-D28k. *Cerebellum* **7,** 406–416 (2008).

128. Jeong, J.-W., Tiwari, V. N., Behen, M. E., Chugani, H. T. & Chugani, D. C. In vivo detection of reduced Purkinje cell fibers with diffusion MRI tractography in children with autistic spectrum disorders. *Front. Hum. Neurosci.* **8,** 1–11 (2014).

129. Levitt, J. G. *et al.* Cerebellar Vermis Lobules VIII-X in Autism. *Prog. Neuropsychopharmacol. Biol. Psychiatry* **23,** 625–633 (1999).

130. Liu, J. *et al.* Gray matter abnormalities in pediatric autism spectrum disorder: a meta-analysis with signed differential mapping. *Eur. Child Adolesc. Psychiatry* **26,** 933–945 (2017).

131. Lange, N. *et al.* Longitudinal Volumetric Brain Changes in Autism Spectrum Disorder Ages 6-35 Years. *Autism Res.* **8,** 82–93 (2015).

132. Haar, S., Berman, S., Behrmann, M. & Dinstein, I. Anatomical Abnormalities in Autism? *Cereb. Cortex* **26,** 1440–1452 (2016).

133. Skefos, J. *et al.* Regional alterations in Purkinje cell density in patients with autism. *PLoS One* **9,** 1–12 (2014).

134. Ritvo, E. R. *et al.* Lower Purkinje cell counts in the cerebella of four autistic subjects: Initial findings of the UCLA-NSAC autopsy research report. *Am. J. Psychiatry* **143,** 862–866 (1986).

135. Bailey, A. *et al.* A clinicopathological study of autism. *Brain* **121,** 889–905 (1998).

136. Fatemi, S. H. *et al.* mRNA and protein levels for GABAAα4, α5, β1 and GABABR1 receptors are altered in brains from subjects with autism. *J. Autism Dev. Disord.* **40,** 743–750 (2010).

137. Whitney, E. R., Kemper, T. L., Rosene, D. L., Bauman, M. L. & Blatt, G. J. Density of cerebellar basket and stellate cells in autism: Evidence for a late developmental loss of Purkinje cells. *J. Neurosci.* **87,** 2245–2254 (2009).

138. Webb, S. J. *et al.* Neuroimaging Cerebellar vermal volumes and behavioral correlates in children with autism spectrum disorder. *Psychiatry Res. Neuroimaging* **172,** 61–67 (2009).

139. D'Mello, A. M., Crocetti, D., Mostofsky, S. H. & Stoodley, C. J. Cerebellar gray matter and lobular volumes correlate with core autism symptoms. *NeuroImage Clin.* **7,** 631–639 (2015).

140. Lee, E., Lee, J. & Kim, E. Excitation/Inhibition Imbalance in Animal Models of Autism Spectrum Disorders. *Biol. Psychiatry* **81,** 838–847 (2017).

141. Fatemi, S. H. *et al.* Glutamic acid decarboxylase 65 and 67 kDa proteins are reduced in autistic parietal and cerebellar cortices. *Biol. Psychiatry* **52,** 805–810 (2002).

142. Yip, J., Soghomonian, J. & Blatt, G. J. Decreased GAD65 mRNA levels in select subpopulations in the cerebellar dentate nuclei in autism: an in situ hybridization study. *Autism Res.* **2,** 50–59 (2009).

143. Yip, J., Soghomonian, J.-J. & Blatt, G. J. Decreased GAD67 mRNA levels in cerebellar Purkinje cells in autism: Pathophysiological implications. *Acta Neuropathol.* **113,** 559–568 (2007).

144. Fatemi, S. H., Reutiman, T. J., Folsom, T. D. & Thuras, P. D. GABAA receptor downregulation in brains of subjects with autism. *J. Autism Dev. Disord.* **39,** 223–230 (2009).

145. Fatemi, S. H., Folsom, T. D., Reutiman, T. J. & Thuras, P. D. Expression of GABAB Receptors Is Altered in Brains of Subjects with Autism. *Cerebellum* **8,** 64–69 (2009).

146. Soghomonian, J.-J., Zhang, K., Reprakash, S. & Blatt, G. J. Decreased parvalbumin mRNA levels in cerebellar Purkinje cells in autism. *Autism Res.* **10,** 1787–1796 (2017).

147. Weber, A. M., Egelhoff, J. C., McKellop, J. M. & Franz, D. N. Autism and the cerebellum: Evidence from tuberous sclerosis. *J. Autism Dev. Disord.* **30,** 511–517 (2000).

148. Eluvathingal, T. J. *et al.* Cerebellar Lesions in Tuberous Sclerosis Complex: Neurobehavioural and Neuroimaging Correlates. *J. Child Neurol.* **21,** 846–851 (2006).

149. Sundberg, M. *et al.* Purkinje cells derived from TSC patients display hypoexcitability and synaptic deficits associated with reduced FMRP levels and reversed by rapamycin. *Mol. Psychiatry* **23,** 2167–2183 (2018).

150. de Vries, P. J. *et al.* Tuberous Sclerosis Associated Neuropsychiatric Disorders (TAND) and the TAND Checklist. *Pediatr. Neurol.* **52,** 25–35 (2015).

151. Dalic, L. & Cook, M. J. Managing drug-resistant epilepsy: challenges and solutions. *Neuropsychiatr. Dis. Treat.* **12,** 2605–2616 (2016).

152. Shepherd, C. *et al.* Understanding the health economic burden of patients with tuberous sclerosis complex (TSC) with epilepsy: a retrospective cohort study in the UK Clinical Practice Research Datalink (CPRD). *BMJ Open* **7,** 7–13 (2017).

153. Zhang, B., McDaniel, S. S., Rensing, N. R. & Wong, M. Vigabatrin Inhibits Seizures and mTOR Pathway Activation in a Mouse Model of Tuberous Sclerosis Complex. *PLoS One* **8,** 1–8 (2013).

154. Wong, M. A Critical Review of mTOR Inhibitors and Epilepsy: from Basic Science to Clinical Trials. *Expert Rev. Neurother.* **13,** 1–21 (2013).

155. Curatolo, P., Jozwiak, S. & Nabbout, R. Management of epilepsy associated with tuberous sclerosis complex (TSC): Clinical recommendations. *Eur. J. Pediatr. Neurol.* **16,** 582–586 (2012).

156. Hemming, K., Maguire, M., Hutton, J. & Marson, A. Vigabatrin for refractory partial epilepsy. *Cochrane Database Syst. Rev.* **31,** 1–22 (2013).

157. Greiner, H. M. *et al.* Vigabatrin for Childhood Partial-Onset Epilepsies. *Pediatr. Neurol.* **46,** 83–88 (2012).

158. Kinirons, P. *et al.* Vigabatrin Retinopathy in an Irish Cohort: Lack of Correlation with Dose. *Epilepsia* **47,** 311–317 (2006).

159. Hu, Q. *et al.* Efficacy and safety of antiepileptic drugs for refractory partial-onset epilepsy: a network meta-analysis. *J. Neurol.* **265,** 1–11 (2018).

160. Androsova, G. *et al.* Comparative effectiveness of antiepileptic drugs in patients with mesial temporal lobe epilepsy with hippocampal sclerosis. *Epilepsia* **58,** 1734–1741 (2017).

161. National Institute for Health and Care Excellence. Epilepsies: diagnosis and management. *NICE Clinical Guideline CG137* (2018). Available at: https://www.nice.org.uk/guidance/cg137/chapter/Appendix-E-Pharmacological-treatment.

162. Jackson, M. C. *et al.* Effect of vigabatrin on seizure control and safety profile in different subgroups of children with epilepsy. *Epilepsia* **58,** 1575–1585 (2017).

163. Camposano, S. E., Major, P., Halpern, E. & Thiele, E. A. Vigabatrin in the treatment of childhood epilepsy: A retrospective chart review of efficacy and safety profile. *Epilepsia* **49,** 1186–1191 (2008).

164. Ben-Menachem, E. Mechanism of action of vigabatrin: correcting misperceptions. *Acta Neurol. Scand.* **124,** 5–15 (2011).

165. Loscher, W. & Rogawski, M. A. How theories evolved concerning the mechanism of action of barbiturates. *Epilepsia* **53,** 12–25 (2012).

166. National Institute for Health and Care Excellence. Epilepsies: diagnosis and management. *NICE Clinical Guideline CG137* (2018).

167. Curatolo, P. & Moavero, R. mTOR Inhibitors in Tuberous Sclerosis Complex. *Curr. Neuropharmacol.* **10,** 404–415 (2012).

168. Franz, D. N. & Capal, J. K. mTOR inhibitors in the pharmacologic management of tuberous sclerosis complex and their potential role in other rare neurodevelopmental disorders. *Orphanet J. Rare Dis.* **12,** 1–9 (2017).

169. Franz, D. N. *et al.* Long-Term Use of Everolimus in Patients with Tuberous Sclerosis Complex: Final Results from the EXIST-1 Study. *PLoS One* **11,** 1–13 (2016).

170. Habib, S. L. *et al.* Is mTOR Inhibitor Good Enough for Treatment All Tumors in TSC Patients? *J. Cancer* **7,** 1621–1631 (2016).

171. Ostendorf, A. P. & Wong, M. mTOR Inhibition in Epilepsy: Rationale and Clinical Perspectives. *CNS Drugs* **29,** 91–99 (2015).

172. Krueger, D. A. *et al.* Everolimus Treatment of Refractory Epilepsy in Tuberous Sclerosis Complex. *Ann. Neurol.* **74,** 679–687 (2013).

173. LaSarge, C. L. & Danzer, S. C. Mechanisms regulating neuronal excitability and seizure development following mTOR pathway hyperactivation. *Front. Mol. Neurosci.* **7,** 1–15 (2014).

174. Takei, N. *et al.* Brain-Derived Neurotrophic Factor Induces Mammalian Target of Rapamycin-Dependent Local Activation of Translation Machinery and Protein Synthesis in Neuronal Dendrites. *J. Neurosci.* **24,** 9760–9769 (2004).

175. Takei, N. & Nawa, H. mTOR signaling and its roles in normal and abnormal brain development. *Front. Hum. Neurosci.* **7,** 1–12 (2014).

176. McDaniel, S. S. & Wong, M. Therapeutic role of mammalian target of rapamycin (mTOR) inhibition in preventing epileptogenesis. *Neurosci. Lett.* **497,** 231–239 (2011).

177. Curatolo, P., Moavero, R., van Scheppingen, J. & Aronica, E. mTOR dysregulation and tuberous sclerosis-related epilepsy. *Expert Rev. Neurother.* **18,** 185–201 (2018).

178. Raab-Graham, K. F., Haddick, P. C. G., Jan, Y. N. & Jan, L. Y. Activity- and mTOR-Dependent Suppression of Kv1.1 Channel mRNA Translation in Dendrites. *Science (80-.).* **314,** 144–148 (2006).

179. Wang, Y., Barbaro, M. F. & Baraban, S. C. A role for the mTOR pathway in surface expression of AMPA receptors. *Neurosci. Lett.* **401,** 35–39 (2006).

180. Wong, M. *et al.* Impaired glial glutamate transport in a mouse tuberous sclerosis epilepsy model. *Ann. Neurol.* **54,** 251–6 (2003).

181. Lozovaya, N. *et al.* Selective supression of excessive GluN2C expression rescues early epilepsy in a tuberous sclerosis murine model. *Nat. Commun.* **5,** 1–15 (2014).

182. Krueger, D. A. *et al.* Everolimus for Subependymal Giant-Cell Astrocytomas in Tuberous Sclerosis. *N. Engl. J. Med.* **363,** 1801–1811 (2010).

183. Franz, D. N. *et al.* Efficacy and safety of everolimus for subependymal giant cell astrocytomas associated with tuberous sclerosis complex (EXIST-1): a multicentre, randomised, placebo-controlled phase 3 trial. *Lancet* **381,** 125–132 (2013).

184. Wiegand, G. *et al.* Everolimus in tuberous sclerosis patients with intractable epilepsy: A treatment option? *Eur. J. Paediatr. Neurol.* **17,** 631–638 (2013).

185. Cardamone, M. *et al.* Mammalian Target of Rapamycin Inhibitors for Intractable Epilepsy and Subependymal Giant Cell Astrocytomas in Tuberous Sclerosis Complex. *J. Pediatr.* **164,** 1195–1200 (2014).

186. Krueger, D. A. *et al.* Long-term treatment of epilepsy with everolimus in tuberous sclerosis. *Neurology* **87,** 2408–2415 (2016).

187. Saxton, R. A. & Sabatini, D. M. mTOR Signaling in Growth, Metabolism, and Disease. *Cell* **168,** 960–976 (2017).

188. Franz, D. N. *et al.* Rapamycin causes regression of astrocytomas in tuberous sclerosis complex. *Ann. Neurol.* **59,** 490–498 (2006).

189. Mingarelli, A. *et al.* Dramatic relapse of seizures after everolimus withdrawal. *Eur. J. Paediatr. Neurol.* **22,** 203–206 (2018).

190. Amin, S. *et al.* The outcome of surgical management of subependymal giant cell astrocytoma in tuberous sclerosis complex. *Eur. J. Paediatr. Neurol.* **17,** 36–44 (2012).

191. Fohlen, M., Ferrand-Sorbets, S., Delalande, O. & Dorfmüller, G. Surgery for subependymal giant cell astrocytomas in children with tuberous sclerosis complex. *Child's Nerv. Syst.* **34,** 1511–1519 (2018).

192. Liang, S., Zhang, J., Yang, Z. & Zhang, S. Long-term outcomes of epilepsy surgery in tuberous sclerosis complex. *J. Neurol.* **264,** 1146–1154 (2017).

193. Fohlen, M. *et al.* Refractory epilepsy in preschool children with tuberous sclerosis complex: Early surgical treatment and outcome. *Seizure Eur. J. Epilepsy* **60,** 71–79 (2018).

194. Fallah, A. *et al.* Resective Epilepsy Surgery for Tuberous Sclerosis in Children: Determining Predictors of Seizure Outcomes in a Multicenter Retrospective Cohort Study. *Neurosurgey* **77,** 517–524 (2015).

195. Wu, Y., Liu, D. & Song, Z. Neuronal Networks and Energy Bursts in Epilepsy. *Neuroscience* **287,** 175–186 (2015).

196. Jansen, F. E., van Huffelen, A. C., Algra, A. & van Nieuwenhuizen, O. Epilepsy Surgery in Tuberous Sclerosis: A Systematic Review. *Epilepsia* **48,** 1477–1484 (2007).

197. Alexander, H. B., Broshek, D. K. & Quigg, M. Quality of life in adults with epilepsy is associated with anticonvulsant polypharmacy independent of seizure status. *Epilepsy Behav.* **78,** 96–99 (2018).

198. Petruzzi, A. *et al.* Psychological features and quality of life in 50 adult patients with epilepsy and their caregivers from the Lecco epilepsy center, Italy. *Epilepsy Behav.* **71,** 13–16 (2017).

199. Richardson, S. P., Farias, S. T., Iii, A. R. L. & Alsaadi, T. M. Improvement in seizure control and quality of life in medically refractory epilepsy patients converted from polypharmacy to monotherapy. *Epilepsy Behav.* **5,** 343–347 (2004).

200. Sun, P., Liu, Z., Krueger, D. & Kohrman, M. Direct medical costs for patients with tuberous sclerosis complex and surgical resection of subependymal giant cell astrocytoma : a US national cohort study. *J. Med. Econ.* **18,** 349–356 (2015).

201. Fallah, A. *et al.* Cost-utility analysis of competing treatment strategies for drug-resistant epilepsy in children with Tuberous Sclerosis Complex. *Epilepsy Behav.* **63,** 79–88 (2016).

202. Arya, R. *et al.* Long-term outcomes of ressective epilepsy surgery after invasive presurgical evaluation in children with tuberous sclerosis complex and bilateral multiple lesions. *J. Neurosurg. Pediatr.* **15,** 26–33 (2015).

203. Spencer, S. & Huh, L. Outcomes of epilepsy surgery in adults and children. *Lancet Neurol.* **7,** 525–537 (2008).

204. Baud, M. O. *et al.* European trends in epilepsy surgery. *Neurology* **91,** 96–106 (2018).

205. de Vries, P. J. & Howe, C. J. The tuberous sclerosis complex proteins- a GRIPP on cognition and neurodevelopment. *Trends Mol. Med.* **13,** 319–326 (2007).

206. Jones, A. C. *et al.* Comprehensive Mutation Analysis of TSC1 and TSC2- and Phenotypic Correlations in 150 Families with Tuberous Sclerosis. *Am. J. Hum. Genet.* **64,** 1305–1315 (1999).

207. Dabora, S. L. *et al.* Mutational Analysis in a Cohort of 224 Tuberous Sclerosis Patients Indicates Increased Severity of TSC2, Compared with TSC1, Disease in Multiple Organs. *Am. J. Hum. Genet.* **68,** 64–80 (2001).

208. Rok, P., Kasprzyk-Obara, J., Domanska-Pakiela, D. & Jozwiak, S. Clinical symptoms of tuberous sclerosis complex in patients with an identical TSC2 mutation. *Med Sci Monit* **11,** CR230-234 (2005).

209. Meikle, L. *et al.* A Mouse Model of Tuberous Sclerosis: Neuronal Loss of Tsc1 Causes Dysplastic and Ectopic Neurons, Reduced Myelination, Seizure Activity, and Limited Survival. *J. Neurosci.* **27,** 5546–5558 (2007).

210. Fernandez, L. C., Torres, M. & Real, F. X. Somatic mosaicism: on the road to cancer. *Nat. Rev. Cancer* **16,** 43–55 (2016).

211. Rohlin, A. *et al.* Parallel Sequencing Used in Detection of Mosaic Mutations: Comparison With Four Diagnostic DNA. *Hum. Mutat.* **30,** 1012–1020 (2009).

212. Liu, Q. *et al.* Quick Genetic Screening Using Targeted Next-Generation Sequencing in Patients With Tuberous Sclerosis. *J. Child Neurol.* **30,** 610–614 (2015).

213. Tyburczy, M. E. *et al.* Mosaic and Intronic Mutations in TSC1/TSC2 Explain the Majority of TSC Patients with No Mutation Identified by Conventional Testing. *PLoS Genet.* **11,** 1–17 (2015).

214. Eeghen, A. M. Van, Black, M. E., Pulsifer, M. B., Kwiatkowski, D. J. & Thiele, E. A. Genotype and cognitive phenotype of patients with tuberous sclerosis complex. *Eur. J. Hum. Genet.* **20,** 510–515 (2011).

215. Cheadle, J. P., Reeve, M. P., Sampson, J. R. & Kwiatkowski, D. J. Molecular genetic advances in tuberous sclerosis. *Hum. Genet.* **107,** 97–114 (2000).

216. Sancak, O. *et al.* Mutational analysis of the TSC1 and TSC2 genes in a diagnostic setting: genotype- phenotype correlations and comparison of diagnostic DNA techniques in Tuberous Sclerosis Complex. *Eur. J. Hum. Genet.* **13,** 731–741 (2005).

217. Lee, J. S. *et al.* Mutational analysis of paediatric patients with tuberous sclerosis complex in Korea: genotype and epilepsy. *Epileptic Disord.* **16,** 449–455 (2014).

218. Eeghen, A. M. Van, Nellist, M., Eeghen, E. E. Van & Thiele, E. A. Central TSC2 missense mutations are associated with a reduced risk of infantile spasms. *Epilepsy Res.* **103,** 83–87 (2013).

219. Kothare, S. V *et al.* Severity of manifestations in tuberous sclerosis complex in relation to genotype. *Epilepsia* **55,** 1025–1029 (2014).

220. Lyczkowski, D. A. *et al.* Intrafamilial phenotypic variability in tuberous sclerosis complex. *J Child Neurol* **22,** 1348–1355 (2007).

221. Overwater, I. E. *et al.* Genotype and brain pathology phenotype in children with tuberous sclerosis complex. *Eur. J. Hum. Genet.* **24,** 1688–1695 (2016).

222. Lyczkowski, D. A. *et al.* Intrafamilial Phenotypic Variability in Tuberous Sclerosis Complex. *J. Child Neurol.* **22,** 1348–1355 (2007).

223. Ryland, G. L. *et al.* Loss of heterozygosity: what is it good for? *BMC Med. Genomics* **8,** 45 (2015).

224. Henske, E. P. *et al.* Allelic Loss Is Frequent in Tuberous Sclerosis Kidney Lesions but Rare in Brain Lesions. *Am. J. Hum. Genet.* **59,** 400–406 (1996).

225. Au, K.-S., Herbert, A. A., Roach, E. S. & Northrup, H. Complete Inactivation of the TSC2 Gene Leads to Formation of Hamartomas. *Am. J. Hum. Genet.* **65,** 1790–1794 (1999).

226. Karbowniczek, M., Yu, J. & Henske, E. P. Renal Angiomyolipomas from Patients with Sporadic Lymphangiomyomatosis Contain Both Neoplastic and Non-Neoplastic Vascular Structures. *Am. J. Pathol.* **162,** 491–500 (2003).

227. Smolarek, T. A. *et al.* Evidence That Lymphangiomyomatosis Is Caused by TSC2 Mutations: Chromosome 16p13 Loss of Heterozygosity in Angiomyolipomas and Lymph Nodes from Women with Lymphangiomyomatosis. *Am. J. Hum. Genet.* **62,** 810–815 (1998).

228. Boer, K. *et al.* Clinicopathological and immunohistochemical findings in an autopsy case of

tuberous sclerosis complex. *Neuropathology* **28,** 577–590 (2008).

229. Patil, V. V *et al.* Activation of extracellular regulated kinase and mechanistic target of rapamycin pathway in focal cortical dysplasia. *Neuropathology* **36,** 146–156 (2015).

230. Crino, P. B., Aronica, E., Baltuch, G. & Nathanson, K. L. Biallelic TSC gene inactivation in tuberous sclerosis complex. *Neurology* **74,** 1716–1723 (2010).

231. Ma, L., Chen, Z., Erdjument-Bromage, H., Tempst, P. & Pandolfi, P. P. Phosphorylation and functional inactivation of TSC2 by Erk implications for tuberous sclerosis and cancer pathogenesis. *Cell* **121,** 179–93 (2005).

232. Waltereit, R. *et al.* Enhanced episodic-like memory and kindling epilepsy in a rat model of tuberous sclerosis. *J. Neurochem.* **96,** 407–413 (2006).

233. Kirschstein, T. & Kohling, R. Animal models of tumour-associated epilepsy. *J. Neurosci. Methods* **260,** 109–117 (2015).

234. Rentz, A. M. *et al.* Tuberous Sclerosis Complex: A Survey of Health Care Resource Use and Health Burden. *Pediatr. Neurol.* **52,** 435–441 (2015).

235. Krymskaya, V. P. Tumour suppressors hamartin and tuberin: intracellular signalling. *Cell. Signal.* **15,** 729–739 (2003).

236. Huang, J. & Manning, B. D. The TSC1- TSC2 complex: a molecular switchboard controlling cell growth. *Biochem. J.* **412,** 179–190 (2008).

237. Hoogeveen-Westerveld, M. *et al.* Analysis of TSC1 truncations de fi nes regions involved in TSC1 stability, aggregation and interaction. *Biochim. Biophys. Acta- Mol. Basis Dis.* **1802,** 774–781 (2010).

238. Hodges, A. K. *et al.* Pathological mutations in TSC1 and TSC2 disrupt the interaction between hamartin and tuberin. *Hum. Mol. Genet.* **10,** 2899–2906 (2001).

239. Qin, J. *et al.* Structural Basis of the Interaction between Tuberous Sclerosis Complex 1 (TSC1) and Tre2-Bub2-Cdc16 Domain Family Member 7 (TBC1D7) *. *J. Biol. Chem.* **291,** 8591–8601 (2016).

240. Lima, A. J. S. *et al.* Identification of Regions Critical for the Integrity of the TSC1-TSC2-TBC1D7 Complex. *PLoS One* **9,** 1–13 (2014).

241. Benvenuto, G. *et al.* The tuberous sclerosis-1 (TSC1) gene product hamartin suppresses cell growth and augments the expression of the TSC2 product tuberin by inhibiting its ubiquitination. *Oncogene* **19,** 6306–6316 (2000).

242. Chong-Kopera, H. *et al.* TSC1 Stabilizes TSC2 by Inhibiting the Interaction between TSC2 and the HERC1. *J. Biol. Chem.* **281,** 8313–8316 (2006).

243. Inoki, K., Zhu, T., Guan, K. & Arbor, A. TSC2 Mediates Cellular Energy Response to Control Cell Growth and Survival. *Cell* **115,** 577–590 (2003).

244. Winter, J. N., Jefferson, L. S. & Kimball, S. R. ERK and Akt signaling pathways function through parallel mechanisms to promote mTORC1 signaling. *Am. J. Physiol. Cell Physiol.* **300,** C1172–C1180 (2011).

245. Dibble, C. C. & Cantley, L. C. Regulation of mTORC1 by PI3K signaling. *Trends Cell Biol.* **25,** 545–555 (2015).

246. Buller, C. L. *et al.* A GSK-3/TSC2/mTOR pathway regulates glucose uptake and GLUT1 glucose transporter expression. *Am. J. Cell Physiol.* **295,** 836–843 (2018).

247. Nellist, M. *et al.* Identification and Characterization of the Interaction between Tuberin and 14-3-3. *J. Biol. Chem.* **277,** 39417–39424 (2002).

248. Morrison, D. K. The 14-3-3 proteins: integrators of diverse signaling cues that impact cell fate and cancer development. *Trends Cell Biol.* **19,** 16–23 (2008).

249. Li, Y., Inoki, K., Yeung, R. & Guan, K.-L. Regulation of TSC2 by 14-3-3 Binding. *J. Biol. Chem.* **277,** 44593–44596 (2002).

250. Maheshwar, M. M. *et al.* The GAP-related domain of tuberin, the product of the TSC2 gene, is a target for missense mutations in tuberous sclerosis. *Hum. Mol. Genet.* **6,** 1991–1996 (1997).

251. Inoki, K., Li, Y., Xu, T. & Guan, K. Rheb GTPase is a direct target of TSC2 GAP activity and regulates mTOR signaling. *Genes Dev.* **17,** 1829–1834 (2003).

252. Li, Y., Inoki, K. & Guan, K. Biochemical and Functional Characterizations of Small GTPase Rheb and TSC2 GAP Activity. *Mol. Cell. Biol.* **24,** 7965–7975 (2004).

253. Zhang, Y. *et al.* Rheb is a direct target of the tuberous sclerosis tumour suppressor proteins. *Nat. Cell Biol.* **5,** 578–582 (2003).

254. Jacobs, B. L. *et al.* Identification of mechanically regulated phosphorylation sites on tuberin (TSC2) that control mechanistic target of rapamycin (mTOR) signaling. *J. Biol. Chem.* **292,** 6987–6997 (2017).

255. Mozaffari, M. *et al.* Identification of a region required for TSC1 stability by functional analysis of TSC1 missense mutations found in individuals with tuberous sclerosis complex. *BMC Med. Genet.* **10,** 1–12 (2009).

256. Xu, L. *et al.* Alternative Splicing to the Tuberous Sclerosis 2 (TSC2) Gene in Human and Mouse Tissues. *Genomics* **27,** 475–480 (1995).

257. Dibble, C. C. *et al.* TBC1D7 Is a Third Subunit of the TSC1-TSC2 Complex Upstream of mTORC1. *Mol. Cell* **47,** 535–546 (2012).

258. Gai, Z. *et al.* Structure of the TBC1D7–TSC1 complex reveals that TBC1D7 stabilizes dimerization of the TSC1 C-terminal coiled coil region. *J. Mol. Cell Biol.* **8,** 411–425 (2016).

259. Hoogeveen-Westerveld, M. *et al.* The TSC1-TSC2 complex consists of multiple TSC1 and TSC2 subunits. *BMC Biochem.* **13,** 1–8 (2012).

260. Capo-Chichi, J.-M. *et al.* Disruption of TBC1D7 , a subunit of the TSC1-TSC2 protein complex, in intellectual disability and megalencephaly. *J. Med. Genet.* **50,** 740–744 (2013).

261. Neuman, N. A. & Henske, E. P. Non-canonical functions of the tuberous sclerosis complex-Rheb signalling axis. *EMBO Mol. Med.* **3,** 189–200 (2011).

262. Brugarolas, J. B., Vazquez, F., Reddy, A., Sellers, W. R. & Kaelin, W. G. TSC2 regulates VEGF through mTOR-dependent and -independent pathways. *Cancer Cell* **4,** 147–158 (2003).

263. Hartman, T. R. *et al.* The tuberous sclerosis proteins regulate formation of the primary cilium via a rapamycin-insensitive and polycystin 1-independent pathway. *Hum. Mol. Genet.*

18, 151–163 (2009).

264. Alves, M. M. *et al.* PAK2 is an effector of TSC1/2 signaling independent of mTOR and a potential therapeutic target for Tuberous Sclerosis Complex. *Sci. Rep.* **5,** 1–12 (2015).

265. Bartolome, A. & Guillen, C. *Role of the Mammalian Target of Rapamycin (mTOR) Complexes in Pancreatic B-Cell Mass Regulation*. **95,** (2014).

266. Tee, A. R. *et al.* Tuberous sclerosis complex-1 and -2 gene products function together to inhibit mammalian target of rapamycin (mTOR)-mediated downstream signaling. *Proc. Natl. Acad. Sci.* **99,** 13571–13576 (2002).

267. Menon, S. *et al.* Spatial control of the TSC complex integrates insulin and nutrient regulation of mTORC1 at the lysosome. *Cell* **156,** 771–785 (2014).

268. Inoki, K., Li, Y., Zhu, T., Wu, J. & Guan, K. TSC2 is phosphorylated and inhibited by Akt and suppresses mTOR signalling. *Nat. Cell Biol.* **4,** 648–657 (2002).

269. Knut & Alice Wallenberg foundation. TSC1. *The Human Protein Atlas* Available at: https://www.proteinatlas.org/ENSG00000165699-TSC1/tissue.

270. Knut & Alice Wallenberg foundation. TSC2. *The Human Protein Atlas* Available at: https://www.proteinatlas.org/ENSG00000103197-TSC2/tissue.

271. Lee, H. Phosphorylated mTOR Expression Profiles in Human Normal and Carcinoma Tissues. *Dis. Markers* **2017,** 1–8 (2017).

272. Johnson, M. W., Kerfoot, C., Bushnell, T., Li, M. & Vinters, H. V. Hamartin and Tuberin Expression in Human Tissues. *Mod. Pathol.* **14,** 202–210 (2011).

273. Plank, T. L., Yeung, R. S. & Henske, E. P. Advances in Brief Hiimartin, the Product of the Tuberous Sclerosis 1 (TSC1) Gene, Interacts with Tuberin and Appears to Be Localized to Cytoplasmic Vesicles. *Cancer Res.* **58,** 4766–4770 (1998).

274. Carroll, B. *et al.* Control of TSC2-Rheb signaling axis by arginine regulates mTORC1 activity. *Elife* **1,** 1–23 (2016).

275. Demetriades, C., Plescher, M. & Teleman, A. A. Lysosomal recruitment of TSC2 is a universal response to cellular stress. *Nat. Commun.* **7,** 1–14 (2016).

276. Gao, X. *et al.* Tsc tumour suppressor proteins antagonize amino-acid-TOR signalling. *Nat. Cell Biol.* **4,** 699–704 (2003).

277. Montagne, J. *et al.* Drosophila S6 Kinase: A Regulator of Cell Size. *Science (80-.).* **24,** 2126–2129 (1999).

278. Kwiatkowski, D. J. *et al.* A mouse model of TSC1 reveals sex-dependent lethality from liver hemangiomas , and up-regulation of p70S6 kinase activity in Tsc1 null cells. *Hum. Mol. Genet.* **11,** 525–534 (2002).

279. Kobayashi, T., Hirayama, Y., Kobayashi, E., Kubo, Y. & Hino, O. A germline insertion in the tuberous sclerosis (Tsc2) gene gives rise to the Eker rat model of dominantly inherited cancer. *Nat. Genet.* **9,** 70–74 (1995).

280. Everitt, J. I., Goldsworthy, T. L., Wolf, D. C. & Walker, C. L. Hereditary Renal Cell Carcinoma in the Eker Rat: A Rodent Familial Cancer Syndrome. *J. Urol.* **148,** 1932–1936 (1992).

281. Kobayashi, T. *et al.* Renal Carcinogenesis, Hepatic Hemangiomatosis, and Embryonic Lethality Caused by a Germ-Line Tsc2 Mutation in Mice. *Cancer Res.* **59,** 1206–1211 (1999).

282. Kenerson, H. L., Aicher, L. D., True, L. D. & Yeung, R. S. Activated Mammalian Target of Rapamycin Pathway in the Pathogenesis of Tuberous Sclerosis Complex Renal Tumors. *Cancer Res.* **62,** 5645–5650 (2002).

283. Betz, C. & Hall, M. N. Where is mTOR and what is it doing there? *J. Cell Biol.* **203,** 563–574 (2013).

284. Sancak, Y., Bar-Peled, L., Zoncu, R., Markhard, A. L. & Nada, S. Ragulator-Rag Complex Targets mTORC1 to the Lysosomal Surface and Is Necessary for Its Activation by Amino Acids. *Cell* **141,** 290–303 (2010).

285. Demetriades, C., Doumpas, N. & Teleman, A. A. Regulation of TORC1 in Response to Amino Acid Starvation via Lysosomal Recruitment of TSC2. *Cell* **156,** 786–799 (2014).

286. Tee, A. R., Manning, B. D., Roux, P. P., Cantley, L. C. & Blenis, J. Tuberous Sclerosis Complex Gene Products , Tuberin and Hamartin , Control mTOR Signaling by Acting as a GTPase-Activating Protein Complex toward Rheb. *Curr. Biol.* **13,** 1259–1268 (2003).

287. Rosner, M., Freilinger, A. & Hengstschla, M. Akt regulates nuclear/cytoplasmic localization of tuberin. *Oncogene* **26,** 521–531 (2007).

288. Long, X., Lin, Y., Ortiz-vega, S., Yonezawa, K. & Avruch, J. Rheb Binds and Regulates the mTOR Kinase. *Curr. Biol.* **15,** 702–713 (2005).

289. Swiech, L., Perycz, M., Malik, A. & Jaworski, J. Role of mTOR in physiology and pathology of the nervous system. *Biochim. Biophys. Acta - Proteins Proteomics* **1784,** 116–132 (2008).

290. Schreiber, K. H. *et al.* Rapamycin-mediated mTORC2 inhibition is determined by the relative expression of FK506-binding proteins. *Aging Cell* **14,** 265–273 (2015).

291. Sarbassov, D. D. *et al.* Prolonged Rapamycin Treatment Inhibits mTORC2 Assembly and Akt / PKB. *Mol. Cell* **22,** 159–168 (2006).

292. Tee, A. R., Sampson, J. R., Pal, D. K. & Bateman, J. M. The role of mTOR signalling in neurogenesis, insights from tuberous sclerosis complex. *Semin. Cell Dev. Biol.* **52,** 12–20 (2016).

293. Heras-Sandoval, D., Pérez-Rojas, J. M., Hernández-Damián, J. & Pedraza-Chaverri, J. The role of PI3K/AKT/mTOR pathway in the modulation of autophagy and the clearance of protein aggregates in neurodegeneration. *Cell. Signal.* **26,** 2694–701 (2014).

294. Iwata, T. N. *et al.* Conditional Disruption of Raptor Reveals an Essential Role for mTORC1 in B Cell Development, Survival, and Metabolism. *J. Immunol.* **197,** 2250–2260 (2016).

295. Guertin, D. A. *et al.* Ablation in Mice of the mTORC Components raptor, rictor, or mLST8 Reveals that mTORC2 Is Required for Signaling to Akt-FOXO and PKCa, but Not S6K1. *Dev. Cell* **11,** 859–871 (2006).

296. Wullschleger, S., Loewith, R. & Hall, M. N. TOR Signaling in Growth and Metabolism. *Cell* **124,** 471–484 (2006).

297. Kim, D. *et al.* GBL, a Positive Regulator of the Rapamycin-Sensitive Pathway Required for the Nutrient-Sensitive Interaction between Raptor and mTOR. *Mol. Cell* **11,** 895–904

(2003).

298. Kakumoto, K., Ikeda, J., Okada, M., Morii, E. & Oneyama, C. mLST8 Promotes mTOR-Mediated Tumor Progression. *PLoS One* **10,** 1–15 (2015).

299. Yang, G., Murashige, D. S., Humphrey, S. J. & James, D. E. A Positive Feedback Loop between Akt and mTORC2 via SIN1 Phosphorylation. *Cell Rep.* **12,** 937–943 (2015).

300. Catena, V. & Fanciulli, M. Deptor: not only a mTOR inhibitor. *J. Exp. Clin. Cancer Res.* **36,** 1–9 (2017).

301. Wiza, C., Nascimento, E. B. M. & Ouwens, D. M. Role of PRAS40 in Akt and mTOR signaling in health and disease. *Am. J. Physiol. Endocrinol. Metab.* **302,** 1453–1460 (2018).

302. Huang, J. & Manning, B. A complex interplay between Akt,TSC2 and the two mTOR complexes. *Biochem Soc Trans* **37,** 217–222 (2010).

303. Bhaskar, P. T. & Hay, N. The Two TORCs and Akt. *Dev. Cell* **12,** 487–502 (2007).

304. Ruvinsky, I. & Meyuhas, O. Ribosomal protein S6 phosphorylation: from protein synthesis to cell size. *Trends Biochem. Sci.* **31,** 342–348 (2006).

305. Puighermanal, E. *et al.* Ribosomal Protein S6 Phosphorylation Is Involved in Novelty-Induced Locomotion, Synaptic Plasticity and mRNA Translation. *Front. Mol. Neurosci.* **10,** 1–16 (2017).

306. Biever, A., Valjent, E. & Puighermanal, E. Ribosomal Protein S6 Phosphorylation in the Nervous System: From Regulation to Function. *Front. Mol. Neurosci.* **8,** 1–14 (2015).

307. Duvel, K. *et al.* Article Activation of a Metabolic Gene Regulatory Network Downstream of mTOR Complex 1. *Mol. Cell* **39,** 171–183 (2010).

308. Showkat, M., Beigh, M. A. & Andrabi, K. I. mTOR Signaling in Protein Translation Regulation: Implications in Cancer Genesis and Therapeutic Interventions. *Mol. Biol. Int.* **2014,** 1–14 (2014).

309. Magri, L. *et al.* Timing of mTOR activation affects tuberous sclerosis complex neuropathology in mouse models. *Dis. Model. Mech.* **6,** 1185–1197 (2013).

310. Way, S. W. *et al.* Loss of Tsc2 in radial glia models the brain pathology of tuberous sclerosis complex in the mouse. *Hum. Mol. Genet.* **18,** 1252–1265 (2009).

311. Sherman, D. L. *et al.* Arrest of Myelination and Reduced Axon Growth when Schwann Cells Lack mTOR. *J. Neurosci.* **32,** 1817–1825 (2015).

312. Choi, Y. *et al.* Tuberous sclerosis complex proteins control axon formation. *Genes Dev.* **22,** 2485–2495 (2008).

313. Tavazoie, S. F., Alvarez, V. a, Ridenour, D. a, Kwiatkowski, D. J. & Sabatini, B. L. Regulation of neuronal morphology and function by the tumor suppressors Tsc1 and Tsc2. *Nat. Neurosci.* **8,** 1727–1734 (2005).

314. Porstmann, T. *et al.* Article SREBP Activity Is Regulated by mTORC1 and Contributes to Akt-Dependent Cell Growth. *Cell Metab.* **8,** 224–236 (2008).

315. Kafri, M., Metzl-Raz, E., Jona, G. & Barkai, N. The Cost of Protein Production. *Cell Rep.* **14,** 22–31 (2016).

316. Kosillo, P. *et al.* Tsc1-mTOR signaling controls the structure and function of midbrain

dopamine neurons. 1–68 (2018). doi:doi.org/10.1101/376814

317. Uhlmann, E. J. *et al.* Astrocyte-specific TSC1 conditional knockout mice exhibit abnormal neuronal organization and seizures. *Ann. Neurol.* **52,** 285–296 (2002).

318. Sosunov, A. A. *et al.* Tuberous sclerosis: A primary pathology of astrocytes? *Epilepsia* **49,** 53–62 (2008).

319. Liddelow, S. A. & Barres, B. A. Reactive Astrocytes: Production, Function, and Therapeutic Potential. *Immunity* **46,** 957–967 (2017).

320. Robertson, J. M. Astrocytes and the evolution of the human brain. *Med. Hypotheses* **82,** 236–239 (2014).

321. Colombo, E. & Farina, C. Astrocytes: Key Regulators of Neuroinflammation. *Trends Immunol.* **37,** 608–620 (2016).

322. Zhang, Y. *et al.* Neuronal mTORC1 Is Required for Maintaining the Nonreactive State of Astrocytes. *J. Biol. Chem.* **292,** 100–111 (2017).

323. Guerrini, R. & Parrini, E. Neuronal migration disorders. *Neurobiol. Dis.* **38,** 154–166 (2010).

324. Tsai, P. T. *et al.* Autistic-like behaviour and cerebellar dysfunction in Purkinje cell Tsc1 mutant mice. *Nature* **488,** 647–651 (2012).

325. Costa, V. *et al.* mTORC1 Inhibition Corrects Neurodevelopmental and Synaptic Alterations in a Human Stem Cell Model of Tuberous Sclerosis Report mTORC1 Inhibition Corrects Neurodevelopmental and Synaptic Alterations in a Human Stem Cell Model of Tuberous Sclerosis. *Cell Rep.* **15,** 86–95 (2016).

326. Talos, D. M. *et al.* Altered inhibition of Tuberous Sclerosis and Type IIb cortical dysplasia. *Ann. Neurol.* **71,** 539–551 (2012).

327. Kim, S.-H., Speirs, C. K., Solnica-Krezel, L. & Ess, K. C. Zebrafish model of tuberous sclerosis complex reveals cell-autonomous and non-cell-autonomous functions of mutant tuberin. *Dis. Model. Mech.* **4,** 255–267 (2011).

328. Rennebeck, G. *et al.* Loss of function of the tuberous sclerosis 2 tumor suppressor gene results in embryonic lethality characterized by disrupted neuroepithelial growth and development. *Proc. Natl. Acad. Sci.* **95,** 15629–15634 (1998).

329. Onda, H., Lueck, A., Marks, P. W., Warren, H. B. & Kwiatkowski, D. J. Tsc2(+/-) mice develop tumors in multiple sites that express gelsolin and are influenced by genetic background. *J. Clin. Invest.* **104,** 687–695 (1999).

330. Goorden, S. M. I., Woerden, G. M. Van, Weerd, L. Van Der, Cheadle, J. P. & Elgersma, Y. Cognitive Deficits in Tsc1+/- Mice in the Absence of Cerebral Lesions and Seizures. *Ann. Clin. Psychiatry* **62,** 648–655 (2007).

331. Feliciano, D. M., Su, T., Lopez, J., Platel, J.-C. & Bordey, A. Single-cell Tsc1 knockout during corticogenesis generates tuber-like lesions and reduces seizure threshold in mice. *J. Clin. Invest.* **121,** 1596–1607 (2011).

332. Kobayashi, T. *et al.* Renal Carcinogenesis, Hepatic Hemangiomatosis, and Embryonic Lethality Caused by a Germ-Line Tsc2 Mutation in Mice. *Cancer Res.* **59,** 1206 LP-1211 (1999).

333. Reith, R. M. *et al.* Loss of Tsc2 in Purkinje cells is associated with autistic-like behavior in a mouse model of tuberous sclerosis complex. *Neurobiol. Dis.* **51,** 93–103 (2013).

334. Reith, R. M., Way, S., Iii, J. M., Haines, K. & Gambello, M. J. Loss of the tuberous sclerosis complex protein tuberin causes Purkinje cell degeneration. *Neurobiol. Dis.* **43,** 113–122 (2011).

335. Ehninger, D. *et al.* Reversal of learning deficits in a Tsc2+/- mouse model of tuberous sclerosis. *Nat. Med.* **14,** 843–848 (2009).

336. Sola, L. & Gornung, E. Classical and molecular cytogenetics of the zebrafish, Danio rerio (Cyprinidae, Cypriniformes): an overview. *Genetica* **111,** 397–412 (2001).

337. Kalueff, A. V., Stewart, A. M. & Gerlai, R. Zebrafish as an emerging model for studying complex brain disorders. *Trends Pharmacol. Sci.* **35,** 63–75 (2014).

338. Bradbury, J. Small fish, big science. *PLoS Biol.* **2,** 568–572 (2004).

339. Streisinger, G., Walker, C., Dower, N., Knauber, D. & Singer, F. Production of clones of homozygous diploid zebra fish (Brachydanio rerio). *Nature* **291,** 293–296 (1981).

340. Grunwald, D. J. & Eisen, J. S. Headwaters of the zebrafish- emergence of a new model vertebrate. *Nat. Rev. Genet.* **3,** 717–724 (2002).

341. Howe, K. *et al.* The zebrafish reference genome sequence and its relationship to the human genome. *Nature* **496,** 498–503 (2013).

342. Kim, S.-H., Kowalski, M. L., Carson, R. P., Bridges, L. R. & Ess, K. C. Heterozygous inactivation of tsc2 enhances tumorigenesis in p53 mutant zebrafish. *Dis. Model. Mech.* **6,** 925–33 (2013).

343. Link, B. A. & Megason, S. G. in *Sourcebook of Models for Biomedical Research* (ed. Conn, P. M.) 103–112 (Humana Press, 2008). doi:10.1007/978-1-59745-285-4_13

344. Hortopan, G. A., Dinday, M. T. & Baraban, S. C. Zebrafish as a model for studying genetic aspects of epilepsy. *Dis. Model. Mech.* **3,** 144–148 (2010).

345. Crosby, E. B., Bailey, J. M., Oliveri, A. N. & Levin, E. D. Neurobehavioral impairments caused by developmental imidacloprid exposure in zebrafish. *Neurotoxicol. Teratol.* **49,** 81–90 (2015).

346. Crawford, A. D., Esguerra, C. V. & De Witte, P. A. M. Fishing for drugs from nature: Zebrafish as a technology platform for natural product discovery. *Planta Med.* **74,** 624–632 (2008).

347. Steenbergen, P. J., Richardson, M. K. & Champagne, D. L. Patterns of avoidance behaviours in the light/dark preference test in young juvenile zebrafis : A pharmacological study. *Behav. Brain Res.* **222,** 15–25 (2011).

348. Meyer, A. & Schartl, M. Gene and genome duplication in vertebrates: the one-to-four (-to-eight in fish) rule and the evolution of novel gene functions. *Curr. Opin. Cell Biol.* **11,** 699–704 (1999).

349. Sourbron, J. *et al.* Serotonergic Modulation as Effective Treatment for Dravet syndrome in a Zebrafish Mutant Model. *ACS Chem. Neurosci.* **7,** 588–598 (2016).

350. Dibella, L. M., Park, A. & Sun, Z. Zebrafish Tsc1 reveals functional interactions between the cilium and the TOR pathway. *Hum. Mol. Genet.* **18,** 595–606 (2009).

351. Kingswood, J. C. *et al.* The economic burden of tuberous sclerosis complex in UK patients with renal manifestations: a retrospective cohort study in the clinical practice research datalink (CPRD). *J. Med. Econ.* **19,** 1116–1126 (2016).

352. Wienecke, R., Konig, A. & DeClue, J. E. Identification of Tuberin, the Tuberous Sclerosis-2 Product. *J. Biol. Chem.* **270,** 16409–16414 (1995).

353. Zeng, L.-H. *et al.* Tsc2 gene inactivation causes a more severe epilepsy phenotype than Tsc1 inactivation in a mouse model of Tuberous Sclerosis Complex. *Hum. Mol. Genet.* **20,** 445–454 (2011).

354. Scheldeman, C. *et al.* mTOR-related neuropathology in mutant tsc2 zebrafish : Phenotypic , transcriptomic and pharmacological analysis. *Neurobiol. Dis.* **108,** 225–237 (2017).

355. Eker, R. Familial renal adenomas in Wistar rats: A Preliminary Report. *Acta Pathol. Microbiol. Scand.* **34,** 554–562 (1954).

356. Yeung, R. S. *et al.* Predisposition to renal carcinoma in the Eker rat is determined by germ-line mutation of the tuberous sclerosis 2 (TSC2) gene. *Proc. Natl. Acad. Sci. U. S. A.* **91,** 11413–6 (1994).

357. Hino, O. & Kobayashi, T. Mourning Dr. Alfred G. Knudson: the two-hit hypothesis, tumour supressor genes, and tuberous sclerosis complex. *Cancer Sci.* **108,** 5–11 (2017).

358. Knudson, A. G. Mutation and cancer: statistical study of retinoblastoma. *Proc. Natl. Acad. Sci.* **68,** 820–823 (1971).

359. Hino, O. *et al.* Spontaneous and radiation-induced renal tumors in the Eker rat model of dominantly inherited cancer. *Proc. Natl. Acad. Sci.* **90,** 327–331 (1993).

360. Yeung, R. S., Buetow, K. H., Testa, J. R. & Knudson, A. G. Susceptibility to renal carcinoma in the Eker rat involves a tumor suppressor gene on chromosome 10. *Proc. Natl. Acad. Sci.* **90,** 8038–8042 (1993).

361. Kobayashi, T., Hirayama, Y., Kobayashi, E., Kudo, Y. & Hino, O. A germline insertion in the tuberous sclerosis (Tsc2) gene gives rise to the Eker rat model of dominantly inherited cancer. *Nat. Genet.* **9,** 70–74 (1995).

362. Kenerson, H., Dundon, T. a & Yeung, R. S. Effects of Rapamycin in the Eker Rat Model of Tuberous Sclerosis Complex. *Pediatr. Res.* **57,** 67–75 (2005).

363. Amin, S. *et al.* Causes of mortality in individuals with tuberous sclerosis complex. *Dev. Med. Child Neurol.* **59,** 612–617 (2017).

364. Yeung, R. S., Katsetos, C. D. & Klein-Szanto, A. Subependymal Astrocytic Hamartomas in the Eker Rat Model of Tuberous Sclerosis. *Am. J. Physiol. Endocrinol. Metab.* **151,** 1477–1486 (1997).

365. Mizuguchi, M. *et al.* Novel Cerebral Lesions in the Eker Rat Model of Tuberous Sclerosis: Cortical Tuber and Anaplastic Ganglioglioma. *J. Neuropathol. Exp. Neurol.* **59,** 188–196 (2000).

366. Takahashi, D. K., Dinday, M. T., Barbaro, N. M. & Baraban, S. C. Abnormal cortical cells and astrocytomas in the Eker rat model of tuberous sclerosis complex. *Epilepsia* **45,** 1525–1530 (2004).

367. Mizuguchi, M. *et al.* Novel Cerebral Lesions in the Eker Rat Model of Tuberous Sclerosis: Cortical Tuber and Anaplastic Ganglioglioma. *J. Neuropathol. Exp. Neurol.* **59,** 188–196

(2000).

368. Jentsch, T. J., Stein, V., Weinreich, F. & Zdebik, A. A. Molecular Structure and Physiological Function of Chloride Channels. *Physiol. Rev.* **82,** 503–568 (2002).

369. Huang, R.-Q. *et al.* Pentylenetetrazole-Induced Inhibition of Recombinant Gamma-Aminobutyric Acid Type A (GABA A) Receptor: Mechanism and Site of Action. *J. Pharmacol. Exp. Ther.* **298,** 986–995 (2001).

370. Waltereit, R., Japs, B., Schneider, M., de Vries, P. J. & Bartsch, D. Epilepsy and Tsc2 haploinsufficiency lead to autistic-like social deficit behaviors in rats. *Behav. Genet.* **41,** 364–72 (2011).

371. Schneider, M., de Vries, P. J., Schönig, K., Rößner, V. & Waltereit, R. mTOR inhibitor reverses autistic-like social deficit behaviours in adult rats with both Tsc2 haploinsufficiency and developmental status epilepticus. *Eur. Arch. Psychiatry Clin. Neurosci.* **267,** 455–463 (2017).

372. Song, X. *et al.* Natural history of patients with tuberous sclerosis complex related renal angiomyolipoma. *Curr. Med. Res. Opin.* **33,** 1277–1282 (2017).

373. Farag, S. & Kayser, O. *Chapter 1- The Cannabis Plant: Botanical Aspects*. *Handbook of Cannabis and Related Pathologies* (Elsevier Inc., 2017). doi:10.1016/B978-0-12-800756-3/00001-6

374. Devinsky, O. *et al.* Cannabidiol: Pharmacology and potential therapeutic role in epilepsy and other neuropsychiatric disorders. *Epilepsia* **55,** 791–802 (2014).

375. Watts, G. Science commentary: Cannabis confusions. *BMJ* **332,** 175–176 (2006).

376. Thomas, B. F. & ElSohly, M. A. in *The Analytical Chemistry of Cannabis* 1–26 (Elsevier, 2016). doi:10.1016/B978-0-12-804646-3.00001-1

377. Hilling, K. W. & Mahlberg, P. G. A Chemotaxic Analysis of Cannabinoid Variation in Cannabis (Cannabaceae). *Am. J. Bot.* **91,** 966–975 (2004).

378. Pollio, A. The Name of Cannabis: A Short Guide for Nonbotanists. *Cannabis Cannabinoid Res.* **1,** 234–238 (2016).

379. Pain, S. A potted history. *Nature* **525,** 5–6 (2015).

380. Szaflarski, J. P. & Martina Bebin, E. Cannabis, cannabidiol, and epilepsy - From receptors to clinical response. *Epilepsy Behav.* **41,** 277–282 (2014).

381. Gertsch, J., Pertwee, R. G. & Di Marzo, V. Phytocannabinoids beyond the Cannabis plant-do they exist? *Br. J. Pharmacol.* **160,** 523–529 (2010).

382. Atakan, Z. Cannabis, a complex plant: different compounds and different effects on individuals. *Ther. Adv. Psychopharmacol.* **2,** 241–254 (2012).

383. Reddy, D. S. & Golub, V. M. The Pharmacological Basis of Cannabis Therapy for Epilepsy. *J. Pharmacol. Exp. Ther.* **357,** 45–55 (2016).

384. Rosenberg, E. C., Tsien, R. W., Whalley, B. J. & Devinsky, O. Cannabinoids and Epilepsy. *Neurotherapeutics* **12,** 747–768 (2015).

385. Costa, M. A., Fonseca, B. M., Marques, F., Teixeira, N. A. & Correia-da-silva, G. The psychoactive compound of Cannabis sativa , D9-tetrahydrocannabinol (THC) inhibits the

human trophoblast cell turnover. *Toxicology* **334,** 94–103 (2015).

386. Gaoni, Y. & Mechoulam, R. Isolation, Structure, and Partial Synthesis of an Active Constituent of Hashish. *J. Am. Chem. Soc.* **86,** 1646–1647 (1964).

387. Lucas, C. J., Galettis, P. & Schneider, J. The Pharmacokinetics and the Pharmacodynamics of Cannabinoids. *Br. J. Clin. Pharmacol.* **12,** (2018).

388. Kumar, R. N., Chambers, W. A. & Pertwee, R. G. Pharmacological actions and therapeutic uses of cannabis and cannabinoids. *Anaesthesia* **56,** 1059–1068 (2001).

389. De Vries, M., Rijckevorsel, D. C. M. Van, Wilder-Smith, O. H. G. & van Goor, H. Dronabinol and chronic pain : importance of mechanistic considerations. *Expert Opin. Pharmacother.* **15,** 1525–1534 (2014).

390. Childs, E., Lutz, J. A. & de Wit, H. Dose-related effects of delta-9-THC on emotional responses to acute psychosocial stress. *Drug Alcohol Depend.* **177,** 136–144 (2017).

391. Malik, Z., Bayman, L., Valestin, J., Hashmi, S. & Schey, R. Dronabinol increases pain threshold in patients with functional chest pain: a pilot double-blind placebo-controlled trial. *Dis. Esophagus* **30,** 1–8 (2016).

392. Kuhlen, M. *et al.* Effective treatment of spasticity using dronabinol in pediatric palliative care. *Eur. J. Paediatr. Neurol.* **20,** 898–903 (2016).

393. Bridgeman, M. B. & Abazia, D. T. Medicinal Cannabis: History, Pharmacology, And Implications for the Acute Care Setting. *Pharm. Ther.* **42,** 180–188 (2017).

394. Issa, M. A. *et al.* The subjective psychoactive effects of oral dronabinol studied in a randomized, controlled crossover clinical trial for pain. *Clin. J. Pain* **30,** 472–478 (2015).

395. Morales, P., Reggio, P. H. & Jagerovic, N. An Overview on Medicinal Chemistry of Synthetic and Natural Derivatives of Cannabidiol. *Front. Pharmacol.* **8,** 1–18 (2017).

396. Ibeas Bih, C. *et al.* Molecular Targets of Cannabidiol in Neurological Disorders. *Neurotherapeutics* **12,** 699–730 (2015).

397. Adams, R., Hunt, M. & Clark, J. H. Structure of Cannabidiol, a Product Isolated from the Marihuana Extract of Minnesota Wild Hemp. I. *J. Am. Chem. Soc.* **62,** 196–200 (1940).

398. Adams, R., Baker, B. . R. & Wearn, R. B. Structure of Cannabinol. III. Synthesis of Cannabinol, 1-Hydroxy-3-n-amyl-6,6,9-trimethyl-6-dibenzopyran. *J. Am. Chem. Soc.* **62,** 2204–2207 (1940).

399. Jacob, A. & Todd, A. R. Cannabidiol and Cannabol, Constituents of Cannabis indica Resin. *Nature* **145,** 350 (1940).

400. Mechoulam, R. & Shvo, Y. Hashish-I- The structure of Cannabidiol. *Tetrahedron* **19,** 2073–2078 (1963).

401. Hanuš, L. O., Meyer, S. M., Munoz, E., Taglialatela-Scafati, O. & Appendino, G. Phytoccanabinoids: a unified critical inventory. *Nat. Prod. Rep.* **33,** 1347–1448 (2016).

402. Devinsky, O. *et al.* Cannabidiol in patients with treatment-resistant epilepsy: an open-label interventional trial. *Lancet. Neurol.* **15,** 270–278 (2016).

403. Hess, E. J. *et al.* Cannabidiol as a new treatment for drug-resistant epilepsy in tuberous sclerosis complex. *Epilepsia* **57,** 1617–1624 (2016).

404. Thiele, E. A. *et al.* Cannabidiol in patients with seizures associated with Lennox-Gastaut syndrome (GWPCARE4): a randomised, double-blind, placebo-controlled phase 3 trial. *Lancet* **391,** 1085–1096 (2018).

405. Fogaca, M. V., de Campos, A. C., Coelho, L. D., Duman, R. S. & Guimarães, F. S. The anxiolytic effects of cannabidiol in chronically stressed mice are mediated by the endocannabinoid system: Role of neurogenesis and dendritic remodeling. *Neuropharmacology* **135,** 22–33 (2018).

406. Sartim, A. G., Sales, A. J., Guimarães, F. S. & Joca, S. R. L. Hippocampal mammalian target of rapamycin is implicated in stress-coping behavior induced by cannabidiol in the forced swim test. *J. Psychopharmacol.* **32,** 922–931 (2018).

407. Crippa, A. S. *et al.* Neural basis of anxiolytic effects of cannabidiol (CBD) in generalized social anxiety disorder: a preliminary report. *J. Psychopharmacol.* **25,** 121–130 (2011).

408. Stevenson, C. C., Campus, S. B. & Le, L. Cannabidiol regulation of emotion and emotional memory processing: relevance for treating anxiety-related and substance abuse disorders. *Br. J. Pharmacol.* **174,** 3242–3256 (2017).

409. Gomes, F. V. *et al.* Decreased glial reactivity could be involved in the antipsychotic-like effect of cannabidiol. *Schizophr. Res.* **164,** 155–163 (2015).

410. Renard, J. *et al.* Cannabidiol Counteracts Amphetamine-Induced Neuronal and Behavioral Sensitization of the Mesolimbic Dopamine Pathway through a Novel mTOR/p70S6 Kinase Signaling Pathway. *J. Neurosci.* **36,** 5160–5169 (2016).

411. Kalenderoglou, N., Macpherson, T. & Wright, K. L. Cannabidiol Reduces Leukemic Cell Size- But Is It Important? *Front. Pharmacol.* **8,** 1–9 (2017).

412. Shrivastava, A., Kuzontkoski, P. M., Groopman, J. E. & Prasad, A. Cannabidiol Induces Programmed Cell Death in Breast Cancer Cells by Coordinating the Cross-talk between Apoptosis and Autophagy. *Mol. Cancer Ther.* **10,** 1161–1172 (2011).

413. Sultan, A. S., Marie, M. A. & Sheweita, S. A. Novel mechanism of cannabidiol-induced apoptosis in breast cancer cell lines. *The Breast* **41,** 34–41 (2018).

414. Elbaz, M. *et al.* Modulation of the tumor microenvironment and inhibition of EGF/EGFR pathway: Novel anti-tumor mechanisms of Cannabidiol in breast cancer. *Mol. Oncol.* **9,** 906–919 (2015).

415. Andre, C. M., Hausman, J. & Guerriero, G. Cannabis sativa: The Plant of the Thousand and One Molecules. *Front. Plant Sci.* **7,** 1–17 (2016).

416. Russo, E. B. Cannabidiol Claims and Misconceptions. *Trends Pharmacol. Sci.* **38,** 198–201 (2017).

417. Merrick, J. *et al.* Identification of Psychoactive Degradants of Cannabidiol in Simulated Gastric and Physiological Fluid. *Canabis Cannabinoid Res.* **1,** 102–112 (2016).

418. Foltz, E. *et al.* An assessment of human gastric fluid composition as a function of PPI usage. *Physiol. Rep.* **3,** 1–13 (2015).

419. Nahler, G., Grotenhermen, F., Zuardi, A. W. & Crippa, J. A. S. A Conversion of Oral Cannabidiol to Delta9-Tetrahydrocannabinol Seems Not to Occur in Humans. *Cannabis Cannabinoid Res.* **2,** 81–86 (2017).

420. Grotenherm, F., Russo, E. & Zuardi, A. W. Even High Doses of Oral Cannabidol Do Not

Cause THC-Like Effects in Humans: Comment on Merrick et al . Cannabis and Cannabinoid Research 2016;1(1):102–112; DOI: 10.1089/can.2015.0004. *Cannabis Cannabinoid Res.* **2,** 1–4 (2017).

421. Hlozek, T. *et al.* Pharmacokinetic and behavioural profile of THC, CBD, and THC + CBD combination after pulmonary, oral, and subcutaneous administration in rats and confirmation of conversion in vivo of CBD to THC. *Eur. Neuropsychopharmacol.* **27,** 1223–1237 (2017).

422. Palazzoli, F. *et al.* Development of a simple and sensitive liquid chromatography triple quadrupole mass spectrometry (LC-MS/MS) method for the determination of cannabidiol (CBD), 9-tetrahydrocannabinol (THC) and its metabolites in rat whole blood after oral administration of . *J. Pharm. Biomed. Anal.* **150,** 25–32 (2018).

423. Shim, S. *et al.* Development of a New Minipig Model to Study Radiation-Induced Gastrointestinal Syndrome and its Application in Clinical Research Development of a New Minipig Model to Study Radiation-Induced Gastrointestinal Syndrome and its Application in Clinical Resear. *Radiat. Res.* **181,** 387–395 (2014).

424. Shulman, R. J., Henning, S. J., Nichols, B. L. & Children, T. The Miniature Pig as an Animal Model for the Study of Intestinal Enzyme Development. *Pediatr. Res.* **23,** 311–315 (1988).

425. Wray, L., Stott, C., Jones, N. & Wright, S. Cannabidiol Does Not Convert to D 9 - Tetrahydrocannabinol in an In Vivo Animal Model. *Cannabis Cannabinoid Res.* **2,** 282–287 (2018).

426. Consroe, P., Kennedy, K. & Schram, K. Assay of Plasma Cannabidiol by Capillary Gas Chromatography/Ion Trap Mass Spectroscopy Following High-Dose Repeated Daily Oral Administration in Humans. *Pharmacol. Biochem. Behav.* **40,** 517–522 (1991).

427. Devinsky, O. *et al.* Trial of Cannabidiol for Drug-Resistant Seizures in the Dravet Syndrome. *N. Engl. J. Med.* **376,** 2011–2020 (2017).

428. Ranganathan, M. *et al.* Tetrahydrocannabinol (THC) impairs encoding but not retrieval of verbal information. *Prog. Neuropsychopharmacol. Biol. Psychiatry* **79,** 176–183 (2017).

429. Karschner, E. L. *et al.* Subjective and Physiological Effects After Controlled Sativex and Oral THC Administration. *Clin. Pharmacol. Ther.* **89,** 400–407 (2009).

430. D'Souza, D. C. *et al.* The Psychotomimetic Effects of Intravenous Delta-9-Tetrahydrocannabinol in Healthy Individuals: Implications for Psychosis. *Neuropharmacology* **29,** 1558–1572 (2004).

431. Friedman, D. & Sirven, J. I. Historical perspective on the medical use of cannabis for epilepsy : Ancient times to the 1980s. *Epilepsy Behav.* **70,** 298–301 (2017).

432. Kalant, H. Medicinal use of cannabis: History and current status. *Pain Res. Manag.* **6,** 80–91 (2001).

433. Grinspoon, L. Medical marihuana in a time of prohibition. *Int. J. Drug Policy* **10,** 145–156 (1999).

434. DEA. Drug Scheduling. Available at: https://www.dea.gov/drug-scheduling.

435. European Monitoring Centre for Drugs and Drug Addiction. Substances and classifications table. (2008). Available at: http://www.emcdda.europa.eu/html.cfm/index5733EN.html.

436. Gross, D. W., Hamm, J., Ashworth, N. L. & Quigley, D. Marijuana use and epilepsy:

Prevalence in patients of a tertiary care epilepsy center. *Neurology* **62,** 2095–2098 (2004).

437. Hamerle, M., Ghaeni, L., Kowski, A., Weissinger, F. & Holtkamp, M. Cannabis and other illicit drug use in epilepsy patients. *Eur. J. Neurol.* **21,** 167–170 (2014).

438. Hill, A. J. *et al.* Voltage-gated sodium (NaV) channel blockade by plant cannabinoids does not confer anticonvulsant effects per se. *Neurosci. Lett.* **566,** 269–274 (2014).

439. Ryan, D., Drysdale, a. J., Lafourcade, C., Pertwee, R. G. & Platt, B. Cannabidiol Targets Mitochondria to Regulate Intracellular Ca2+ Levels. *J. Neurosci.* **29,** 2053–2063 (2009).

440. Ledgerwood, C. J., Greenwood, S. M., Brett, R. R., Pratt, J. A. & Bushell, T. J. Cannabidiol inhibits synaptic transmission in rat hippocampal cultures and slices via multiple receptor pathways. *Br. J. Pharmacol.* **162,** 286–294 (2011).

441. Karler, R. & Turkanis, S. A. Subacute cannabinoid treatment: anticonvulsant activity and withdrawal excitability in mice. *Br. J. Pharmacol.* **68,** 479–484 (1980).

442. Wallace, M. J., Wiley, J. L., Martin, B. R. & DeLorenzo, R. J. Assessment of the role of CB1 receptors in cannabinoid anticonvulsant effects. *Eur. J. Pharmacol.* **428,** 51–57 (2001).

443. Izquierdo, I. & Tannhauser, M. The effect of cannabidiol on maximal electroshock seizures in rats. *J. Pharm. Pharmacol.* **25,** 916–917 (1973).

444. Consroe, P., Benedito, M. A. C., Leite, J. R., Carlini, E. A. & Mechoulam, R. Effects of cannabidiol on behavioural seizures caused by convulsant drugs or current in mice. *Eur. J. Pharmacol.* **83,** 293–298 (1982).

445. Jones, N. a *et al.* Cannabidiol displays antiepileptiform and antiseizure properties in vitro and in vivo. *J Pharmacol Exp Ther* **332,** 569–577 (2010).

446. Jones, N. A. *et al.* Cannabidiol exerts anti-convulsant effects in animal models of temporal lobe and partial seizures. *Seizure* **21,** 344–352 (2012).

447. Hill, A. J., Hill, T. D. M. & Whalley, B. J. in *Endocannabinoids: Molecular, Pharmacological, Behavioural and Clinical Features* (eds. Murillo-Rodriguez, E., Onaivi, E. S., Darmani, N. A. & Wagner, E.) 164–204 (Bentham Science Publishers, 2013). doi:10.2174/97816080502841130101

448. Gobira, P. H. *et al.* Cannabidiol, a Cannabis sativa constituent, inhibits cocaine-induced seizures in mice: Possible role of the mTOR pathway and reduction in glutamate release. *Neurotoxicology* **50,** 116–121 (2015).

449. Rosenberg, E. C., Patra, P. H. & Whalley, B. J. Therapeutic effects of cannabinoids in animal models of seizures , epilepsy , epileptogenesis , and epilepsy-related neuroprotection. *Epilepsy Behav.* **70,** 319–327 (2016).

450. Price, J. A., Morris, Z. A. & Costello, S. The Application of Adaptive Behaviour Models: A Systematic Review. *Behav. Sci. (Basel).* **8,** 1–17 (2018).

451. Devinsky, O. *et al.* Effect of Cannabidiol on Drop Seizures in the Lennox–Gastaut Syndrome. *N. Engl. J. Med.* **378,** 1888–1897 (2018).

452. Xie, J., Wang, X. & Proud, C. G. mTOR inhibitors in cancer therapy. *F1000Research* **5,** 3–11 (2016).

453. Giacoppo, S., Pollastro, F., Grassi, G., Bramanti, P. & Mazzon, E. Target regulation of PI3K/Akt/mTOR pathway by cannabidiol in treatment of experimental multiple sclerosis.

Fitoterapia **116,** 77–84 (2017).

454. Sales, A. J. *et al.* Cannabidiol Induces Rapid and Sustained Antidepressant-Like Effects Through Increased BDNF Signaling and Synaptogenesis in the Prefrontal Cortex. *Mol. Neurol.* 1–12 (2018). doi:10.1007/s12035-018-1143-4

455. Schiavon, A. P. *et al.* Protective Effects of Cannabidiol Against Hippocampal Cell Death and Cognitive Impairment Induced by Bilateral Common Carotid Artery Occlusion in Mice. *Neurotoxicology Res.* **26,** 307–316 (2014).

456. Esposito, G. *et al.* Cannabidiol Reduces Ab-Induced Neuroinflammation and Promotes Hippocampal Neurogenesis through PPAR gamma Involvement. *PLoS One* **6,** 1–8 (2011).

457. Vasheghani, F. *et al.* PPARγ deficiency results in severe, accelerated osteoarthritis associated with aberrant mTOR signalling in the articular cartilage. *Ann. Rheum. Dis.* **74,** 569–578 (2015).

458. Laplante, M. & Sabatini, D. M. mTOR Signaling in Growth Control and Disease. *Cell* **149,** 274–293 (2012).

459. Crino, P. B. The mTOR signalling cascade : paving new roads to cure neurological disease. *Nat. Rev. Neurol.* **12,** 379–392 (2016).

460. van Eeghen, A. M., Chu-Shore, C. J., Pulsifer, M. B., Camposano, S. E. & Thiele, E. A. Cognitive and adaptive development of patients with tuberous sclerosis complex : A retrospective , longitudinal investigation. *Epilepsy Behav.* **23,** 10–15 (2012).

461. Klein, B. D. *et al.* Evaluation of Cannabidiol in Animal Seizure Models by the Epilepsy Therapy Screening Program (ETSP). *Neurochem. Res.* **42,** 1939–1948 (2017).

462. Vilela, L. R. *et al.* Anticonvulsant effect of cannabidiol in the pentylenetetrazole model: Pharmacological mechanisms, electroencephalographic profile, and brain cytokine levels. *Epilepsy Behav.* **75,** 29–35 (2017).

463. Ramer, R. *et al.* COX-2 and PPAR- gamma Confer Cannabidiol-Induced Apoptosis of Human Lung Cancer Cells. *Mol. Cancer Ther.* **12,** 69–82 (2012).

464. Solinas, M. *et al.* Cannabidiol, a Non-Psychoactive Cannabinoid Compound, Inhibits Proliferation and Invasion in U87-MG and T98G Glioma Cells through a Multitarget Effect. *PLoS Biol.* **8,** 1–9 (2013).

465. Fisher, T. *et al.* In vitro and in vivo efficacy of non-psychoactive cannabidiol in neuroblastoma. *Curr. Oncol.* **23,** 15–22 (2016).

466. Lukhele, S. T. & Motadi, L. R. Cannabidiol rather than Cannabis sativa extracts inhibit cell growth and induce apoptosis in cervical cancer cells. *BMC Complement. Altern. Med.* **16,** 1–16 (2016).

467. Mcallister, S. D. *et al.* Pathways mediating the effects of cannabidiol on the reduction of breast cancer cell proliferation, invasion, and metastasis. *Breast Cancer Res. Treat.* **129,** 37–47 (2011).

468. Ramer, R. *et al.* Cannabidiol inhibits lung cancer cell invasion and metastasis via intercellular adhesion molecule-1. *FASEB J.* **26,** 1535–1548

469. Wong, M. Animal models of focal cortical dysplasia and tuberous sclerosis complex: Recent progress toward clinical applications. *Epilepsia* **50,** 34–44 (2009).

470. Roubertoux, P. L. *Organism Models of Autism Spectrum Disorders*. (Humana Press, New York, NY, 2015). doi:https://doi.org/10.1007/978-1-4939-2250-5

471. Orellana-Paucar, A. M. *et al.* Anticonvulsant activity of bisabolene sesquiterpenoids of Curcuma longa in zebrafish and mouse seizure models. *Epilepsy Behav.* **24,** 14–22 (2012).

472. Li, Q. *et al.* Differential behavioral responses of zebrafish larvae to yohimbine treatment. *Psychopharmacology (Berl).* **232,** 197–208 (2015).

473. Ji, Y. *et al.* Behavioural responses of zebrafish larvae to acute ethosuximide exposure. *Behav. Pharmacol.* **28,** 428–440 (2017).

474. Carmean, V. & Ribera, A. B. Genetic Analysis of the Touch Response in Zebrafish (Danio rerio). *Int. J. Comp. Psychol.* **23,** 91–102 (2010).

475. Schindelin, J. *et al.* Fiji: an open-source platform for biological-image analysis. *Nat. Methods* **9,** 676–682 (2012).

476. Vermoesen, K. *et al.* Assessment of the convulsant liability of antidepressants using zebrafish and mouse seizure models. *Epilepsy Behav.* **22,** 450–460 (2011).

477. Schnörr, S. J., Steenbergen, P. J., Richardson, M. K. & Champagne, D. L. Measuring thigmotaxis in larval zebrafish. *Behav. Brain Res.* **228,** 367–374 (2012).

478. Burgess, H. A. & Granato, M. Modulation of locomotor activity in larval zebrafish during light adaptation. *J. Exp. Biol.* **210,** 2526–2539 (2007).

479. Ramcharitar, J. & Ibrahim, R. M. Ethanol modifies zebrafish responses to abrupt changes in light intensity. *J. Clin. Neurosci.* **20,** 476–477 (2013).

480. Ellis, L. D., Seibert, J. & Soanes, K. H. Distinct models of induced hyperactivity in zebrafish larvae. *Brain Res.* **1449,** 46–59 (2012).

481. Peng, X. *et al.* Anxiety-related behavioral responses of pentylenetetrazole-treated zebrafish larvae to light-dark transitions. *Pharmacol. Biochem. Behav.* **145,** 55–65 (2016).

482. Griffiths, B. B. *et al.* A zebrafish model of glucocorticoid resistance shows serotonergic modulation of the stress response. *Front. Behav. Neurosci.* **6,** 1–10 (2012).

483. Meyuhas, O. & Dreazen, A. *Chapter 3 Ribosomal Protein S6 Kinase. From TOP mRNAs to Cell Size*. *Progress in Molecular Biology and Translational Science* **90,** (Elsevier Inc., 2009).

484. Blessing, E. M., Steenkamp, M. M., Manzanares, J. & Marmar, C. R. Cannabidiol as a Potential Treatment for Anxiety Disorders. *Neurotherapeutics* **12,** 825–836 (2015).

485. Solati, J., Salari, A. A. & Bakhtiari, A. 5HT1Aand 5HT1Breceptors of medial prefrontal cortex modulate anxiogenic-like behaviors in rats. *Neurosci. Lett.* **504,** 325–329 (2011).

486. Bordukalo-Niksic, T. *et al.* 5HT-1A receptors and anxiety-like behaviours: Studies in rats with constitutionally upregulated/downregulated serotonin transporter. *Behav. Brain Res.* **213,** 238–245 (2010).

487. Koek, W., Mitchell, N. C. & Daws, L. C. Biphasic effects of selective serotonin reuptake inhibitors on anxiety: rapid reversal of escitalopram's anxiogenic effects in the novelty-induced hypophagia test in mice? *Behav. Pharmacol.* **29,** 365–369 (2017).

488. Russo, E. B., Burnett, A., Hall, B. & Parker, K. K. Agonistic Properties of Cannabidiol at 5-

HT1a Receptors. *Neurochem. Res.* **30,** 1037–1043 (2005).

489. Hind, W. H., England, T. J. & O'Sullivan, S. E. Cannabidiol protects an in vitro model of the blood – brain barrier from oxygen-glucose deprivation via PPARγ and 5- HT 1A receptors. *Br. J. Pharmacol.* **173,** 815–825 (2016).

490. Herculano, A. M. & Maximino, C. Serotonergic modulation of zebrafish behavior: Towards a paradox. *Prog. Neuropsychopharmacol. Biol. Psychiatry* **55,** 50–66 (2014).

491. Maximino, C. *et al.* Role of serotonin in zebrafish (Danio rerio) anxiety: Relationship with serotonin levels and effect of buspirone, WAY 100635, SB 224289, fluoxetine and para-chlorophenylalanine (pCPA) in two behavioral models. *Neuropharmacology* **71,** 83–97 (2013).

492. Carty, D. R., Thornton, C., Gledhill, J. H. & Willett, K. L. Developmental Effects of Cannabidiol and Δ9-Tetrahydrocannabinol in Zebrafish. *Toxicol. Sci.* **162,** 137–145 (2018).

493. Chugani, H. T. & Chugani, D. C. Imaging of Serotonin Mechanisms in Epilepsy. *Epilepsy Curr.* **5,** 201–206 (2005).

494. Sarikaya, I. PET studies in epilepsy. *Am. J. Nucl. Med. Mol. Imaging* **5,** 416–430 (2015).

495. Chugani, H. T. *et al.* a-[11C]-Methyl-L-tryptophan–PET in191 patients with tuberous sclerosis complex. *Neurology* **81,** 674–680 (2013).

496. French, J. *et al.* Cannabidiol (CBD) significantly reduces drop seizure frequency in Lennox-Gastaut syndrome (LGS): results of a multi-center, randomized, double-blind, placebo controlled trial (GWPCARE4) (S21.001). *Neurology* **88,** (2017).

497. Fu, C. & Ess, K. C. Conditional and domain-specific inactivation of the Tsc2 gene in neural progenitor cells. *Genesis* **51,** 284–292 (2013).

498. Scheldeman, C. *et al.* Neurobiology of Disease mTOR-related neuropathology in mutant tsc2 zebrafish: phenotypic, transcriptomic and pharmacological analysis. *Neurobiol. Dis.* **108,** 225–237 (2017).

499. Feliciano, D. M. *et al.* A circuitry and biochemical basis for tuberous sclerosis symptoms: From epilepsy to neurocognitive deficits. *Int. J. Dev. Neurosci.* **31,** 667–678 (2013).

500. Elisia, I. *et al.* DMSO represses inflammatory cytokine production from human blood cells and reduces autoimmune arthritis. *PLoS One* **11,** 1–24 (2016).

501. Varela, M., Dios, S., Novoa, B. & Figueras, A. Characterisation, expression and ontogeny of interleukin-6 and its receptors in zebrafish (Danio rerio). *Dev. Comp. Immunol.* **37,** 97–106 (2012).

502. Timm, M., Saaby, L., Moesby, L. & Hansen, E. W. Considerations regarding use of solvents in in vitro cell based assays. *Cytotechnology* **65,** 887–894 (2013).

503. Pinno, J. *et al.* Interleukin-6 influences stress-signalling by reducing the expression of the mTOR-inhibitor REDD1 in a STAT3-dependent manner. *Cell. Signal.* **28,** 907–916 (2016).

504. Kim, H. Y. *et al.* Interleukin-6 upregulates Th17 response via mTOR/STAT3 pathway in acute-on-chronic hepatitis B liver failure. *J. Gastroenterol.* **49,** 1264–1273 (2014).

505. Huang, J., Dibble, C. C., Matsuzaki, M. & Manning, B. D. The TSC1-TSC2 Complex Is Required for Proper Activation of mTOR Complex 2. *Mollecular Cell. Biol.* **28,** 4104–4115 (2008).

506. Sancak, Y. *et al.* PRAS40 Is an Insulin-Regulated Inhibitor of the mTORC1 Protein Kinase. *Mol. Cell* **25,** 903–915 (2007).

507. Cardis, M. A. & DeKlotz, C. M. C. Cutaneous manifestations of tuberous sclerosis complex and the paediatrician's role. *Arch. Dis. Child.* **102,** 858–863 (2017).

508. Lin, J. Medical Care Burden of Children with Autism Spectrum Disorders. *Rev. J. Autism Dev. Disord.* **1,** 242–247 (2014).

509. Derguy, C., Roux, S., Portex, M. & M'bailara, K. An ecological exploration of individual, family, and environmental contributions to parental quality of life in autism. *Psychiatry Res.* **268,** 87–93 (2018).

510. Cooper, K., Loades, M. E. & Russell, A. Adapting psychological therapies for autism. *Res. Autism Spectr. Disord.* **45,** 43–50 (2018).

511. Howes, O. D. & Group, E. P. F. Autism Spectrum Disorder: consensus guidelines on assessment, treatment and research from the British Association for Psychopharmacology. *J. Psychopharmacol.* **32,** 3–29 (2018).

512. Harding, S. D. *et al.* The IUPHAR / BPS Guide to PHARMACOLOGY in 2018: updates and expansion to encompass the new guide to IMMUNOPHARMACOLOGY. *Nucleic Acids Res.* **46,** 1091–1106 (2018).

513. Sharma, S. R., Gonda, X. & Tarazi, F. I. Autism Spectrum Disorder: Classification, diagnosis and therapy. *Pharmacol. Ther.* **190,** 91–104 (2018).

514. Eissa, N. *et al.* Current Enlightenment About Etiology and Pharmacological Treatment of Autism Spectrum Disorder. *Front. Neurosci.* **12,** 1–26 (2018).

515. Williams, K., Brignell, A., Randall, M., Silove, N. & Hazell, P. Selective serotonin reuptake inhibitors (SSRIs) for autism spectrum disorders (ASD). *Cochrane Database Syst. Rev.* **20,** 1–39 (2013).

516. Hirsch, L. & Pringsheim, T. Aripiprazole for autism spectrum disorders (ASD) (Review). *Cochrane Database Syst. Rev.* 1–3 (2016). doi:10.1002/14651858.CD009043.pub3

517. Evangeliou, A. *et al.* Application of a Ketogenic Diet in Children With Autistic Behavior: Pilot Study. *J. Child Neurol.* **18,** 113–118 (2003).

518. Randell, E. *et al.* The use of everolimus in the treatment of neurocognitive problems in tuberous sclerosis (TRON): study protocol for a randomised controlled trial. *Trials* **17,** 1–10 (2016).

519. Krueger, D. A. *et al.* Everolimus for treatment of tuberous sclerosis complex-associated neuropsychiatric disorders. *Ann. Clin. Transl. Neurol.* **4,** 877–887 (2017).

520. Ding, L. *et al.* mTOR: An attractive therapeutic target for osteosarcoma? *Oncotarget* **7,** 50805–50813 (2016).

521. Kezic, A., Popovic, L. & Lalic, K. mTOR Inhibitor Therapy and Metabolic Consequences: Where Do We Stand? *Oxid. Med. Cell. Longev.* **2018,** 1–8 (2018).

522. Yi, Z. & Ma, F. Breast Cancer Biomarkers of Everolimus Sensitivity in Hormone Receptor-Positive Breast Cancer. *J. Breast Cancer* **20,** 321–326 (2017).

523. Tanaka, K. *et al.* Oncogenic EGFR Signaling Activates an mTORC2- NF-kB Pathway That Promotes Chemotherapy Resistance. *Cancer Discov.* **1,** 524–532 (2011).

524. Gupta, M. *et al.* Inhibition of histone deacetylase overcomes rapamycin-mediated resistance in diffuse large B-cell lymphoma by inhibiting Akt signaling through mTORC2. *Lymphoid Neoplasia* **114,** 2926–2936 (2018).

525. Ritvo, E. R. *et al.* Lower Purkinje Cell counts in the Cerebella of Four Autistic Subjects : Initial Findings of the UCLA-NSAC autopsy research Report. *Am. J. Psychiatry* **143,** 862–866 (1986).

526. Fatemi, S. H. *et al.* Purkinje cell size is reduced in cerebellum of patients with autism. *Cell. Mol. Neurobiol.* **22,** 171–175 (2002).

527. Traut, N. *et al.* Cerebellar volume in autism: Literature meta-analysis and analysis of the ABIDE cohort. *Biol. Psychiatry* **83,** 579–588 (2017).

528. Riva, D. *et al.* Gray Matter Reduction in the Vermis and CRUS-II Is Associated with Social and Interaction Deficits in Low-Functioning Children with Autistic Spectrum Disorders: a VBM-DARTEL Study. *Cerebellum* **12,** 676–685 (2013).

529. Foster, N. E. V *et al.* Structural Gray Matter Differences During Childhood Development in Autism Spectrum Disorder: A Multimetric Approach. *Pediatr. Neurol.* **53,** 350–359 (2015).

530. Mello, A. M. D., Moore, D. M., Crocetti, D., Mostofsky, S. H. & Stoodley, C. J. Cerebellar Gray Matter Differentiates Children With Early Language Delay in Autism. *Autism Res.* **9,** 1191–1204 (2016).

531. Laidi, C. *et al.* Cerebellar anatomical alterations and attention to eyes in autism. *Sci. Rep.* **7,** 1–11 (2017).

532. Ming, X., Brimacombe, M. & Wagner, G. C. Prevalence of motor impairment in autism spectrum disorders. *Brain Dev.* **29,** 565–570 (2007).

533. Sur, E. *et al.* Comparative Histometrical Study: The cerebellum and the determination of some AgNOR parameters in different avian species. *Bull. Vet. Inst. Pulawy* **55,** 261–265 (2011).

534. Donald, S. *et al.* P-Rex2 regulates Purkinje cell dendrite morphology and motor coordination. *Proc. Natl. Acad. Sci.* **105,** 4483–4488 (2008).

535. Thored, P. *et al.* Long-Term Accumulation of Microglia with Proneurogenic Phenotype Concomitant with Persistent Neurogenesis in Adult Subventricular Zone After Stroke. *Glia* **57,** 835–849 (2009).

536. Haynes, S. E. *et al.* The P2Y12 receptor regulates microglial activation by extracellular nucleotides. *Nat. Neurosci.* **9,** 1512–1519 (2006).

537. Field, A. *Discovering Statistics using IBM SPSS Statistics*. (Sage Publications Ltd., 2013).

538. Effron, B. & Tibshirani, R. J. *An introduction to the bootstrap*. (Chapman & Hall, 1993).

539. Marzban, H. *et al.* Cellular commitment in the developing cerebellum. *Front. Cell. Neurosci.* **8,** 1–26 (2015).

540. Pisu, M. B. *et al.* Proliferation and Migration of Granule Cells in the Developing Rat Cerebellum: Cisplatin Effects. **1235,** 1226–1235 (2005).

541. Ka, M., Condorelli, G., Woodgett, J. R. & Kim, W.-Y. mTOR regulates brain morphogenesis by mediating GSK3 signaling. *Development* **141,** 4076–4086 (2014).

542. Ka, M., Smith, A. L. & Kim, W. Y. MTOR controls genesis and autophagy of GABAergic interneurons during brain development. *Autophagy* **13,** 1348–1363 (2017).

543. Khundrakpam, B. S., Lewis, J. D., Kostopoulos, P., Carbonell, F. & Evans, A. C. Cortical Thickness Abnormalities in Autism Spectrum Disorders Through Late Childhood, Adolescence, and Adulthood: A Large-Scale MRI Study. *Cereb. Cortex* **27,** 1721–1731 (2017).

544. Chomez, P. *et al.* Increased cell death and delayed development in the cerebellum of mice lacking the rev-erbA α orphan receptor. *Development* **127,** 1489–1498 (2000).

545. Piochon, C. *et al.* Cerebellar plasticity and motor learning deficits in a copy-number variation mouse model of autism. *Nat. Commun.* **5,** 1–12 (2014).

546. Krysko, O. *et al.* Neocortical and Cerebellar Developmental Abnormalities in Conditions of Selective Elimination of Peroxisomes From Brain or From Liver. *J. Neurosci. Res.* **85,** 58–72 (2007).

547. Carletti, B. & Rossi, F. Neurogenesis in the Cerebellum. *Neurosci.* **14,** 91–100 (2008).

548. Purves, D., Augustine, G. & Fitzpatrick, D. in *Neuroscience* (Sunderland (MA): Sinauer Associates, 2001).

549. Esclapez, M., Tillakaratne, N. J., Kaufman, D. L., Tobin, a J. & Houser, C. R. Comparative localization of two forms of glutamic acid decarboxylase and their mRNAs in rat brain supports the concept of functional differences between the forms. *J. Neurosci.* **14,** 1834–1855 (1994).

550. Moffett, J. R., Palkovits, M., Namboodiri, M. A. A. & Neale, J. H. Comparative distribution of N-Acetylaspartylglutamate and GAD67 in the cerebellum and precerebellar nuclei of the rat utilizing enhanced carbodiimide fixation and immunohistochemistry. *J. Comp. Neurol.* **347,** 598–618 (1994).

551. Simat, M., Ambrosetti, L., Lardi-Studler, B. & Fritschy, J. M. GABAergic synaptogenesis marks the onset of differentiation of basket and stellate cells in mouse cerebellum. *Eur. J. Neurosci.* **26,** 2239–2256 (2007).

552. Eggermann, E. & Jonas, P. How the 'slow' Ca 2+ buffer parvalbumin affects transmitter release in nanodomain-coupling regimes. *Nat. Neurosci.* **15,** 20–22 (2012).

553. Collin, T. *et al.* Developmental Changes in Parvalbumin Regulate Presynaptic Ca2+ Signaling. *J. Neurosci.* **25,** 96–107 (2005).

554. Schmidt, H., Arendt, O., Brown, E. B., Schwaller, B. & Eilers, J. Parvalbumin is freely mobile in axons, somata and nuclei of cerebellar Purkinje neurones. *J. Neurochem.* **100,** 727–735 (2007).

555. Schwaller, B., Meyer, M. & Schiffmann, S. 'New' functions for 'old' proteins: The role of the calcium-binding proteins calbindin D-28k, calretinin and parvalbumin, in cerebellar physiology. Studies with knockout mice. *Cerebellum* **1,** 241–258 (2002).

556. Sergaki, M. C. *et al.* Compromised Survival of Cerebellar Molecular Layer Interneurons Lacking GDNF Receptors GFRα1 or RET Impairs Normal Cerebellar Motor Learning. *Cell Rep.* **19,** 1977–1986 (2017).

557. Nellist, M. *et al.* Distinct effects of single amino-acid changes to tuberin on the function of the tuberin-hamartin complex. *Eur. J. Hum. Genet.* **13,** 59–68 (2005).

558. Zhao, X. *et al.* Noninflammatory Changes of Microglia Are Sufficient to Cause Epilepsy. *Cell Rep.* **22,** 2094–2106 (2018).

559. Hayakawa, K. *et al.* Cannabidiol prevents a post-ischemic injury progressively induced by cerebral ischemia via a high-mobility group box1-inhibiting mechanism. *Neuropharmacology* **55,** 1280–1286 (2008).

560. Fernández-Arjona, M. del M., Grondona, J. M., Granados-Durán, P., Fernández-Llebrez, P. & López-Ávalos, M. D. Microglia Morphological Categorization in a Rat Model of Neuroinflammation by Hierarchical Cluster and Principal Components Analysis. *Front. Cell. Neurosci.* **11,** 1–22 (2017).

561. Ito, D. *et al.* Microglia-specific localisation of a novel calcium binding protein, Iba1. *Mol. Brain Res.* **57,** 1–9 (1998).

562. Stowell, R. D. *et al.* Cerebellar microglia are dynamically unique and survey Purkinje neurons in vivo. *Dev. Neurobiol.* **78,** 627–644 (2018).

563. Petković, F., Campbell, I. L., Gonzalez, B. & Castellano, B. Reduced cuprizone-induced cerebellar demyelination in mice with astrocyte-targeted production of IL-6 is associated with chronically activated, but less responsive microglia. *J. Neuroimmunol.* **310,** 97–102 (2017).

564. Savchenko, V. L., Mckanna, J. A., Nikonenko, I. R. & Skibo, G. G. Microglia and astrocytes in the adult rat brain: comparative immunocytochemical analysis demonstrates de efficacy of lipocortin 1 immunoreactivity. *Neuroscience* **96,** 195–203 (2000).

565. Kaplan, J. S., Stella, N., Catterall, W. A. & Westenbroek, R. E. Cannabidiol attenuates seizures and social deficits in a mouse model of Dravet syndrome. *Proc. Natl. Acad. Sci.* **114,** 11229–11234 (2017).

566. Osborne, A. L., Solowij, N., Babic, I., Huang, X. & Weston-green, K. Improved Social Interaction , Recognition and Working Memory with Cannabidiol Treatment in a Prenatal Infection (poly I:C) Rat Model. *Neuropsychopharmacology* **42,** 1447–1457 (2017).

567. Tschuluun, N., Wenzel, H. J. & Schwartzkroin, P. A. Irradiation exacerbates cortical cytopathology in the Eker rat model of Tuberous Sclerosis Complex, but does not induce hyperexcitability. *Epilepsy Res.* **73,** 53–64 (2007).

568. Rensing, N., Han, L. & Wong, M. Intermittent dosing of rapamycin maintains antiepileptogenic effects in a mouse model of tuberous sclerosis complex. *Epilepsia* **56,** 1088–1097 (2015).

569. Zeng, L. *et al.* Tsc2 gene inactivation causes a more severe epilepsy phenotype than Tsc1 inactivation in a mouse model of Tuberous Sclerosis Complex. *Hum. Mol. Genet.* **20,** 445–454 (2011).

570. Magri, L. *et al.* Sustained Activation of mTOR Pathway in Embryonic Neural Stem Cells Leads to Development of Tuberous Sclerosis Complex-Associated Lesions. *Stem Cell* **9,** 447–462 (2011).

571. Carson, R. P., Nielen, D. L. Van, Winzenburger, P. A. & Ess, K. C. Neuronal and glia abnormalities in Tsc1 -de fi cient forebrain and partial rescue by rapamycin. *Neurobiol. Dis.* **45,** 369–380 (2012).

572. Ehninger, D. & Silva, A. J. Increased levels of anxiety-related behaviours in a Tsc2 dominant negative transgenic mouse model of tuberous sclerosis. *Behav. Genet.* **41,** 357–363 (2011).

573. Bhatia, B. *et al.* Tuberous sclerosis complex suppression in cerebellar development and medulloblastoma: separate regulation of mTOR activity and p27Kip1 localization. *Cancer Res.* **69,** 7224–7234 (2009).

574. Boronat, S., Anne, E. & Paul, T. Cerebellar lesions are associated with TSC2 mutations in tuberous sclerosis complex: a retrospective record review study. *Dev. Med. Child Neurol.* **59,** 1071–1076 (2017).

575. Espinosa, S. J. & Luo, L. Timing Neurogenesis and Differentiation: Insights from Quatitative Clonal Analyses of Cerebellar Granule Cells. *J. Neurosci.* **28,** 2301–2312 (2008).

576. Altman, J. Morphological Development of the Rat Cerebellum and Some of Its Mechanisms. *Exp. Brain Res.* **Supp. 6,** (1982).

577. Butts, T., Green, M. J. & Wingate, R. J. T. Development of the cerebellum: simple steps to make a 'little brain'. *Development* **141,** 4031–4041 (2014).

578. Lewis, P. M., Gritli-Linde, A., Smeyne, R., Kottmann, A. & McMahon, A. P. Sonic hedgehog signaling is required for expansion of granule neuron precursors and patterning of the mouse cerebellum. *Dev. Biol.* **270,** 393–410 (2004).

579. Ha, T. *et al.* CbGRiTS: Cerebellar gene regulation in time and space. *Dev. Biol.* **397,** 18–30 (2015).

580. Govindarajan, B. *et al.* Transgenic expression of dominant negative tuberin through a strong constitutive promoter results in a tissue-specific tuberous sclerosis phenotype in the skin and brain. *J. Biol. Chem.* **280,** 5870–4 (2005).

581. Zimatkin, S. M. & Karnyushko, O. A. Expression of Doublecortin and NeuN in Developing Neurons in the Rat Cerebellum. *Neurosci. Behav. Physiol.* **47,** 122–126 (2017).

582. Weyer, A. & Schilling, K. Developmental and Cell Type-Specific Expression of the Neuronal Marker NeuN in the Murine Cerebellum. *J. Neurosci. Res.* **73,** 400–409 (2003).

583. Korbo, L., Andersen, B. B., Ladefoged, O. & Moller, A. Total numbers of various cell types in rat cerebellar cortex estimated using an unbiased stereological method. *Brain Res.* **609,** 262–268 (1993).

584. Buffo, A. & Rossi, F. Origin, lineage and function of cerebellar glia. *Prog. Neurobiol.* **109,** 42–63 (2013).

585. Suzuki, K. *et al.* Microglial Activation in Young Adults With Autism Spectrum Disorder. *JAMA Psychiatry* **70,** 49–58 (2013).

586. Vargas, D. L., Nascimbene, C., Krishnan, C., Zimmerman, A. W. & Pardo, C. A. Neuroglial Activation and Neuroinflammation in the Brain of Patients with Autism. *Ann. Neurol.* **57,** 67–81 (2005).

587. Hendrickx, D. A. E., van Eden, C. G., Schuurman, K. G., Hamann, J. & Huitinga, I. Staining of HLA-DR, Iba1 and CD68 in human microglia reveals partially overlapping expression depending on cellular morphology and pathology. *J. Neuroimmunol.* **309,** 12–22 (2017).

588. Jay, V., Edwards, V., Musharbash, A. & Rutka, J. T. Cerebellar Pathology in Tuberous Sclerosis. *Ultrastruct. Pathol.* **22,** 331–339 (1998).

589. Liber, A. F. Tuberous Sclerosis with Cerebellar Involvment. *Am. J. Clin. Pathol.* **10,** 483–492 (1940).

590. Uhlmann, E. J. *et al.* Heterozygosity for the tuberous sclerosis complex (TSC) gene products results in increased astrocyte numbers and decreased p27-Kip1 expression in TSC2+/- cells. *Oncogene* **21,** 4050–4059 (2002).

591. Sofroniew, M. V. & Vinters, H. V. Astrocytes: Biology and pathology. *Acta Neuropathol.* **119,** 7–35 (2010).

592. Anlauf, E. & Derouiche, A. Glutamine Synthetase as an Astrocytic Marker: Its Cell Type and Vesicle Localization. *Front. Endocrinol. (Lausanne).* **16,** 1–5 (2013).

593. Raponi, E. *et al.* S100B Expression Defines a State in Which GFAP- Expressing Cells Lose Their Neural Stem Cell Potential and Acquire a More Mature Developmental Stage. *Glia* **55,** 1416–1425 (2007).

594. Yoon, H., Walters, G., Paulsen, A. R. & Scarisbrick, I. A. Astrocyte heterogeneity across the brain and spinal cord occurs developmentally, in adulthood and in response to demyelination. *PLoS One* **12,** 1–19 (2017).

595. Thomanetz, V. *et al.* Ablation of the mTORC2 component rictor in brain or Purkinje cells affects size and neuron morphology. *J. Cell Biol.* **201,** 293–308 (2013).

596. Shiota, C., Woo, J., Lindner, J., Shelton, K. D. & Magnuson, M. A. Multiallelic Disruption of the rictor Gene in Mice Reveals that mTOR Complex 2 Is Essential for Fetal Growth and Viability. *Dev. Cell* **11,** 583–589 (2006).

597. Burnett, L. C. *et al.* Loss of the imprinted, non-coding Snord116 gene cluster in the interval deleted in the Prader Willi syndrome results in murine neuronal and endocrine pancreatic developmental phenotypes. *Hum. Mol. Genet.* **26,** 4606–4616 (2018).

598. Chen, J., Holguin, N., Shi, Y., Silva, M. J. & Long, F. mTORC2 Signaling Promotes Skeletal Growth and Bone Formation in Mice. *J. Bone Miner. Res.* **30,** 369–378 (2015).

599. Oh, W. J. & Jacinto, E. mTOR complex 2 signaling and functions. *Cell Cycle* **10,** 2305–2316 (2011).

600. Huang, J., Wu, S., Wu, C. & Manning, B. D. Signaling Events Downstream of Mammalian Target of Rapamycin Complex 2 Are Attenuated in Cells and Tumors Deficient for the Tuberous Sclerosis Complex Tumor Suppressors. *Cancer Res.* **69,** 6107–6115 (2009).

601. Tsuchiya, H., Orimoto, K., Kobayashi, T. & Hino, O. Presence of Potent Transcriptional Activation Domains in the Predisposing Tuberous Sclerosis (Tsc2) Gene Product of the Eker Rat Model. *Cancer Res.* **56,** 429–433 (1996).

602. Aicher, L. D., Campbell, J. S. & Yeung, R. S. Tuberin Phosphorylation Regulates Its Interaction with Hamartin. *J. Biol. Chem.* **276,** 21017–21021 (2001).

603. Angliker, N., Burri, M., Zaichuk, M., Fritschy, J. M. & Rüegg, M. A. mTORC1 and mTORC2 have largely distinct functions in Purkinje cells. *Eur. J. Neurosci.* **42,** 2595–2612 (2015).

604. Saito, N. & Shirai, Y. Protein Kinase C gamma (PKCgamma): Function of Neuron Specific Isotype. *J. Biochem.* **132,** 683–687 (2002).

605. Ignatowska-Jankowska, B., Jankowski, M. M. & Swiergiel, A. H. Cannabidiol decreases body weight gain in rats: Involvement of CB2 receptors. *Neurosci. Lett.* **490,** 82–84 (2011).

606. Strackx, E., Gantert, M., Moers, V., Kooten, I. A. J. Van & Kramer, B. W. Increased Number of Cerebellar Granule Cells and Astrocytes in the Internal Granule Layer in Sheep

Following Prenatal Intra-amniotic Injection of Lipopolysaccharide. *Cerebellum* **11,** 132–144 (2012).

607. Deiana, S. *et al.* Plasma and brain pharmacokinetic profile of cannabidiol (CBD), cannabidivarine (CBDV), Δ9 -tetrahydrocannabivarin (THCV) and cannabigerol (CBG) in rats and mice following oral and intraperitoneal administration and CBD action on obsessive-compulsive behav. *Psychopharmacology (Berl).* **219,** 859–873 (2012).

608. Mori, M. A. *et al.* Cannabidiol reduces neuroinflammation and promotes neuroplasticity and functional recovery after brain ischemia. *Prog. Neuropsychopharmacol. Biol. Psychiatry* **3,** 94–105 (2016).

609. Schiavon, A. P., Bonato, J. M., Milani, H., Guimaraes, F. S. & de Oliveira, M. R. W. Influence of single and repeated cannabidiol administration on emotional behavior and markers of cell proliferation and neurogenesis in non-stressed mice. *Prog. Neuropsychopharmacol. Biol. Psychiatry* **64,** 27–34 (2016).

610. Mori, M. A. *et al.* Cannabidiol reduces neuroinflammation and promotes neuroplasticity and functional recovery after brain ischemia. *Prog. Neuropsychopharmacol. Biol. Psychiatry* **75,** 94–105 (2017).

611. Chang, J. C. *et al.* Mitotic Events in Cerebellar Granule Progenitor Cells that Expand Cerebellar Surface Area Are Critical for Normal Cerebellar Cortical Lamination in Mice. *J. Neuropathol. Exp. Neurol.* **74,** 261–272 (2015).

612. Gomez-Nicola, D. & Perry, V. H. Microglial Dynamics and Role in the Healthy and Diseased Brain: A Paradigm of Functional Plasticity. *Neurosci.* **21,** 169–184 (2015).

613. Lafuente, H. *et al.* Cannabidiol Reduces Brain Damage and Improves Functional Recovery After Acute Hypoxia-Ischemia in Newborn Pigs. *Pediatr. Res.* **70,** 272–277 (2011).

614. Ceprian, M. *et al.* Cannabidiol reduces brain damage and improves functional recovery in a neonatal rat model of arterial ischemic stroke. *Neuropharmacology* **116,** 151–159 (2017).

615. Serra, I. *et al.* Cannabidiol modulates phosphorylated rpS6 signalling in a zebrafish model of Tuberous Sclerosis Complex. *Behav. Brain Res.* **363,** 135–144 (2019).

616. WHALLEY, B. *et al.* USE OF CANNABIDIOL IN THE TREATMENT OF TUBEROUS SCLEROSIS COMPLEX. (2018).

617. Hosseinzadeh, M., Nikseresht, S., Khodagholi, F., Naderi, N. & Maghsoudi, N. Cannabidiol Post-Treatment Alleviates Rat Epileptic-Related Behaviors and Activates Hippocampal Cell Autophagy Pathway Along with Antioxidant Defense in Chronic Phase of Pilocarpine-Induced Seizure. *J. Mol. Neurosci.* **58,** 432–440 (2016).

618. Iannotti, F. A. *et al.* Effects of non-euphoric plant cannabinoids on muscle quality and performance of dystrophic mdx mice. *Br. J. Pharmacol.* **8,** 1–17 (2018).

619. Campos, A. C. *et al.* Plastic and Neuroprotective Mechanisms Involved in the Therapeutic Effects of Cannabidiol in Psychiatric Disorders. *Front. Pharmacol.* **8,** 1–18 (2017).

620. Bernard, M. *et al.* Autophagy fosters myofibroblast differentiation through MTORC2 activation and downstream upregulation of CTGF. *Autophagy* **10,** 2193–2207 (2014).

621. Lampada, A. *et al.* mTORC1-independent autophagy regulates receptor tyrosine kinase phosphorylation in colorectal cancer cells via an mTORC2-mediated mechanism. *Cell Death Differ.* **24,** 1045–1062 (2017).

622. Mckay, B. E. & Turner, R. W. Physiological and morphological development of the rat cerebellar Purkinje cell. *J. Physiol.* **567,** 829–850 (2005).

623. Tadayonnejad, R. *et al.* Rebound Discharge in Deep Cerebellar Nuclear Neurons In Vitro. *Cerebellum* **9,** 352–374 (2010).

624. Peter, S. *et al.* Dysfunctional cerebellar Purkinje cells contribute to autism-like behaviour in Shank2-deficient mice. *Nat. Commun.* **7,** 1–14 (2016).

625. Skalicky, A. M. *et al.* Economic burden, work, and school productivity in individuals with tuberous sclerosis and their families. *J. Med. Econ.* **21,** 953–959 (2018).

626. Leclerc, S. & Easley, D. Pharmacological Therapies for Autism Spectrum Disorder: A Review. *Pharm. Ther.* **40,** 389–397 (2015).

627. DeFilippis, M. & Wagner, K. D. Treatment of Autism Spectrum Disorder in Children and Adolescents. *Evid. Based. Med.* **46,** 18–41 (2016).

628. Matson, J. L. & Hess, J. A. Psychotropic drug efficacy and side effects for persons with autism spectrum disorders. *Res. Autism Spectr. Disord.* **5,** 230–236 (2011).

629. van Heijst, B. F. C. & Geurts, H. M. Quality of life in autism across the lifespan: A meta-analysis. *Autism* **19,** 158–167 (2015).

630. Baxter, A. J. *et al.* The epidemiology and global burden of autism spectrum disorders. *Psychol. Med.* **45,** 601–613 (2015).

631. Mugno, D., Ruta, L., D'Arrigo, V. G. & Mazzone, L. Impairment of quality of life in parents of children and adolescents with pervasive developmental disorder. *Health Qual. Life Outcomes* **5,** 1–9 (2007).

632. Wang, Y. *et al.* Social Impairment of Children with Autism Spectrum Disorder Affects Parental Quality of Life in Different Ways. *Psychiatry Res.* **266,** 168–174 (2018).

633. Guimaraes, F. S., Chiaretti, T. M., Graeff, F. G. & Zuardi, A. Antianxiety effect of cannabidiol in the elevated plus-maze. *Psychopharmacology (Berl).* **100,** 558–559 (1990).

634. Servadio, M., Vanderschuren, L. J. M. J. & Trezza, V. Modeling autism-relevant behavioral phenotypes in rats and mice: Do 'autistic' rodents exist? *Behav. Pharmacol.* **26,** 522–540 (2015).

635. Marco, E. M. *et al.* Social encounter with a novel partner in adolescent rats: Activation of the central endocannabinoid system. *Behav. Brain Res.* **220,** 140–145 (2011).

636. Grandgeorge, M. & Bourreau, Y. Interest towards human, animal and object in children with autism spectrum disorders: an ethological approach at home. *Eur. Child Adolesc. Psychiatry* **24,** 83–93 (2014).

637. Silverman, J. L., Yang, M., Lord, C. & Crawley, J. N. Behavioural phenotyping assays for mouse models of autism. *Nat. Rev. Neurosci.* **11,** 490–502 (2011).

638. Antunes, M. & Biala, G. The novel object recognition memory: neurobiology, test procedure, and its modifications. *Cogn. Process.* **13,** 93–110 (2012).

639. Silvers, J. M., Harrod, S. B., Mactutus, C. F. & Booze, R. M. Automation of the novel object recognition task for use in adolescent rats. *J. Neurosci. Methods* **166,** 99–103 (2007).

640. Broadbent, N. J., Gaskin, S., Squire, L. R. & Clark, R. E. Object recognition memory and

the rodent hippocampus. *Learn. Mem.* **17,** 5–11 (2010).

641. Ridler, K. *et al.* Neuroanatomical Correlates of Memory Deficits in Tuberous Sclerosis Complex. *Cereb. Cortex* **14,** 261–271 (2007).

642. Pulsifer, M. B., Winterkorn, E. B. & Thiele, E. A. Psychological profile of adults with tuberous sclerosis complex. *Epilepsy Behav.* **10,** 402–406 (2007).

643. Shephard, E. *et al.* Early developmental pathways to childhood symptoms of attention-deficit hyperactivity disorder, anxiety and autism spectrum disorder. *J. Child Psychol. Psychiatry* (2018). doi:10.1111/jcpp.12947

644. La Buissonnière-Ariza, V. *et al.* Presentation and Correlates of Hoarding Behaviors in Children with Autism Spectrum Disorders and Comorbid Anxiety or Obsessive-Compulsive Symptoms. *J. Autism Dev. Disord.* **48,** 4167–4178 (2018).

645. Lamprea, M. R., Cardenas, F. P., Setem, J. & Morato, S. Thigmotactic responses in an open-field. *Brazilian J. Med. Biol. Res.* **41,** 135–140 (2008).

646. Sousa, N., Almeida, O. F. X. & Wotjak, C. T. A hitchhiker's guide to behavioral analysis in laboratory rodents. *Genes, Brain Behav.* **5,** 5–24 (2006).

647. Ennaceur, A., Michalikova, S. & Chazot, P. L. Models of anxiety: Responses of rats to novelty in an open space and an enclosed space. *Behav. Brain Res.* **171,** 26–49 (2006).

648. Medeiros, G. F. De, Pereira, E., Granzotto, N. & Ramos, A. Low-Anxiety Rat Phenotypes Can Be Further Reduced through Genetic Intervention. *PLoS One* **8,** 1–12 (2013).

649. Speight, A., Davey, W. G., McKenna, E. & Voigt, J.-P. W. Exposure to a maternal cafeteria diet changes open-field behaviour in the developing offspring. *Int. J. Dev. Neurosci.* **57,** 34–40 (2016).

650. Schulz, D. Acute food deprivation separates motor-activating from anxiolytic effects of caffeine in a rat open field test model. *Behav. Pharmacol.* **29,** 543–546 (2018).

651. Liu, F. *et al.* Effectiveness of low dose of rapamycin in preventing seizure-induced anxiety-like behavior, cognitive impairment and defects in neurogenesis in developing rats. *Int. J. Neurosci.* **8,** 1–20 (2018).

652. Aguilar, B. L., Malkova, L., Gouemo, P. N. & Forcelli, P. A. Genetically Epilepsy-Prone Rats Display Anxiety-Like Behaviors and Neuropsychiatric Comorbidities of Epilepsy. *Front. Neurol.* **9,** 1–15 (2018).

653. Song, C., Berridge, K. C. & Kalueff, A. V. 'Stressing' rodent self-grooming for neuroscience research. *Nat. Rev. Neurosci.* **17,** 591 (2016).

654. Kalueff, A. V *et al.* Neurobiology of rodent self-grooming and its value for translational neuroscience. *Nat. Rev. Neurosci.* **17,** 45–59 (2016).

655. Kalueff, A. V & Tuohimaa, P. The grooming analysis algorithm discriminates between different levels of anxiety in rats : potential utility for neurobehavioural stress research. *J. Neurosci. Methods* **143,** 169–177 (2005).

656. Reimer, A. E. *et al.* Rats with differential self-grooming expression in the elevated plus-maze do not differ in anxiety-related behaviors. *Behav. Brain Res.* **292,** 370–380 (2015).

657. Rodgers, J., Glod, M., Connolly, B. & McConachie, H. The Relationship Between Anxiety and Repetitive Behaviours in Autism Spectrum Disorder. *J. Autism Dev. Disord.* **42,** 2404–

2409 (2012).

658. Lidstone, J. *et al.* Relations among restricted and repetitive behaviors, anxiety and sensory features in children with autism spectrum disorders. *Res. Autism Spectr. Disord.* **8,** 82–92 (2014).

659. Kilincaslan, A. *et al.* Beneficial Effects of Everolimus on Autism and Attention-Deficit/ Hyperactivity Disorder Symptoms. *J. Child Adolesc. Psychopharmacol.* **27,** 838–388 (2017).

660. Eden, K. E., Vries, P. J. De, Moss, J., Richards, C. & Oliver, C. Self-injury and aggression in tuberous sclerosis complex : cross syndrome comparison and associated risk markers. *J. Dev. Disord.* **6,** 1–11 (2014).

661. Vlaskamp, C. *et al.* Bumetanide As a Candidate Treatment for Behavioral Problems in Tuberous Sclerosis Complex. *Front. Neurol.* **8,** 1–7 (2017).

662. Hassan, I. K. *et al.* Psychosis with obsessive-compulsive symptoms in tuberous sclerosis. *J. Clin. Neurosci.* **21,** 867–869 (2014).

663. Thomas, A. *et al.* Marble burying reflects a repetitive and perseverative behavior more than novelty-induced anxiety. *Psychopharmacology (Berl).* **204,** 361–373 (2009).

664. Casarotto, P. C., Gomes, F. V, Resstel, L. B. M. & Guimara, F. S. Cannabidiol inhibitory effect on marble-burying behaviour: involvement of CB1 receptors. *Behav. Pharmacol.* **21,** 353–358 (2010).

665. Egashira, N., Okuno, R., Harada, S., Matsushita, M. & Mishima, K. Effects of glutamate-related drugs on marble-burying behavior in mice: Implications for obsessive-compulsive disorder. *Eur. J. Pharmacol.* **586,** 164–170 (2008).

666. Cops, E. J. *et al.* Tissue-type plasminogen activator is an extracellular mediator of Purkinje cell damage and altered gait. *Exp. Neurol.* **249,** 8–19 (2013).

667. Angoa-Pérez, M., Kane, M. J., Briggs, D. I., Francescutti, D. M. & Kuhn, D. M. Marble Burying and Nestlet Shredding as Tests of Repetitive, Compulsive-like Behaviors in Mice. *jove* **24,** 50978 (2013).

668. Schneider, T. *et al.* Gender-specific behavioral and immunological alterations in an animal model of autism induced by prenatal exposure to valproic acid. *Psychoneuroendocrinology* **33,** 728–740 (2008).

669. Shoval, G. & Hershkovitz, L. Prohedonic Effect of Cannabidiol in a Rat Model of Depression. *Neuropsychobiology* **73,** 123–129 (2016).

670. Schneider, M., Schömig, E. & Leweke, F. M. Acute and chronic cannabinoid treatment differentially affects recognition memory and social behavior in pubertal and adult rats. *Addict. Biol.* **13,** 345–357 (2008).

671. Cai, L., Gibbs, R. B. & Johnson, D. A. Recognition of novel objects and their location in rats with selective cholinergic lesion of the medial septum. *Neurosci. Lett.* **506,** 261–265 (2012).

672. Westbrook, S. R., Brennan, L. E. & Stanton, M. E. Ontogeny of Object Versus Location Recognition in the Rat: Acquisition and Retention Effects. *Dev. Psychobiol.* **56,** 1492–1506 (2014).

673. Heck, D. H., Zhao, Y., Roy, S., Ledoux, M. S. & Reiter, L. T. Analysis of cerebellar function in Ube3a -eficient mice reveals novel genotype-specific behaviors. *Hum. Mol. Genet.* **17,** 2181–2189 (2008).

674. Yan, M. *et al.* EGb761 improves histological and functional recovery in rats with acute spinal cord contusion injury. *Spinal Cord* **54,** 259–265 (2016).

675. Patra, P. H. *et al.* Cannabidiol reduces seizures and associated behavioral comorbidities in a range of animal seizure and epilepsy models. *Epilepsia* **60,** 303–314 (2018).

676. Using ImageJ to quantify blots. *The University of Queensland* Available at: https://di.uq.edu.au/community-and-alumni/sparq-ed/sparq-ed-services/using-imagej-quantify-blots.

677. Gallo-Oller, G., Ordoñez-Ciriza, R. & Dotor, J. A new background subtraction method for Western blot densitometry band quantification through image analysis software. *J. Immunol. Methods* **457,** 1–5 (2018).

678. Invitrogen. Normalization in western blotting to obtain relative quantitation. *Technical Note* Available at: https://assets.thermofisher.com/TFS-Assets/BID/Technical-Notes/ibright-normalization-western-blotting-relative-quantitation-technical-note.pdf.

679. Deacon, R. M. J. Housing, husbandry and handling of rodents for behavioral experiments. *Nat. Protoc.* **1,** 936–946 (2006).

680. Xia, Y., Ye, Q., Gao, Q., Lu, Y. & Zhang, D. Symmetry Analysis of Gait between Left and Right Limb Using Cross-Fuzzy Entropy. *Comput. Math. Methods Med.* **2016,** 1–9 (2016).

681. Santos, P. M., Williams, S. L. & Thomas, S. S. Neuromuscular evaluation using rat gait analysis. *J. Neurosci ence Methods* **61,** 79–84 (1995).

682. Peres, F. F. *et al.* Cannabidiol Administered During Peri-Adolescence Prevents Behavioral Abnormalities in an Animal Model of Schizophrenia. *Front. Pharmacol.* **9,** 1–15 (2018).

683. Jakubczak, L. F. Food and Water Intakes of Rats as a Function of Strain, Age, Temperature, and Body Weight. *Physiol. Behav.* **17,** 251–258 (1976).

684. Rodd, C., Metzger, D. L. & Sharma, A. Extending World Health Organization weight-for-age reference curves to older children. *BMC Pediatr.* **14,** 1–7 (2014).

685. Humphrey, A., Williams, J., Pinto, E. & Bolton, P. F. A prospective longitudinal study of early cognitive development in tuberous sclerosis. *Eur. Child Adolesc. Psychiatry* **13,** 159–165 (2004).

686. Kaur, M., Srinivasan, S. M. & Bhat, A. N. Comparing motor performance, praxis, coordination, and interpersonal synchrony between children with and without Autism Spectrum Disorder (ASD). *Res. Dev. Disabil.* **72,** 79–95 (2018).

687. Yuan, E. *et al.* Graded loss of tuberin in an allelic series of brain models of TSC correlates with survival, and biochemical, histological and behavioral features. *Hum. Mol. Genet.* **21,** 4286–4300 (2012).

688. Louis, E. D. *et al.* Reduced Purkinje cell dendritic arborization and loss of dendritic spines in essential tremor. *Brain* **137,** 3142–3148 (2014).

689. Axelrad, J. E. *et al.* Reduced Purkinje Cell Number in Essential Tremor: A Postmortem Study. *Arch. Neurol.* **65,** 101–107 (2008).

690. Parker, A. J. & Clarke, K. A. Gait Topography in Rat Locomotion. *Physiol. Behav.* **48,** 41–47 (1990).

691. Horner, A. M., Russ, D. W. & Biknevicius, A. R. Effects of early-stage aging on locomotor

dynamics and hindlimb muscle force production in the rat. *J. Exp. Biol.* **214,** 3588–3595 (2011).

692. Hruska, R. E. & Silbergeld, E. K. Abnormal locomotion in rats after bilateral intrastriatal injection of kainic acid. *Life Sci.* **25,** 181–194 (1979).

693. Elbatsh, M. M., Assareh, N., Marsden, C. A. & Kendall, D. A. Anxiogenic-like effects of chronic cannabidiol administration in rats. *Psychopharmacology (Berl).* **221,** 239–247 (2012).

694. El-Alfy, A. T. *et al.* Antidepressant-like effect of Δ 9-etrahydrocannabinol and other cannabinoids isolated from Cannabis sativa L. *Pharmacol. Biochem. Behav.* **95,** 434–442 (2010).

695. Long, L. E. *et al.* A behavioural comparison of acute and chronic D9-tetrahydrocannabinol and cannabidiol in C57BL/6JArc mice. *Int. J. Neuropsychopharmacol.* **13,** 861–876 (2010).

696. Drai, D., Kafkafi, N., Benjamini, Y., Elmer, G. & Golani, I. Rats and mice share common ethologically relevant parameters of exploratory behavior. *Behav. Brain Res.* **125,** 133–140 (2001).

697. Seibenhener, M. L. & Wooten, M. C. Use of the Open Field Maze to Measure Locomotor and Anxiety-like Behavior in Mice. *J. Vis. Exp.* **e52434,** 1–6 (2015).

698. Saiki, A., Kimura, R., Samura, T., Fujiwara-Tsukamoto, Y. & Sakai, Y. Different Modulation of Common Motor Information in Rat Primary and Secondary Motor Cortices. *PLoS One* **9,** 1–13 (2014).

699. Schonfeld, L.-M., Dooley, D., Jahanshahi, A., Temel, Y. & Hendrix, S. Evaluating rodent motor functions: Which tests to choose? *Neurosci. Biobehav. Rev.* **83,** 298–312 (2017).

700. Ho, Y., Eichendorff, J. & Schwarting, R. K. W. Individual response profiles of male Wistar rats in animal models for anxiety and depression. *Behav. Brain Res.* **136,** 1–12 (2002).

701. Shaw, F. Z., Chuang, S. H., Shieh, K. R. & Wang, Y. J. Depression- and anxiety-like behaviors of a rat model with absence epileptic discharges. *Neuroscience* **160,** 382–393 (2009).

702. Raznahan, A., Joinson, C., Callaghan, F. O., Osborne, J. P. & Bolton, P. F. Psychopathology in tuberous sclerosis: an overview and findings in a population-based sample of adults with tuberous sclerosis. *J. Intellect. Disabil. Res.* **50,** 561–569 (2006).

703. World Health Organization, . *Depression and Other Common Mental Disorders: Global Health Estimates*. (2017).

704. Nardo, M., Casarotto, P. C., Gomes, F. V. & Guimaraes, F. S. Cannabidiol reverses the mCPP-induced increase in marble-burying behavior. *Fundam. Clin. Pharmacol.* **28,** 544–550 (2014).

705. Campbell, C. T., Phillips, M. S. & Manasco, K. Cannabinoids in Pediatrics. *J. Pediatr. Pharmacol. Ther.* **22,** 176–185 (2016).

706. Rex, A., Voigt, J.-P., Gustedt, C., Beckett, S. & Fink, H. Anxiolytic-like profile in Wistar, but not Sprague-Dawley rats in the social interaction test. *Psychopharmacology (Berl).* **177,** 23–34 (2004).

707. Fogaça, M. V., Reis, F. M. C. V. & Campos, A. C. Effects of intra-prelimbic prefrontal cortex injection of cannabidiol on anxiety-like behavior: Involvement of 5HT1A receptors

and previous stressful experience. *Eur. Neuropsychopharmacol.* **24,** 410–419 (2014).

708. Varlinskaya, E. I. & Spear, L. P. Social interactions in adolescent and adult Sprague-Dawley rats: Impact of social deprivation and test context familiarity. *Behav. Brain Res.* **188,** 398–405 (2008).

709. Garau, A., Marti, M. A., Sala, J. & Balada, F. Age Effects on the Social Interaction Test in Early Adulthood Male Rats. *Depress. Anxiety* **12,** 226–231 (2000).

710. Perkins, A. E. *et al.* A working model for the assessment of disruptions in social behavior among aged rats: The role of sex differences, social recognition, and sensorimotor processes. *Exp. Gerontol.* **76,** 46–57 (2016).

711. Morellini, F. Spatial memory tasks in rodents: what do they model? *Cell Tissue Res.* **354,** 273–286 (2013).

712. Blaser, R., Heyser, C. & Parker, M. O. Spontaneous object recognition: a promising approach to the comparative study of memory. *Front. Behav. Neurosci.* **9,** 1–12 (2015).

713. Sara, S. J., Dyon-Laurent, C. & Herve, A. Novelty seeking behavior in the rat is dependent upon the integrity of the noradrenergic system. *Cogn. Brain Res.* **2,** 181–187 (1995).

714. Dudchenko, P. A. An overview of the tasks used to test working memory in rodents. *Neurosci. Biobehav. Rev.* **28,** 699–709 (2004).

715. Morellini, F. & Schachner, M. Enhanced novelty-induced activity, reduced anxiety, delayed resynchronization to daylight reversal and weaker muscle strength in tenascin-C-deficient mice. *Eur. J. Neurosci.* **23,** 1255–1268 (2006).

716. Hauser, M. J., Isbrandt, D. & Roeper, J. Disturbances of novel object exploration and recognition in a chronic ketamine mouse model of schizophrenia. *Behav. Brain Res.* **332,** 316–326 (2017).

717. Kabbaj, M., Devine, D. P., Savage, V. R. & Akil, H. Neurobiological Correlates of Individual Differences in Novelty-Seeking Behavior in the Rat: Differential Expression of Stress-Related Molecules. *J. Neurosci.* **20,** 6983–6988 (2000).

718. Vivanti, G. *et al.* Attention to novelty versus repetition: Contrasting habituation profiles in Autism and Williams syndrome. *Dev. Cogn. Neurosci.* **29,** 54–60 (2018).

719. Orekhova, E. V & Stroganova, T. A. Arousal and attention re-orienting in autism spectrum disorders: evidence from auditory event-related potentials. *Front. Hum. Neurosci.* **8,** 1–17 (2014).

720. Pazos, M. R. *et al.* Cannabidiol administration after hypoxia-ischemia to newborn rats reduces long-term brain injury and restores neurobehavioral function. *Neuropharmacology* **63,** 776–783 (2012).

721. Stern, C. A. J., Gazarini, L., Takahashi, R. N., Guimaraes, F. S. & Bertoglio, L. J. On Disruption of Fear Memory by Reconsolidation Blockade: Evidence from Cannabidiol Treatment. *Neuropsychopharmacology* **37,** 2132–2142 (2012).

722. Song, C., Stevenson, C. W., Guimaraes, F. S. & Lee, J. L. C. Bidirectional Effects of Cannabidiol on Contextual Fear Memory Extinction. *Front. Pharmacol.* **7,** 1–7 (2016).

723. Nazario, L. R. *et al.* Caffeine protects against memory loss induced by high and non-anxiolytic dose of cannabidiol in adult zebrafish (Danio rerio). *Pharmacol. Biochem. Behav.* **135,** 210–216 (2015).

724. Fagherazzi, E. V *et al.* Memory-rescuing effects of cannabidiol in an animal model of cognitive impairment relevant to neurodegenerative disorders. *Psychopharmacology (Berl).* **219,** 1133–1140 (2012).

725. Warburton, E. C. & Brown, M. W. Neural circuitry for rat recognition memory. *Behav. Brain Res.* **285,** 131–139 (2015).

726. Thiele, E. *et al.* Cannabidiol in patients with Lennox-Gastaut syndrome: Interim analysis of an open-label extension study. *Epilepsia* **60,** 419–428 (2019).

727. Devinsky, O. *et al.* Long-term cannabidiol treatment in patients with Dravet syndrome: An open-label extension trial. *Epilepsia* **60,** 294–302 (2019).

728. Panic, L. *et al.* Ribosomal Protein S6 Gene Haploinsufficiency Is Associated with Activation of a p53-Dependent Checkpoint during Gastrulation. *Mol. Cell. Biol.* **26,** 8880–8891 (2006).

729. Volarevic, S. *et al.* Proliferation, But Not Growth, Blocked by Conditional Deletion of 40S Ribosomal Protein S6. *Science (80-.).* **288,** 2045–2047 (2000).

730. Knoll, M. *et al.* The ribosomal protein S6 in renal cell carcinoma: functional relevance and potential as biomarker. *Oncogene* **7,** 418–432 (2015).

731. Levoe, S. N. *et al.* Factors influencing adverse skin responses in rats receiving repeated subcutaneous injections and potential impact on neurobehavior. *Curr. Neurobiol.* **5,** 1–10 (2014).

732. Lodzki, M. *et al.* Cannabidiol-transdermal delivery and anti-inflammatory effect in a murine model. *J. Control. Release* **93,** 377–387 (2003).

733. Rosenberg, E. C., Louik, J., Conway, E., Devinsky, O. & Friedman, D. Quality of Life in Childhood Epilepsy in pediatric patients enrolled in a prospectiv, open-label clinical study with cannabidiol. *Epilepsia* **58,** 96–100 (2017).

734. Sparagana, S. P., Delgado, M. R., Batchelor, L. L. & Roach, S. Seizure Remission and Antiepileptic Drug Discontinuation in Children With Tuberous Sclerosis Complex. *Arch. Neurol.* **60,** 1286–1289 (2016).

735. Overwater, I. E. *et al.* Epilepsy in children with tuberous sclerosis complex: Chance of remission and response to antiepileptic drugs. *Epilepsia* **56,** 1239–1245 (2015).

736. Perucca, P., Scheffer, I. E. & Kiley, M. The managment of epilepsy in children and adults. *Med. J. Aust.* **208,** 226–233 (2018).

737. Allers, K. *et al.* The economic impact of epilepsy: a systematic review. *BMC Neurol.* **15,** 1–16 (2015).

738. Jackson, M. J. & Turkington, D. Depression and anxiety in epilepsy. *J. Neurol. Neurosurg. Psychiatry* **76,** 45–47 (2005).

739. Strasser, L., Downes, M., Kung, J., Cross, J. H. & Haan, M. D. E. Prevalence and risk factors for autism spectrum disorder in epilepsy: a systematic review and meta-analysis. *Dev. Med. Child Neurol.* **60,** 19–29 (2018).

740. Gerlach, A. C. & Krajewski, J. L. Antiepileptic Drug Discovery and Development: What Have We Learned and Where Are We Going? *Pharmaceuticals* **3,** 2884–2899 (2010).

741. Loscher, W. & Schmidt, D. Modern antiepileptic drug development has failed to deliver: Ways out of the current dilemma. *Epilepsia* **52,** 657–678 (2011).

742. Amada, N., Yamasaki, Y., Williams, C. M. & Whalley, B. J. Cannabidivarin (CBDV) suppresses pentylenetetrazole (PTZ)-induced increases in epilepsy-related gene expression. *PeerJ* **1,** 1–18 (2013).

743. Zhang, B. & Wong, M. Pentylenetetrazole-induced seizures cause acute, but not chronic, mTOR pathway activation in rat. *Epilepsia* **53,** 506–511 (2012).

744. Watanabe, T. *et al.* Amygdala-kindled and pentylenetetrazole-induced seizures in glutamate transporter GLAST-deficient mice. *Brain Res.* **845,** 92–96 (1999).

745. Sircar, R., Veliskova, J. & Moshe, S. L. Chronic neonatal phencyclidine treatment produces age-related changes in pentylenetetrazol-induced seizures. *Dev. Brain Res.* **81,** 185–191 (1994).

746. Bialer, M. & White, H. S. Key factors in the discovery and development of new antiepileptic drugs. *Nat. Rev. Drug Discov.* **9,** 68–82 (2010).

747. Smith, M., Wilcox, K. S. & White, H. S. Discovery of Antiepileptic Drugs. *Neurotherapeutics* **4,** 12–17 (2007).

748. Löscher, W. Critical review of current animal models of seizures and epilepsy used in the discovery and development of new antiepileptic drugs. *Seizure* **20,** 359–368 (2011).

749. Kliouеva, I. A., Luijtelaar, E. L. J. M. Van, Chepurnova, N. E. & Chepurnov, S. A. PTZ-induced seizures in rats: effects of age and strain. *Psychol. Behav.* **72,** 421–426 (2001).

750. Tchekalarova, J., Kubová, H. & Mares, P. Effects of postnatal caffeine exposure on seizure susceptibility in developing rats. *Brain Res.* **1150,** 21–39 (2007).

751. Guillet, R. Neonatal caffeine exposure alters seizure susceptibility in rats in an age-related manner. *Dev. Brian Res.* **89,** 124–128 (1995).

752. Dhir, A. Pentylenetetrazol (PTZ) Kindling Model of Epilepsy. *Curr. Protoc. Neurosci.* **Supplement,** 1–12 (2012).

753. Ferraro, T. N. *et al.* Mapping Loci for Pentylenetetrazol-Induced Seizure Susceptibility in Mice. *J. Neurosci.* **19,** 6733–6739 (1999).

754. Motulsky, H. J. & Brown, R. E. Detecting outliers when fitting data with nonlinear regression- a new method based on robust nonlinear regression and the false discovery rate. *BMC Bioinformatics* **7,** 1–20 (2006).

755. Adikaram, K. K. L. B., Hussein, M. A., Effenberger, M. & Becker, T. Data Transformation Techniques to Improve the Outlier Detection Power of Grubbs' Test for Data Expected to Follow Linear Relation. *J. Appl. Math.* **2015,** 1–9 (2015).

756. Wong, M., Wozniak, D. F. & Yamada, K. A. An animal model of generalized nonconvulsive status epilepticus: immediate characteristics and long-term effects. *Exp. Neurol.* **183,** 87–99 (2003).

757. Hill-Yardin, E. L. *et al.* Reduced susceptibility to induced seizures in the Neuroligin-3 R451C mouse model of autism. *Neurosci. Lett.* **589,** 57–61 (2015).

758. Snead III, O. C. Pharmacological models of generalized absence seizures in rodents. *J. Neural Transm.* **35,** 7–19 (1992).

759. Reddy, D. S. & Rogawski, M. A. Enhanced Anticonvulsant Activity of Neuroactive Steroids in a Rat Model of Catamenial Epilepsy. *Epilepsia* **42,** 337–344 (2001).

760. Bogdanov, N. N., Poletaeva, I. I. & Popova, N. V. Pentylenetetrazol and strychnine convulsions in brain weight selected mice. *Seizure* **6,** 135–138 (1997).

761. Eells, J. B., Clough, R. W., Browning, R. A. & Jobe, P. C. Comparative FOS immunoreactivity in the brain after forebrain, brainstem, or combined seizures induced by electroshock, pentylenetetrazol, focally induced and audiogenic seizures in rats. *Neuroscience* **123,** 279–292 (2004).

762. Chesher, G. B. & Jackson, D. M. Anticonvulsant Effects of Cannabinoids in Mice: Drug Interactions within Cannabinoids and Cannabinoid Interactions with Phenytoin. *Psycopharmacologia* **37,** 255–264 (1974).

763. Fuente-Martín, E. *et al.* Early nutritional changes induce sexually dimorphic long-term effects on body weight gain and the response to sucrose intake in adult rats. *Metabolism* **61,** 812–822 (2012).

764. Prager, G., Stefanski, V., Hudson, R. & Rödel, H. G. Family matters: Maternal and litter-size effects on immune parameters in young laboratory rats. *Brain, Behav. Immun.* **24,** 1371–1378 (2010).

765. Viana, L. C. *et al.* Litter size, age-related memory impairments, and microglial changes in rat dentate gyrus: stereological analysis and three dimentional morphometry. *Neuroscience* **238,** 280–296 (2013).

766. Nery, C. da S. *et al.* Murinometric Evaluations and Feed Efficiency in Rats from Reduced Litter During Lactation and Submitted or Not to Swimming Exercise. *Ciencias do Exerc. e do Esporte* **17,** 49–55 (2011).

767. Roma, P. G., Huntsberry, M. E. & Riley, A. L. Separation stress, litter size, and the rewarding effects of low-dose morphine in the dams of maternally separated rats. *Prog. Neuropsychopharmacol. Biol. Psychiatry* **31,** 429–433 (2007).

768. de Lima, D. S. C., Francisco, E. da S., Lima, C. B. & Guedes, R. C. A. Neonatal L-glutamine modulates anxiety-like behavior, cortical spreading depression, and microglial immunoreactivity: analysis in developing rats suckled on normal size- and large size litters. *Amino Acids* **49,** 337–346 (2016).

769. Millar, S. A., Stone, N. L., Yates, A. S. & O'Sullivan, S. E. A Systematic Review on the Pharmacokinetics of Cannabidiol in Humans. *Front. Pharmacol.* **9,** 1–13 (2018).

770. Hesdorffer, D. C. *et al.* Combined analysis of risk factors for SUDEP. *Epilepsia* **52,** 1150–1159 (2011).

771. Shorvon, S. & Tomson, T. Sudden unexpected death in epilepsy. *Lancet* **378,** 2028–2038 (2011).

772. Vasconcelos, A. P. De, Gizard, F., Marescaux, C. & Nehlig, A. Role of Nitric Oxide in Pentylenetetrazol-Induced Seizures: Age-Dependent Effects in the Immature Rat. *Epilepsia* **41,** 363–371 (2000).

773. Lüttjohann, A., Fabene, P. F. & van Luijtelaar, G. A revised Racine's scale for PTZ-induced seizures in rats. *Physiol. Behav.* **98,** 579–586 (2009).

774. Chachua, T. *et al.* Rapamycin has age- , treatment paradigm- , and model-specific anticonvulsant effects and modulates neuropeptide Y expression in rats. *Epilepsia* **53,** 2015–2025 (2015).

775. Siebel, A. M., Menez, F. P., Schaefer, I. da C., Petersen, B. D. & Bonan, C. D. Rapamycin

suppresses PTZ-induced seizures at different developmental stages of zebrafish. *Pharmacol. Biochem. Behav.* **139,** 163–168 (2015).

776. Talos, D. M. *et al.* Mechanistic Target of Rapamycin Complex 1 and 2 in Human Temporal Lobe Epilepsy. *Ann. Neurol.* **83,** 311–327 (2018).

777. Sabatini, D. M. Twenty-five years of mTOR: Uncovering the link from nutrients to growth. *Proc. Natl. Acad. Sci.* **114,** 11818–11825 (2017).

778. Hara, K. *et al.* Raptor, a Binding Partner of Target of Rapamycin (TOR), Mediates TOR Action. *Cell* **110,** 177–189 (2002).

779. Baybis, M. *et al.* mTOR Cascade Activation Distinguishes Tubers from Focal Cortical Dysplasia. *Ann. Neurol.* **56,** 478–487 (2004).

780. Bissler, J. J. *et al.* Everolimus long-term use in patients with tuberous sclerosis complex: Four-year update of the EXIST-2 study. *PLoS One* **12,** 1–16 (2017).

781. Corroon, J. & Phillips, J. A. A Cross-Sectional Study of Cannabidiol Users. *Cannabis Cannabinoid Res.* **3,** 152–161 (2018).

782. Cenci, M. A., Whishaw, I. Q. & Schallert, T. Animal models of neurological deficits: how relevant is the rat? *Nat. Rev. Neurosci.* **3,** 574–579 (2002).

783. Ellenbroek, B. & Youn, J. Rodent models in neuroscience research: is it a rat race? *Dis. Model. Mech.* **9,** 1079–1087 (2016).

784. Ryan, D., Drysdale, A. J., Lafourcade, C., Pertwee, R. G. & Platt, B. Cannabidiol targets mitochondria to regulate intracellular Ca2+ levels. *J. Neurosci.* **29,** 2053–63 (2009).

785. Drysdale, A. J., Ryan, D., Pertwee, R. G. & Platt, B. Cannabidiol-induced intracellular Ca2+ elevations in hippocampal cells. *Neuropharmacology* **50,** 621–631 (2006).

786. Parray, H. A. & Yun, J. W. Cannabidiol promotes browning in 3T3-L1 adipocytes. *Mol. Cell. Biochem.* **416,** 131–139 (2016).

787. Xie, J. & Proud, C. G. Signaling crosstalk between the mTOR complexes Signaling crosstalk between the mTOR complexes. *Translation* **2,** 1–11 (2014).

788. Agoston, D. V. How to Translate Time? The Temporal Aspect of Human and Rodent Biology. *Front. Neurol.* **8,** 17–19 (2017).

789. Pahl, P. J. Growth curves for body weight of the laboratory rat. *Aust. Joural Biol. Sci.* **22,** 1077–1080 (1969).

790. Szaflarski, J. P. *et al.* Long-term safety and treatment effects of cannabidiol in children and adults with treatment-resistant epilepsies: Expanded access program results. *Epilepsia* **59,** 1540–1548 (2018).

791. Hazekamp, A. The Trouble with CBD Oil. *Med. Cannabis Cannabinoids* **1,** 65–72 (2018).

792. Smart, R., Caulkins, J. P., Kilmer, B., Davenport, S. & Midgette, G. Variation in Cannabis potency and prices in a newly-legal market: Evidence from 30 million cannabis sales in Washington State. *Addiction* **112,** 2167–2177 (2017).

793. Lippiello, P. *et al.* From Cannabis to Cannabidiol to Treat Epilepsy, Where Are We? *Curr. Pharm. Des.* **22,** 1–8 (2016).